Physical effects of anthropogenic aerosols on wheat production in the eastern Indo Gangetic Plain

Shreemat Shrestha

Open Researcher and Contributor ID (ORCID): 0000-0002-3054-0126

Submitted in total fulfillment of the requirements

of the degree of Doctor of Philosophy

September 2019

Environmental Hydrology and Water Resources Group

Department of Infrastructure Engineering

The University of Melbourne

Australia

Declaration

This is to certify that:

1. this thesis comprises only my original work towards the degree of Doctor of Philosophy,
2. due acknowledgement has been made in the text to all other material used,
3. the thesis is fewer than 100,000 words in length exclusive of tables, maps, bibliographies and appendices.

Shreemat Shrestha

Melbourne

September 2019

Abstract

The Indo Gangetic Plain (IGP) is home to 800 million people and is considered a hot spot of air pollution due to persistently high anthropogenic atmospheric aerosol loading. High levels of anthropogenic aerosols in the IGP not only affect the health of people, but also affect the health of the natural system and climate of the region in terms of their effect (physical) on surface dimming, monsoon pattern, evapotranspiration, fog events, glacial retreat, reduction of stream discharge during dry season, etc. Since the IGP is a food bowl of south Asia, it is crucial to understand the effect of anthropogenic aerosols on crop production for the food security and livelihood of the millions of people of the region. In this context, this study is conducted to address the need for a study on the effect of anthropogenic aerosols on crop production in the IGP. Here, the eastern IGP is selected as a study area due to comparatively higher aerosol loading, population density and dominance of smallholders in agriculture compared to the western IGP. Similarly, the effect of atmospheric aerosols on wheat is studied because wheat is a widely cultivated winter crop and high-level atmospheric aerosol loading during the winter season is reported in the IGP. Hence, this thesis seeks to address the main research question "What are the physical effects of atmospheric aerosols on winter crop (wheat) production in the eastern IGP?".

To address the main research question, the study is conducted in the following 4 steps. Firstly, in the context of increased trend of persistent winter fog along with increased level of atmospheric aerosols across the IGP in past 2 decades, its possible effect on the crop production and to address current knowledge gap on the status of fog in the Nepal component of IGP, this step examined the trend of winter fog events in the Terai region of Nepal (Chapter 3). After analysing the historical visibility data of 4 Terai stations in Nepal, the fog was also found to be an important weather phenomenon at Nepal component of IGP due to a significant number of average foggy days (24 to 56 days) during winter and its increasing trend in past 35 years. Secondly, in the scenario of an increased number of cold days in the Indian component of IGP due to the increased level of fog and haze, this step pursued to address the knowledge gap on the extreme cold events and to document farmer's perception on effect of cold and fog events on their agriculture. In this step, the study on cold waves in the Terai region of Nepal and farmer's perception of the effect of fog events and cold waves on agriculture was conducted (Chapter 4). Analysis of the historical daily temperature data of 6 Terai stations during 1970-2015 showed that the annual number of cold and extreme cold days were at increasing trend during past 4 decades supporting the trend of fog events during winter. Focus group discussion with the farmer groups of Dhanusha and Sunsari districts (Terai region of Nepal) revealed that the increased fog and cold events during winter have affected their winter crop and livestock significantly. Thirdly, to assess the impact of reduced solar radiation, due

to anthropogenic aerosols on crop production a regression modelling study was conducted to estimate daily radiative forcing due to atmospheric aerosols from Moderate Resolution Imaging Spectrometers (MODIS) data in the IGP region (Chapter 5). A simple regression model was developed by utilising Aerosol Robotic Network's (AERONET's) aerosol optical depth (AOD), atmospheric water vapour and radiative forcing at the surface data during 2002 to 2015 at 10 stations in the IGP. After calibration and evaluation of the model, the model was also evaluated by using MODIS Terra and Aqua products of AOD and water vapour to use the developed model beyond the AERONET stations in the IGP. Finally, by using the daily radiative forcing from the developed model and the calibrated Agricultural Production Systems sIMulator (APSIM) model at the Sustainable Resilient Farming Systems Intensifications (SRFSI) project sites of eastern IGP region, the effect on the principal winter crop, wheat production due to anthropogenic atmospheric aerosols was studied (Chapter 6). In the eastern IGP, in average the anthropogenic aerosols have reduced the wheat grain yield, biomass yield, and crop evapotranspiration by 11.2-13.5%, 21.2-22%, and 13.5-15.1% respectively during 2015-2017 at the SRSFI nodes of eastern IGP. Moreover, the loss of wheat grain yield due to anthropogenic aerosols in the eastern IGP is estimated to be more than 300 million USD per annum during the study period. Hence, this study established the effect of anthropogenic aerosols on winter crop (wheat) production by using process-based model APSIM in the IGP for the first time.

There are several possible applications of the outputs of this research. For example, the findings of an increasing trend in fog and cold days and their implications for agriculture in the Nepal component of the IGP could be utilised by policymakers to minimise the effect of fog and cold events on the Terai region of Nepal. Likewise, the simple regression model developed in this study to estimate radiative forcing due to atmospheric aerosols could also be used to assess the effect of aerosols on the terrestrial ecosystem of the IGP. Similarly, the quantification of the reduction in the wheat grain yield in the eastern IGP from this study could be utilised by policymakers and stakeholders to justify more investment in air quality improvement within the region and to build awareness among farmers and citizens to reduce air pollution not only for their health benefit, but also for food security of the region. The major limitations of this study are non-consideration of the effect of anthropogenic aerosols on direct and diffuse radiation availability and the effect of deposited aerosols on the leaves, which would both be expected to influence crop production. Methods developed and used in this research could be applied in future research to investigate the effect of anthropogenic aerosols on other crops (maize, lentil, boro rice, potato, etc.).

Acknowledgements

First and foremost, I would like to extend my sincere gratitude to my present principal supervisor Murray C. Peel, for providing me with the great opportunity to complete my PhD thesis under his supervision, it is truly an honour. Thank you for your encouragement and continuous support and guidance in this study. I am also grateful to my former principal supervisor Graham A. Moore for his support and guidance for the first two years and continuous supervision even after his retirement. Thank you for your guidance and expert advice throughout the study period. I really feel honoured to complete my PhD under your supervision.

I would also like to thank my committee chair A. Prof. Dongryeol Ryu for your invaluable comments and suggestions.

I am indebted to Don Gaydon and Perry Poulton from CSIRO, Brisbane for their support for their guidance in using calibrated APSIM model for SRSFI sites in this research.

I also would like to acknowledge the Australian Centre for International Agricultural Research (ACIAR) for providing John Allwright Fellowship (JAF) to pursue my PhD at the University of Melbourne.

Special thanks to Renuka Shrestha, SRFSI Nepal coordinator, Mahesh Gathala, and Thakur P Tiwari, Project Leader SRFSI for their support and encouragement to pursue my PhD in Australia.

Many thanks to Sanjeet, Bikash and Mukti for assisting during transcribing the fog data and their support during my fieldwork in the Terai region of Nepal.

Thanks to my fellow PhD students Seema, Suwash, Tilak, Smriti, Mukta, Naveen and others for their company and support.

I also would like to thank my wife Ahana for walking together on this journey in Australia and for all the support by taking care of home and children during my PhD work.

I am grateful to my mother and brother for your continued support, love and blessing in my life. Specially, I also would like to thank my brother Manohar Shrestha for taking all the responsibility of the family including taking care my mother and without his support I would not have come to Australia for my PhD study.

I would like to express my deep sense of gratitude to my father Late Shyam Bahadur Shrestha for his inspiration, guidance and all the support in my life. Finally, I would like to thank my eternal spiritual father for his guidance, support and blessings in every step of my journey in this life.

Preface

The research described in this thesis is entirely my own work, and the contributions of others are limited to supervision, technical assistance and/or manuscript review. No part of this thesis has been submitted for another qualification, and no part was carried out prior to PhD enrolment.

Chapters 3 to 6 are formatted as journal articles and have been submitted or accepted & published in the Journals as below.

- Chapter 3 has been published as "*Shrestha, S., Moore, G.A., Peel, M.C., 2018. Trends in winter fog events in the Terai region of Nepal. Agric. For. Meteorol. 259, 118–130. https://doi.org/10.1016/j.agrformet.2018.04.018*".
- Chapter 4 has been submitted as "*Shrestha, S., Peel, M.C., Moore, G.A. Cold waves in Terai region of Nepal and farmer's perception of the effect of fog events and cold waves on agriculture*"; submitted for publication in Theoretical and Applied Climatology on June 6, 2019.
- Chapter 5 has been published as "*Shrestha, S., Peel, M.C., Moore, G.A., 2018. Development of a Regression Model for Estimating Daily Radiative Forcing Due to Atmospheric Aerosols from Moderate Resolution Imaging Spectrometers (MODIS) Data in the Indo Gangetic Plain (IGP). Atmosphere (Basel). 9, 1–26.* https://doi.org/10.3390/atmos9100405".
- Chapter 6 has been submitted for publication as "*Shrestha, S., Peel, M.C., Moore, G.A., Don, G., Poulton, P and Dutta, S K. Physical effects of anthropogenic aerosols on wheat production in the eastern Indo Gangetic Plain"* in Agricultural and Forest Meteorology on September 5, 2019

Abbreviations

ABC	atmospheric brown cloud
ACIAR	Australian Centre for International Agricultural Research
ADRF	direct radiative forcing due to atmospheric aerosols
AE	Angstrom exponent
AERONET	AErosol RObotic NETwork
AOD	Aerosol Optical Depth
APSIM	agricultural production systems simulator
ARF	Aerosol Radiative Forcing
ARIMA	autoregressive integrated moving average
AUD	Australian Dollar
BC	Black Carbon
BOA	bottom of atmosphere
BS	Bharat Stage
BSRN	Baseline Surface Radiation
CA	Conservation Agriculture
CCN	cloud condensation nuclei
CERES	crop environment resource synthesis
cfu	colony-forming unit
CLM	Community Land Model
CRM	column radiation model
DB	deep blue
DHM	Department of Hydrology and Meteorology
DJF	December January February
DSSAT	Decision support system for agrotechnology transfer
DT	dark target
EHP	elevated heat pump
EOS	Earth observing system
ET	Evapotranspiration
ETCCDI	Expert Team on Climate Change Detection and Indices
FGD	focus group discussion
GC	GEOS-Chem
GEBA	Global Energy Balance Archive
Gg y^{-1}	Giga gram per year

GLOF	Glacial Lake Outburst Flood
GPP	gross primary productivity
ha	Hectare
HI	hazard index
HKH	Hindu Kush Himalaya
IGP	Indo Gangetic Plain
ILCR	Incremental Lifetime Cancer Risk
IMD	Indian Meteorological Department
INDOEX	INDian Ocean Experiment
ISCCP	International Satellite Cloud Climatology Project
JJAS	June July August September
Km	Kilometre
Ktons	Kilo tons
m ha	million hectare
m.a.s.l.	meter above sea level
MAE	mean absolute error
MAM	March April May
MARKAL	MARKet and ALlocation
ME	mean error
MERRA	Modern-Era Retrospective Analysis for Research and Application
METAR	Meteorological Terminal Air Report
MI	myocardial infarction
MISR	Multiangle Imaging Spectro Radiometer
MK	Mann Kendall
mm	milli meter
MODIS	Moderate Resolution Imaging Spectroradiometer
Mt.	Mount
NASA	National Aeronautics and Space Administration
NCO-P	Nepal Climate Observation-Pyramid
NCP	North China Plain
NDSWR	net downward shortwave radiation
NPP	net primary productivity
PAR	photosynthetic active radiation
PM	Particulate Matter
PMF	Positive Matrix Factorization
RMSE	root mean square error

RUE	radiation use efficiency
SBDART	Santa Barbara DISTORT Atmospheric Radiative Transfer
SLCP	short-lived climate pollutant
SMOG	Speciated Multi-pOllutant Generator
SolRad-Net	Solar Radiation Networks
SRFSI	Sustainable Resilient Farming System Intensification
SSP	shared socio-economic pathway
TOA	top of atmosphere
TUV	Tropospheric Ultraviolet-Visible
UP	Utter Pradesh
USD	United States Dollar
UTC	Coordinated Universal Time
W m^{-2}	Watt per meter square
WHO	World Health Organization
WIA	water-insoluble aerosol
WMO	World Meteorological Organization
YIB	Yale interactive terrestrial biosphere

Table of Contents

Chapter 1

Chapter 2

Chapter 3

Chapter 4

Chapter 5

Chapter 6

Chapter 7

List of Figures

Chapter 1

Chapter 2

Chapter 3

Chapter 4

Chapter 5

Chapter 6

List of Tables

Chapter 3

Chapter 4

Chapter 5

Chapter 6

Annexes

Annex 1: Supplement Figures of Chapter 5 (Comparison of MODIS and AERONET data)

Annex 2 : Supplement Tables of Chapter 6

Chapter 1

Introduction

1.0 Introduction

The Indo Gangetic Plain (IGP) is the food basket of the South Asian region and home to about 800 Million people with the world's highest concentration of rural poverty (Ericksen et al., 2012; Taneja et al., 2014). The IGP is also considered a hot spot with respect to high atmospheric aerosol loading (Mehta, 2015). Increasing aerosol loading in the IGP has significantly affected people's health and natural systems of the region. This study seeks to better understand the physical effects of atmospheric aerosols on crop production in the IGP. This chapter introduces the thesis by covering the study context, study area, study rationale, framework of this study, an overview of chapters and the scope of this study in the following sections.

Air pollution is not a new phenomenon, it was a feature of the industrial revolution in Europe and America in the early twentieth century. The peak impact of air pollution in Europe and America is reported in the form of 'London Fog' and 'Los Angeles Smog' respectively by the mid twentieth century, which caused a large number of sick people and took the lives of thousands (Davis et al., 2002; Fenger, 2009; Mahoney and Bernardino, 1976). In spite of the increase of population, traffic, and industrial activities, the air quality of the US and Europe improved over the past 5 decades due to the adoption of strong regulation to minimize pollution by using cleaner energy sources and efficient technology (Crippa et al., 2016; Sullivan et al., 2018). However, the history of poor air quality in developed countries is repeating in the developing countries at South and East Asia in the form of 'Great Indo Asian haze' / 'Atmospheric Brown Cloud', 'Chinese haze'/ 'Chinese smog' in the twenty-first century (Ramanathan et al., 2001; Ramanathan and Crutzen, 2003; Shi et al., 2016; Wang et al., 2016). Emissions of anthropogenic aerosols from increased urbanization, industrialization, and economic activities in the two most populous countries, China and India, are responsible for the high level of air pollution in the region. The World Health Organization (WHO) database on the levels of annual average fine particulate matter reveals that of the 50 most polluted cities in the world, 45 lie in the Indo Asia Pacific region (WHO, 2018). The high levels of air pollution in these countries is reported to have severe effects on the health of people in this region. For

example, globally the highest mortality burden due to exposure to air pollution is reported in China and India, with 1.2 million deaths each in the year 2017 (Health Effects Institute, 2019). In the Indo Asia Pacific Region, the IGP is recognized as a hot spot for air pollution due to persistently high levels of atmospheric aerosols (Ramanathan et al., 2007; Zhao et al., 2018).

2.0 Study Context / Problem area:

The Indo Gangetic Plain (IGP) is one of the most highly polluted regions of the world partially due to persistent heavy aerosol loading in its atmosphere due to rapid urbanization, industrialization and lack of effective monitoring and control on pollution (Srivastava et al., 2012a; M. Kumar et al., 2018). High atmospheric pollution in this region is not only due to emissions from increased use of fossil fuel in transportation and the industrial sector, but also due to a high dependence on biomass being used mainly for cooking in the rural residential sector (Venkataraman et al., 2006). Moreover, the practice of burning of crop residue (rice and wheat) in the field has significantly contributed to atmospheric aerosols during the rice and wheat harvesting seasons in the IGP (Kaskaoutis et al., 2014; Rajput et al., 2014; Rastogi et al., 2016). The combined effect of increasing emissions of anthropogenic aerosols with the region's unique topography and synoptic meteorological conditions has resulted in alarming levels of atmospheric aerosols in the IGP (Dey and Di Girolamo, 2010; Di Girolamo et al., 2004; Srivastava et al., 2012). The WHO (2018a) showed that 17 cities of the IGP are listed in the 20 most polluted cities of the world, based upon annual mean $PM_{2.5}$ concentration. This high level of pollution has a serious impact on the health of people in the IGP. Among countries with the highest mortality burden attributable to air pollution in 2017, 3 IGP countries India (1.2 million), Pakistan (128,000) and Bangladesh (123,000) secured the second and third and fifth position. (Health Effects Institute, 2019).

This high level of atmospheric aerosols not only affects the health of people, but also the health of the ecosystem and the local climate through its effect on surface dimming, monsoon rainfall pattern, fog, and cryosphere (Bonasoni et al., 2012; Gautam et al., 2011; Kambezidis et al., 2012; Li et al., 2016; Ramanathan and Ramana, 2005; Srivastava et al., 2016). The reduction of surface solar radiation through absorption and scattering by atmospheric aerosols is known as surface dimming, and it is continuing in India even after 2000 at the rate of 10 W m^{-2}decade $^{-1}$ (Wild et al., 2009). Moreover, Dey and Tripathi (2007) also estimated that about 19 % of net incoming radiation is reduced by

atmospheric aerosols in the Ganga basin. Because of reduced solar radiation, evapotranspiration in this region is reduced significantly. For example, Padmakumari et al. (2013) showed a decreasing trend in pan evaporation for the Indian region at the rate of 9.24 mm per annum^2 during 1971-2010. Solar dimming in the IGP not only reduces surface evapotranspiration, but also weakens the land-sea temperature gradient, which results in a shift in the Asian monsoon circulation southward and decreases its intensity (Ramanathan et al., 2005). Moreover, the increased aerosol loading in the atmosphere is also believed to be responsible for increase in persistent fog and haze across the IGP (Figure 1) during the winter(Gautam et al., 2007).

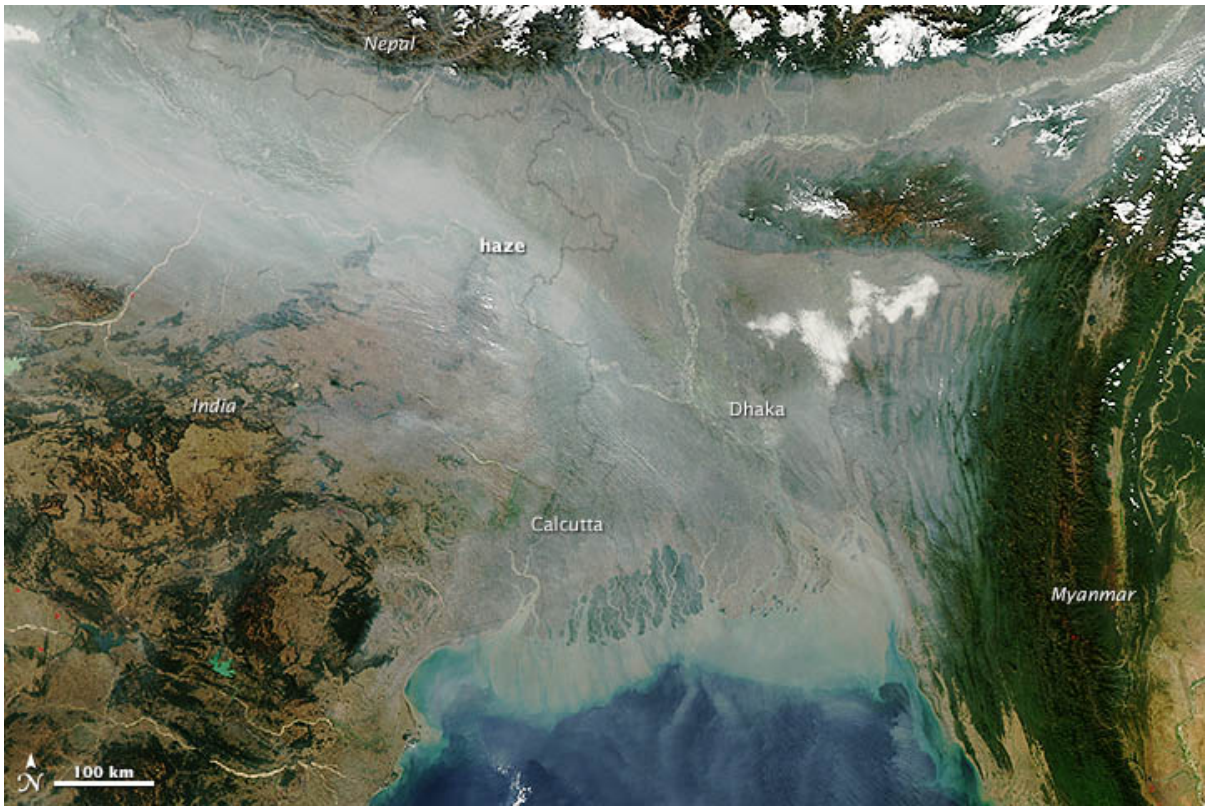

Figure 1: A thick blanket of haze over the eastern IGP, an image captured by MODIS Terra on January 3, 2016 (NASA - Earth Observatory, 2016)

The atmospheric aerosols, especially black carbon, have a major role in the reduction of snow cover area and glacial retreat in the Hindu Kush Himalayan (HKH) region due to the reduction of snow albedo through aerosol deposition (Menon et al., 2010). Increasing glacial retreat in the HKH has a direct effect on streamflow especially decline during the dry season, which may affect the livelihood of people in the whole IGP region (Shrestha and Aryal, 2011). In summary, all these effects of increased atmospheric aerosols such as reduction of solar radiation, reduction of evapotranspiration, change in monsoon pattern,

increased fog events, reduction in stream discharge during the dry season have potential to impact crop production in the IGP. A finding from the literature review in this thesis is that there is a lack of comprehensive study on the effects of atmospheric aerosols on crop production in the IGP. As the IGP is a food basket for the whole region, the effect of atmospheric aerosols on crop production is expected to affect the food security and livelihood of more than a billion people living in the region. In this context, the study on the physical effect of atmospheric aerosols on crop production in the eastern IGP region is conducted. Within the IGP, the eastern IGP is selected as a study area due to persistent and comparatively high atmospheric aerosols (Figure 2).

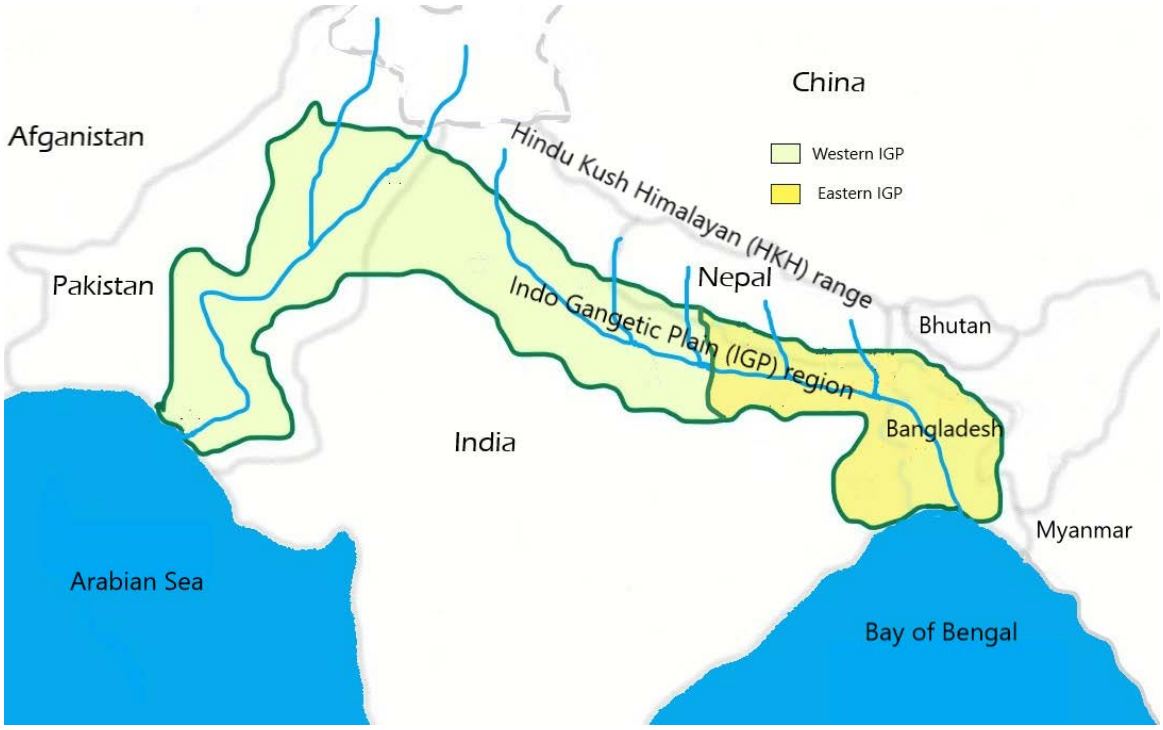

Figure 2: The study area (eastern IGP)

3.0 Study Area:

The Indo Gangetic Plain (IGP) is a fertile alluvium plain area of two neighbouring river basins (the Indus and Ganga) below the foothills of the Hindu Kush Himalaya (Figure 2). The IGP region extends from the delta of the Indus river at the Arabian sea to the delta of the Ganga at the Bay of Bengal (Mani, 1974) and encompasses the eastern plain area of Pakistan, most of northern and eastern India, the southern plain area of Nepal and almost all of Bangladesh (Figure 2). The IGP is one of the most densely populated regions of the world with an average population density of more than 550 people km^{-2}. Moreover, the IGP consists of five mega cities (New Delhi, Karachi, Dhaka, Kolkata, and Lahore) and

dozens of cities with a population of more than 1 million (United Nations, 2015). By considering the biophysical condition and socioeconomic development, the IGP region can be divided into two broad categories: western IGP and eastern IGP (Taneja et al., 2014). The eastern IGP is the study area in this thesis.

The eastern IGP encompasses eastern Utter Pradesh, Bihar and West Bengal of India, Eastern Terai area of Nepal and the plain area of Bangladesh (Figure 2). Apart from the geographical locations, the characteristics of the eastern IGP are distinctly different from the western IGP, with respect to biophysical and socio-economic factors. There is a clear gradient in annual average precipitation in the IGP with 654 mm in Punjab (western IGP) to 1462 mm in West Bengal (eastern IGP) (Erenstein et al., 2007). The climate of the Eastern IGP is hot and sub-humid, the monsoon season (June to September) is the rainy season, and about 85% of total precipitation occurs during this period (Gupta and Seth, 2007). In spite of higher precipitation in the eastern IGP compared to western IGP, the crop productivity in eastern IGP is comparatively less due to a lack of assured irrigation facility, a low level of agricultural input, traditional agricultural techniques and climate extremes (flood and droughts) (Taneja et al., 2014). The major characteristic of the eastern IGP land is the low lying flood prone plain, which is believed to be formed by alluvium deposit brought by the Ganga river system from the Himalayas (Pal et al., 2009). Moreover, the average land holding in eastern IGP is small (only 0.59 ha/household) and less mechanized compared to western IGP (3.55 ha/household) (Balasubramanian et al., 2013). The IGP is considered to be one of the densely populated regions with a clear gradient (ascending) of population density west to east (Erenstein et al., 2007). From the census data of respective countries in 2011, the total population of eastern IGP is more than 360 million with the average population density of 991 people per square kilometre.

4.0 Rationale

Agricultural production from the eastern IGP is important with respect to the livelihood of the farmers within this region and the food security of the wider region. The high level of anthropogenic aerosols in the eastern IGP reduces solar radiation, increases fog events and alters the temperature, which can affect agricultural production significantly. However, there and only a few studies on the effect of aerosols on crop production in this region. There is a lack of systematic study on the effect of atmospheric aerosols on crop production in the IGP. In this context, this study is expected to provide a clear picture of the impact of aerosols on crop production in the eastern IGP. Outputs from this study will

not only help to fill a knowledge gap in this area, but also inform policymakers to prioritize air quality improvement programs in the region for the livelihood of the farmers and food security of the region. In addition to the health benefit of air pollution control in the IGP, this study may provide quantification of likely crop yield benefits of air pollution control in the region. This will help policymakers and stakeholders to justify more investment and adopt clean technologies for air quality improvement in the region. In addition, the study output is also expected to motivate air polluters of unorganized sectors, such as the farmers, and individuals to adopt improved technology to reduce air pollution for their economic benefit to avoid crop yield reduction and improved health. For example, outputs from this study may increase awareness of the importance of minimizing air pollution (through use of improved cook stove, avoid crop residue burning, etc.) to obtain crop yield and health benefits. The regional nature of this study in the eastern IGP, which encompasses the Terai area of Nepal, Bihar and West Bengal states of India and Plain area of Bangladesh, may provide background information for the initiation of a regional program between the three countries to combat air pollution to ensure a healthy environment and food security for the people of this region.

5.0 Framework of this study

High atmospheric aerosols can chemically and physically affect crop production. Among the air pollutants, gaseous pollutants such as O_3, SO_2, NO_2, etc. are highly phytotoxic and directly affect the plant (Saxena and Kulshrestha, 2016). Moreover, pollutants like SO_2 and NO_2 can transform into H_2SO_4 and HNO_3 and causes acid rain (Larssen et al., 2006), which negatively affects plant growth through acidification of soils (Singh and Agrawal, 2008). Since several studies on the effect of ozone on crop production have already been conducted in this region (Ghude et al., 2014; Oksanen et al., 2013; Roy et al., 2009; Singh et al., 2018; Singh and Agrawal, 2017) and acid rain is not a problem in the IGP (Bisht et al., 2014; Kulshrestha et al., 2001), this study focuses on the physical effects of atmospheric aerosols on crop production. The major direct physical effect of atmospheric aerosols on crop production is the reduction of both direct and diffuse radiation available to the plants, which lower crop yield (Burney and Ramanathan, 2014). Apart from the direct physical effect of aerosols through reduction of surface solar radiation, aerosols also indirectly affect crop production through their effect on temperature (both surface and atmosphere) and occurrence of events like fog and cold spells. Hence, in order to

assess the physical effects of aerosols on winter crops in the eastern IGP, research is planned in the following sequence.

a. Fog is an important event affecting winter crops in the IGP. In the context of an increasing trend of fog events in the IGP and a knowledge gap on the trend of fog events in the Nepal component of IGP, a study on fog events in the Terai area of Nepal and its effect on crop production is conducted.
b. The increased frequency and extent of fog events in the IGP region, has also reduced the day time temperature due to blockage of incoming radiation, resulting in extreme cold events in the IGP. To fill a knowledge gap in the Nepal component of the IGP, a study on extreme cold events and their effect on crop production is also conducted. Since there is also a lack of 'ordinary voices' in studies related to air pollution in India (Bhalla et al., 2018), the perception of local farmers on the impact of fog and extreme cold events on their winter crop is also studied in the Nepal component of IGP.
c. Quantification of the reduction in solar radiation due to atmospheric aerosols is important to assess its effect on crop production. To address a lack of a simple method to assess the radiative forcing due to atmospheric aerosols in the IGP, a study is also conducted to develop a simple regression model to estimate daily radiative forcing due to anthropogenic aerosols in the IGP.
d. In the context of high aerosols loading during winter and wheat being an important winter crop in the eastern IGP, the effect of anthropogenic atmospheric aerosols on winter crop (wheat) production in the eastern IGP is estimated by using a calibrated crop simulation model for selected representative districts of eastern IGP in Nepal, India, and Bangladesh.

6.0 Scope of study

The scope of this study is the assessment of the physical effect of atmospheric aerosols on winter crop (wheat) production in the eastern IGP. While considering the physical effects, the reduction of solar radiation due to anthropogenic aerosols is considered in the study. Other physical effects such as the effect of deposited aerosols on crop production is not considered. Similarly, with respect to the winter crops, the major winter cereal crop of the IGP, wheat is considered for this study. In addition, the indirect effect of aerosols on crop production like change in monsoon rainfall pattern, water availability of crops, and cloud cover have not been covered in this study.

7.0 Overview of Chapter

This thesis consists of seven chapters in total. This chapter is the introduction chapter. The second chapter contains a review of the literature concerning the atmospheric aerosols status in the IGP, and the effects of aerosols on various aspects including crop production. In addition, knowledge gaps on the physical effects of aerosols on crop production in this region are identified and the research questions are formulated. Chapters 3-6 describe the research conducted. Each of these chapters has been formulated as a standalone research article as described in the preface. The third chapter includes an investigation into fog events in the Nepal component of IGP and their effect on agriculture. The third chapter is published as "*Shrestha, S., Moore, G.A., Peel, M.C., 2018. Trends in winter fog events in the Terai region of Nepal. Agric. For. Meteorol. 259, 118–130. https://doi.org/10.1016/j.agrformet.2018.04.018*". The fourth chapter presents an investigation into cold spells in the Nepal component of IGP and their effect in agriculture. The forth chapter is submitted as "*Shrestha, S., Peel, M.C., Moore, G.A. Cold waves in Terai region of Nepal and farmer's perception of the effect of fog events and cold waves on agriculture"; s*ubmitted for publication in Theoretical and Applied Climatology on June 6, 2019. The fifth chapter introduces the regression model to estimate daily radiative forcing in the IGP by using remotely sensed AOD and atmospheric water vapor. The fifth chapter is published as "Shrestha, S., Peel, M.C., Moore, G.A., 2018. Development of a Regression Model for Estimating Daily Radiative Forcing Due to Atmospheric Aerosols from Moderate Resolution Imaging Spectrometers (MODIS) Data in the Indo Gangetic Plain (IGP). Atmosphere (Basel). 9, 1–26. https://doi.org/10.3390/atmos9100405". The sixth chapter presents an investigation into the effect of atmospheric aerosols on wheat production in the eastern IGP based upon results of a calibrated crop simulation model at representative districts within Nepal, India and Bangladesh. Lastly, the final chapter, synthesizes the findings of all the chapters and presents the summary and conclusion of this thesis. Moreover, the final chapter also covers the limitations of the study and the areas of future research.

References

Balasubramanian, V., Adhya, T.K., Ladha, J.K., 2013. Enhancing eco-efficiency in the intensive cereal-based systems of the Indo-Gangetic plains, in: Hershey, C.H., Neate, P. (Eds.), Eco-Efficiency: From Vision to Reality (Issues in Tropical Agriculture Series). International Center for Tropical Agriculture, Cali, Colombia, pp. 99–115. https://doi.org/doi:10.1201/b17133-197

Bhalla, N., Boyle, J.O., Haun, D.A.N., 2018. Who Is Responsible for Delhi Air Pollution ? Indian Newspapers ' Framing of Causes and Solutions. Int. J. Commun. 12, 41–64.

Bisht, D.S., Tiwari, S., Srivastava, A.K., Singh, J. V., Singh, B.P., Srivastava, M.K., 2014. High concentration of acidic species in rainwater at Varanasi in the Indo-Gangetic Plains, India. Nat. Hazards 75, 2985–3003. https://doi.org/10.1007/s11069-014-1473-0

Bonasoni, P., Cristofanelli, P., Marinoni, A., Vuillermoz, E., 2012. Atmospheric pollution in the Hindu Kush – Himalaya region. Mt. Res. Dev. 32, 468–479. https://doi.org/10.1659/MRD-JOURNAL-D-12-00066.1

Burney, J., Ramanathan, V., 2014. Recent climate and air pollution impacts on India agriculture. Proc. Natl. Acad. Sci. 111, 16319–16324. https://doi.org/10.1073/pnas.1317275111

Crippa, M., Janssens-maenhout, G., Dentener, F., Guizzardi, D., Sindelarova, K., Muntean, M., Dingenen, R. Van, Granier, C., 2016. Forty years of improvements in European air quality : regional policy-industry interactions with global impacts. Atmos. Chem. Phys 16, 3825–3841. https://doi.org/10.5194/acp-16-3825-2016

Davis, D.L., Bell, M.L., Davis, D.L., Bell, M.L., Bates, D., 2002. A Look Back at the London Smog of 1952 and the Half Century Since A Half Century Later 110, 734–735.

Dey, S., Di Girolamo, L., 2010. A climatology of aerosol optical and microphysical properties over the Indian subcontinent from 9 years (2000–2008) of Multiangle Imaging Spectroradiometer (MISR) data. J. Geophys. Res. 115, D15204. https://doi.org/10.1029/2009JD013395

Dey, S., Tripathi, S.N., 2007. Estimation of aerosol optical properties and radiative effects in the Ganga basin, northern India, during the wintertime. J. Geophys. Res. 112, D03203. https://doi.org/10.1029/2006JD007267

Di Girolamo, L., Bond, T.C., Bramer, D., Diner, D.J., Fettinger, F., Kahn, R.A., Martonchik, J. V., Ramana, M. V., Ramanathan, V., Rasch, P.J., 2004. Analysis of multi-angle Imaging SpectroRadiometer (MISR) aerosol optical depths over greater India during winter 2001-2004. Geophys. Res. Lett. 31, 1–5. https://doi.org/10.1029/2004GL021273

Erenstein, O., Thorpe, W., Singh, J., Varma, A., 2007. Crop–livestock interactions and livelihoods in the Trans-Gangetic Plains, India.

Ericksen, P., Thornton, P., Notenbaert, A., Cramer, L., Jones, P., Herrero, M., Ericksen, P., Thornton, P., Cramer, L., Jones, P., 2012. Mapping hotspots of climate change and food insecurity in the global tropics. Copenhagen, Denmark.

Fenger, J., 2009. Air pollution in the last 50 years - From local to global. Atmos. Environ. 43, 13–22. https://doi.org/10.1016/j.atmosenv.2008.09.061

Gautam, R., Hsu, N.C., Kafatos, M., Tsay, S.C., 2007. Influences of winter haze on fog/low cloud over the Indo-Gangetic plains. J. Geophys. Res. Atmos. 112, 1–11. https://doi.org/10.1029/2005JD007036

Gautam, R., Hsu, N.C., Tsay, S.C., Lau, K.M., Holben, B., Bell, S., Smirnov, A., Li, C., Hansell, R., Ji, Q., Payra, S., Aryal, D., Kayastha, R., Kim, K.M., 2011. Accumulation of aerosols over the Indo-

Gangetic plains and southern slopes of the Himalayas: distribution, properties and radiative effects during the 2009 pre-monsoon season. Atmos. Chem. Phys. 11, 12841–12863. https://doi.org/10.5194/acp-11-12841-2011

Ghude, S.D., Jena, C., Chate, D.M., Beig, G., Pfister, G.G., Kumar, R., Ramanathan, V., 2014. Reductions in India's crop yield due to ozone. Geophys. Res. Lett. 41, 5685–5691. https://doi.org/10.1002/2014GL060930

Gupta, R., Seth, A., 2007. A review of resource conserving technologies for sustainable management of the rice-wheat cropping systems of the Indo-Gangetic plains (IGP). Crop Prot. 26, 436–447. https://doi.org/10.1016/j.cropro.2006.04.030

Health Effects Institute, 2019. State of Global Air 2019. Special Report. Boston, MA.

Kambezidis, H.D., Kaskaoutis, D.G., Kharol, S.K., Moorthy, K.K., Satheesh, S.K., Kalapureddy, M.C.R., Badarinath, K.V.S., Sharma, A.R., Wild, M., 2012. Multi-decadal variation of the net downward shortwave radiation over south Asia: The solar dimming effect. Atmos. Environ. 50, 360–372. https://doi.org/10.1016/j.atmosenv.2011.11.008

Kaskaoutis, D.G., Kumar, S., Sharma, D., Singh, R.P., Kharol, S.K., Sharma, M., Singh, A.K., Singh, S., Singh, A., Singh, D., 2014. Effects of crop residue burning on aerosol properties, plume characteristics, and long-range transport over northern India. J. Geophys. Res. Atmos. 119, 5424–5444. https://doi.org/10.1002/2013JD021357

Kulshrestha, U., Kulshrestha, M.J., Vairamani, R.S.M., Sarkar, A.K., Parashar, D.C., 2001. Investigation of alkaline nature of rain water in India. Water Air Soil Pollut. 131, 1685–1690.

Kumar, M., Parmar, K.S., Kumar, D.B., Mhawish, A., Broday, D.M., Mall, R.K., Banerjee, T., 2018. Long-term aerosol climatology over Indo-Gangetic Plain: Trend, prediction and potential source fields. Atmos. Environ. 180, 37–50. https://doi.org/10.1016/j.atmosenv.2018.02.027

Larssen, T., Lydersen, E., Tang, D., He, Y., Gao, J., Liu, H., Duan, L., Seip, H.M., Vogt, R.D., Mulder, J., Shao, M., Wang, Y., Shang, H., Zhang, X., Solberg, S., Aas, W., Økland, T., Eilertsen, O., Angell, V., Liu, Q., Zhao, D., Xiang, R., Xiao, J., Luo, J., 2006. Acid rain in China. Environ. Sci. Technol. 40, 418–425. https://doi.org/10.1021/es0626133

Li, Z., Lau, W.K.-M., Ramanathan, V., G. Wu, Ding, Y., Manoj, M.G., Liu, J., Qian, Y., J. Li, Zhou, T., Fan, J., Rosenfeld, D., Ming, Y., Wang, Y., Huang0, J., Wang, B., Xu, X., Lee, S.-S., Cribb, M., Zhang, F., Yang, X., Zhao, C., Takemura, T., Wang, K., Xia, X., Yin, Y., Zhang, H., Guo, J., Zhai, P.M., Sugimoto, N., Babu, S.S., Brasseur, G.P., 2016. Aerosol and monsoon climate interactions over Asia. Rev. Geophys. 56, 866–929. https://doi.org/10.1002/2015RG000500

Mahoney, L.E., Bernardino, S., 1976. Air Pollution and Respiratory Mortality in Los Angeles. Environ. Heal. 159–166.

Mani, M.S., 1974. Biogeography of the Indo-Gangetic Plain, in: Mani, M.S. (Ed.), Ecology and Biogeography in India. Springer Netherlands, Dordrecht, pp. 689–697. https://doi.org/10.1007/978-94-010-2331-3_23

Mehta, M., 2015. A study of aerosol optical depth variations over the Indian region using thirteen years (2001–2013) of MODIS and MISR Level 3 data. Atmos. Environ. 109, 161–170.

Menon, S., Koch, D., Beig, G., Sahu, S., Fasullo, J., Orlikowski, D., 2010. Black carbon aerosols and the third polar ice cap. Atmos. Chem. Phys. 10, 4559–4571. https://doi.org/10.5194/acp-10-4559-2010

NASA - Earth Observatory, 2016. Haze over the Indo-Gangetic Plain [WWW Document]. URL https://earthobservatory.nasa.gov/images/87273/haze-over-the-indo-gangetic-plain (accessed 3.3.18).

Oksanen, E., Pandey, V., Pandey, A.K., Keski-saari, S., Kontunen-soppela, S., 2013. Impacts of increasing ozone on Indian plants. Wnvironmental Pollut. 177, 189–200.

Padmakumari, B., Jaswal, A.K., Goswami, B.N., 2013. Decrease in evaporation over the Indian monsoon region: Implication on regional hydrological cycle. Clim. Change 121, 787–799. https://doi.org/10.1007/s10584-013-0957-3

Pal, D.K., Bhattacharyya, T., Srivastava, P., Chandran, P., Ray, S.K., 2009. Soils of the Indo-Gangetic Plains : their historical perspective and management. Curr. Sci. 96, 1193–1202.

Rajput, P., Sarin, M., Sharma, D., Singh, D., 2014. Characteristics and emission budget of carbonaceous species from post-harvest agricultural-waste burning in source region of the Indo-Gangetic Plain Characteristics and emission budget of carbonaceous species from post-harvest agricultural-waste burning i. Tellus B Chem. Phys. Meteorol. 0889, 0–11. https://doi.org/10.3402/tellusb.v66.21026

Ramanathan, V., Chung, C., Kim, D., Bettge, T., Buja, L., Kiehl, J.T., Washington, W.M., Fu, Q., Sikka, D.R., Wild, M., 2005. Atmospheric brown clouds: impacts on South Asian climate and hydrological cycle. Proc. Natl. Acad. Sci. U. S. A. 102, 5326–33. https://doi.org/10.1073/pnas.0500656102

Ramanathan, V., Crutzen, P.J., 2003. New directions: Atmospheric Brown "Clouds." Atmos. Environ. 37, 4033–4035. https://doi.org/10.1016/S1352-2310(03)00536-3

Ramanathan, V., Crutzen, P.J., Lelieveld, J., Mitra, a. P., Althausen, D., Anderson, J., Andreae, M.O., Cantrell, W., Cass, G.R., Chung, C.E., Clarke, a. D., Coakley, J. a., Collins, W.D., Conant, W.C., Dulac, F., Heintzenberg, J., Heymsfield, a. J., Holben, B., Howell, S., Hudson, J., Jayaraman, a., Kiehl, J.T., Krishnamurti, T.N., Lubin, D., McFarquhar, G., Novakov, T., Ogren, J. a., Podgorny, I. a., Prather, K., Priestley, K., Prospero, J.M., Quinn, P.K., Rajeev, K., Rasch, P., Rupert, S., Sadourny, R., Satheesh, S.K., Shaw, G.E., Sheridan, P., Valero, F.P.J., 2001. Indian Ocean Experiment: An integrated analysis of the climate forcing and effects of the great Indo-Asian haze. J. Geophys. Res. 106, 28371. https://doi.org/10.1029/2001JD900133

Ramanathan, V., Ramana, M. V, 2005. Persistent, Widespread, and Strongly Absorbing Haze Over the Himalayan Foothills and the Indo-Gangetic Plains. Pure Appl. Geophys. 162, 1609–1626.

Ramanathan, V., Ramana, M. V, Roberts, G., Kim, D., Corrigan, C., Chung, C., Winker, D., 2007. Warming trends in Asia amplified by brown cloud solar absorption. Nature 448, 575–8. https://doi.org/10.1038/nature06019

Rastogi, N., Singh, A., Sarin, M.M., Singh, D., 2016. Temporal variability of primary and secondary aerosols over northern India: Impact of biomass burning emissions. Atmos. Environ. 125, 396–403. https://doi.org/10.1016/j.atmosenv.2015.06.010

Roy, S.D., Beig, G., Ghude, S.D., 2009. Exposure-plant response of ambient ozone over the tropical Indian region. Atmos. Chem. Phys. 5253–5260.

Saxena, P., Kulshrestha, U., 2016. Biochemical Effects of Air Pollutants on Plants, in: Kulshrestha, U., Saxena, P. (Eds.), Plant Responses to Air Pollution. Springer, pp. 59–70. https://doi.org/10.1007/978-981-10-1201-3

Shi, H., Wang, Y., Chen, J., Huisingh, D., 2016. Preventing smog crises in China and globally. J. Clean. Prod. 112, 1261–1271. https://doi.org/10.1016/j.jclepro.2015.10.068

Shrestha, A.B., Aryal, R., 2011. Climate change in Nepal and its impact on Himalayan glaciers. Reg. Environ. Chang. 11, 65–77. https://doi.org/10.1007/s10113-010-0174-9

Singh, A., Agrawal, M., 2008. Acid rain and its ecological consequences. J Env. Biol. 29, 15:24.

Singh, A.A., Agrawal, S.B., 2017. Tropospheric ozone pollution in India : effects on crop yield and

product quality. Environ. Sci. Pollut. Res. 24, 4367–4382. https://doi.org/10.1007/s11356-016-8178-8

Singh, A.A., Fatima, A., Mishra, A.K., Chaudhary, N., 2018. Assessment of ozone toxicity among 14 Indian wheat cultivars under field conditions : growth and productivity. Env. Monit Assess 190, 1–14.

Srivastava, A.K., Dey, S., Tripathi, S.N., 2012. Aerosol Characteristics over the Indo-Gangetic Basin: Implications to Regional Climate, in: Hayder Abdul-Razzak (Ed.), Atmospheric Aerosols - Regional Characteristics - Chemistry and Physics. InTech, pp. 47–79. https://doi.org/DOI: 10.5772/47782

Srivastava, S.K., Sharma, A.R., Sachdeva, K., 2016. Spatial and Temporal Variability of Fog Over the Indo-Gangetic Plains, India. Int. J. Environ. Ecol. Eng. 10, 1042–1057.

Sullivan, T.J., Driscoll, C.T., Beier, C.M., Burtraw, D., Fernandez, I.J., Galloway, J.N., Gay, D.A., Goodale, C.L., Likens, G.E., Lovett, G.M., Watmough, S.A., 2018. Air pollution success stories in the United States : The value of long-term observations. Environ. Sci. Policy 84, 69–73. https://doi.org/10.1016/j.envsci.2018.02.016

Taneja, G., Pal, B.D., Joshi, P.K., Aggarwal, P.K., N. K., T., 2014. Farmerss Preferences for Climate-Smart Agriculture: An Assessment in the Indo-Gangetic Plain (No. 01337), Discussion Paper. New Delhi. https://doi.org/10.2139/ssrn.2420547

United Nations, 2015. World Urbanization Prospects, 2014 Revisions (ST/ESA/SER.A/366), United Nations. New York. https://doi.org/10.4054/DemRes.2005.12.9

Venkataraman, C., Habib, G., Kadamba, D., Shrivastava, M., Leon, J.F., Crouzille, B., Boucher, O., Streets, D.G., 2006. Emissions from open biomass burning in India: Integrating the inventory approach with high-resolution Moderate Resolution Imaging Spectroradiometer (MODIS) active-fire and land cover data. Global Biogeochem. Cycles 20, 1–12. https://doi.org/10.1029/2005GB002547

Wang, G., Zhang, R., Gomez, M.E., Yang, L., Levy, M., Hu, M., Lin, Y., 2016. Persistent sulfate formation from London Fog to Chinese haze. PNAS 113, 2–7. https://doi.org/10.1073/pnas.1616540113

WHO, 2018. Ambient Air Quality Database, WHO, April 2018 [WWW Document]. URL http://www.who.int/airpollution/en/ (accessed 3.20.19).

Wild, M., Trüssel, B., Ohmura, A., Long, C.N., König-Langlo, G., Dutton, E.G., Tsvetkov, A., 2009. Global dimming and brightening: An update beyond 2000. J. Geophys. Res. 114, D00D13. https://doi.org/10.1029/2008JD011382

Zhao, D., Chen, H., Li, X., Ma, X., 2018. Air pollution and its in fl uential factors in China ' s hot spots. J. Clean. Prod. 185, 619–627. https://doi.org/10.1016/j.jclepro.2018.02.181

Chapter 2

Review of Literature

1.0 Introduction

This chapter presents a literature review of studies on the physical effects of atmospheric aerosols on crop production in the Indo Gangetic Plain (IGP) region. This review covers literature related to atmospheric aerosols in the IGP including their distribution (spatial and temporal), sources and trend. Furthermore, it also incorporates a review of the effects of atmospheric aerosols on human health and natural systems, particularly crop production in the IGP and the methodologies used to assess the effects of atmospheric aerosols on crop production. Following the literature review, gaps in the literature are identified and the research questions for this study are elaborated.

2.0 Atmospheric Aerosols

Atmospheric aerosols are defined as "a collection of airborne solid or liquid particles, with a typical size between 0.01 and 10 micrometre (a millionth of a metre, µm) that reside in the atmosphere for at least several hours" (IPCC, 2007, p. 76). The IPCC definition of atmospheric aerosols is broad enough to also include hydrometeors, which in this study it is important to differentiate aerosols from hydrometeors (cloud droplets, rain droplets, ice/snow particles, etc.). Therefore, in this study atmospheric aerosols are defined as solid and liquid particles suspended in the atmosphere, as defined by the IPCC (2007), but without hydrometeors. Because of the short lifetime of aerosols in the atmosphere (few days), they are also called short-lived climate pollutants (SLCPs)(Burney and Ramanathan, 2014).

Aerosols are classified according to their formation process, source environment, origin, and particle size distribution. Aerosol formation processes are classified as primary or secondary, where primary aerosols are particles directly emitted into the atmosphere and secondary aerosols are not directly emitted particles, but form via condensation in the atmosphere (Boucher, 2015). Aerosols are emitted from different source environments, such as urban, rural, sea, and desert. Aerosols from these sources are termed as urban aerosols, rural aerosols, marine aerosols, desertic aerosols respectively. The origin of aerosols is either natural or anthropogenic. Natural aerosols are aerosols from natural

sources such as sea, desert, soil, vegetation, natural fires, volcano, etc. (Lagzi et al., 2013). Whereas, aerosols emitted from human activities are called anthropogenic aerosols, such as particulate emissions from burning fossil fuel, biofuel, and other fuels. Based on their particle size distribution, aerosols are categorised into three major aerosol classes: aerosols with a radius greater than 0.5 μm; 0.05 μm to 0.5 μm; and less than 0.05 μm, which are called coarse mode, accumulation mode and fine mode aerosols respectively (Boucher, 2015).

Aerosols are also classified with respect to the size of particulate matter (PM) viz. PM10, PM2.5, and PM1. Here the subscript describes the aerodynamic diameter cut-off limit in microns, which is measured in microgram per cubic metre of air. Similarly, aerosols are also often expressed in terms of the concentration of black carbon (BC) in the atmosphere. The BC concentration provides the light-absorbing capacity of the aerosols because it absorbs visible light at all wavelengths (United States Environmental Protection Agency, 2012). Apart from mass concentration, atmospheric aerosols can also be measured in terms of aerosol optical depth (AOD). AOD is defined as the vertical integral through the entire height of the atmosphere of the fraction of incident light either scattered or absorbed by airborne particles (US Climate Change Science Program, 2009). The AOD is dependent upon the wavelength of the radiation, so wavelength should be specified for the AOD. The dependence of AOD on the wavelength of radiation is expressed by the Angstrom Exponent (AE) (Ångström, 1929). As the AE provides information regarding the size of scattering particles, it is widely used as a qualitative indicator of aerosol particle size, AE with values greater than 2 indicate small particles (mainly combustion by-product) and AE less than 1 indicate large particles like sea salts and mineral dust (Schuster et al., 2006).

3.0 Atmospheric aerosols in the IGP

The IGP region is one of the most polluted regions of the world (M. Kumar et al., 2018; Wester et al., 2019). This region consists of a thick layer of absorbing aerosols which are also known as atmospheric brown clouds (Ramanathan and Crutzen, 2003). Atmospheric aerosols from both natural and anthropogenic sources contribute to the atmospheric aerosol loading in the IGP (Singh et al., 2015). In this subsection, the atmospheric aerosols in the IGP are reviewed in terms of AOD and PM. In addition, the sources of aerosols (natural and anthropogenic), temporal distribution (diurnal distribution, seasonal

distribution, past trend, and projected future trend) of atmospheric aerosols in the IGP are also discussed in the following subsections.

3.1 AOD in the IGP

Ground-based observations from the AERosol RObotic NETwork (AERONET), the network of aerosol observatories established under the Aerosols Radiative Forcing over India (ARFINET), and field campaigns, as well as satellite-based observations (MODerate Resolution Imaging Spectroradiometer (MODIS) and Multiangle Imaging Spectro Radiometer (MISR)), clearly show a persistent high AOD loading over the IGP (Aloysius et al., 2008; Giles et al., 2011; Babu et al., 2013; Bibi et al., 2016; Soni et al., 2016; Mehta, 2015; Sen et al., 2017; Kumar et al., 2018). David et al. (2018) also found that the IGP has the highest AOD compared to other regions of India when they simulated AOD over India using the Goddard Earth Observing System (GEOS)-Chem, a global 3-D chemical-transport model using SMOG (Speciated Multi-pOllutant Generator from the Indian Institute of Technology, Bombay) and GEOS-Chem (GC) inventories for 2012. In an analysis of MODIS and MISR data over India during 2001 to 2013, Mehta (2015) found that annual AOD loading was highest in the IGP in all years and two cities in the IGP, New Delhi and Kolkata, were the most polluted cities among the populous cities of India. In brief, the IGP is considered a hotspot for aerosol studies in the region, due to the persistent high aerosol loading in the region (Srivastava et al., 2012a).

In order to understand the geographical distribution of atmospheric aerosols in the IGP, the decadal AOD and Angstrom exponent derived from MODIS Terra Deep Blue satellite data during 2006-2015 for the region are reproduced from Kumar et al. (2018) in Figures 1 and 2 respectively. The area weighted average AOD over the IGP region determined by Kumar et al. (2018) is 0.5 ± 0.25, which is close to the IGP AOD estimated by David et al. (2018) using the Goddard Earth Observing System (GEOS)-Chem 3D chemical transport model. The AOD of the IGP is found to be significantly higher than other parts of the world (4 times that of the global average and 5 times that of North America)(Mao et al., 2014). It is observed in Figure 1 that the AOD of the western IGP is less, except in the densely populated settlements along the Indus. The distribution of Angstrom exponent in the IGP (Figure 2) indicates that atmospheric aerosols in the western IGP are coarse and mixed, which is due to mineral dust from the nearby desert and South West Asia (Sen et al., 2017). Figure 1 also clearly indicates that the central IGP and the Eastern IGP have high AOD (>0.6). The persistence of higher AOD (>0.8) in the eastern IGP (Eastern Uttar Pradesh (UP)

and northern Bihar area) is documented by Kumar et al. (2018) and Sen et al. (2017) and was designated as “the Bihar pollution pool” by Di Girolamo et al. (2004). This persistent high pollution pool overlaps with an area of high population density (Sehgal et al., 2013) and with an area of maximum atmospheric subsidence (Di Girolamo et al., 2004) due to the topography of the area. In addition, the aerosols emitted locally by the combustion of biofuels for domestic cooking, fossil fuels in industries and transport, burning of crop residue as well as aerosols transported by westerly winds are also responsible for the high AODs in the central and eastern IGP (Kumar et al., 2015; Sen et al., 2017; David et al., 2018). The eastern IGP is dominated by fine aerosols (Figure 2), which may be due to the settlement of the transported coarse particles by the westerlies at western and central IGP and local residential and industrial emissions (fine aerosols) from the biomass and fossil fuel combustion (Gautam et al., 2011; M. Kumar et al., 2018). In summary, the majority of area in the IGP has high AOD, with higher AOD values observed over the central and eastern IGP.

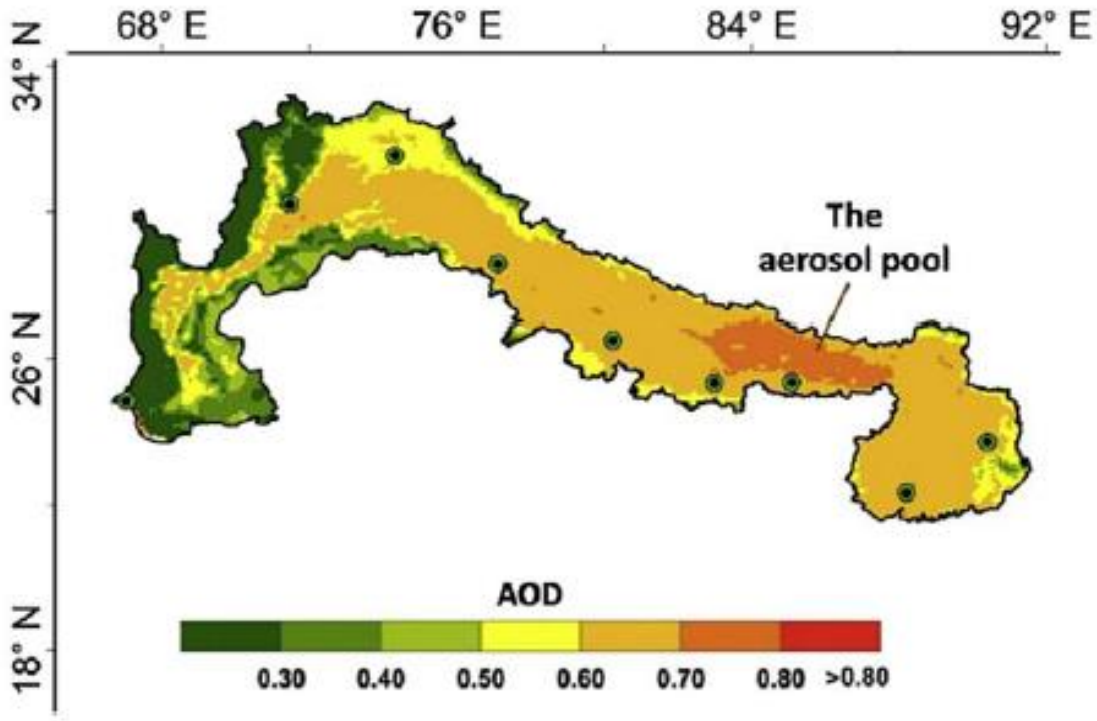

Figure 1: Decadal AOD (2006-2015) of IGP (from M. Kumar et al., 2018)

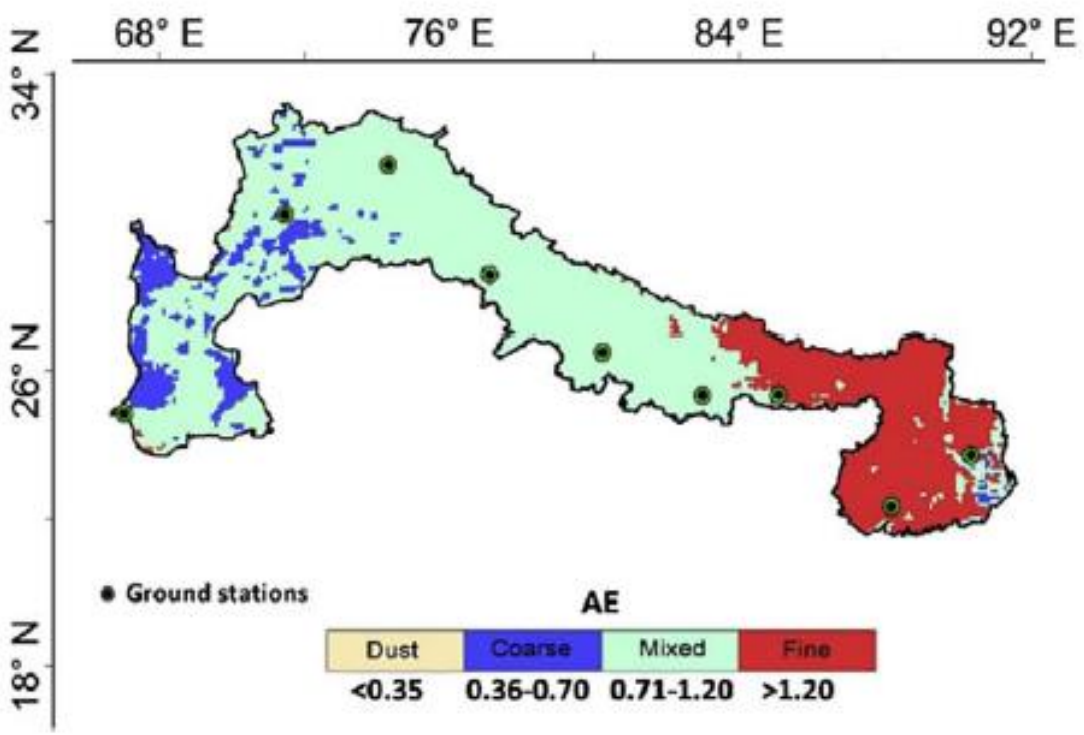

Figure 2: Decadal Angstrom exponent (2006-2015) of IGP (from M. Kumar et al., 2018)

3.2 Particulate Matter in IGP

Particulate matter (PM) is an important indicator of air quality related to human health effects because of the increased risks of myocardial infarction (MI), stroke, arrhythmia, and heart failure exacerbation within hours to days of exposure to aerosols (Brook et al., 2010). PM related indicators are generally described as the mass concentration of the particulates with an aerodynamic diameter less than 10 µm (PM_{10}) or 2.5 µm ($PM_{2.5}$). When considering the health hazard of exposure to PM, the WHO Air Quality guidelines recommend threshold values of $PM_{2.5}$ exposure as 10 μgm^{-3} (annual mean); 25 μgm^{-3} (24 hour mean) and PM_{10} exposure as 20 μgm^{-3} (annual mean); 50 μgm^{-3} (24 hour mean) (WHO, 2006). However, the national ambient air quality standards in all IGP countries (Pakistan, India, Nepal, and Bangladesh) have higher threshold values, by many times those of the WHO thresholds (Wester et al., 2019). For example, in India the threshold values of $PM_{2.5}$ are 40 μgm^{-3} (annual mean); 60 μgm^{-3} (24 hour mean) and PM_{10} are 60 μgm^{-3} (annual mean); 100 μgm^{-3} (24 hour mean) according to their National Ambient Air Quality Standard (NAAQS) (CPCB, 2012). Despite these high threshold values of the Indian Nation standard (NAAQS), the average annual PM_{10} level in all Indian IGP cities with a population > 1 million was at the critical level, defined as the annual mean concentration

of PM_{10} exceeded the NAAQS threshold value by 1.5 times, during 2014-2015 (CPCB, 2015). Bran and Srivastava (2017) used a regional climate model to investigate $PM_{2.5}$ over India and found the Indo Gangetic basin has high $PM_{2.5}$ ranging from 60 to 200 μgm^{-3} throughout the year. Figure 3 shows the annual concentration of $PM_{2.5}$ in the major cities of the IGP based on measured data from the WHO (2018). As illustrated in Figure 3, the recent annual average $PM_{2.5}$ (in 2018) in all cities exceeded the WHO threshold of 10 μgm^{-3} by many times. Among the cities in the IGP, Kanpur, and Faridabad have the highest and the second highest annual average $PM_{2.5}$ with values of 173 and 172 μgm^{-3} respectively (WHO, 2018). North Indian cities in the central IGP have comparatively higher $PM_{2.5}$, which may be due to geographical location, high population, and economic activities. Not only do the cities of the IGP have high PM levels, but also rural areas like Lumbini, in the Terai area of Nepal and Surya village in UP have high levels of PM (Rehman et al., 2011; Rupakheti et al., 2017). In summary, the concentration of particulate matter throughout the IGP exceeds the WHO and national standard by many times, which indicates a critical condition with respect to the impact of aerosols on the heath of people in the region.

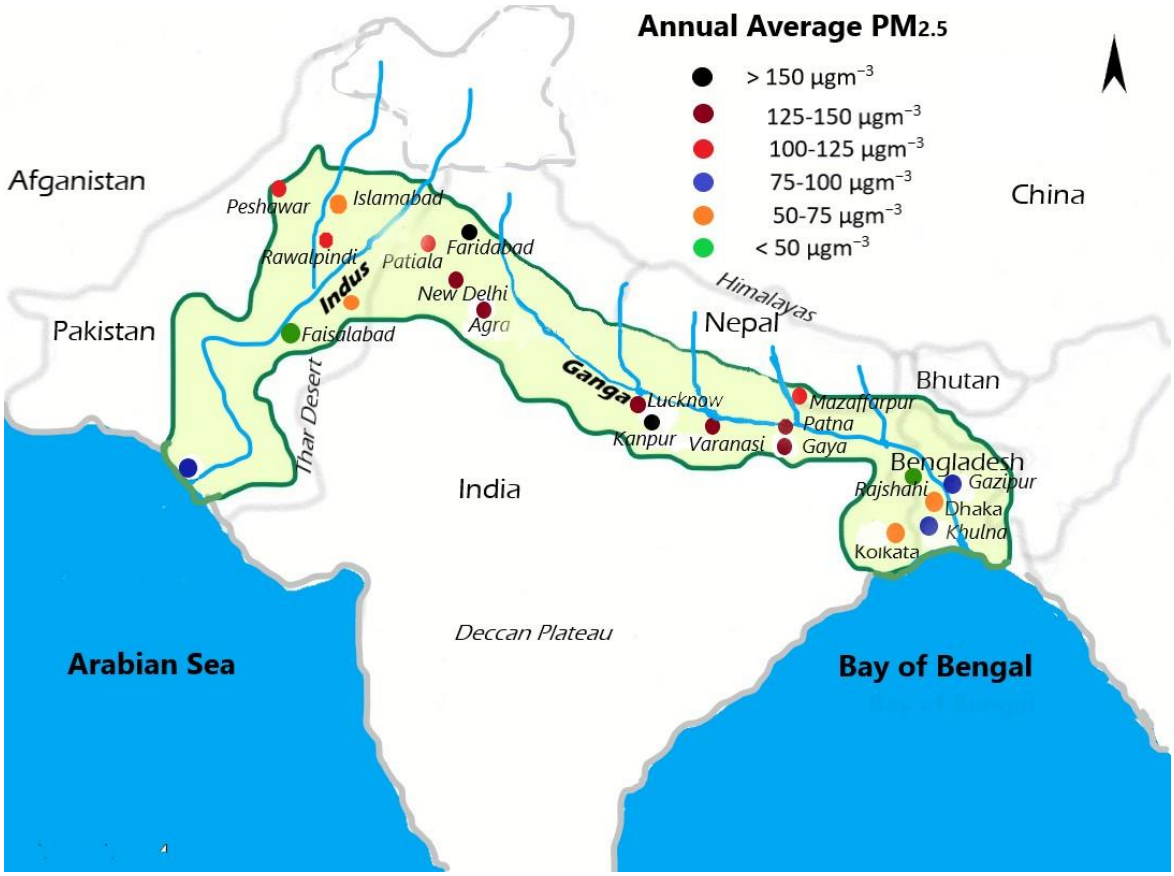

Figure 3: Annual average concentration of PM2.5 in the cities of IGP. Data source WHO (2018)

3.3 Sources of aerosols in IGP

The atmospheric aerosols in the IGP are from both natural and anthropogenic sources. The natural and anthropogenic sources of atmospheric aerosols in the IGP are discussed in following subsections.

3.3.1 Natural sources

Mineral dust from the deserts and sea salts from the ocean are the two important sources of aerosols of natural origin in the IGP and they are discussed in the following paragraphs.

Mineral dust: Mineral dust blown by the wind from the arid and semi-arid regions of the south west region of Asia viz. Iran, Afghanistan, Pakistan, Arabian Peninsula, and Thar desert in north western India is considered an important source of natural aerosols over the IGP region and even over South Asia (Pan et al., 2015). The contribution of dust to AOD_{550} in the IGP is 10% and 14% based on the SMOG (Speciated Multi-pOllutant Generator) and GC (GEOS-Chem) inventories respectively (David et al., 2018), which clearly indicates the significant contribution of mineral dust to the AOD of the region. Moreover, based on the annual data and Positive Matrix Factorization (PMF) analysis, Singh et al. (2016) found that the mineral dust contributed 9% of the total $PM_{<0.95}$ atmospheric aerosols loading in Patiala, a north western city of the IGP. The contribution of mineral dust to the AOD of IGP is mainly concentrated in the pre-monsoon season by the dust transported by the westerly wind and the coarse mode volume concentration is increased by 3 times after dust events (Dey et al., 2004). However, during winter season, the transport of dust is not significant due to low wind speed in the IGP (Prasad et al., 2007).

Sea salt: Sea salt is the next most important natural aerosol after mineral dust in the IGP. By using global aerosol models (GOCART and MOZART), Ramachandran et al. (2015) studied the spatiotemporal characteristics of aerosols in India and found that sea salt contributed to total AOD in the range of 1- 11% (with higher values at sites near the sea) during monsoon months and less than 1% in other months. During the monsoon season, the wind in the Indian ocean is south-westerly and directed from sea to land, which results in a significant contribution of sea-salts to the atmospheric aerosol loads in the IGP (Babu et al., 2013). The AOD of western IGP (Karachi), which is in proximity to the Arabian sea, is also affected by the westerly wind due to the transportation of sea salt during monsoon season (Mansha et al., 2012; Bilal et al., 2016). In Dhaka, a city in proximity to the Bay of Bengal, the sea salt shares 2.1% mass of the total particulate matter in the atmosphere

(Begum et al., 2013). There is a significant share of sea salt in the total particulate matter during monsoon season not only in areas near to the sea, but also at in-land stations like Kanpur and Gandhi College (Srivastava and Ramachandran, 2013). Hence, sea salt is also an important natural aerosol in the IGP with a significant presence during the monsoon season.

3.3.2 Anthropogenic sources

Anthropogenic aerosols are the aerosols emitted from human activities. The major anthropogenic sources of aerosols are the emissions from the combustion of fossil fuels, biofuels and vegetation fires caused by human activities. The increased industrialization and urbanization, as well as a high population density of IGP, has resulted in the increased demand for fossil fuel and at the same time, high reliance of rural communities on traditional solid fuels (fuelwood, dung cake and crop residue) to meet domestic energy demand, which has resulted in the IGP being a hot spot of anthropogenic aerosol emission in south Asia (Tripathi et al., 2006; Kedia et al., 2014b; R. Kumar et al., 2015; Pan et al., 2015; Sen et al., 2017b). It is estimated that the anthropogenic aerosols contributed about 72% on the annual AOD in New Delhi (Srivastava et al., 2012b). By using positive matrix factorization (PMF) model Lodhi et al. (2009), Mansha et al. (2012) and Singh et al. (2016) analysed the source of particulate matter in western IGP cities Lahore, Karachi, and Patiala respectively and all findings showed a strong share of anthropogenic aerosols (at the range of 91 to 95%) in the total particulate matter in those western IGP cities. The major anthropogenic sources of emission in those cities were from biomass combustion, vehicular emissions, power plant emissions, industrial emissions, road dust, etc. The emission from biomass combustion is still important in India because more than 85% of rural households are dependent upon traditional biomass for cooking and space heating in India (Paliwal et al., 2016). In addition to residential emissions from biofuel, the crop residue burning in the open field during October-November has also significantly contributed to the aerosols in the IGP (Sarkar et al., 2018). This is also supported by the findings of Villalobos et al. (2015) and Chakraborty et al. (2015) who indicated that aerosols from biomass combustion are a major contributor of particulate matter in Agra and Kanpur. In addition, the sources of PM in the Eastern IGP city Kolkata and Dhaka are also dominated by anthropogenic sources like road traffic induced dust, industrial emissions, vehicle exhaust and municipal waste incineration, emission from brick kilns, vehicles and biomass combustion (Begum et al., 2013; Das et al., 2015). In summary, the

anthropogenic aerosols from biomass combustion, industrial emission, vehicle emissions, etc. have a strong contribution to the aerosol loading in the IGP.

In order to study the anthropogenic aerosols in the IGP, it is important to understand the major sectors contributing the anthropogenic aerosols in the region. The residential, industrial, transport, power plants, agriculture, etc. are the major sectors of anthropogenic aerosols in the IGP and each of them is discussed separately in the following paragraphs.

Residential Sector: The residential sector is important with respect to contribution in atmospheric aerosols because this sector contributed a major share (15 to >40%) of the surface $PM_{2.5}$ over the major regions of the world including South Asia (Butt et al., 2016). This sector is a leading sector emitting carbonaceous aerosols and the radiative forcing from BC is highest among all sectors even at the global scale (Koch et al., 2007). The emission from the residential sector is mainly from domestic cooking and space heating. The percentage of the population relying on fuelwood and dung cake for domestic cooking and heating in IGP countries Pakistan, India, Nepal, and Bangladesh were 67.1, 68.5, 83.2, and 90.9 respectively (Gwénaëlle Legros et al., 2009). In India alone, 700 million people are still using open biomass *chulha* (traditional cookstove) resulting in health hazard to girls and women due to indoor air pollution (Smith and Sagar, 2014). In addition, India and Bangladesh are ranked as 2nd and 4th among countries emitting the highest carbonaceous cookstove emissions (Lacey and Henze, 2015). Pandey et al., (2014) estimated the $PM_{2.5}$ and BC emission from the residential sector of India from residential cooking as 2580 and 330 Gg y^{-1} for the year 2015. By using regional numerical weather prediction model online-coupled with atmospheric chemistry, Conibear et al., (2018) estimated that the emission of residential emission alone contributes about 70% of $PM_{2.5}$ in the IGP, which is mainly due to the dependence upon the traditional fuels for cooking and space heating. In summary, this sector is not only important due to its high contribution to outdoor atmospheric aerosols but also for its absolute contribution in indoor air pollution in the IGP.

Industrial sector: The Industrial sector emits 32% of BC and is considered to be the second most important sector regarding emission of BC in Asia, after the residential sector (55%) (Zhang et al., 2009). Industrial emission is also recognised as an important source of fine particulate matter with extensive contribution to $PM_{2.5}$ (greater than 30%) in the south Asian countries, Bangladesh (Dhaka, Rajshahi, Chittagong, and Khulna), India (Agra and

Hyderabad) and Pakistan (Karachi and Islamabad) (Singh et al., 2017b). In Karachi, Pakistan Mansha et al. (2012) estimated that industrial emissions (industrial oil burning, smelting, steel industry) contributed up to 53% during 2006-2008**.** In India, the industry sector emissions contribute 22% (198 Gg) of the total emissions in the country and in this sector, brick and sugar production contribute the maximum emissions (37% each), followed by steel production (11%) and cement (8%) (Paliwal et al., 2016). In India, the IGP area is reported as a hotspot with respect to industrial emission due to the majority of brick and sugar industries located in this region (Paliwal et al., 2016). It may be due to the densely situated sugar industries (Lal et al., 2012) and a large number of brick industries in the IGP region of India contributing 85% in total brick production (Singh and Asgher, 2005). Similarly, there are more than 800 coal-fired inefficient brick kilns in operation in Nepal (Climate and Clean Air Coalition Secretariat, 2016). It is estimated that the total emissions from the brick kilns around Dhaka are 23,300 t of $PM_{2.5}$, 15,500 t of sulphur dioxide (SO_2), 302,000 t of carbon monoxide (CO), 6000 t of black carbon, and 1.8 million tons of CO_2 emissions to produce 3.5 billion bricks per year (Guttikunda et al., 2013). Hence due to densely situated industries in the IGP region using fossil fuel and biofuel, industrial emissions make a significant contribution to the aerosol loading in the IGP.

Power sector: Thermal power stations are the major source of electricity generation in the IGP. In India, 68.4% of total electricity is generated from thermal power plants and 57.3% of electricity is produced by the coal-fired thermal power plant (MOP, 2018). Likewise, in Pakistan and Bangladesh, 60.8% and 93.39% of total electricity are produced from thermal power plants (BPDB, 2016; Khan and Ashraf, 2015). By analysing the aerosol parameter derived from Multiangle Imaging Spectro Radiometer (MISR) level 3 data and the locations of thermal power plants in India, Prasad et al. (2006) concluded that thermal power plants are the key point source of air pollution in the Indo Gangetic basin. The total emission from India from the power plants is estimated to be 15.09 Gg $year^{-1}$ (Paliwal et al., 2016). Similarly in India, 111 thermal plants, with an installed capacity of 121 GW, consumed 503 million tons of coal in 2011/12 with estimated emission of 580 ktons of $PM_{2.5}$, 2100 ktons of SO_2, 2000 ktons of NO_x, 1100 ktons of CO, 100 ktons of VOC, and 665 million tons of CO_2 (Guttikunda and Jawahar, 2014). Moreover, very high mean tropospheric NO_2 (up to 14.2 × 1015 molecules cm^2) due to emission from the thermal power plants in specific pockets over India especially over the IGP is also reported (Prasad et al., 2012). Since the majority of the thermal power plants in India are coal-fired, it is the

major source of SO_2 emission in India (Streets et al., 2003). The SO_2 emission is increased by 50% in India since 2007 and the power sector has become the largest emitter of SO_2 mainly from its coal-fired power plants and industries (C. Li et al., 2017). Similarly, in Pakistan, the Industrial sector and power plants contributed 33.3% and 55% of the total SO_2 emission respectively (Shahid et al., 2015). Thus, there is significant contribution of aerosols from the power sector in the IGP due to the high dependence on coal and fossil fuel-fired power plants for electricity in India, Pakistan and Bangladesh.

Transport Sector: Road transport is an important sector with respect to connectivity and regional development in the South Asian region (ESCAP, 2017). Due to increased population, urbanization and more development of infrastructure, the number of road vehicles is increased significantly in South Asia including the IGP (Pandey, 2017). The emissions of $PM_{2.5}$ from the transport sector increased by 1.3 times from 1996 level, which is less than the increase in energy consumption because of the introduction of emission standards Bharat Stage (BS) II in 2005 and BS III in 2010 all over India (Sadavarte and Venkataraman, 2014). Pandey and Venkataraman (2014) estimated that the transportation sector emitted $PM_{2.5}$, BC and OC at the rate of 276, 144 and 99 Gg y^{-1} respectively in the year 2010 in India. They also found that the on-road vehicles are the major emitter of BC and $PM_{2.5}$ in the transportation sector and that old vehicles (pre-2005) contributed about 70% of $PM_{2.5}$ whereas they are only 46% of the vehicle population. Accordingly, in the IGP region the transportation sector is an important sector with respect to $PM_{2.5}$ and BC emissions because it consists of 4 megacities and dozens of cities with populations over a million. For example, the annual emissions of PM_{10} in Karachi from road vehicles are estimated at over 6,100 tons in 2009 and one-third of this is contributed by 2 stroke motorcycle and rickshaws (Sánchez-Triana et al., 2014). The emission from the transportation sector is also affected by government policy and regulations. For example in Dhaka, the contribution of emissions from the vehicles to particulate matter was increased while that to BC decreased in 2007-2009 compared to 2005-2007, which was due to the banning the 2 stroke motorcycles and the increased number of cars and other vehicles (Begum et al., 2013). Not only banning inefficient vehicles (like 2 stroke bikes in Dhaka), appropriate government policy leading towards the improvement of fuel quality, vehicle standard, public transport, vehicle management system can also significantly control emissions from the transport sector in the IGP countries. In summary, the transport sector significantly contributed to the atmospheric

aerosols in the IGP (mainly in the urban areas) and government policy plays an important role in its control.

Open burning of agricultural residue: Burning of biomass (mainly the crop residue of rice and wheat) in the open field has become one of the important sources of atmospheric aerosols in the IGP. In this subsection, the background and the extent of open burning of crop residue in the IGP are discussed and in addition, its contribution to particulate matter and AOD in the IGP is also covered.

Rice and wheat are the major staple food crops sharing more than 80% of total cereal production of the countries in the Indo Gangetic basin viz. Pakistan, India, Nepal, and Bangladesh (Gupta and Seth, 2007). The rice-wheat cropping system is the key cropping system of IGP because rice and wheat are cultivated in more than 13.5 m ha. The attractive benefits of using combine harvesters in rice harvesting, through reduced turnaround time for wheat sowing and cost of cultivation, has led to their increased popularity over the last few decades in the western IGP (Gupta et al., 2004). In Punjab (one of the states of western IGP) 91 and 82% of rice and wheat are harvested by combine harvester (Dhiman and Dhiman, 2015). Moreover, the adoption and the market of combine harvester is reported to be growing at the rate of 28% per annum in India since 2006 (Mehta et al., 2014) and custom hiring service has a major role in the increased use of combine harvester in the western IGP states (Singh, 2015). After harvesting, the combine harvester leaves behind a large volume of loose crop residue in the field, with the resulting difficulty of handling and utilization of crop residue in a short period of time. This situation compels farmers in this region to burn the residue in the field itself to clear the field to sow the following wheat crop (Gupta et al., 2003). The crop residue burning practice is mainly concentrated in the western IGP states of India (Punjab, Haryana and western UP) (Gupta et al., 2004). This may be due to high land holding per household and a high level of mechanization compared to eastern IGP states (Balasubramanian et al., 2013). It is estimated that 74% of rice residues are burned after combine harvesting, whereas only 10% of wheat residue is burned after combine harvesting in the western IGP (Erenstein, 2011). The burning practice of wheat residue is less compared to rice because wheat residue is considered to be valuable and it is used as animal feed. It is reported that 23 million tons of rice residue is burnt annually in the western IGP of India from 15 October to 15 November (NAAS, 2017).

Burning of crop residue generates a significant quantity of atmospheric aerosols in the IGP in that period. Even though the share of annual atmospheric aerosols from crop residue burning is not significantly high compared to the other sources of atmospheric aerosols in Indian sub-continent, its effect is noticed significantly because of the short window of one month (mid-October to mid-November) in which the huge amount (about 24 million tons) of rice straw is burnt in western IGP. From 1 ton of burning rice and wheat residue, about 4 and 12 kg of $PM_{2.5}$ is emitted respectively. Rajput et al. (2014) studied the emission from rice and wheat residue burning from western IGP through field measurements of aerosols and found that atmospheric $PM_{2.5}$ concentration in the study area during rice residue burning season (October and November; n=59), wheat residue burning season (April and May; n=31) and fossil fuel and biofuel emission months (December to March; n=51) are 195± 87, 50±23 and 124±58 respectively. Similarly, the study estimated the total organic carbon emission from rice and wheat residue burning from IGP as 436±68 Gg y^{-1} and 69±2 Gg y^{-1} respectively. Not only the particulate matter, but also a high amount of CO_2, CO, NO_X, SO_2 is emitted in the atmosphere due to burning of crop residue. Badarinath et al. (2009a) estimated that 5504 km^2 of wheat stubble is burnt in the month of May while 12,685 km^2 of rice stubble is burnt in the month of October. The rice and wheat burning have led to the emission of 19.8 and 8.6 Gg of NO_x and 28.3 and 12 Gg of $PM_{2.5}$ respectively. It not only resulted in air pollution but also resulted in nutrient loss viz. 3.85 M ton of organic carbon, 59,000 t of Nitrogen, 20,000 t of Phosphorus and 34,000 t of Potash. (P. Kumar et al., 2015)

By using MODIS data, Vadrevu et al. (2011) studied the crop residue burning and its effect on AOD in Punjab and found that the increase in AOD during winter has well coincided with the fire count during rice residue burning season. Similarly, Mishra and Shibata (2012) analysed and confirmed that the dominance of aerosols due to crop residue burning during October and November in the IGP by using MODIS fire count, MODIS AOD and PARASOL data. The study also revealed that a large concentration of aerosols due to crop residue burning remain below 1 km in altitude. During peak crop residue burning period (15 October to 15 November), a thick smoke/hazy aerosol layer below 2–2.5 km in the atmosphere covering nearly the entire IGP is observed through MODIS images (Kaskaoutis et al., 2014). The emission from the burning of the crop residue is blamed for the increased level of PM level in Delhi and western IGP cities. Moreover, it is observed that there is a strong gradient of AOD in IGP from west to east during peak crop residue burning period (15 October to 15 November) because north westerly wind help to spread

the smoke plume throughout the IGP (Kaskaoutis et al., 2014). The increased crop residue burning in the north western region of India has not only resulted in an increased impact on eastern IGP but also the central and southern India (Sarkar et al., 2018). Hence the emission from the burning crop residue in the western IGP is very important with respect to the effect of atmospheric aerosol in the entire IGP.

3.4 Temporal distribution of atmospheric aerosols in the IGP

The temporal distribution of the atmospheric aerosols is dependent upon sources and sinks of aerosols, interaction of aerosols with the environment and transport of aerosols (Boucher, 2015). For mixing and transportation of the aerosols, the meteorological parameters like wind and temperature play an important role. Since the meteorological parameters, emission from source and removal at sink vary according to daily and seasonal cycles, the temporal distribution of aerosols in the IGP is also expected to vary accordingly. In this context, the diurnal and seasonal distribution of aerosols in IGP is reviewed in the following subsections. In addition, the past historical trend and projected future trend of aerosols in the IGP are also discussed.

3.4.1 Diurnal variation of atmospheric aerosols in the IGP

The diurnal variation of the atmospheric aerosols is dependent upon the extent of emission and timing as well as boundary layer height. The local meteorology controls the diurnal variation of the boundary layer and its understanding is essential for the interpretation of the atmospheric constituents (Bright and Mullen, 2002). The boundary layer is shallow during the night and early morning and it increases as the day progress (Nair et al., 2007). Figure 4 presents the diurnal distribution of BC concentration at indoor (kitchen) and the outdoor (ambient) environment in the month of November at Surya village in the IGP. The outdoor diurnal variation of BC in the Surya village in the IGP followed the similar trend of indoor BC diurnal trend with two peaks one in the morning (05:00 to 08:00 hours) and next in the evening (17:00 to 19:00) following the cooking cycle (Rehman et al., 2011). From the figure, it is also observed that the day time BC outside the cooking hour is less than that in the night time which may be due to shallow boundary layer during the night compared to day time. By using long term (2009-2012) measurements of aerosol BC at Pantnagar (located at western IGP near the Himalayan foothill), Joshi et al. (2016) also found a similar diurnal trend of BC with two peaks, one at the morning and one at the evening. Not only in the rural area, but also in the cities of IGP (Kanpur, Varanasi, and Agra), average diurnal variation of PM_{10} peaked twice a day, once

during the morning (8-10 am) and next during the evening (8-10 pm) (Chitranshi et al., 2015). Tiwari et al. (2016b) also found a similar diurnal distribution of PM_{10} at Patna (a city at eastern IGP) with the first peak in the morning (07:00– 11:00 am) and second in the evening (6:00–9:00 pm) hours. In the rural areas the morning peak is probably due to biomass burning for cooking, whereas in urban areas the peak is probably due to traffic rush hours along with cooking. Similarly, the evening peak in rural areas could be due to biomass combustion for cooking the evening meal, while for urban areas it could be due to emission from traffic, domestic cooking and heating as well as a decreased boundary layer height. Moreover, the average weekdays PM_{10} in New Delhi (urban background site) is found to be about 12% higher than that of a weekend, which is mainly due to vehicular emissions (Suresh Tiwari et al., 2015). In general, diurnal distribution of the atmospheric aerosols in the IGP is bimodal with two peaks one in the evening and one in the morning.

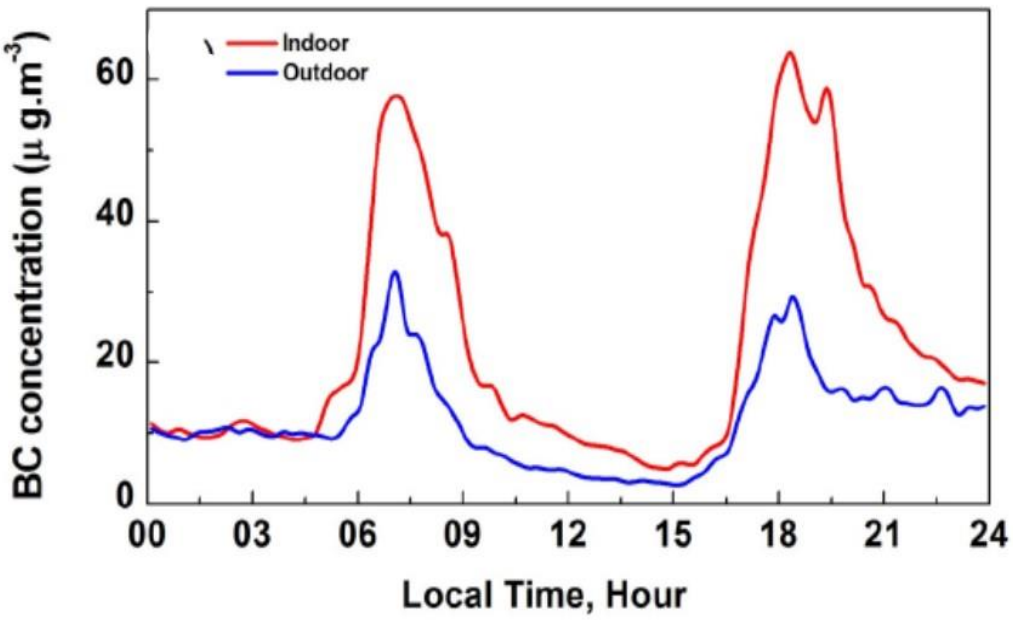

Figure 4: Diurnal variation of BC mass concentration in an indoor kitchen and outdoor ambient at Surya village (adapted from Rehman et al. (2011))

3.4.2 Seasonal distribution of aerosols

Due to the seasonal change of meteorology and emissions, transport and deposition of aerosols, there is a wide seasonal variation of aerosols in IGP. In this subsection, the seasonal variation of AOD and PM in the IGP is discussed. Kumar et al. (2018) found comparatively low average AOD (0.45±0.10) in the IGP during pre-monsoon season

(MAM) with low AE (0.72±0.30). In this season, atmospheric aerosol loads in western IGP is mainly due to dust transported from western Thar desert and west Asian dry region by south westerly winds (Dey et al., 2004; Giles et al., 2011; Singh et al., 2017). This is also supported by the findings of Kumar et al. (2018) which reported the increasing gradient of AE from west to east indicating aerosols with a coarse mode in the west, mixed mode in the central and fine mode in the eastern IGP during the pre-monsoon season. Here the fine mode aerosols in the eastern IGP are due to anthropogenic emission from biomass burning, industries, and vehicular emission. During the post-monsoon season (October, November), average AOD of IGP region is comparatively higher at the range of 0.55±0.20, with fine aerosols in central and eastern IGP and mixed type in western IGP (Kumar et al., 2018). In this season, higher AOD is observed in the central IGP, which may be due to the aerosol build up after monsoon and rice crop residue burning in the Punjab, Haryana and Utter Pradesh (Rastogi et al., 2016). During the monsoon season (JJAS), the average AOD of IGP is 0.54±0.17 and the aerosols in this season are due to the local emission and sea salt from the Indian Ocean in western IGP and from the Bay of Bengal in eastern IGP (Kumar et al., 2018). Heavy precipitation during the summer monsoon naturally reduces the local build-up and long-range transport of aerosol particles in the atmosphere through enhanced removal by wet deposition (UNEP & WMO, 2011). During winter (DJF) the average AOD of the IGP is 0.52±0.20 with the dominance of fine aerosols almost throughout the IGP (except a few patches in western IGP) (Kumar et al., 2018). In summary, there is a distinct regional pattern of aerosols in the IGP in different seasons due to seasonal variation in the emission by different sources and the meteorological parameters for aerosol transportation.

Various literature explained the distinct seasonality in the distribution of PM in the IGP. For example, the average monthly $PM_{2.5}$ in Dhaka (a city at eastern IGP) during 2002-2010 clearly indicated the highest concentration during winter (from December to February) and lowest during the monsoon (from June to August)(Clean Air Asia, 2016). The findings of Pawar et al. (2015) on the PM at Mohali (the western IGP) during 2011-2013 is also in line because their findings showed that in 95% of days during winter and post-monsoon season the 24 hour average $PM_{2.5}$ exceeded 60 μgm^{-3} (NAAQS threshold for 24 hr average), whereas during monsoon season in only 36% of days the daily average $PM_{2.5}$ exceeded the national threshold limit. Similarly at the central IGP city of Kanpur there is a strong seasonal trend of PM, with a factor of two-to-three higher concentrations in the wintertime compared to those in summer season (Ram and Sarin, 2015). Along with $PM_{2.5}$,

the distribution of BC also varies in a similar pattern with high concentration during post-monsoon and winter and minimum during summer (Joshi et al., 2016; Kumar et al., 2015). Since, the major source of emission of PM in IGP during winter is biomass and coal (Singh et al., 2017a), the high level of PM during winter could be due to high emission from crop residue burning, biomass burning in the residential sector (AWC Research Group, 2018) and from coal operated power plants (Guttikunda and Jawahar, 2014). Moreover, the shallow boundary level height and calm wind during winter compared to other seasons has also caused higher $PM_{2.5}$ in IGP during this season (Kumar et al., 2017). The low concentration of PM during monsoon season could be due to scavenging of atmospheric aerosols due to rain. The aerosols are also found to be transported from western to the eastern plain of IGP due to north-westerly winds during the winter and pre-monsoon season (Dey and Di Girolamo, 2010). During the pre-monsoon season, the mineral dust brought by westerly wind is predominant at the western and central IGP (Dey et al., 2004; Giles et al., 2011; Singh et al., 2017). In IGP, there is not only the seasonal variation on PM concentration but also on the variation on the dominance of aerosols types based on the sources. For example, at the central IGP city Kanpur, the aerosol episodes during post-monsoon and winter are found to be related to the anthropogenic emissions whereas those during pre-monsoon consists of significant components of mineral dust (Kaskaoutis et al., 2014). In summary, there is a distinct seasonality in the PM concentration and dominance of particular type of PM in the IGP region caused by seasonality in emission, deposition (both wet and dry), transportation, and boundary level height.

3.4.3 Historical and future projected trend of aerosols

This section presents reviews of studies on historical and future projected trends in atmospheric aerosols based on ground observations as well as satellite data in the IGP. Both the historical trend and future projected trend of aerosols in the IGP are covered in the following subsections.

Historical trend: Before discussing the historical trend of aerosols in the IGP region, it is important to understand the trend of aerosols in the whole Indian sub-continent. In this context, Novakov (2003) estimated historical trends of fossil- fuel BC emissions of India and China from 1875 onward and indicated that the emission trend showed rapid increase in the latter part of the 1800s, a levelling off in the first half of the 1900s, and the re-acceleration in the past 50 years due to increased development activities in China and India. Regarding aerosol trend in this sub-continent after 2000, a study on global AOD

variation and trend using MODIS and MISR during 2001-2014 clearly indicated an increasing trend in economically growing regions of Asia and surrounding oceans, especially the Arabian sea and Bay of Bengal, whereas it is at a decreasing trend over Europe, South and North America (Mehta et al., 2016). That study also illustrated the increasing trend of AOD in India and Pakistan during the winter season and in India and Bangladesh during post-monsoon season mainly due to an increase in anthropogenic aerosols. Provençal et al. (2017) The findings of the study after analysing the AOD in 200 of the world's most populated cities during 2003 to 2015 by using Modern-Era Retrospective Analysis for Research and Application (MERRA) data and found that in contrast to cities in North America, Europe, and Japan, a strong increase in AOD, sulphate and carbonaceous aerosols is observed in most cities of India and Bangladesh. Similarly, Dey and Di Girolamo (2011) studied the trend of AOD in the Indian sub-continent from 2000 to 2010 by using MISR data and found that AOD increased in this sub-continent over that decade. Likewise, Srivastava, (2016) studied the trend of AOD in south Asia during 2001 to 2014 by using MODIS Aqua imagery and found more than 70% of the Indian sub-continent showed a positive trend in AOD. He also found that the annual mean AOD of north and eastern region (Indo Gangetic Basin) has an increasing trend at the rate of 0.1 to 1% per annum. Similarly, Prijith et al. (2018) studied the trends of scattering, absorption and total aerosol optical depth in Indian sub-continent and found very strong positive trends over land regions in November with a trend of AOD greater than 0.01 $year^{-1}$, especially over Indo-Gangetic Plain (IGP). They also concluded that the increase of AOD over IGP in post-monsoon is mainly due to absorbing aerosols, which are increasing at the rate of ~ 0.005 AAOD $year^{-1}$. By using data from 35 aerosol observatories in India during 1986 to 2011, Krishna Moorthy et al. (2013) also found that AOD is increasing at a rate of 2.3% (of its value in 1985) per year and more rapidly (~4%) during 2001-2011. In summary, the historical global and regional trend analysis of aerosols indicate that there is an increasing trend of aerosols in the Indian subcontinent.

Like the AOD trend of Indian sub-continent, AOD trend of entire IGP is also at increasing trend. The AOD of entire IGP derived from MODIS Terra Deep Blue from 2006 to 2015 is increasing at statistically insignificant trend of 0.002 year-1 and the station wise trend of AOD is at increasing trend in all stations of IGP, specifically for the stations in the eastern IGP, the trend is comparatively higher and statistically significant (Kumar et al., 2018). Interestingly in all the 4 stations located in the eastern IGP viz. Varanasi, Patna, Kolkata and Dhaka the AOD trend is statistically significant and strongly increasing at the rate of

0.0174, 0.0206, 0.0200, 0.0181 year^{-1} respectively. In summary, there is an increasing trend of AOD in all the stations in the IGP and more pronounced and stronger increasing trend at the stations in the eastern IGP.

A distinct seasonal trend of AOD over IGP region is also reported in several studies. During the post-monsoon season, the AOD at all the stations in the central and eastern IGP (Delhi, Kanpur, Varanasi, Patna, Kolkata, and Dhaka) showed a statistically significant increasing trend during 2006-2015 (Kumar et al., 2018). That study also showed an increasing trend during winter in all the stations in the IGP, but a statistically significant trend in only 4 stations - Lahore, Patna, Kolkata, and Dhaka. The increasing trend of AOD during post-monsoon and winter season is also reported by Kaskaoutis et al., (2012) and Pandey et al. (2016) at Kanpur and eastern IGP region respectively. The increasing trend of AOD in the IGP is due to increase in anthropogenic aerosols both from fossil fuel and biomass in the region. During the pre-monsoon season, all the stations in the IGP except Multan and Kolkota showed a declining trend of AOD whereas during monsoon no definitive trend is reported (M. Kumar et al., 2018). Pandey et al. (2016) also indicated a slight declining trend of AOD during the pre-monsoon season in the IGP. They also observed the decreased dust loading during pre-monsoon and monsoon season in the north western IGP. Likewise, by using aerosol measurements of multiple satellites during 2000 to 2015, Pandey et al. (2017) also found that the dust loading in the western IGP during pre-monsoon season is decreased by 10 to 20% compared with that of the start of the twenty-first century. The decrease of dust load is also in agreement with the findings of Prijith et al. (2018), which clearly concluded about the decreased trend of AOD in the north western region of India and western IGP during pre-monsoon season. This reduction of atmospheric aerosol during pre-monsoon period is supported by the reduced wind speed and increased pre-monsoon precipitation at the north western part of the Indian subcontinent, which results in increased wet scavenging and reduced erodibility (Pandey et al., 2017). Simulation results of an increasing trend in the contribution of an anthropogenic component and decreasing trend of dust in the Indian subcontinent while simulating AOD over ARFNET stations by using the Goddard Chemistry Aerosol Radiation and Transport (GOCART) model (Babu et al., 2013) also aligns with the seasonal trend of AOD in the IGP. In summary, there is an increasing trend of AOD during post-monsoon and winter due to increased anthropogenic aerosols whereas declining trend in pre-monsoon season with a decline of mineral dust in the western IGP.

Projected Future Trend: Regarding the future projection of AOD in the IGP, Soni et al. (2016) developed an autoregressive integrated moving average (ARIMA) to model the AOD in the IGP by using AERONET and MODIS data during 2001 to 2012 and showed that it is possible to predict the AOD by statistical modelling using time series obtained from past data of MODIS and AERONET as input data. But due to the univariate nature of the model, ARIMA models are not able to provide accuracy in estimation of future values especially during monsoon season (Taneja et al., 2016). Moreover, this model predicts the future trend only based upon the past historical data, while the effect on the future scenario due to policy and technological interventions cannot be represented.

There are some studies on the future scenario of air quality with respect to $PM_{2.5}$ concentration in the IGP. Using Sulphur Transport and dEposition Model (STEM) a regional chemical transport model, Carmichael et al. (2009) simulated the atmospheric aerosols in Asia by 2030 and the scenario shows that an annual increase of $PM_{2.5}$ mass concentration of more than 15 μgm^{-3} over the Ganga valley and eastern China regions. By using the European Monitoring and Evaluation Programme (EMEP) Model, Pommier et al. (2018) showed that on average the $PM_{2.5}$ will increase by 37% for the short term scenario (2030) and 67% for the medium term scenario (2050) in India due to increasing anthropogenic emissions. They also predicted that maximum increment of $PM_{2.5}$ will occur during the post-monsoon season with 117% and 172% increase in the 2030s and 2050s in India. TERI (2016) projected decadal the future emissions (including particulate matter) till 2051 by energy scenario modelling using the MARKet and Allocation (MARKAL) model along with the emission inventory of India and considering future policy and technological interventions. The scenario shows that the total PM_{10} emission reached a peak (almost double the value of that at 2011) by 2031 showing a very alarming situation for air quality. The future scenario of $PM_{2.5}$ in India is also simulated by Chowdhury et al. (2018) by using CMIP5 model with shared socio-economic pathway (SSP) at two scenarios of representative concentration pathways RCP4.5 and RCP8.5 and found that the ambient exposure is expected to peak by 2030 under RCP4.5 and 2040 under RCP8.5 scenario with significant increment of PM in the IGP region. The projected future scenario of atmospheric aerosols shows an alarming scenario in the near future i.e. in 2030s and 2040s. Hence the projected future scenario of aerosols will not only motivate/help to assess the impact of air pollution in the future but also to support/justify the policy and technological intervention to improve the air quality.

4.0 Effect of atmospheric aerosols in the IGP

Atmospheric aerosols have a direct impact on human health, whereas they have both a direct and indirect effect on climate. The effect of atmospheric aerosols on climate due to direct absorbing and scattering of solar radiation is known as a direct effect. When aerosols act as cloud condensation nuclei (CCN) and affect the climate by altering cloud albedo and lifetime, this type of effect is termed an indirect effect (Chung, 2012). Both direct and indirect effects of the atmospheric aerosols on different sectors are discussed in this subsection.

4.1 Effect on public health

Exposure to atmospheric fine particulate matter ($PM_{2.5}$) is one of the major reasons behind premature death globally. Apte et al. (2018) found that exposure to $PM_{2.5}$ has resulted in the reduction of average global life expectancy at birth by about 1 year, with a reduction of 1.2 to 1.9 years in the polluted countries of Asia and Africa respectively. Moreover, exposure to the fine particulate matter ($PM_{2.5}$) has also led to 4.2 million premature deaths and 103.1 million disability-adjusted life years (DALYs) in 2015 (Cohen et al., 2017). Diseases caused by $PM_{2.5}$ exposure include stroke, ischaemic heart disease, acute lower respiratory disease, chronic obstructive pulmonary disease, and lung cancer (WHO, 2015). Among the 10 countries with the highest mortality burden attributable to air pollution in 2017 in the world, 3 IGP countries India (1.2 million), Pakistan (128,000) and Bangladesh (123,000) secured the second, third and fifth positions (Health Effects Institute, 2019). Particulate matter emitted from the major sources viz. residential biomass burning, coal burning, open burning of agricultural residue, brick industries, and the transportation sector contributed 25%, 15.5%, 6.1%, 2.2%, 2.1% of death attributable to particulate matter in India respectively (MAPS Working Group, 2018). By using a high resolution online coupled model Conibear et al., (2018) found that the disease burden due to exposure to $PM_{2.5}$ in the year 2050 will increase by 75% relative to 2015 due to population growth. The map of population-weighted mean concentration across India (MAPS Working Group, 2018) clearly indicates that the mean $PM_{2.5}$ level in the IGP states are more than 85 μgm^{-3}. After a model study on particulate matter sources in India, the AWC Research Group (2018) concluded that PM emissions from residential followed by industry, agriculture, energy sector are responsible for the high premature mortality in the IGP. The atmospheric aerosols in the IGP not only consist of BC and dust but also bioaerosols. The bioaerosols in the IGP consist of microbial (bacterial as well as fungal)

load at the rate of 100-1000 cfu m^{-3} which can transfer epidemic disease in the region (Mamta et al., 2015). Along with the severe effects on physical health, a significant reduction on intelligence is also reported due to cumulative and transitory exposures to air pollution (Chen et al., 2018). In addition to the direct impact of aerosols on health, there may be also several indirect impacts on the health condition of people due to reduction in agricultural production (food security risk), water availability risk and increased risk of a natural disaster like flood and drought in the IGP. In summary, there is a severe health impact on human health in the IGP due to atmospheric fine particulate matter.

4.2 Effect on solar radiation in the IGP

Atmospheric aerosols absorb and scatter incoming solar radiation in the atmosphere and reduce the incidence of solar radiation at the surface of the earth. Due to the high loading of atmospheric aerosols in the IGP, it is expected to have a significant effect on the incoming solar radiation in the region. Here, the effect of atmospheric aerosols on solar radiation is reviewed under the heading of radiative forcing and dimming in the following subsections.

4.2.1 Radiative forcing

The effect of atmospheric aerosols on climate is generally measured in terms of aerosol radiative forcing, which is defined as the effect of anthropogenic aerosols on the radiative fluxes (Chung, 2012). The radiative forcing is estimated at the top of atmosphere (TOA), the bottom of the atmosphere (BOA) and in the atmosphere. Bellouin et al. (2005) estimated the global aerosol direct radiative forcing by using satellite measurements (MODIS) of aerosols. They estimated the global average clear-sky direct radiative forcing as -1.9 ± 0.3 Wm^{-2} at the top of the atmosphere and -4.4 ± 0.6 Wm^{-2} at the bottom of the atmosphere. Ramanathan and Ramana (2005) also studied the direct radiative forcing of atmospheric brown clouds in the Himalayan foothills and Indo Gangetic Plains (IGPs) by using MODIS Terra satellite data from 2001 to 2003 and found the average surface radiative forcing during the dry season (October to May) in the region is about -32 ± 5 Wm^{-2}. Likewise, Dey and Tripathi (2008) studied the direct radiative effect of aerosols in the IGP during 2001 - 2005 by using an aerosol optical model and found the annual average radiative forcing at the surface at Kanpur was -31.8 ± 10.9 Wm^{-2}. Their study also concluded that anthropogenic aerosols contributed 80% of the radiative forcing at Kanpur from October to February. Similar results are also obtained by Ramachandran and Kedia

(2012)'s study on seasonal variation of aerosol radiative forcing at Kanpur and Gandhi college during January 2006 to December 2007 by using AERONET data and SBDART model. Study on the radiative effect of winter haze in the eastern Indo Gangetic Basin through ground measurements and SBDART model showed that the radiative forcing at the BOA during winter months of 2013/14 in Silguri, Kolkata, and Sunderban were -39.3, -70.3 and -38 Wm^{-2} respectively (Das et al., 2015a; Das et al., 2015b). Similarly, the estimation of radiative forcing at the eastern IGP cities Varanasi and Ranchi during February- March 2011 and 2012 were at the range of -30 to -55 Wm^{-2} (Latha et al., 2017). In summary, all the studies indicated a significant radiative forcing impact due to atmospheric aerosols in the IGP.

4.2.2 Surface Dimming

The reduction of surface solar radiation (SSR) due to aerosols in the atmosphere is described as Global Dimming (Stanhill and Cohen, 2001). By analysing the shortwave irradiance around the globe stored in the Global Energy Balance Archive (GEBA) during 1950 to 1990, Gilgen et al. (1998) found that shortwave irradiance is decreasing at more than 2% per decade in the large area of Africa, Asia, Europe, and North America. Similarly, after an extensive review, Wild (2012) found that the majority of the locations in the world global dimming is reported during 1950s- 1980s, but the global dimming is reversed which is termed as global brightening during 1980s -2000 with increase in SSR at the range of 2-8 watt m^{-2} $decade^{-1}$ in most of the locations except India (dimming) where there was still a reduction of SSR at the rate of 8 watt m^{-2} $decade^{-1}$. He also showed the decline of SSR in China/ Mongolia and India (dimming) at the rate of 4 and 10 watt m^{-2} $decade^{-1}$ respectively after 2000 in contrast to increase of SSR (continued brightening) at USA and Europe at the rate of 8 and 3 watt m^{-2} $decade^{-1}$ respectively. He explained the global dimming and brightening phenomena related to anthropogenic atmospheric aerosol emissions, which were governed by economic development and air pollution regulations. Similarly, Alpert et al. (2005) found the dimming is of regional nature with highly populated sites are having a high rate of reduction of solar radiation at 0.41 W $m^{-2}yr^{-1}$ compared to only 0.16 W $m^{-2}yr^{-1}$ for sparsely populated sites (<0.1 million). Moreover, they also found that the dimming rate is also directly related to the areas with industrial activity, clearly indicating the responsibility of anthropogenic aerosols in dimming. Similarly, by using the 20 years dimming phase (1960- 1980) and 15 years (1990-2005) brightening phase of majority area of the globe, Ohmura (2009) found that both aerosol

direct and indirect effects are responsible for changing global solar radiation. In addition, Streets et al. (2006) compared the two decadal rate of decline of global aerosol loading due to emission change at the rate of 0.13% per year with the increase in solar radiation of 0.10% per year during 1983 to 2001 and termed these phenomena as brightening after dimming. Unlike other parts of the world, global dimming remains prominent in India and China even after 2000 with the reduction of SSR at the rate of -10 and -4 W m^{-2}decade $^{-1}$ respectively (Wild, 2009; Wild et al., 2009). Similarly, the analysis of net downward shortwave radiation (NDSWR) over south Asia for the period of 1979-2004 indicated that solar dimming continued in South Asia with a trend of -0.54 W $m^{-2}yr^{-1}$ (Kambezidis et al., 2012). Moreover, after analysis of solar radiation and evaporation trends of 4 metrological stations in India during 1975-1995, Singh et. al (2012) concluded that in all the stations surface diming occurred at the range of 1.5% to 3.4% per decade. By using the SBDART model, Dey and Tripathi, (2007) estimated that about 19% net incoming radiation is reduced by the atmospheric aerosol loading in the Ganga Basin. Similarly, daily sunshine hour data at the plain area of Nepal showed a statistically significant interannual declining trend of monthly total sunshine duration at the rate of -0.56% per annum, which clearly indicates surface dimming also occurring in the Nepal component of IGP (Niroula et al., 2015). Likewise, based upon sunshine duration at 9 stations in Bangladesh during 1961-2006, decreasing annual average sunshine duration at a rate of 0.3 hrs per decade also indicates surface dimming in Bangladesh (Zaman, 2009). After analysis of the monthly mean solar radiation of 12 stations in India during 1981-2004, Kumari et al. (2007) concluded that average dimming in India is occurring at the rate of -0.86 Wm^{-2}. Among the 12 stations, 3 stations are in IGP regions viz. New Delhi, Varanasi, and Kolkata where dimming was occurring at the rate of -1.44, -0.67 and -1.28 Wm^{-2} respectively during 1981-2004. Hence, significant surface dimming is experienced in IGP due to the increasing level of atmospheric aerosols. This continued surface dimming is expected to affect the natural systems in the IGP significantly.

4.3 Effect on evaporation and evapotranspiration

The reduction of solar radiation due to atmospheric aerosols leads to reduced evaporation and evapotranspiration. In this subsection, the effect on the change in evapotranspiration due to surface dimming led by atmospheric aerosols at the global/regional scale and particularly at the IGP region is reviewed.

At the global scale, Liu et.al. (2014) evaluated the atmospheric aerosol's direct radiative effects on the surface heat fluxes of global terrestrial ecosystems during 2003–2010 by using a coupled modelling framework of a terrestrial ecosystem model and an atmospheric radiative transfer model and found that aerosol loadings decreased the mean latent heat flux by 2.4 Wm^{-2} (or evapotranspiration by 28 mm) and sensible heat flux by 16 Wm^{-2} resulting in the increase of global mean soil moisture and water evaporative fraction by 0.5% and 4%, respectively. In Europe and Eastern US region, the results of global offline simulation to study the effects of solar forcing on evapotranspiration and runoff by using Community Land Model (CLM) for the period 1948-2004, showed the reduction of evapotranspiration at 1.5 Wm^{-2} during 1960-90 due to global dimming leading to 5% enhancement of runoff, however during 1990-2004 an increase in evapotranspiration occurred, due to global brightening, which led to a decrease in runoff by 7-10% (Oliveira et al., 2011). The pan evaporation data of 126 stations in China during the second half of the twentieth century also indicated the declining pan evaporation mainly due to the reduction of solar radiation caused by increased level of atmospheric aerosols (Shen et al., 2010). By using satellite radiation measurements and surface radiometer observations, Satheesh and Ramanathan (2000) reported that solar radiation is reduced in the north Indian ocean surface at the range of 12 to 30 Wm^{-2}. The reduced solar radiation resulted in less evaporation from the ocean thereby reducing the moisture inflow to south Asia and weakening the monsoon precipitation (Ramanathan et al., 2005).

The declining trend of evapotranspiration is also observed in the Indian subcontinent. In India, after analysing the solar radiation and evaporation trends of 4 meteorological stations during 1975-1995, Singh et al. (2012) found global dimming at all stations at the rate of 1.5% to 3.4% per decade. Moreover, the results of a wider scale study in India, by analysing pan evaporation data of 58 stations over India during 1971-2010, showed a decreasing trend of pan evaporation at the rate of 9.24 mm per $annum^2$ with a statistically significant confidence level of 99.9% (Padmakumari et al., 2013). The study also concluded that there is a higher decreasing trend in the dry season (October to December and January to May) of -6.16 mm per $annum^2$ compared to the wet season (June to September) of -3.08 mm per $annum^2$. After also analysing the historical wind data in India, Padmakumari et al. (2013) also concluded that along with solar dimming, persistent decreases in surface wind over the Indian sub-continent at the rate of -0.02 $ms^{-1}y^{-1}$ is also responsible for the reduction in evapotranspiration in India. However, after analysing the

trend of reference evapotranspiration and meteorological parameters in China, Zhang et al. (2010) could not find a good relationship between reference evapotranspiration and wind speed in the highly urbanised region of eastern China. Instead of wind speed, they found that declining solar radiation due to aerosols is the main cause behind the declining reference evapotranspiration in those areas. Moreover, at Ranchi a station at south eastern IGP, a study to assess the effect of aerosols on evapotranspiration through observations showed the role of atmospheric aerosols because the atmospheric aerosol radiative forcing (ARF) reduced latent heat (LE) and sensible heat (H) fluxes by 14% and 16% respectively (Murthy et al., 2014). In summary, the reduction of evapotranspiration occurs in the IGP because of surface dimming caused by high atmospheric aerosol loading in the IGP. The reduced evapotranspiration caused by increased atmospheric aerosols may change (increase) soil moisture as suggested by Robock and Li (2006) and may also increase the flow of Indus and Ganga as shown by Gedney et al. 2014 in the runoff of rivers in the northern hemisphere.

4.4 Effect on Monsoon Precipitation

Monsoon precipitation is very important for agriculture production in the IGP because the summer monsoon provides 75-90% of the total precipitation. The atmospheric aerosols affect precipitation by the direct microphysical effect of cloud condensation nuclei (CCN) and the radiative effect (direct and cloud-mediated) on the atmospheric cycle (Rosenfeld et al., 2008). The anthropogenic aerosols Indian Ocean Experiment (INDOEX) documented the Indo Asian haze and analysed the effect of absorbing aerosols on the monsoon and found that it decreased the solar radiation by an amount comparable to 50% of the total ocean heat flux and nearly doubled the lower tropospheric solar heating (V. Ramanathan et al., 2001). In addition, Ramanathan et al. (2001) also found that the anthropogenic aerosols heat the atmosphere, change the atmospheric temperature structure, suppress rainfall and affect the hydrological cycle. A thick layer of anthropogenic aerosols was noticed over the IGP by Ramanathan and Crutzen (2003) and they termed it as ‘atmospheric brown cloud (ABC)’ and the ABC reduced the solar radiation flux by about 20% during the dry season in the IGP (October to May) (Ramanathan and Ramana, 2005). This reduction of solar radiation (dimming) in the IGP weakens the land-sea temperature gradient and results in shifting of the Asian monsoon circulation southward and decreases its intensity (Ramanathan et al., 2005). Likewise, Gautam et al. (2009) also recognized that the high loading of the aerosols in the IGP during pre-monsoon season affect the land-sea

thermal gradient which is one of the most important drivers in the Indian monsoon which drives the circulation pattern between the equatorial Indian Ocean and the Indian sub-continent. However, by using the elevated heat pump (EHP) hypothesis, Lau and Kim (2006) and Meehl et al. (2008) indicated that increased loading of aerosols in the IGP in pre-monsoon season is responsible for increased heating of the upper troposphere with the formation of upper-level warm core anticyclone over the Tibetan Plateau in April to May, resulting in the advance of the monsoon in northern India and subsequent increase of rainfall in the Indian sub-continent. Regarding the effect of atmospheric aerosols on the monsoon precipitations, Tao et al. (2012) made a comprehensive review of aerosol-cloud-precipitation interactions with analysis of theories, models, and limitations. Similarly, Li et al. (2016) also performed an extensive review of studies on Asian monsoon, aerosols, and their interactions and explained the aerosol's effect on Asian monsoon at both continental as well as local scale. In spite of different school of thoughts on the effect of atmospheric aerosols on the Indian monsoon, it is widely recognised that atmospheric aerosols play an important role in the monsoon in the south Asian region. In return, the monsoon transitions also significantly affect the level of atmospheric aerosols in the Indian sub-continent; for example, the high aerosol radiative forcing in the region is resulted by the arrival of dry monsoon (Corrigan et al., 2006).

4.5 Effect on Fog in IGP

In this subsection, the relation between atmospheric aerosols and fog occurrence, coverage of fog, its frequency and trend, and its impact in the IGP are reviewed.

Fog is defined as a suspension of very small, usually microscopic, water droplets in the air that reduce visibility to less than 1000 m at the surface of Earth (WMO, 1975). Apart from the negative correlation between the visibility and atmospheric aerosol concentration (Tiwari et al., 2011), the occurrence of fog is also directly related with the concentration of atmospheric aerosols due to the contribution of aerosol as cloud condensation nuclei (CCN) in fog formation. By using MODIS images and ground data, Gautam et al. (2007) showed that wide areas of IGP spreading from Pakistan at the west to Bangladesh is engulfed by fog/low cloud during winter (December & January) and also indicated that the fine mode aerosols which form haze during the winter months are coupled significantly to the widespread occurrence of fog events over the IGP. Likewise, the cloud-aerosol lidar and infrared pathfinder satellite observation (CALIPSO) observation also showed that thick layers of fog/aerosols up to above the northern/central Indian region

with a thickness ranging from 1.5 to 3 km (K. V S Badarinath et al., 2009). Yasmeen et al. (2012) studied the fog events of Punjab and Sindh region of Pakistan during 2000-2010 and reported that higher aerosol loading during winter, mainly due to biomass burning in IGP during October to November, has amplified the fog frequency/duration under favourable meteorological conditions. The entire IGP area of Punjab, Haryana, Delhi, Uttar Pradesh, Bihar, and West Bengal area can be engulfed by dense fog during winter (Badarinath, Kharol, Sharma, & Roy, 2009; Jenamani, 2012; Syed, Körnich, & Tjernström, 2012; Sathiyamoorthy, Arya, & Kishtawal, 2016).

By analysing the fog events recorded at Hisar from 1992/3 to 2007/8, Singh and Singh (2010) indicated that the occurrence of fog events is increasing at the rate of 2 days per season. After analysis of the visibility data of 82 stations in the IGP across India, Pakistan, and Bangladesh during 1976–2010, Syed et al. (2012) reported that the fog frequency increased by 3 times during the last 35 years. Syed, Körnich, & Tjernström (2012) suggested that along with the atmospheric aerosols, the moisture available from the western disturbances and from vast irrigated agricultural land in western IGP region could be the reason behind the high fog frequency in the region. Srivastava et al. (2016) analysed the trend of winter fog over IGP during 1971-2015 and found that fog frequency has increased by 118.4% during the winter months of December and January. The study also found the spatial variation of foggy frequency in the IGP with 66.29%, 41.94% and 33.06% average fog days at central IGP, western IGP, and eastern IGP respectively. The study indicated that increased anthropogenic aerosol level in the IGP is the possible reason behind the alarming rate of increase in fog frequency in the region. Along with the increased occurrence of fog in the IGP, Gautam and Singh (2018) also found that highest frequency and largest extent of fog holes (holes in fog) over Delhi indicating the effect of urban heat impact on fog. In summary, the high level of anthropogenic atmospheric aerosols is one of the important reasons behind the high coverage of fog as well as increased fog frequency in the IGP.

An increasing trend on the occurrence of dense fog events during winter months in the IGP has affected the life of people and the environment in many ways. For example, it has affected the day-to-day life of millions of people living in this region, by frequent flight/train delay due to poor visibility (Jenamani, 2007). Along with the serious impact on air and surface transportation, fog events also cause more risks to health. The air quality is worsened during foggy days because a study conducted at Agra (a city at western IGP) indicated that the air quality exceeded by 3.2 and 2.2 times of air quality standard of India

during foggy days and non-foggy days respectively (Agarwal et al., 2017). The study also found that the hazard index (HI) and Incremental Lifetime Cancer Risk (ILCR) was 1.4 and 1.2 times more in foggy period than a non-foggy period. Moreover, the aerosol size distribution is also changed due to the fog events (Das et al., 2008). After analysing the gaseous and aerosols pollutants during clear and fog episodes in Lahore, Pakistan, Biswas et al. (2008) found that fog influenced the process of formation of particulates SO_4 from SO_2 resulting in more $PM_{2.5}$ in the atmosphere. Moreover, after analysis of aerosol optical properties during wintertime in Delhi, Tiwari et al. (2015) found that the mass concentration of $PM_{2.5}$ and BC is substantially (~1.8 times) higher during foggy days compared to clear days. Similarly, Das et al. (2015b) also found that compared to non-foggy days in the Sundarban, the AOD is increased by almost a factor of 3 and atmospheric black carbon concentration was increased by 30% during foggy days. The increased aerosol level during foggy season further deteriorate the air quality and affect the health of people living in the IGP. Along with the effects of aerosols on transportation and health, fog also affects the natural system of IGP due to its effect on solar radiation. Sathiyamoorthy et al. (2016) studied the radiative forcing of fog in IGP during 2001 to 2008 by using monthly International Satellite Cloud Climatology Project (ISCCP-D2) cloud data and found that a 10 Wm^{-2} decrease in net cloud radiative forcing decreases the surface temperature by 0.6 ^{o}C over the IGP, which indicates colder foggy winters than non-foggy winters. This is also supported by the observations made by Poulton et al. (2011) on the reduction of solar radiation by 9 to 15 $MJm^{-2}day^{-1}$ and maximum reduction of daily temperature by up 10 $^{\circ}C$ during fog events during early January 2006 at Dinajpur, Jessore, and Patuakhali of Bangladesh. Due to the increased fog events, the growth and development of wheat crop in north India are adversely affected due to reduced photo-synthetically active radiation (PAR) available for photosynthesis, cold stress and favourable condition for disease and insect pest development (Singh and Singh, 2010). Hence, the increasing trend on the occurrence of dense fog events during winter in the IGP have a significant effect on the people and environment of IGP by deteriorating the air quality, transportation schedule, and crop production during winter.

4.6 Effect on cold events

The reduction of solar radiation at the surface of the IGP due to persistent high level of anthropogenic aerosols and fog events during winter is expected to reduce the temperature which may affect the occurrence of extreme cold events. In this context, the

review on the extreme cold events in the IGP and its possible linkage with the atmospheric aerosols is discussed in this subsection.

A cold wave is a regular event occurring during winter in the northern region of Indian sub-continent. After analysis of daily temperature data of 103 stations in India during 1961-2010, Pai, Srivastava, & Nair (2017) concluded that cold wave is a regular phenomena of most areas of India, except southern Peninsula and north-east India. Likewise, after analysing the extreme weather events of India during 1978 to 2006, Singh and Patwardhan (2012) reported that cold wave is the 4th topmost important event with respect to impact (mortality) in that period. Among the extreme cold waves, cold wave during 1st week to 3rd week of January 2003 is reported as one of the severe events affecting the northern states of India with more than 900 reported cases of death out of which 813 were from Uttar Pradesh alone (De, U. S., Dube & Rao, 2005). Pai, Thapliyal, & Kokate (2004) studied the cold wave conditions of meteorological sub-divisions of India during 1971 to 2000 and found a significant increase in the frequency, persistence and spatial coverage of cold wave events in the decade 1991-2000 compared to the previous two decades. Similarly, Mahdi & Dhekale (2016) studied the cold wave situation of southern Bihar by analysing the temperature during 1969 to 2013 and found that January, February, and December are the months with higher cold events with the average duration of 3.98, 3.5 and 3 consecutive days respectively in southern Bihar. In contrast to the findings of Pai, Thapliyal, & Kokate (2004), this study indicated a declining trend of cold wave in the study area. Moreover, Revadekar et al. (2012) studied Indian weather extremes by using data from 121 temperature stations during 1970 to 2003 and found that 75% of stations showed declining trend on the number of cold events. These studies adopted the Indian Meteorological Department (IMD)'s definition of cold wave, which only considered minimum temperature. In contrast to the aforementioned studies, Dash and Mamgain (2011) studied the extreme events of Indian stations by analysing the daily maximum and minimum temperature during 1969-2005 and found a significant increase of cold days in winter in northern India (Indian component of IGP region). This increase of cold days in the IGP during winter months could be due to the reduction of maximum temperature led by increased fog events in the IGP region. This justification is supported by the observations made by Samra et al. (2003) on the below normal maximum temperature during foggy days and on prolonged foggy days bringing cold events. Moreover, Gautam (2014) explained that the cold events with moist air and atmospheric aerosols help the formation of fog and the dense fog, which also reduces the solar

insolation, results in low temperature and providing positive feedback to the persistence of foggy and cold conditions. Foggy winter is colder than non-foggy winter in the IGP and the cooling of the entire IGP occurs at a rate of -0.6˚C with every 10 Wm^{-2} increase in radiative forcing due to fog (Sathiyamoorthy et al., 2016). After a western disturbance, fog is normally observed due to ground cooling at night and the fog blocks solar radiation and further reduces the temperature to make the cold event more intense (Bedekar et al., 1974). Hence, the reviewed literature indicates a linkage between extreme cold events and fog events in the IGP.

4.7 Effect on glacial retreat

The air quality of the Hindu Kush Himalayan (HKH) region, the third most glaciated region on Earth after the Arctic and Antarctic, has worsened over the past two decades due to the nearby IGP region, which is recognised as one of the most polluted regions of the world (Wester et al., 2019). The HKH region consists of more than 54,000 glaciers covering a total area of more than 60,000 km^2 (Shrestha et al., 2015). Glaciers are regarded as a sensitive indicator of climate change and these glaciers are the source of water for more than billions of people living in the region. In this context, the review on the effect of atmospheric aerosols on glacial retreat in the HKH region is covered in this subsection.

Glacial retreat and loss of glacier mass has been observed since the mid-19^{th} century in this region (Shrestha et al., 2015). For example during 2003 and 2009, the Himalayan glaciers lost about 174 gigatons of water (Gardner et al., 2013). Favourable meteorological conditions coupled with the high emission of atmospheric aerosols in the IGP favour the increasing level of the atmospheric aerosols in the Himalayan region (Bonasoni et al., 2012). Highest seasonal black carbon (316.9 ngm^{-3}) and coarse particles/dust (0.37 cm^{-3}) were measured at Nepal Climate Observatory – Pyramid (NCO-P) located at 5079 m.a.s.l. on the southern foothills of Mt. Everest region in the pre-monsoon season, which indicates that the atmospheric brown cloud (ABC) has also affected the pristine atmospheric composition of the Himalayan region (Bonasoni et al., 2010). Lau and Kim (2006) proposed and explained the 'Elevated Heat Pump' (EHP) effect as being caused by a high level of absorbing aerosols (black carbon and dust) in the IGP in late spring and early summer that could lead to the heating the upper troposphere, which further transport of aerosols from the IGP to the southern slopes of the Himalaya and Tibetan plateau causing early and accelerated melting of Himalayan snow packs via aerosol-induced atmosphere-land surface feedback. The transported absorbing aerosols due to

the EHP effect results in heating of the atmosphere, as well as aerosol deposition on the snow, causes darkening of snow (reduction of snow albedo)(Lau et al., 2010; Xu et al., 2016). The deposition of black carbon over the southern Himalayan range during the pre-monsoon season is estimated to be in the range of 900-1300 microgram per sq. m. By using the atmospheric black carbon loading at Nepal Climate Observation-Pyramid (NCO-P) at 5079 m.a.s.l. in the Himalayan region, Yasunari et al. (2010) estimated that the reduction of snow albedo by 2 to 5.2% resulted in the corresponding 10 to 30% increase of annual runoff from a typical glacier of the Tibetan region. Aerosol/dust cover of 400 g m^{-2} of thickness about 2 mm has the maximum effect on the melting of glaciers in the Indian region of Himalaya and this impact is maximum in the north facing glaciers in the month of September (Raina, 2009). From 1990 to 2000, the snow/ice cover over the Himalayan region is said to have reduced by 0.9% and the contribution of BC in this decline is estimated to be 36% (Menon et al., 2010)**.** Similarly, Ménégoz et al. (2014) used climate – chemistry global model to study the BC deposition on snow in the Himalayan region during 1998 to 2008 and found that BC deposited on mountains decreases the snow cover duration by 1-8 days per year. After analysing 30 years atmospheric temperature data acquired from ultra-sonic sounding technique (from 1979 to 2008), the warming trend of the western Himalaya is significant for 6 months (December to May) at the rate of 0.016 ± 0.005 deg K $year^{-1}$, whereas for the other 6 months (June to November) it is cooling at the rate of 0.068 ± 0.033 deg K $year^{-1}$. The reverse trend during the month of June to November is due to aerosol loading in these Himalayan regions (Prasad et al., 2009).

Glacial retreat directly effects the natural system through alteration in water supply, flow pattern and availability of water for agriculture and ecosystem. Glacial retreat also increases the risk of Glacial Lake Outburst Flood (GLOF) events and avalanches (Chen et al., 2013). The GLOF is one of the major impacts of climate change in the Himalayan region and 35 GLOF events have been documented in the recent past in the Himalayan region (5 in Bhutan, 16 in China, 14 in Nepal) causing considerable loss of life and property (Shrestha et al., 2015). Widespread deglaciation evident in the Himalayan region has a direct effect on stream discharge of rivers in Nepal and India, especially in dry season and it will affect the water resource of the whole region itself (Shrestha and Aryal, 2011). Hence, the glacial retreat affects the sustainability of the whole region and livelihood of the billions of people in this part of the world.

4.8 Physical effects on crop production

The physical effects of atmospheric aerosols on crop production include the physical effect of the reduction of solar radiation due to atmospheric aerosols (dimming) and the deposited aerosols on the leaves and are reviewed in the following subsections.

4.8.1 Effect of dimming

High loading of atmospheric aerosols in the IGP results in significant reduction of solar radiation (dimming) in the IGP. As the main energy input for crop production is solar radiation (Monteith, 1977), the dimming in IGP is expected to affect crop production. Crop production in the IGP, a food basket of the region, is not only important with respect to the food security of South Asia, but also the livelihood of the people living in the region. In this context, the effect of dimming on crop production in highly polluted regions of the world, including the IGP region, is reviewed in this subsection.

Due to the increasing level of anthropogenic aerosols in the atmosphere, widespread decrease in solar radiation (dimming) during the second half of the twentieth century occurred throughout the globe (Wild, 2009). Unlike other parts of the world, the dimming continued in China and India after 2000 (Wild, 2009). A crop response simulation model has shown a 1:1 relationship between the increase (decrease) in solar irradiance and increase (decrease) in rice and wheat yield in China and estimated that a 5 to 30% reduction in wheat and rice yield occurred in China during 1979-1990 due to atmospheric aerosols and regional haze (Chameides et. al. 1999). A statistical model of historical rice harvest in India coupled with a regional climate scenario indicated that due to an increased brown cloud and greenhouse gas there has been a slowdown in harvest growth in last two decades (Auffhammer et al., 2006). Similarly, it is also reported that the combined effect of climate change and short-lived climate pollutants (SLCPs) from 1980 to 2010 have reduced the wheat yield up to 36% in India (Burney and Ramanathan, 2014). In order to study the effect of atmospheric aerosols on crop production, Latha et al. (2017) used the SBDART model to obtain the reduction of solar radiation due to atmospheric aerosols at two locations in the IGP, Varanasi and Ranchi, and found that the incoming radiation was reduced by about 5% due to black carbon (BC) at Varanasi and 4% at Ranchi. Furthermore, by using the empirical model developed by Ahmed and Hassan (2011), they estimated the loss of −149 kg/ha and −141 kg/ha wheat grain yield at Varanasi and Ranchi respectively due to the reduction in solar radiation caused by absorbing aerosols. Apart from dimming, the growth and development of wheat crop in north India is adversely

affected due to reduced or no PAR (photosynthetic active radiation) available for photosynthesis, cold stress and congenial condition for disease and insect pest development due to increasing fog events in the region (Singh and Singh, 2010). In summary, the reviewed studies indicate that there is a significant effect of atmospheric aerosols on crop production in India. While considering a high level of atmospheric aerosols in the IGP in the present context, the review also indicates the need for a comprehensive study on the effect of atmospheric aerosols on crop production in this region.

It is also necessary to review the studies on the effect of atmospheric aerosols on crop production in other polluted regions like the IGP to understand the extent of effect and the methodology adopted for their assessment. Cohan et al. 2002 used the Norman (Norman and Hesketh, 1980) and MAESTRA (Wang and Jarvis, 1990) models to estimate the effect on net primary productivity (NPP) of crop due to aerosols in the mid-latitudes and concluded that both total and diffuse PAR should be considered and also found that the response is sensitive to cloudiness of the site. They also found that in clear-sky conditions, the presence of aerosol enhances NPP whereas in a cloudy condition the aerosol reduces the NPP. Bergin (2004) studied aerosol loading and its effect on PAR reaching the surface of the Yangtze Delta agricultural region in China by using the coupled atmospheric radiative transfer crop model (described by Greenwald et al., 2006) and found that there is 15-20% reduction of PAR similar to the findings of Xu et al., (2003). Furthermore, they estimated about 10% reduction in rice production due to a decrease in PAR due to anthropogenic aerosols. Greenwald et al. 2006 used the modified crop environment resource synthesis (CERES) crop model to study the influence of aerosol on rice, wheat and maize production under various atmospheric conditions. For the most realistic set of model results based on location-specific aerosol loadings and crop-specific assumptions of radiation use efficiency (RUE) change, they found that, the influence of aerosols is estimated to be 10% on maize yield, ±5% on wheat yield, and ±10% on rice yield except for when grown under exceptionally sunny conditions as found in California central valley, in which case, yields are predicted to increase by up to 30%. In addition, aerosols also tend to decrease plant water stress by reducing soil evaporation and transpiration and when crops are grown under rainfed conditions, this reduction in water loss from evapotranspiration may offset the decrease in the photosynthetic rate and cause aerosols to have a positive influence on final grain yields. In these CERES models, the impact on direct and diffused light of the atmospheric aerosols is considered. Wild et

al. (2012) reviewed the agricultural implications of global dimming and brightening and concluded that the effect of increased diffused radiation on the crop productivity depends largely upon the crop canopy structure of crop viz. the tall trees are benefitted by global dimming whereas short grasses are less benefitted due to less enhanced diffused fraction of PAR. Not only the modified CERES crop model, but also the Agricultural Production Systems Simulator (APSIM) is also used to assess the effect of atmospheric aerosols on crop production. For example, Yang et al. (2013) evaluated the impact of 'global dimming' and climate change on wheat yield and water use in three regions of China (Beijing, Chengdu and Urumqi) during the past four decades using APSIM and found that crop production in low solar radiation environment (Chengdu 7.85 MJm^{-2} during wheat growing season) is significantly decreased (by 32%) during the past 42 years due to dimming. Likewise, APSIM model was also used by Liu et al. (2016) and Xiao and Tao (2014) to assess the effect of aerosols on wheat and maize production in the North China Plain. In summary, a significant loss resulted due to atmospheric aerosols in the polluted area and the crop model is an effective tool to assess the effect of atmospheric aerosols on crop production.

Statistical models are also widely used to assess the effect of aerosols on crop production in polluted regions. For example, Tie et al. (2016) studied the implications on rice and wheat productivity due to heavy haze and air pollution in China by using a statistical model based upon experimental measurements of crop yield data and solar radiation reduction estimated by the Tropospheric Ultraviolet-Visible (TUV) model by using MODIS AOD data. They found that the reduction in solar radiation by aerosols resulted in the reduction of wheat and rice yield in the study area by 10-14% and 3-8% respectively. Similarly, Ozdes (2012) studied a statistical correlation between crop (rice, wheat, cotton & soybean) yield, temperature, precipitation, and aerosol optical depth (AOD) in 5 countries of central Asia and found that the correlation not only varies across the countries but also in different agricultural regions.

4.8.2 Effect of aerosols deposited on the leaves

The effect of aerosol on crop is not only due to diffusion of incoming solar radiation, change in temperature and moisture availability, but also due to deposition of aerosol on crop leaves. Bergin et al. 2001 proposed a model to account for the reduction of PAR due to dry deposition of water-insoluble aerosol (WIA) particles on leaves. The model estimated that over a two-month period during a growing season, dry deposition of WIA

may account for a 35% reduction in PAR available for plant photosynthesis in the Yangtze delta region of China. Recently, Mina et al. (2018) conducted an experiment at the Indian Agricultural Research Institute(IARI), New Delhi to study the effect of particulate matter deposition on growth, physiology and yield attributes of rice and found that the deposited particulate matter clogged the stomata and increased the leaf temperature resulting in up to 14% reduction of yield of the basmati rice variety. Hence, the physical deposition of atmospheric aerosols on the leaves also affects crop production.

4.9 Acid rain and crop production

India and China are the leading countries (number one and two respectively) responsible for the emission of SO_2 due to high consumption of coal in power plants and industries (Li et al., 2017). Similarly, high level of emissions of nitrous oxide, carbon dioxide in India and China is reported due to increasing use of fossil fuel in industrial and transport sector as well as dependence upon biomass to meet domestic energy demand (Novakov, 2003; Stohl et al., 2015; Lacey and Henze, 2015). The sulphur dioxide, nitrogen oxides, carbon dioxide, etc. emitted in the atmosphere are oxidised and hydrolysed in the atmosphere to form acid rain (Likens et al., 1979). Acid rain-affected areas in China are mainly distributed over east China, southwest China, and parts of south China, including the middle and lower parts of the Yangtze River (Hu et al., 2010). A significant effect of acid rain on crop production is reported in China, for example, vegetable yield was reduced by 7.8%, wheat by 5.4%, soybeans by 5.7%, and cotton by 5.0% (Yang et al., 2002). In addition to the effect on crop production, the acid rain is also assisting landslide by developing failure mechanism in limestone rocks in southwest China (Zhang and Mcsaveney, 2018).

Regarding acid rain in the IGP region, after the analysis of the rainwater samples across the region during the summer monsoon seasons from 2009 and 2011, it was found that only about 16% of the rainwater samples were acidic (pH<5.61)(Tiwari et al., 2016). In this study, the mean ratio of $H^+/(NO3^- + SO4^{2-})$ was 0.02, and the ratios $(Ca^{2+} + Mg^{2+} + NH_4^+)/(NO^{3-} + SO_4^{2-})$ was 2.2. (greater than 1), which indicate that most of the acidity in rainwater was neutralised and Ca^{2+}, Mg^{2+}, and NH_4^+ played a crucial role in neutralisation. The neutralisation of acid rain by neutralising agents originated from both anthropogenic as well as crustal sources in the IGP is reported in the findings of several studies (Jain et al., 2000; Kulshrestha et al., 2003; Singh and Singh, 2007; Bisht et al., 2014). Unlike China, generally rainwater in India is alkaline in nature due to buffering of acidity by the soil derived aerosols rich in Calcium (Kulshrestha et al., 2001). However, in the late phase of

monsoon, the rainwater near industrial areas (like Dhanbad) is found to be acidic due to non-availability of proper neutraliser for acidic ion (Singh et al., 2007).

4.10 Other Effects

Under the heading of other effects, the effect of atmospheric aerosols on solar energy production and lightning is covered in this subsection.

Along with the effect on the natural systems, the effect of atmospheric aerosol on solar energy production is also reported in different countries. Based on 12 years data (2003 to 2014), Li et al. (2017) estimated that due to severe air pollution, the annual average reduction on point of array irradiance (POIA) over both northern and eastern China is about 20-25%. Hence, along with the other benefits of air quality improvements, the photovoltaic system performance will also be improved significantly in northern and eastern China to provide emission-free electricity. Similarly, Bergin et al. (2017) studied the reduction of solar energy from photovoltaic panel due to atmospheric and deposited aerosol particles in India, China, and Arabian Peninsula through field observations and modelling and found that at present the aerosols have reduced the power production by 17-25% across those regions.

Lightning is one of the important disaster events in India which takes thousands of lives (on average 2234 death per year) every year (Siingh et al., 2014). Recent studies show that there is a relation between atmospheric aerosol concentration and lightning events. For example, the results of Lal et al. (2018)'s study on the relation between atmospheric aerosols and lightning events in the IGP showed that lightning activity increases (decreases) with increasing aerosols during normal (deficient) monsoon rainfall years. However, in the case of deficient rainfall years and the average value of AOD less than 0.88, lightning increases with increasing aerosol. They also found that the role of AOD is more prominent for lightning activity in western IGP than that in eastern IGP.

5.0 Methods adopted to assess the effects of atmospheric aerosols on crop production

The atmospheric aerosols affect crop production through both chemical and physical features. Even though the chemical effects of atmospheric pollutants on crop production is also important, but by considering the scope of this study, only the physical effects of atmospheric aerosols on the crop production are reviewed. Regarding the direct physical effects, the reduction of solar radiation availability for the plants due to dispersion and

absorption by the atmospheric aerosols and deposition of aerosols on the leaves are important with respect to crop yield. Apart from the direct physical effects, the indirect effect of atmospheric aerosols, for example, effect on change in temperature, evapotranspiration, precipitation, extreme events, etc. also have a major role in crop production. In this context, the reduction of solar radiation by the atmospheric aerosol is a key input parameter for the assessment of the effect of aerosols on crop production. So, in this section, firstly, the review of methods used to assess the effect of atmospheric aerosols on solar radiation, secondly the review of the methodology used to assess the effect on crop production are covered.

5.1 Assessment of radiative forcing due to aerosols

The review of methodologies for the assessment on the effect of aerosols on the solar radiation covers two widely used methods based on the AERONET estimation and the estimation based on the SBDART model in this subsection.

As a global network of ground-based remote sensing aerosol stations initiated by NASA, AERONET (AErosol RObotic NETwork) stations are in operation throughout the globe (Holben et al., 1998). AERONET ground observation data are widely used to study the optical properties of atmospheric aerosols and their radiative effects (Zhuang et al., 2013; Kaskaoutis et al., 2014; Fu et al., 2017). The AERONET network provides long-term continuous monitoring and characterisation of aerosols, at a regional and global scale as well as aerosol information from spectral data of direct sun radiation extinction and angular measurement of sky radiance (Holben et al., 1998; Dubovikl and King, 2000). In addition, the inversion AERONET products provide aerosol parameters (e.g. size distribution, complex refractive index, partition of spherical and non-spherical particles) and properties (e.g. phase function, refractive index, spectral and broadband fluxes etc.) including radiative forcing at the top of atmosphere and bottom of atmosphere (NASA, n.d.). García et al. (2008) validated the AERONET estimated radiative forcing against ground-based broad band measurements from the Baseline Surface Radiation (BSRN) and the Solar Radiation Networks (SolRad-Net) and found that AERONET estimated radiative forcing is very close to ground measurements with uncertainty less than 15 Wm^{-2} for all stations which is within the uncertainty of BSRN and SolRad-Net observed data. In spite of consideration of AERONET data as a benchmark for the atmospheric aerosol's optical properties and radiative forcing, these point data on aerosol optical properties and

radiative forcing due to atmospheric aerosols at the surface and top of the atmosphere are limited to the location of the AERONET stations.

SBDART (Santa Barbara DISTORT Atmospheric Radiative Transfer) (Ricchiazzi et al., 1998) model is used to estimate the plane-parallel radiative transfer in clear and cloudy conditions within the earth's atmosphere and at the surface. It consists of a cloud model, gas absorption model, standard aerosol model, standard atmospheric model, extra-terrestrial source spectra, surface models, etc. The source code of SBDART is in FORTRAN 77. This model is found to be widely utilized to estimate the radiative forcing due to aerosols at the top of the atmosphere, in the atmosphere and at the bottom of atmosphere (i.e. at the surface of Earth)(Alam et al., 2011; Badarinath et al., 2009; Sadavarte et al., 2015; Singh et al., 2010; Tzanis and Varotsos, 2016; Xia et al., 2007). However, it requires a large number of input parameters (and therefore assumptions) and high processing time, making it unrealistic for use with large amounts of data across spatial and temporal scales (Gautier and Landsfeld, 1997).

5.2 Assessment of effect on crop production.

Review on the methodology used for the assessment of the effect of aerosols on crop production, the field experimental methods and the methods based on global models, statistical models, and crop models are covered in the following subsections.

5.2.1 Field experimentations (radiation-controlled greenhouse / Lysimetric study)

Several field experiments using open top field chambers to study the effect of ozone exposure to the crop growth are reported (Heagle et al., 1987; Maggs et al., 1995; Wahid and Campus, 1995). But, only limited field experiments to study the impact of particulate matter on crop production are reported. By using a special chamber Hirano et al. (1995) found that the dust deposition on the leaf surface due to atmospheric pollution affected the stomatal conductance, photosynthesis, and transpiration by shading, plugging of stomata and increasing the leaf temperature. In IGP, Agrawal et al. (2003) studied the effect of air pollution on peri-urban agriculture at Varanasi by monitoring the exposure to SO_2, NO_2, and O_3 of mung bean, wheat, mustard, and spinach crops and their response in terms of physiological characteristics, pigment, biomass, and yield. Similarly, Rajput and Agrawal (2005) also found that the negative impact of air pollution on the physiological characteristics of pea plants leading to low yield and inferior quality seeds in peri-urban areas of Varanasi city with a higher level of air pollutants. Seyyednejad et al. (2011) reviewed the effects of air pollution on plants and found that the air pollution reduces the

leaf area, reduces chlorophyll content, depletes sugar content and increases free proline content (indicating stress to the plants). Likewise, Dhir (2016) also found that the absorption/deposition of air pollutants on the leaves of the plants induce physiological and biological alterations in plants causing reduction of leaf area, closure of stomata and damage to the photosynthesis apparatus and reduces the photosynthesis capacity/efficiency of the plants. Regarding the factors affecting the deposition of particulate matter on vegetation, Przybysz et al. (2014) reported that pollution level, rainfall, and passage of time are the major factors. Moreover, by using natural and synthetic leaves in the experiments on the accumulation of particulate matter, Weerakkody et al. (2018) found that all three characteristics of leaves viz. leaf size, leaf shapes, and leaf surface characteristics are influential in the capture and retention of particulate matter. Recently, to assess the effect of deposition of atmospheric aerosols on the leaves of rice during rice growing season, Mina et al. (2018) conducted an experiment in New Delhi and found that the yield of Basmati rice varieties PS-5 and PB-1509 was reduced by 7-14% and 4-11% due to deposition of atmospheric aerosols on the leaves. In summary, the experimental studies are mainly focussed on the effect on crop production due to the deposited particulate matter on the leaves of the plants. These experimental studies do not include the effect of the change in solar radiation on the crop production, so there is need of further study of the effect of the change in solar radiation due to atmospheric aerosols on crops in the region (Mina et al., 2018).

5.2.2 Global models

In this subsection, the global models used to study the effect of atmospheric aerosols on crop production are reviewed.

By using a climate-biosphere model, Steiner and Chameides (2005) indicated that apart from the radiation effect of the aerosols, in certain conditions thermal responses of aerosols can also have a greater impact on photosynthesis and transpiration of plants. Mercado et al. (2009) estimated that the variations in diffuse fraction contribute about one quarter on the land carbon sink between 1960 and 1999 by using a global model modified to account for the effect of both direct and diffuse radiation on canopy photosynthesis. In order to investigate the aerosol-induced effects on land carbon fluxes (gross primary productivity (GPP) and isoprene emission), Strada and Unger (2016) used a coupled global-vegetation-chemistry-climate model and found that at the global scale land carbon fluxes are not sensitive to pollution aerosols even at significant reduction of

surface solar radiation of 9%, but at the regional scale, GPP and isoprene emission show robust but opposite sensitivity to anthropogenic aerosols. By using a column radiation model (CRM) and the Yale interactive terrestrial biosphere (YIB) model, Yue and Unger (2017) found that aerosols decreased the net plant productivity by 2-4% in both Northern plain and southwest region of China. In summary, these global models are used to study the effect of aerosols on forest productivity and at the regional scale, these models found a significant effect of atmospheric aerosols on plant productivity.

5.2.3 Statistical Modelling

The statistical models used to assess the effect of atmospheric aerosols on crop production in the polluted regions of China and in India is reviewed in this subsection.

In order to investigate the impact of aerosols on crop production in Jiangsu province of China, Shuai et al. (2013) analysed the historical sunshine data during 1980 to 2008 and found a decreasing trend of sunshine hours (0.37h decade^{-1}) due to the increased level of atmospheric aerosols. Then after multiple regression of historical sunshine duration, temperature, and rice yield data, they concluded that the increasing level of atmospheric aerosols offset the benefits of global warming on rice production during 1980 to 2008 in Jiangsu province, China. To investigate the relation between the level of air pollution to solar radiation, Wang et al. (2012) analysed the historical data on air pollution index (API) and sunshine hours in 38 cities of China and found that the sunshine hours of 84% of the cities declined significantly ($p<0.05$) by an average of 16.7% during 1960-2000 and winter seasons had high API along with highest sunshine hour decline (21.5%). Moreover, by analysing the surface solar irradiance, wind speed and air pollution of 27 cities across China, Wang et al. (2014) concluded that wind speed is also an important factor which regulates solar radiation especially in the cities and seasons with high air pollution. To study the direct impact of $PM_{2.5}$ on the production of wheat, rice and maize in 303 prefectural level administrative divisions in 25 provinces of China during 2001 to 2010, Zhou et al. (2018) used an econometric model and found that $PM_{2.5}$ has a significant direct negative impact on the yield of wheat and corn.

In India by using a statistical model of historical rice harvest data coupled with regional climate scenario, Auffhammer et al. (2006) indicated that due to increased brown clouds and greenhouse gas there has been a slowdown in harvest growth over the last two decades. Similarly, by using a statistical model, Burney and Ramanathan (2014) found that up to 36% of the reduction in wheat yield took place due to the combined effect of

atmospheric aerosols and climate change in India during 1980 to 2010. Gupta et al. (2017) analysed the impact of temperature and solar radiation (due to atmospheric aerosols) on wheat production through regression analysis of the data from 208 districts in India during 1981 to 2009 and found that every 1°C increase in average daily maximum and minimum temperature tended to lower yield by 2-4% each and 1% increase in solar radiation increased yield by 1%. By using historical MODIS AOD data during 2001 to 2013, the study also indicated that one standard deviation decrease of AOD is estimated to increase the wheat yield by about 4.8% in India (Gupta et al., 2017). In summary, statistical models applied in the polluted regions of China and India indicate a significant negative impact on crop production due to the increased level of atmospheric aerosols.

5.2.4 Crop simulation modelling

Crop simulation modelling simulates the processes involved in crop growth and predicts the response of the system to change in boundary condition and inputs related to weather, soil, crop management, etc. (Hoogenboom et al., 2004). Decision support system for agrotechnology transfer (DSSAT) (Hoogenboom et al., 2004; Jones et al., 2003) and agricultural production systems simulator (APSIM) (Keating et al., 2003; McCown et al., 1996) are widely used crop simulation models as decision-making tools and for scientific investigations viz. yield forecasting, production and resource management, ecological and environmental research, climate change etc (Holzworth et al., 2014; Jones et al., 2016). DSSAT uses the crop environment resource synthesis (CERES) model for simulation of cereals (Hoogenboom et al., 2004), whereas APSIM uses ORIZA for rice and WHEAT model for wheat crop simulation (Holzworth et al., 2014). The physical effect of atmospheric aerosols on the agricultural crop is difficult to measure experimentally. In this context, crop simulation models used to assess the effect of atmospheric aerosols in crop (cereals: wheat and maize) production is reviewed in this subsection.

Chameides et al. (1999) used crop environment resource synthesis (CERES) - 3.1 rice and wheat models to study the effects of atmospheric aerosols on crop production in which the major input variable related to atmospheric aerosols was a reduction in the surface irradiance due to aerosols. Likewise, Greenwald et al. 2006 used modified CERES crop model to study the influence of aerosol on rice, wheat and maize production under various atmospheric conditions. They obtained the change in solar radiation due to atmospheric aerosols by using the National Center for Atmospheric Research (NCAR) Tropospheric Ultraviolet-Visible (TUV) radiation model. Not only the DSSAT crop model

but also the APSIM model is also widely used to assess the effect of atmospheric aerosols on crop production. For example, by using the APSIM model Chen et al. (2010) found that an increase of temperature and reduction in solar radiation during 1961-2003 in the north China plain (NCP) reduced the potential yield of wheat and maize under full irrigation by 45.3 and 51.4 kg ha^{-1} a^{-1} respectively. Moreover, by using APSIM, Xiao and Tao (2014) found that the dimming caused by air pollution in the North China Plain (NCP) during 1980-2009 reduced the wheat yield by 3-12% across the stations. Similarly, by using APSIM model, Liu et al. (2016) investigated the impact of air pollution on wheat yield at NCP during 2000- 2012 and found that the reduction of solar radiation caused by air pollution reduced the wheat yield significantly. Likewise for the maize crop by using APSIM, Xiao and Tao (2016) investigated the relative contribution of climate change, cultivar shift and management change on the maize yield during 1981 to 2009 in NCP and found that the change in climate variables reduced maize yield by 15 to 30% and among the change in climate variables, the highest reduction of the maize yield 12-24% is due to the change in solar radiation during that period. The reduction of maize yield due to the reduction in solar radiation caused by air pollution is also supported by the findings of Sun et al. (2016). In addition to the study on the effect of aerosols on wheat and maize at China, the study on the effect of dimming on boro rice at Bangladesh is investigated by Zaman (2009) by using ORYZA 2000 developed by the International Rice Research Institute (IRRI). In summary, the crop simulation models DSSAT and APSIM are successfully used for the studies on the effect of atmospheric aerosols on crop production.

6.0 Knowledge gaps

The IGP region is a hotspot with respect to a high level of atmospheric aerosols because of high population density, increasing urbanisation/industrialization as well as physiographic conditions (Srivastava et al., 2012a). Compared to other parts of the IGP, high levels of atmospheric aerosols and even persistent higher pollution pool is reported at the eastern IGP due to higher population density, topographical feature, local meteorology and high emissions from biomass and fossil fuel from these area (David et al., 2018; Di Girolamo et al., 2004; M. Kumar et al., 2018). A seasonally higher level of atmospheric aerosols is noticed during winter season in the eastern IGP due to increased emissions from biomass and fossil combustion and shallow boundary layer height and calm wind during this season (Clean Air Asia, 2016; Guttikunda et al., 2014; Kumar et al., 2017; Kumar et al., 2018). Regarding atmospheric aerosol loading trend in the IGP, various

studies have analysed the past historical data (Kumar et al., 2018) and future aerosol scenario of IGP (Kumar et al., 2018; Venkataraman et al., 2018), indicating increasing trend in previous decades and alarming scenario of the future if the present trend continues. After reviewing the studies on the effect of atmospheric aerosols in the IGP, it is noticed that there are several studies on the effects of atmospheric aerosols on public health, but only a few studies on the effect on crop production. In addition, the systematic study on the effect of atmospheric aerosols on crop production in the IGP by using crop simulation is not noticed so far. However, the reviewed literature clearly indicated that significant decline of solar radiation due to an increase of atmospheric aerosols in several locations in the IGP (Das et al., 2015b; Kumari et al., 2007; Latha et al., 2017; Niroula et al., 2015; Zaman, 2009). Moreover, several studies through crop simulation and modelling in NCP, a hot spot in China clearly indicated that the yield of wheat and maize is seriously affected by the decline of solar radiation due to increased atmospheric aerosols (Chen et al., 2010; Liu et al., 2016; Sun et al., 2016; Xiao and Tao, 2014). In the present scenario of IGP being a food basket of the region, the impact of aerosols on the crop production in the IGP is an important issue with respect to the food security of the region (Ramanathan and Ramana, 2005). Since the atmospheric aerosols alter several factors affecting crop growth viz. incoming solar radiation, ambient temperature (maximum as well as minimum temperature), potential evapotranspiration (ET_o), precipitation, etc., the effect of atmospheric aerosols on crop production in a highly polluted region like the IGP is expected to be significant. In addition, the effect of atmospheric aerosols on the major winter crop (wheat) production will further increase vulnerability of the livelihood of people in the eastern IGP because of a dominance of smallholders (Balasubramanian et al., 2013) and low crop productivity (Taneja et al., 2014) in the eastern IGP. In this context, the main research question of this study is "**What are the physical effects of atmospheric aerosols on winter crop (wheat) production in the eastern IGP?"**

In order to address the main research question for the assessment of the physical effects of atmospheric aerosols on winter crop (wheat) production in the eastern IGP, the relevant studies were extensively reviewed. After review, the identified important factors related to atmospheric aerosols affecting winter crop production in the IGP were winter fog events, extreme cold events, and the radiative forcing due to atmospheric aerosols.

The fog event in the IGP is reported to be increasing at an alarming rate during the past four decades along with the increasing air pollution in the IGP (Srivastava et al., 2016). The persistence of fog events occurring during winter in the IGP have strong implications

for air and surface transport (Jenamani and Kumar, 2013) and also affect crop production significantly (Singh and Singh, 2010). Regarding, the geographical coverage and trend of fog events in the IGP, several studies explained about the increased level of fog events in Indian and Pakistani and even Bangladesh portion of the IGP and all showed the increasing trend (Muslehuddin et al., 2004; Singh and Singh, 2010; Syed et al., 2012; Yasmeen et al., 2012; S K Srivastava et al., 2016). However, studies on fog events and their trend in the Nepal section of IGP, which is popularly known as the Terai region of Nepal, is not reported so far. Hence the study on the trend of fog events in the Nepal section of IGP i.e. the foothill of the Himalayan region will complete the picture of fog event trends for the entire IGP. Moreover, the extent of fog events and their trend in the Terai region of Nepal will also indicate its effect on crop production in Terai, which is also the food basket of Nepal. Hence, to obtain the trend of fog in the Nepal portion of IGP, a research sub-question for this study is, "**What is the status and trend of fog in Terai area of Nepal?"**

After review of cold events, in the IGP, it is noticed that several studies were conducted on the cold events in the Indian section of IGP (Pai et al., 2004; De, U. S., Dube and Rao, 2005; Revadekar et al., 2012; Singh and Patwardhan, 2012; Nair et al., 2016; Pai et al., 2017; Roshan et al., 2018) but the literature regarding cold events in the Nepal section of IGP (Terai region of Nepal) is not noticed so far. Even though news regarding cold waves and its effect on humans and agriculture in the Terai region of Nepal is reported in the national/local media during winter in almost every year, the scientific studies in this regard in the Terai region of Nepal are not noticed so far. It indicates the need for a systematic scientific study of cold events and its effect on agriculture in the Terai region of Nepal. However, the scientific studies in the past that are too one-dimensional and have ignored important cross correlations that are obvious to lay-people. Therefore, the incorporation of citizen science is also regarded as a tool for ecological research and climate change (Dickinson et al., 2012). Hence, the perspective of the farmers on the effects of cold events and fog on their crop production is also very important to assess the severity of its effect on agriculture at the ground level along with scientific study of the cold events based on historical temperature data. In this context, the next important research sub-question to address the main research question is "**What is the status of cold wave in the Terai region of Nepal and what is the farmer's perception on the effect of fog and cold wave on their crop production?"**

From the review of the literature, it is understood that the reduction of solar radiation due to an increasing level of atmospheric aerosols is a key factor causing a larger impact

on the natural system and in crop production in the IGP. To assess the severity of alarming increased atmospheric aerosols in the IGP, the radiative forcing due to atmospheric aerosols is estimated in the IGP in several studies (Ramanathan and Ramana, 2005; Sarkar et al., 2006; Gautam et al., 2010; Alam et al., 2011; Ramachandran and Kedia, 2012; Praveen et al., 2012; Srivastava et al., 2012; Das et al., 2015a; Tiwari et al., 2016a; Bibi et al., 2017). These studies used complicated models like SBDART for the assessment of radiative forcing due to atmospheric aerosols and these models require many input parameters and requires more time to process the data. Similarly, AERONET inversion product provides the radiative forcing at the top of the atmosphere, at the bottom of the atmosphere and the atmosphere at the AERONET stations throughout the globe (NASA, n.d.). The AERONET optical/radiative properties derived by using a continuous measurement of sun photometers are considered to be a benchmark in aerosol studies (Xia et al., 2015), but those point data are limited to the respective AERONET stations only. In this context, there is a need for a simple model which can assess the effect the atmospheric aerosols on the solar radiation availability. In this context, an important research sub-question is **How the availability of solar radiation is affected by atmospheric aerosol in the IGP?**

Regarding the studies to assess the effect of atmospheric aerosols on the crop production in the IGP, only a few studies were noticed during the review and Auffhammer et al., (2006) and Burney and Ramanathan (2014) are two well-cited studies in this regard. Both those studies and other studies used statistical and empirical models to assess the effect of atmospheric aerosols on crop production. The studies by using the crop models to assess the effect of atmospheric aerosols on crop production are found to be very limited in the IGP region. Since, at present the effect of atmospheric aerosols is mainly focussed on their effect on people's health and climate change, the assessment of the effect on winter crop production due to atmospheric aerosols in the eastern IGP will also provide the complete picture of the effect of atmospheric aerosols by including its effect on food security of the region. Hence, it is realised that there is a need for a comprehensive study to find the implication of aerosols on crops through crop simulation modelling in the IGP. In this context, the sub-question of this study is **What is the effect of atmospheric aerosols on the winter crop production in the eastern IGP?**

7.0 Research Questions:

Based on the knowledge/data gaps the major research question of this study is listed below

---

"What are the physical effects of atmospheric aerosols in winter crop (wheat) production in the eastern IGP?"

To address this main research question following sub-questions are to be addressed.

Sub-question no 1 : What is the status and trend of fog in the Terai region of Nepal?

Sub-question no 2 : What is the status and trend of cold wave in the Terai region of Nepal?

Sub-question no 3 : What is the farmer's perception on the effect of fog and cold wave in their crop production?

Sub-question no 4 : How the availability of solar radiation is affected by atmospheric aerosol in IGP? and

Sub-question no 5 : What is the effect of atmospheric aerosols in the winter crop production in the eastern IGP?

References:

Agarwal, A., Mangal, A., Satsangi, A., Lakhani, A., Maharaj Kumari, K., 2017. Characterization, sources and health risk analysis of PM2.5bound metals during foggy and non-foggy days in sub-urban atmosphere of Agra. Atmos. Res. 197, 121–131. https://doi.org/10.1016/j.atmosres.2017.06.027

Agrawal, M., Singh, B., Rajput, M., Marshall, F., Bell, J.N.B., 2003. Effect of air pollution on peri-urban agriculture : a case study. Environ. Pollut. 126, 323–329. https://doi.org/10.1016/S0269-7491(03)00245-8

Ahmed, M., Hassan, F., 2011. Cumulative effect of temperature and solar radiation on wheat yield. Not. Bot. Horti Agrobot. Cluj-Napoca 39, 146–152. https://doi.org/10.15835/NBHA3925406

Alam, K., Trautmann, T., Blaschke, T., 2011. Aerosol optical properties and radiative forcing over mega-city Karachi. Atmos. Res. 101, 773–782. https://doi.org/10.1016/j.atmosres.2011.05.007

Aloysius, M., Mohan, M., Parameswaran, K., George, S.K., Nair, P.R., 2008. Aerosol transport over the Gangetic basin during ISRO-GBP land campaign-II. Ann. Geophys. 26, 431–440. https://doi.org/10.5194/angeo-26-431-2008

Alpert, P., Kishcha, P., Kaufman, Y.J., Schwarzbard, R., 2005. Global dimming or local dimming?: Effect of urbanization on sunlight availability. Geophys. Res. Lett. 32, 1–4. https://doi.org/10.1029/2005GL023320

Ångström, A., 1929. On the atmospheric transmission of sun radiation and on dust in the air. Geogr. Ann. 11, 156–166.

Apte, J.S., Brauer, M., Cohen, A.J., Ezzati, M., Pope, C.A., 2018. Ambient PM 2.5 reduces global and regional life expectancy. Environ. Sci. Technol. Lett. 5, 546–551. https://doi.org/10.1021/acs.estlett.8b00360

Auffhammer, M., Ramanathan, V., Vincent, J.R., 2006. Integrated model shows that atmospheric brown clouds and greenhouse gases have reduced rice harvests in India. PNAS 103.

AWC Research Group, 2018. Source apportionment , health effects and potential reduction of fine. Baton Rouge, LA.

Babu, S.S., Manoj, M.R., Moorthy, K.K., Gogoi, M.M., Nair, V.S., Kompalli, S.K., Satheesh, S.K., Niranjan, K., Ramagopal, K., Bhuyan, P.K., Singh, D., 2013. Trends in aerosol optical depth over Indian region: Potential causes and impact indicators. J. Geophys. Res. Atmos. 118, 11794–11806. https://doi.org/10.1002/2013JD020507

Badarinath, K. V S, Kharol, S.K., Sharma, A.R., Roy, P.S., 2009. Fog over Indo-Gangetic Plains - A study using multisatellite data and ground observations. IEEE J. Sel. Top. Appl. Earth Obs. Remote Sens. 2, 185–195. https://doi.org/10.1109/JSTARS.2009.2019830

Badarinath, K V S, Kumar Kharol, S., Rani Sharma, A., 2009. Long-range transport of aerosols from agriculture crop residue burning in Indo-Gangetic Plains—A study using LIDAR, ground measurements and satellite data. J. Atmos. Solar-Terrestrial Phys. 71, 112–120.

Balasubramanian, V., Adhya, T.K., Ladha, J.K., 2013. Enhancing eco-efficiency in the intensive cereal-based systems of the Indo-Gangetic plains, in: Hershey, C.H., Neate, P. (Eds.), Eco-Efficiency: From Vision to Reality (Issues in Tropical Agriculture Series). International Center for Tropical Agriculture, Cali, Colombia, pp. 99–115. https://doi.org/doi:10.1201/b17133-197

Bangladesh Power Development Board, 2016. Annual Report 2015-2016. Dhaka.

Bedekar, V.C., Dekate, M. V, Banerjee, A.K., 1974. Heat and cold waves in India forcasting manual part IV (FMU Rep. No. IV-6). Poona< India.

Begum, B.A., Hopke, P.K., Markwitz, A., 2013. Air pollution by fine particulate matter in Bangladesh. Atmos. Pollut. Res. 4, 75–86. https://doi.org/10.5094/APR.2013.008

Bellouin, N., Boucher, O., Haywood, J., Reddy, M.S., 2005. Global estimate of aerosol direct radiative forcing from satellite measurements. Nature 438, 1138–1141. https://doi.org/10.1038/nature04348

Bergin, M.H., 2004. Radiative forcing by anthropogenic aerosols: sources and impacts, in: Urbanization, Energy, and Air Pollution in China: The Challenges Ahead: Proceedings of a Symposium. THE NATIONAL ACADEMIES PRESS, Washington DC, pp. 155–167. https://doi.org/10.17226/11192

Bergin, M.H., Ghoroi, C., Dixit, D., Schauer, J.J., Shindell, D., 2017. Large reductions in solar energy production due to dust and particulate air pollution. Environ. Sci. Technol. Lett. acs.estlett.7b00197. https://doi.org/10.1021/acs.estlett.7b00197

Bergin, M.H., Greenwald, R., Xu, J., Berta, Y., Chameides, W.L., 2001. Influence of aerosol dry deposition on pjotosynthetically active radiation available to plants: Acase study in the Yangtze delta region of China. Geophys. Res. Lett. 28, 3605–3608.

Bibi, H., Alam, K., Bibi, S., 2017. Estimation of shortwave direct aerosol radiative forcing at four locations on the Indo-Gangetic plains: Model results and ground measurement. Atmos. Environ. 163, 166–181.

Bibi, H., Alam, K., Blaschke, T., Bibi, S., Iqbal, M.J., 2016. Long-term (2007 – 2013) analysis of aerosol optical properties over four locations in the Indo-Gangetic plains. Appl. Opt. 55, 6199–6211. https://doi.org/10.1364/AO.55.006199

Bilal, M., Nichol, J.E., Nazeer, M., 2016. Validation of Aqua-MODIS C051 and C006 operational aerosol products using AERONET measurements over Pakistan. IEEE J. Sel. Top. Appl. Earth Obs. Remote Sens. 9, 2074–2080. https://doi.org/10.1109/JSTARS.2015.2481460

Bisht, D.S., Tiwari, S., Srivastava, A.K., Singh, J. V., Singh, B.P., Srivastava, M.K., 2014. High concentration of acidic species in rainwater at Varanasi in the Indo-Gangetic Plains, India. Nat. Hazards 75, 2985–3003. https://doi.org/10.1007/s11069-014-1473-0

Biswas, K.F., Ghauri, B.M., Husain, L., 2008. Gaseous and aerosol pollutants during fog and clear episodes in South Asian urban atmosphere. Atmos. Environ. 42, 7775–7785. https://doi.org/10.1016/j.atmosenv.2008.04.056

Bonasoni, P., Cristofanelli, P., Marinoni, A., Vuillermoz, E., 2012. Atmospheric Pollution in the Hindu Kush – Himalaya Region. Mt. Res. Dev. 32, 468–479. https://doi.org/10.1659/MRD-JOURNAL-D-12-00066.1

Bonasoni, P., Laj, P., Marinoni, A., Sprenger, M., Angelini, F., Arduini, J., 2010. Atmospheric Brown Clouds in the Himalayas : first two years of continuous observations at the Nepal-Climate Observatory at Pyramid (5079 m) 4823–4885.

Boucher, O., 2015. Atmospheric aerosols -properties and climate impacts, Springer. Springer, Paris. https://doi.org/10.1017/CBO9781107415324.004

Bran, S.H., Srivastava, R., 2017. Investigation of PM2.5mass concentration over India using a regional climate model. Environ. Pollut. 224, 484–493. https://doi.org/10.1016/j.envpol.2017.02.030

Bright, D.R., Mullen, S.L., 2002. The sensitivity of the numerical simulation of the southwest monsoon boundary layer to the choice of PBL turbulence parameterization in MM5. Weather

Forecast. 17, 99–114. https://doi.org/10.1175/1520-0434(2002)017<0099:TSOTNS>2.0.CO;2

Brook, R.D., Rajagopalan, S., Pope, C.A., Brook, J.R., Bhatnagar, A., Diez-Roux, A. V., Holguin, F., Hong, Y., Luepker, R. V., Mittleman, M.A., Peters, A., Siscovick, D., Smith, S.C., Whitsel, L., Kaufman, J.D., 2010. Particulate matter air pollution and cardiovascular disease: An update to the scientific statement from the american heart association, Circulation. https://doi.org/10.1161/CIR.0b013e3181dbece1

Burney, J., Ramanathan, V., 2014. Recent climate and air pollution impacts on India agriculture. Proc. Natl. Acad. Sci. 111, 16319–16324. https://doi.org/10.1073/pnas.1317275111

Butt, E.W., Rap, A., Schmidt, A., Scott, C.E., Pringle, K.J., Reddington, C.L., Richards, N.A.D., Woodhouse, M.T., Ramirez-Villegas, J., Yang, H., Vakkari, V., Stone, E.A., Rupakheti, M., Praveen, P.S., Van Zyl, P.G., Beukes, J.P., Josipovic, M., Mitchell, E.J.S., Sallu, S.M., Forster, P.M., Spracklen, D. V., 2016. The impact of residential combustion emissions on atmospheric aerosol, human health, and climate. Atmos. Chem. Phys. 16, 873–905. https://doi.org/10.5194/acp-16-873-2016

Carmichael, G.R., Adhikary, B., Kulkarni, S., D'Allura, A., Tang, Y., Streets, D., Zhang, Q., Bond, T.C., Ramanathan, V., Jamroensan, A., Marrapu, P., 2009. Asian aerosols: Current and year 2030 distributions and implications to human health and regional climate change. Environ. Sci. Technol. 43, 5811–5817. https://doi.org/10.1021/es8036803

Chakraborty, Aj. of G.R.: A., Bhattu, D., Gupta, T., Tripathi, S.N., Canagaratna, M.R., 2015. Real-time measurements of ambient aerosols in a polluted Indian city: Sources, characteristics, and processing of organic aerosols during foggy and nonfoggy periods. J. Geophys. Res. Atmos. 120, 9006–9019. https://doi.org/10.1002/2015JD023419.Received

Chameides, W.L., Yu, H., Liu, S.C., Bergin, M., Zhou, X., Mearns, L., Wang, G., Kiang, C.S., Saylor, R.D., Luo, C., Huang, Y., Steiner, A., Giorgi, F., 1999. Case study of the effects of atmospheric aerosols and regional haze on agriculture: an opportunity to enhance crop yields in China through emission controls?, in: Proceedings of the National Academy of Sciences of the United States of America. pp. 13626–13633. https://doi.org/10.1073/pnas.96.24.13626

Chen, C., Wang, E., Yu, Q., Zhang, Y., 2010. Quantifying the effects of climate trends in the past 43 years (1961-2003) on crop growth and water demand in the North China Plain. Clim. Change 100, 559–578. https://doi.org/10.1007/s10584-009-9690-3

Chen, J.L., Wilson, C.R., Tapley, B.D., 2013. Contribution of ice sheet and mountain glacier melt to recent sea level rise. Nat. Geosci. 6, 549.

Chen, X., Zhang, Xiaobo, Zhang, Xin, 2018. The impact of exposure to air pollution on cognitive performance. PNAS 115, 9193–9197. https://doi.org/10.1073/pnas.1809474115

Chitranshi, S., Sharma, S.P., Dey, S., 2015. Spatio-temporal variations in the estimation of PM10 from MODIS-derived aerosol optical depth for the urban areas in the Central Indo-Gangetic Plain. Meteorol. Atmos. Phys. 127, 107–121. https://doi.org/10.1007/s00703-014-0347-z

Chowdhury, S., Dey, S., Smith, K.R., 2018. Ambient PM2.5 exposure and expected premature mortality to 2100 in India under climate change scenarios. Nat. Commun. 9, 1–10. https://doi.org/10.1038/s41467-017-02755-y

Chung, C.E., 2012. Aerosol direct radiative forcing : a review, in: Abdul-Razzak, H. (Ed.), Atmospheric Aerosols – Regional Characteristics – Chemistry and Physics. InTech, pp. 379–394. https://doi.org/http://dx.doi.org/10.5772/50248

Clean Air Asia, 2016. Guidance framework for better air quality in Asian cities.

Climate and Clean Air Coalition Secretariat, 2016. Annual Report. Paris. https://doi.org/10.1039/C1DT90165F

Cohan, D.S., Xu, J., Greenwald, R., Bergin, M.H., Chameides, W.L., 2002. Impact of atmospheric aerosol light scattering and absorption on terrestrial net primary productivity - art. no. 1090. Global Biogeochem. Cycles 16, 1090. https://doi.org/10.1029/2001GB001441

Cohen, A.J., Brauer, M., Burnett, R., Anderson, H.R., Frostad, J., Estep, K., Balakrishnan, K., Brunekreef, B., Dandona, L., Dandona, R., Feigin, V., Freedman, G., Hubbell, B., Jobling, A., Kan, H., Knibbs, L., Liu, Y., Martin, R., Morawska, L., Pope, C.A., Shin, H., Straif, K., Shaddick, G., Thomas, M., van Dingenen, R., van Donkelaar, A., Vos, T., Murray, C.J.L., Forouzanfar, M.H., 2017. Estimates and 25-year trends of the global burden of disease attributable to ambient air pollution: an analysis of data from the Global Burden of Diseases Study 2015. Lancet 389, 1907–1918. https://doi.org/10.1016/S0140-6736(17)30505-6

Conibear, L., Butt, E.W., Knote, C., Arnold, S.R., Spracklen, D. V., 2018. Stringent emission control policies can provide large improvements in air quality and public health in India. GeoHealth 1–16. https://doi.org/10.1029/2018GH000139

Corrigan, C.E., Ramanathan, V., Schauer, J.J., 2006. Impact of monsoon transitions on the physical and optical properties of aerosols. J. Geophys. Res. 111, D18208. https://doi.org/10.1029/2005JD006370

CPCB, 2015. Annual Report 2014-15. New Delhi.

CPCB, 2012. National ambient air quality status & trends in India -2010. Central Pollution Control Board, New Delhi.

Das, R., Khezri, B., Srivastava, B., Datta, S., Sikdar, P.K., Webster, R.D., Wang, X., 2015. Trace element composition of PM2.5 and PM10 from Kolkata – a heavily polluted Indian metropolis. Atmos. Pollut. Res. 6, 742–750. https://doi.org/10.5094/APR.2015.083

Das, S.K., Chatterjee, A., Ghosh, S.K., Raha, S., 2015a. Fog-induced changes in optical and physical properties of transported aerosols over Sundarban, India. Aerosol Air Qual. Res. 15, 1201–1212. https://doi.org/10.4209/aaqr.2014.11.0287

Das, S.K., Chatterjee, A., Ghosh, S.K., Raha, S., 2015b. An integrated campaign for investigation of winter-time continental haze over Indo-Gangetic Basin and its radiative effects. Sci. Total Environ. 533, 370–82. https://doi.org/10.1016/j.scitotenv.2015.06.085

Das, S.K., Jayaraman, a., Misra, a., 2008. Fog-induced variations in aerosol optical and physical properties over the Indo-Gangetic Basin and impact to aerosol radiative forcing. Ann. Geophys. 26, 1345–1354. https://doi.org/10.5194/angeo-26-1345-2008

Dash, S.K., Mamgain, A., 2011. Changes in the frequency of different categories of temperature extremes in India. J. Appl. Meteorol. Climatol. 50, 1842–1858. https://doi.org/10.1175/2011JAMC2687.1

David, L.M., Ravishankara, A.R., Kodros, J.K., Venkataraman, C., Sadavarte, P., Pierce, J.R., Chaliyakunnel, S., Millet, D.B., 2018. Aerosol optical depth over India. J. Geophys. Res. Atmos. 123, 1–16. https://doi.org/10.1002/2017JD027719

De, U.S., Dube, R.K., Rao, G.S.P., 2005. Extreme weather events over India in the last 100 years. J. Indian Geophys. Union 9, 173–187.

Dey, S., Di Girolamo, L., 2011. A decade of change in aerosol properties over the Indian subcontinent. Geophys. Res. Lett. 38, 1–5. https://doi.org/10.1029/2011GL048153

Dey, S., Di Girolamo, L., 2010. A climatology of aerosol optical and microphysical properties over the Indian subcontinent from 9 years (2000–2008) of Multiangle Imaging Spectroradiometer

(MISR) data. J. Geophys. Res. 115, D15204. https://doi.org/10.1029/2009JD013395

Dey, S., Tripathi, S.N., 2008. Aerosol direct radiative effects over Kanpur in the Indo-Gangetic basin, northern India: Long-term (2001-2005) observations and implications to regional climate. J. Geophys. Res. Atmos. 113, 1–20. https://doi.org/10.1029/2007JD009029

Dey, S., Tripathi, S.N., Singh, R.P., Holben, B.N., 2004. Influence of dust storms on the aerosol optical properties over the Indo-Gangetic basin. J. Geophys. Res. 109, 1–13. https://doi.org/10.1029/2004JD004924

Dhiman, M., Dhiman, J., 2015. Infusion of farm mechanization technologies in Indian agriculture: progress and impact. Indian J. Econ. Dev. 11, 111–122. https://doi.org/10.5958/2322-0430.2015.00014.1

Dhir, B., 2016. Air pollutants and photosynthetic efficiency of plants, in: Kulshrestha, U., Saxena, P. (Eds.), Plant Responses to Air Pollution. Springer, p. 71.

Di Girolamo, L., Bond, T.C., Bramer, D., Diner, D.J., Fettinger, F., Kahn, R.A., Martonchik, J. V., Ramana, M. V., Ramanathan, V., Rasch, P.J., 2004. Analysis of multi-angle Imaging SpectroRadiometer (MISR) aerosol optical depths over greater India during winter 2001-2004. Geophys. Res. Lett. 31, 1–5. https://doi.org/10.1029/2004GL021273

Dickinson, J.L., Shirk, J., Bonter, D., Bonney, R., Crain, R.L., Martin, J., Phillips, T., Purcell, K., 2012. The current state of citizen science as a tool for ecological research and public engagement In a nutshell : Front. Ecol. Environ. 10, 291–297. https://doi.org/10.1890/110236

Dubovikl, O., King, M.D., 2000. A flexible inversion algorithm for retrieval of aerosol optical properties from Sun and sky radiance measurements. J. Geophys. Res. 105, 20,673-20,696. https://doi.org/10.1029/2000JD900282

Erenstein, O., 2011. Cropping systems and crop residue management in the Trans-Gangetic Plains: Issues and challenges for conservation agriculture from village surveys. Agric. Syst. 104, 54–62. https://doi.org/10.1016/j.agsy.2010.09.005

ESCAP, 2017. Review of development in transportation in asia and the Pacific. Bangkok, Thailand.

Fu, Y., Zhu, J., Yang, Y., Yuan, R., Liu, G., Xian, T., Liu, P., 2017. Grid-cell aerosol direct shortwave radiative forcing calculated using the SBDART model with MODIS and AERONET observations: An application in winter and summer in eastern China. Adv. Atmos. Sci. 34, 952–964. https://doi.org/10.1007/s00376-017-6226-z

García, O.E., Díez, A.M., Expósito, F.J., Díaz, J.P., Dubovik, O., Dubuisson, P., Roger, J.C., Eck, T.F., Sinyuk, A., Derimian, Y., Dutton, E.G., Schafer, J.S., Holben, B., García, C.A., 2008. Validation of AERONET estimates of atmospheric solar fluxes and aerosol radiative forcing by ground-based broadband measurements. J. Geophys. Res. Atmos. 113, 1–16. https://doi.org/10.1029/2008JD010211

Gardner, A.S., Moholdt, G., Cogley, J.G., Wouters, B., Arendt, A.A., Wahr, J., Berthier, E., Hock, R., Pfeffer, W.T., Kaser, G., Ligtenberg, S.R.M., Bolch, T., Sharp, M.J., Hagen, J.O., Van Den Broeke, M.R., Paul, F., 2013. A reconciled estimate of glacier contributions to sea level rise: 2003 to 2009. Science (80-.). 340, 852–857. https://doi.org/10.1126/science.1234532

Gautam, R., 2014. Challenges in early warning of the persistent and widespread winter fog over the Indo- Gangetic plains: a satellite perspective, in: Singh, Z.Z. and A. (Ed.), Reducing Disaster: Early Warning Systems for Climate Change. Springer Science+Business Media Dordrecht, pp. 51–61. https://doi.org/10.1007/978-94-017-8598-3

Gautam, R., Hsu, N.C., Kafatos, M., Tsay, S.C., 2007. Influences of winter haze on fog/low cloud over the Indo-Gangetic plains. J. Geophys. Res. Atmos. 112, 1–11.

https://doi.org/10.1029/2005JD007036

Gautam, R., Hsu, N.C., Lau, K.-M., Kafatos, M., 2009. Aerosol and rainfall variability over the Indian monsoon region: distribution, trends, and coupling. Ann. Geophys. 27, 3691–3703.

Gautam, R., Hsu, N.C., Lau, K.M., 2010. Premonsoon aerosol characterization and radiative effects over the Indo-Gangetic plains: Implications for regional climate warming. J. Geophys. Res. Atmos. 115, 1–15. https://doi.org/10.1029/2010JD013819

Gautam, R., Hsu, N.C., Tsay, S.C., Lau, K.M., Holben, B., Bell, S., Smirnov, A., Li, C., Hansell, R., Ji, Q., Payra, S., Aryal, D., Kayastha, R., Kim, K.M., 2011. Accumulation of aerosols over the Indo-Gangetic plains and southern slopes of the Himalayas: distribution, properties and radiative effects during the 2009 pre-monsoon season. Atmos. Chem. Phys. 11, 12841–12863. https://doi.org/10.5194/acp-11-12841-2011

Gautam, R., Singh, M.K., 2018. Urban heat island over Delhi punches holes in widespread fog in the Indo-Gangetic plains. Geophys. Res. Lett. 45, 1114–1121. https://doi.org/10.1002/2017GL076794

Gautier, C., Landsfeld, M., 1997. Surface solar radiation flux and cloud radiative forcing for the atmospheric radiation measurement (ARM) Southern Great Plains (SGP): a satellite, surface observations, and radiative transfer model study. J. Atmos. Sci. 54, 1289–1307. https://doi.org/10.1175/1520-0469(1997)054<1289:SSRFAC>2.0.CO;2

Gedney, N., Huntingford, C., Weedon, G.P., Bellouin, N., Boucher, O., Cox, P.M., 2014. Detection of solar dimming and brightening effects on Northern Hemisphere river flow. Nat. Geosci 7, 796–800. https://doi.org/10.1038/NGEO2263

Giles, D.M., Holben, B.N., Tripathi, S.N., Eck, T.F., Newcomb, W.W., Slutsker, I., Dickerson, R.R., Thompson, A.M., Mattoo, S., Wang, S.H., Singh, R.P., Sinyuk, A., Schafer, J.S., 2011. Aerosol properties over the Indo-Gangetic Plain: A mesoscale perspective from the TIGERZ experiment. J. Geophys. Res. Atmos. 116, 1–19. https://doi.org/10.1029/2011JD015809

Gilgen, H., Wild, M., Ohmura, A., 1998. Means and trends of shortwave irradiance at the surface estimated from global energy balance archive data. J. Clim. 11, 2042–2061. https://doi.org/10.1175/1520-0442-11.8.2042

Greenwald, R., Bergin, M.H., Xu, J., Cohan, D., Hoogenboom, G., Chameides, W.L., 2006. The influence of aerosols on crop production: A study using the CERES crop model. Agric. Syst. 89, 390–413. https://doi.org/10.1016/j.agsy.2005.10.004

Gupta, P.K., Sahai, S., Singh, N., Dixit, C.K., Singh, D.P., Sharma, C., Tiwari, M.K., Gupta, R.K., Garg, S.C., 2004. Residue burning in rice – wheat cropping system : Causes and implications. Curr. Sci. 87, 1713–1717.

Gupta, R., Seth, A., 2007. A review of resource conserving technologies for sustainable management of the rice-wheat cropping systems of the Indo-Gangetic plains (IGP). Crop Prot. 26, 436–447. https://doi.org/10.1016/j.cropro.2006.04.030

Gupta, R., Somanathan, E., Dey, S., 2017. Global warming and local air pollution have reduced wheat yields in India. Clim. Change 140, 593–604. https://doi.org/10.1007/s10584-016-1878-8

Gupta, R.K., Naresh, R.K., Hobbs, P.R., Jiaguo, Z., Ladha, J.K., 2003. Sustainability of post-green revolution agriculture: the rice– wheat cropping systems of the Indo-Gangetic Plains and China. and impacts, in: Ladha, J.K., Hill, J.E., Duxbury, J.M., Gupta, R.K., Buresh, R.J. (Eds.), Improving the Productivity and Sustainability of Rice-Wheat Systems: Issues. American Society of Agronomy, Crop Science Society of America, Soil Science Society of America, Madison, Wisconsin, pp. 1–26. https://doi.org/10.1016/j.agsy.2003.10.004

Guttikunda, S.K., Begum, B.A., Wadud, Z., 2013. Particulate pollution from brick kiln clusters in the Greater Dhaka region, Bangladesh. Air Qual. Atmos. Heal. 6, 357–365. https://doi.org/10.1007/s11869-012-0187-2

Guttikunda, S.K., Goel, R., Pant, P., 2014. Nature of air pollution, emission sources, and management in the Indian cities. Atmos. Environ. 95, 501–510.

Guttikunda, S.K., Jawahar, P., 2014. Atmospheric emissions and pollution from the coal-fired thermal power plants in India. Atmos. Environ. 92, 449–460. https://doi.org/10.1016/j.atmosenv.2014.04.057

Gwénaëlle Legros, Havet, I., Bruce, N., Bonjour, S., 2009. The energy access situation in developing countries - A review focussing on the least developed countries and Sub Saharan Africa, UNDP WHO New York. New York.

Heagle, A.S., Kress, L.W., Temple, P.J., Kohut, R.J., Miller, J.E., Heggestad, H.E., 1987. Factors influencing ozone dose-yield response relationships in open-top field chamber studies, in: Heck, W.W., Taylor, O.C., Tingey, D.T. (Eds.), Assessment of Crop Loss from Air Pollution. Elsevier Appplied Science, London and New York, pp. 141–180.

Health Effects Institute, 2019. State of Global Air 2019. Special Report. Boston, MA.

Hirano, T., Kiyota, M., Aiga, I., 1995. Physical effects of dust on leaf physiology of cucumber and kidney bean plants. Environ. Pollut. 89, 255–261.

Holben, B.N., Eck, T.F., Slutsker, I., Tanré, D., Buis, J.P., Setzer, A., Vermote, E., Reagan, J.A., Kaufman, Y.J., Nakajima, T., Lavenu, F., Jankowiak, I., Smirnov, A., 1998. AERONET - A federated instrument network and data archive for aerosol characterization. Remote Sens. Environ. 66, 1–16. https://doi.org/10.1016/S0034-4257(98)00031-5

Holzworth, D.P., Huth, N.I., Peter, G., Zurcher, E.J., Herrmann, N.I., Mclean, G., Chenu, K., Oosterom, E.J. Van, Snow, V., Murphy, C., Moore, A.D., Brown, H., Whish, J.P.M., Verrall, S., Fainges, J., Bell, L.W., Peake, A.S., Poulton, P.L., Hochman, Z., Thorburn, P.J., Gaydon, D.S., Dalgliesh, N.P., Rodriguez, D., Cox, H., Chapman, S., Doherty, A., Teixeira, E., Sharp, J., Cichota, R., Vogeler, I., Li, F.Y., Wang, E., Hammer, G.L., Robertson, M.J., Dimes, J.P., Whitbread, A.M., Hunt, J., Rees, H. Van, Mcclelland, T., Carberry, P.S., Hargreaves, J.N.G., Macleod, N., Mcdonald, C., Harsdorf, J., Wedgwood, S., Keating, B.A., 2014. APSIM- evolution towards a new generation of agricultural systems. Environ. Model. Softw. 62, 327–350. https://doi.org/10.1016/j.envsoft.2014.07.009

Hoogenboom, G., White, J.W., Messina, C.D., 2004. From genome to crop:integration through simulation modelling. F. Crop. Res. 90, 145–163.

Hu, H., Yang, Q., Lu, X., Wang, W., Wang, S., Fan, M., 2010. Air pollution and control in different areas of China. Crit. Rev. Environ. Sci. Technol. 40, 452–518. https://doi.org/10.1080/10643380802451946

IPCC, 2007. Climate Change 2007 Synthesis Report, Intergovernmental Panel on Climate Change. https://doi.org/10.1256/004316502320517344

Jain, M., Kulshrestha, U.C., Sarkar, A.K., Parashar, D.C., 2000. Influence of crustal aerosols on wet deposition at urban and rural sites in India. Atmos. Enivronment 34, 5129–5137.

Jenamani, R.K., 2012. Micro-climatic study and trend analysis of fog characteristics at IGI airport New Delhi using hourly data (1981-2005). Mausam 63, 203–218.

Jenamani, R.K., 2007. Alarming rise in fog and pollution causing a fall in maximum temperature over Delhi. Curr. Sci. 93, 313–322.

Jenamani, R.K., Kumar, A., 2013. Bad weather and aircraft accidents – global vis-à-vis Indian

scenario. Curr. Sci. 104, 316–325.

Jones, J.W., Antle, J.M., Basso, B., Boote, K.J., Conant, R.T., Foster, I., Godfray, H.C.J., Herrero, M., Howitt, R.E., Janssen, S., Keating, B.A., Munoz-carpena, R., Porter, C.H., Rosenzweig, C., Wheeler, T.R., 2016. Brief history of agricultural systems modeling. Agric. Syst. 155, 240–254. https://doi.org/10.1016/j.agsy.2016.05.014

Jones, J.W., Hoogenboom, G., Porter, C.H., Boote, K.J., Batchelor, W.D., Hunt, L. a., Wilkens, P.W., Singh, U., Gijsman, a. J., Ritchie, J.T., 2003. The DSSAT cropping system model, European Journal of Agronomy. https://doi.org/10.1016/S1161-0301(02)00107-7

Joshi, H., Naja, M., Singh, K.P., Kumar, R., Bhardwaj, P., Babu, S.S., Satheesh, S.K., Moorthy, K.K., Chandola, H.C., 2016. Investigations of aerosol black carbon from a semi-urban site in the Indo-Gangetic Plain region. Atmos. Environ. 125, 346–359. https://doi.org/10.1016/j.atmosenv.2015.04.007

Kambezidis, H.D., Kaskaoutis, D.G., Kharol, S.K., Moorthy, K.K., Satheesh, S.K., Kalapureddy, M.C.R., Badarinath, K.V.S., Sharma, A.R., Wild, M., 2012. Multi-decadal variation of the net downward shortwave radiation over south Asia: The solar dimming effect. Atmos. Environ. 50, 360–372. https://doi.org/10.1016/j.atmosenv.2011.11.008

Kaskaoutis, D G, Houssos, E.E., Goto, D., Bartzokas, A., Nastos, P.T., Sinha, P.R., Kharol, S.K., Kosmopoulos, P.G., Singh, R.P., Takemura, T., 2014. Synoptic weather conditions and aerosol episodes over Indo-Gangetic Plains, India. Clim. Dyn. 43, 2313–2331. https://doi.org/10.1007/s00382-014-2055-2

Kaskaoutis, D. G., S.Kumar, Sharma, D., Singh, R.P., Kharol, S.K., Sharma, M., Singh, A.K., Singh, S., Singh, A., Singh, D., 2014. Effectsof crop residue burningonaerosol properties, plume characteristics, and long-range transport over northern India. J. Geophys. Res. Atmos. 5424–5444. https://doi.org/10.1002/2013JD021350.Received

Keating, B.A., Carberry, P.S., Hammer, G.L., Probert, M.E., Robertson, M.J., Holzworth, D., Huth, N.I., Hargrea, J.N.G., 2003. An o v er v iew of APSIM , a model designed for farming systems simulation. Eur. J. Agron. 18, 267–288.

Kedia, S., Ramachandran, S., Holben, B.N., Tripathi, S.N., 2014. Quantification of aerosol type, and sources of aerosols over the Indo-Gangetic Plain. Atmos. Environ. 98, 607–619. https://doi.org/10.1016/j.atmosenv.2014.09.022

Khan, S., Ashraf, H.F., 2015. Analysis of Pakistan' s electric power sector. BlekingeTekniska Hogskola BTH.

Koch, D., Bond, T.C., Streets, D., Unger, N., Werf, G.R. Van Der, 2007. Global impacts of aerosols from particular source regions and sectors. J. Geophys. Res. 112, 1–24. https://doi.org/10.1029/2005JD007024

Krishna Moorthy, K., Suresh Babu, S., Manoj, M.R., Satheesh, S.K., 2013. Buildup of aerosols over the Indian Region. Geophys. Res. Lett. 40, 1011–1014. https://doi.org/10.1002/grl.50165

Kulshrestha, U., Kulshrestha, M.J., Vairamani, R.S.M., Sarkar, A.K., Parashar, D.C., 2001. Investigation of alkaline nature of rain water in India. Water Air Soil Pollut. 131, 1685–1690.

Kulshrestha, U.C., Kulshrestha, M.J., Sekar, R., Sastry, G.S.R., Vairamani, M., 2003. Chemical characteristics of rainwater at an urban site of south-central India. Atmos. Environ. 37, 3019–3026. https://doi.org/10.1016/S1352-2310(03)00266-8

Kumar, M., Parmar, K.S., Kumar, D.B., Mhawish, A., Broday, D.M., Mall, R.K., Banerjee, T., 2018. Long-term aerosol climatology over Indo-Gangetic Plain: Trend, prediction and potential source fields. Atmos. Environ. 180, 37–50. https://doi.org/10.1016/j.atmosenv.2018.02.027

Kumar, M., Raju, M.P., Singh, R.K., Singh, A.K., Singh, R.S., Banerjee, T., 2017. Wintertime characteristics of aerosols over middle Indo-Gangetic Plain: Vertical profile, transport and radiative forcing. Atmos. Res. 183, 268–282.

Kumar, M., Tiwari, S., Murari, V., Singh, A.K., Banerjee, T., 2015. Wintertime characteristics of aerosols at middle Indo-Gangetic Plain: Impacts of regional meteorology and long range transport. Atmos. Environ. 104, 162–175. https://doi.org/10.1016/j.atmosenv.2015.01.014

Kumar, P., Kumar, S., Joshi, L., 2015. Socioeconomic and environmental implications of agricultural residue burning a case study of Punjab, India. Springer Open, New Delhi. https://doi.org/10.1007/978-81-322-2014-5

Kumar, R., Barth, M.C., Nair, V.S., Pfister, G.G., Suresh Babu, S., Satheesh, S.K., Krishna Moorthy, K., Carmichael, G.R., Lu, Z., Streets, D.G., 2015. Sources of black carbon aerosols in South Asia and surrounding regions during the Integrated Campaign for Aerosols, Gases and Radiation Budget (ICARB). Atmos. Chem. Phys. 15, 5415–5428. https://doi.org/10.5194/acp-15-5415-2015

Kumar, R., Barth, M.C., Pfister, G.G., Delle Monache, L., Lamarque, J.F., Archer-Nicholls, S., Tilmes, S., Ghude, S.D., Wiedinmyer, C., Naja, M., Walters, S., 2018. How will air quality change in South Asia by 2050? J. Geophys. Res. Atmos. 123, 1840–1864. https://doi.org/10.1002/2017JD027357

Kumar, R., Barth, M.C., Pfister, G.G., Nair, V.S., Ghude, S.D., Ojha, N., 2015. What controls the seasonal cycle of black carbon aerosols in India? J. Geophys. Res. 120, 7788–7812. https://doi.org/10.1002/2015JD023298

Kumari, B.P., Londhe, A.L., Daniel, S., Jadhav, D.B., 2007. Observational evidence of solar dimming : Offsetting surface warming over India 34, 1–5. https://doi.org/10.1029/2007GL031133

Lacey, F., Henze, D., 2015. Global climate impacts of country-level primary carbonaceous aerosol from solid-fuel cookstove emissions. Environ. Res. Lett. 10, 114003. https://doi.org/10.1088/1748-9326/10/11/114003

Lagzi, I., Mészáros, R., Gelybó, G., Leelőssy, Á., 2013. Atmospheric chemistry. Eötvös Loránd University. https://doi.org/10.1039/c2cs90076a

Lal, D.M., Ghude, S.D., Mahakur, M., Waghmare, R.T., Tiwari, S., Srivastava, M.K., Meena, G.S., Chate, D.M., 2018. Relationship between aerosol and lightning over Indo-Gangetic Plain (IGP), India. Clim. Dyn. 50, 3865–3884. https://doi.org/10.1007/s00382-017-3851-2

Lal, D.M., Ghude, S.D., Patil, S.D., Kulkarni, S.H., Jena, C., Tiwari, S., Srivastava, M.K., 2012. Tropospheric ozone and aerosol long-term trends over the Indo-Gangetic Plain (IGP), India. Atmos. Res. 116, 82–92. https://doi.org/10.1016/j.atmosres.2012.02.014

Latha, R., Murthy, B.S., Lipi, K., Srivastava, M.K., Kumar, M., 2017. Absorbing aerosols, possible implication to crop yield - a comparison between IGB stations. Aerosol Air Qual. Res. 17, 693–705. https://doi.org/10.4209/aaqr.2016.02.0554

Lau, K.M., Kim, K.M., 2006. Observational relationships between aerosol and Asian monsoon rainfall, and circulation. Geophys. Res. Lett. 33, 1–5. https://doi.org/10.1029/2006GL027546

Lau, W.K.M., Kim, M., Kim, K., 2010. Enhanced surface warming and accelerated snow melt in the Himalayas and Tibetan Plateau induced by absorbing aerosols. https://doi.org/10.1088/1748-9326/5/2/025204

Li, C., McLinden, C., Fioletov, V., Krotkov, N., Carn, S., Joiner, J., Streets, D., He, H., Ren, X., Li, Z., Dickerson, R.R., 2017. India is overtaking China as the world's largest emitter of

anthropogenic sulfur dioxide. Sci. Rep. 7, 1–7. https://doi.org/10.1038/s41598-017-14639-8

Li, X., Wagner, F., Peng, W., Yang, J., Mauzerall, D.L., 2017. Reduction of solar photovoltaic resources due to air pollution in China. Proc. Natl. Acad. Sci. 114, 11867–11872. https://doi.org/10.1073/pnas.1711462114

Li, Z., Lau, W.K.-M., Ramanathan, V., G. Wu, Ding, Y., Manoj, M.G., Liu, J., Qian, Y., J. Li, Zhou, T., Fan, J., Rosenfeld, D., Ming, Y., Wang, Y., Huang0, J., Wang, B., Xu, X., Lee, S.-S., Cribb, M., Zhang, F., Yang, X., Zhao, C., Takemura, T., Wang, K., Xia, X., Yin, Y., Zhang, H., Guo, J., Zhai, P.M., Sugimoto, N., Babu, S.S., Brasseur, G.P., 2016. Aerosol and monsoon climate interactions over Asia. Rev. Geophys. 56, 866–929. https://doi.org/10.1002/2015RG000500

Likens, G.E., Wright, R.F., Galloway, J.N., Butler, T.J., 1979. Acid rain. Sci. Amer. 241, 43–51.

Liu, X., Sun, H., Feike, T., Zhang, X., Shao, L., Chen, S., 2016. Assessing the impact of air pollution on grain yield of winter wheat - a case study in the North China plain. PLoS One 11, 1–16. https://doi.org/10.1371/journal.pone.0162655

Lodhi, A., Ghauri, B., Khan, M.R., Rahman, S., Shafique, S., 2009. Particulate matter (PM 2.5) concentration and source apportionment in Lahore. Artic. J. Braz. Chem. Soc 20, 1811–1820. https://doi.org/10.1590/S0103-50532009001000007

Maggs, R., Wahid, A., Shamsi, S.R.A., Ashmore, M.R., 1995. Effects of ambient air pollution on wheat and rice yield in Pakistan. Water. Air. Soil Pollut. 85, 1311–1316.

Mamta, Shrivastava, J., Satsangi, G., Kumar, R., 2015. Assessment of bioaerosol pollution over Indo-Gangetic plain. Environ. Sci. Pollut. Res. 22, 6004–6009.

Mansha, M., Ghauri, B., Rahman, S., Amman, A., 2012. Characterization and source apportionment of ambient air particulate matter (PM2.5) in Karachi. Sci. Total Environ. 425, 176–183. https://doi.org/10.1016/j.scitotenv.2011.10.056

Mao, K.B., Ma, Y., Xia, L., Chen, W.Y., Shen, X.Y., He, T.J., Xu, T.R., 2014. Global aerosol change in the last decade: An analysis based on MODIS data. Atmos. Environ. 94, 680–686. https://doi.org/10.1016/j.atmosenv.2014.04.053

MAPS Working Group, G., 2018. Burden of disease attributable to major air pollution sources in India. Boston, MA.

McCown, R.L., Hammer, G.L., Hargreaves, J.N.G., Holzworth, D.P., Freebairn, D.M., 1996. APSIM : a novel software system for model development , model testing and simulation in agricultural systems research 50, 255–271.

Meehl, G.A., Arblaster, J.M., Collins, W.D., 2008. Effects of black carbon aerosols on the Indian monsoon. J. Clim. 21, 2869–2882. https://doi.org/10.1175/2007jcli1777.1

Mehta, C.R., Chandel, N.S., Senthilkumar, T., 2014. Status, challenges and strategies for farm mechanization in India. AMA, Agric. Mech. Asia, Africa Lat. Am. 45, 43–50.

Mehta, M., 2015. A study of aerosol optical depth variations over the Indian region using thirteen years (2001–2013) of MODIS and MISR Level 3 data. Atmos. Environ. 109, 161–170.

Mehta, M., Singh, R., Singh, A., Singh, N., Anshumali, 2016. Recent global aerosol optical depth variations and trends - A comparative study using MODIS and MISR level 3 datasets. Remote Sens. Environ. 181, 137–150. https://doi.org/10.1016/j.rse.2016.04.004

Ménégoz, M., Krinner, G., Balkanski, Y., Boucher, O., Cozic, A., Lim, S., Ginot, P., Laj, P., Gallée, H., Wagnon, P., Marinoni, A., Jacobi, H.W., 2014. Snow cover sensitivity to black carbon deposition in the Himalayas: From atmospheric and ice core measurements to regional climate simulations. Atmos. Chem. Phys. 14, 4237–4249. https://doi.org/10.5194/acp-14-

4237-2014

Menon, S., Koch, D., Beig, G., Sahu, S., Fasullo, J., Orlikowski, D., 2010. Black carbon aerosols and the third polar ice cap. Atmos. Chem. Phys. 10, 4559–4571.

Mina, U., Chandrashekara, T.K., Kumar, S.N., Meena, M.C., Yadav, S., Tiwari, S., Singh, D., Kumar, P., Kumar, R., 2018. Impact of particulate matter on basmati rice varieties grown in Indo-Gangetic Plains of India: Growth, biochemical, physiological and yield attributes. Atmos. Environ. 188, 174–184. https://doi.org/10.1016/j.atmosenv.2018.06.015

Mishra, A.K., Shibata, T., 2012. Synergistic analyses of optical and microphysical properties of agricultural crop residue burning aerosols over the Indo-Gangetic Basin (IGB). Atmos. Environ. 57, 205–218. https://doi.org/10.1016/j.atmosenv.2012.04.025

Monteith, J.L., 1977. Climate and the efficiency of crop production in Britain. Phil. Trans. R. Soc. Lond. 281, 277–294.

MOP, 2018. Power sector at a glance all India [WWW Document]. India Minist. Power, Policies Publ. URL https://powermin.nic.in/en/content/power-sector-glance-all-india

Murthy, B.S., Latha, R., Manoj Kumar, Mahanti, N.C., 2014. Effect of aerosols on evapo-transpiration. Atmos. Environ. 89, 109–118. https://doi.org/10.1016/j.atmosenv.2014.02.029

Muslehuddin, B.M., Mir, H., Faisal, N., 2004. Recent occurrence of fog over Pakistan (1997 to 2000). Pakistan J. Meteorol. 1, 3–18.

NAAS, 2017. Innovative viable solution to rice residue burning in rice-wheat cropping system through concurrent use of super straw management system-fitted combines and turbo happy seeder. New Delhi.

Nair, S.A., Pai, D.S., Rajeevan, M., 2016. Climatology and trend of cold waves over India during 1971-2010. Mausam 67, 651–658.

Nair, V.S., Moorthy, K.K., Alappattu, D.P., Kunhikrishnan, P.K., George, S., Nair, P.R., Babu, S.S., Abish, B., Satheesh, S.K., Tripathi, S.N., Niranjan, K., Madhavan, B.L., Srikant, V., Dutt, C.B.S., Badarinath, K.V.S., Reddy, R.R., 2007. Wintertime aerosol characteristics over the Indo-Gangetic Plain (IGP): Impacts of local boundary layer processes and long-range transport. J. Geophys. Res. Atmos. 112, 1–15. https://doi.org/10.1029/2006JD008099

NASA, n.d. AERONET Inversion Products [WWW Document]. URL https://aeronet.gsfc.nasa.gov/new_web/Documents/Inversion_products_V2.pdf (accessed 7.5.16).

Niroula, N., Kobayashi, K., Xu, J., 2015. Sunshine duration is declining in Nepal across the period from 1987 to 2010. J. Agric. Meteorol. 71, 15–23. https://doi.org/10.2480/agrmet.D-14-00025

Norman, J.M., Hesketh, J.D., 1980. Micrometeorological methods for predicting environmental effects on photosynthesis, in: Hesketh, J.D., James W. Jones (Eds.), Predicting Photosynthesis for Ecosystem Models. CRC Press, pp. 9–36.

Novakov, T., 2003. Large historical changes of fossil-fuel black carbon aerosols. Geophys. Res. Lett. 30, 1–4. https://doi.org/10.1029/2002GL016345

Ohmura, A., 2009. Observed decadal variations in surface solar radiation and their causes. J. Geophys. Res 114, 0–5. https://doi.org/10.1029/2008JD011290

Oliveira, P.J.C., Davin, E.L., Levis, S., Seneviratne, S.I., 2011. Vegetation-mediated impacts of trends in global radiation on land hydrology: A global sensitivity study. Glob. Chang. Biol. 17, 3453–

3467. https://doi.org/10.1111/j.1365-2486.2011.02506.x

Ozdes, M., 2012. The effect of climate and aerosol on crop production : a case study of Central Asia. Georgia Institute of Technology.

Padmakumari, B., Jaswal, A.K., Goswami, B.N., 2013. Decrease in evaporation over the Indian monsoon region: Implication on regional hydrological cycle. Clim. Change 121, 787–799. https://doi.org/10.1007/s10584-013-0957-3

Pai, D.S., Srivastava, A.K., Nair, S.A., 2017. Heat and cold waves over India, in: Rajeevan, M.N., Nayak, S. (Eds.), Observed Climate Variability and Change over the Indian Region. Springer Geology, pp. 51–72. https://doi.org/10.1007/978-981-10-2531-0

Pai, D.S., Thapliyal, V., Kokate, P.D., 2004. Decadal variation in the heat and cold waves over India during 1971-2000. Mausam 2, 281–292.

Paliwal, U., Sharma, M., Burkhart, J.F., 2016. Monthly and spatially resolved black carbon emission inventory of India: Uncertainty analysis. Atmos. Chem. Phys. 16, 12457–12476. https://doi.org/10.5194/acp-16-12457-2016

Pan, X., Chin, M., Gautam, R., Bian, H., Kim, D., Colarco, P.R., Diehl, T.L., Takemura, T., Pozzoli, L., Tsigaridis, K., Bauer, S., Bellouin, N., 2015. A multi-model evaluation of aerosols over South Asia: Common problems and possible causes. Atmos. Chem. Phys. 15, 5903–5928. https://doi.org/10.5194/acp-15-5903-2015

Pandey, A., Sadavarte, P., Rao, A.B., Venkataraman, C., 2014. Trends in multi-pollutant emissions from a technology-linked inventory for India: II. Residential, agricultural and informal industry sectors. Atmos. Environ. 99, 341–352. https://doi.org/10.1016/j.atmosenv.2014.09.081

Pandey, A., Venkataraman, C., 2014. Estimating emissions from the Indian transport sector with on-road fleet composition and traffic volume. Atmos. Environ. 98, 123–133. https://doi.org/10.1016/j.atmosenv.2014.08.039

Pandey, S.K., Bakshi, H., Vinoj, V., 2016. Recent changes in dust and its impact on aerosol trends over the Indo-Gangetic Plain (IGP), in: SPIE 9876, Remote Sensing of the Atmosphere, Clouds, and Precipitation VI, 98761Z (5 May 2016). pp. 98761Z-9876–10.

Pandey, S.K., Vinoj, V., Landu, K., Babu, S.S., 2017. Declining pre-monsoon dust loading over South Asia: Signature of a changing regional climate. Sci. Rep. 7, 1–10. https://doi.org/10.1038/s41598-017-16338-w

Pandey, V., 2017. Screaming Urbanization and Infrastructural Gap in South Asia: A Critical Analysis, in: Bandyopadhyay, S., Casaca, P., Torre, A., Dentinho, T. (Eds.), Regional Cooperation in South Asia: Socio-Economic, Spatial, Ecological and Institutional Aspects. Springer, pp. 113–130.

Pawar, H., Garg, S., Kumar, V., Sachan, H., Arya, R., Sarkar, C., Chandra, B.P., Sinha, B., 2015. Quantifying the contribution of long-range transport to particulate matter (PM) mass loadings at a suburban site in the north-western Indo-Gangetic Plain (NW-IGP). Atmos. Chem. Phys. 15, 9501–9520. https://doi.org/10.5194/acp-15-9501-2015

Pommier, M., Fagerli, H., Gauss, M., Simpson, D., Sharma, S., Sinha, V., Ghude, S.D., Landgren, O., Nyiri, A., Wind, P., 2018. Impact of regional climate change and future emission scenarios on surface O 3 and PM 2.5 over India. Atmos. Chem. Phys 185194, 103–127. https://doi.org/10.5194/acp-18-103-2018

Poulton, P.L., Rawson, H.M., Dalgliesh, N.P., 2011. Physical constraints to cropping in southern Bangladesh, in: Rawson, H.M. (Ed.), Sustainable Intensification of Rabi Cropping in Southern

Bangaladesh Using Wheat and Mungbean. ACIAR, Canberra, pp. 49–106.

Prasad, A.K., Singh, R.P., Kafatos, M., 2012. Influence of coal-based thermal power plants on the spatial-temporal variability of tropospheric NO2column over India. Environ. Monit. Assess. 184, 1891–1907. https://doi.org/10.1007/s10661-011-2087-6

Prasad, A.K., Singh, R.P., Kafatos, M., 2006. Influence of coal based thermal power plants on aerosol optical properties in the Indo-Gangetic basin. Geophys. Res. Lett. 33, 3–6. https://doi.org/10.1029/2005GL023801

Prasad, A.K., Singh, S., Chauhan, S.S., Srivastava, M.K., Singh, R.P., Singh, R., 2007. Aerosol radiative forcing over the Indo-Gangetic plains during major dust storms. Atmos. Environ. 41, 6289–6301. https://doi.org/10.1016/j.atmosenv.2007.03.060

Prasad, A.K., Yang, K.-H.S., El-Askary, H.M., Kafatos, M., 2009. Melting of major Glaciers in the western Himalayas: evidence of climatic changes from long term MSU derived tropospheric temperature trend (1979–2008).

Praveen, P.S., Ahmed, T., Kar, A., Rehman, I.H., Ramanathan, V., 2012. Link between local scale BC emissions in the Indo-Gangetic plains and large scale atmospheric solar absorption. Atmos. Chem. Phys. 12, 1173–1187. https://doi.org/10.5194/acp-12-1173-2012

Prijith, S.S., Venkata, P., Rao, N., Mohan, M., 2018. Trends of absorption , scattering and total aerosol optical depths over India and surrounding oceanic regions from satellite observations : role of local production , transport and atmospheric dynamics. Environ. Sci. Pollut. Res.

Provençal, S., Kishcha, P., da Silva, A.M., Elhacham, E., Alpert, P., 2017. AOD distributions and trends of major aerosol species over a selection of the world's most populated cities based on the 1st version of NASA's MERRA Aerosol Reanalysis. Urban Clim. 20, 168–191. https://doi.org/10.1016/j.uclim.2017.04.001

Przybysz, A., Sæbø, A., Hanslin, H.M., Gawro, S.W., 2014. Accumulation of particulate matter and trace elements on vegetation as affected by pollution level , rainfall and the passage of time. Sci. Total Environ. 481, 360–369. https://doi.org/10.1016/j.scitotenv.2014.02.072

Raina, V.K., 2009. Himalayan glaciers a state-of-art review of glacial studies, glacial retreat and climate change, MOEF Discussion Paper.

Rajput, M., Agrawal, M., 2005. Physiological and yield responses of pea plants to ambient air pollution. Indian J. Plant Physiol. 9, 9–14.

Rajput, P., Sarin, M., Sharma, D., Singh, D., 2014. Characteristics and emission budget of carbonaceous species from post-harvest agricultural-waste burning in source region of the Indo-Gangetic plain. Tellus, Ser. B Chem. Phys. Meteorol. 66, 1–12. https://doi.org/10.3402/tellusb.v66.21026

Ram, K., Sarin, M.M., 2015. Atmospheric carbonaceous aerosols from Indo-Gangetic Plain and Central Himalaya: Impact of anthropogenic sources. J. Environ. Manage. 148, 153–163.

Ramachandran, S., Kedia, S., 2012. Radiative effects of aerosols over Indo-Gangetic plain: environmental (urban vs. rural) and seasonal variations. Environ. Sci. Pollut. Res. 19, 2159–2171.

Ramachandran, S., Kedia, S., Sheel, V., 2015. Spatiotemporal characteristics of aerosols in India: Observations and model simulations. Atmos. Environ. 116, 225–244. https://doi.org/10.1016/j.atmosenv.2015.06.015

Ramanathan, V., Chung, C., Kim, D., Bettge, T., Buja, L., Kiehl, J.T., Washington, W.M., Fu, Q., Sikka, D.R., Wild, M., 2005. Atmospheric brown clouds: impacts on South Asian climate and

hydrological cycle. Proc. Natl. Acad. Sci. U. S. A. 102, 5326–33. https://doi.org/10.1073/pnas.0500656102

Ramanathan, V., Crutzen, P.J., 2003. New directions: Atmospheric Brown "Clouds." Atmos. Environ. 37, 4033–4035. https://doi.org/10.1016/S1352-2310(03)00536-3

Ramanathan, V, Crutzen, P.J., Kiehl, J.T., Rosenfeld, D., 2001. Aerosols, climate, and the hydrological cycle. Science (80-.). 294, 2119–2124.

Ramanathan, V., Crutzen, P.J., Lelieveld, J., Mitra, a. P., Althausen, D., Anderson, J., Andreae, M.O., Cantrell, W., Cass, G.R., Chung, C.E., Clarke, a. D., Coakley, J. a., Collins, W.D., Conant, W.C., Dulac, F., Heintzenberg, J., Heymsfield, a. J., Holben, B., Howell, S., Hudson, J., Jayaraman, a., Kiehl, J.T., Krishnamurti, T.N., Lubin, D., McFarquhar, G., Novakov, T., Ogren, J. a., Podgorny, I. a., Prather, K., Priestley, K., Prospero, J.M., Quinn, P.K., Rajeev, K., Rasch, P., Rupert, S., Sadourny, R., Satheesh, S.K., Shaw, G.E., Sheridan, P., Valero, F.P.J., 2001. Indian Ocean Experiment: An integrated analysis of the climate forcing and effects of the great Indo-Asian haze. J. Geophys. Res. 106, 28371. https://doi.org/10.1029/2001JD900133

Ramanathan, V., Ramana, M.V., 2005. Persistent , widespread , and strongly absorbing haze over the Himalayan foothills and the Indo-Gangetic Plains. Pure Appl. Geophys. 162, 1609–1626. https://doi.org/10.1007/s00024-005-2685-8

Rastogi, N., Singh, A., Sarin, M.M., Singh, D., 2016. Temporal variability of primary and secondary aerosols over northern India: Impact of biomass burning emissions. Atmos. Environ. 125, 396–403. https://doi.org/10.1016/j.atmosenv.2015.06.010

Rehman, I.H., Ahmed, T., Praveen, P.S., Kar, A., Ramanathan, V., 2011. Black carbon emissions from biomass and fossil fuels in rural India. Atmos. Chem. Phys. 11, 7289–7299. https://doi.org/10.5194/acp-11-7289-2011

Revadekar, J. V., Kothawale, D.R., Patwardhan, S.K., Pant, G.B., Rupa Kumar, K., 2012. About the observed and future changes in temperature extremes over India, in: Natural Hazards. pp. 1133–1155. https://doi.org/10.1007/s11069-011-9895-4

Ricchiazzi, P., Yang, S., Gautier, C., Sowle, D., 1998. SBDART: A research and teaching software tool for plane-parallel radiative transfer in the earth's atmosphere. Bull. Am. Meteorol. Soc. 79, 2101–2114. https://doi.org/10.1175/1520-0477(1998)079<2101:SARATS>2.0.CO;2

Robock, A., Li, H., 2006. Solar dimming and CO2 effects on soil moisture trends. Geophys. Res. Lett. 33, 1–5. https://doi.org/10.1029/2006GL027585

Rosenfeld, D., Rosenfeld, D., Lohmann, U., Raga, G.B., Dowd, C.D.O., Kulmala, M., Fuzzi, S., Reissell, A., Andreae, M.O., 2008. Flood or drought : How do aerosols affect precipitation ? Science (80-.). 321, 1309–1313. https://doi.org/10.1126/science.1160606

Roshan, G.R., Ghanghermeh, A.A., Kong, Q., 2018. Spatial and temporal analysis of outdoor human thermal comfort during heat and cold waves in Iran. Weather Clim. Extrem. 1–10. https://doi.org/10.1016/j.wace.2018.01.005

Rupakheti, D., Adhikary, B., Praveen, P.S., Rupakheti, M., Kang, S., Mahata, K.S., Naja, M., Zhang, Q., Panday, A.K., Lawrence, M.G., 2017. Pre-monsoon air quality over Lumbini, a world heritage site along the Himalayan foothills. Atmos. Chem. Phys. 17, 11041–11063. https://doi.org/10.5194/acp-17-11041-2017

Sadavarte, P., Venkataraman, C., 2014. Trends in multi-pollutant emissions from a technology-linked inventory for India: I. Industry and transport sectors. Atmos. Environ. 99, 353–364. https://doi.org/10.1016/j.atmosenv.2014.09.081

Sadavarte, P., Venkataraman, C., Cherian, R., Patil, N., Madhavan, B.L., Gupta, T., Kulkarni, S.,

Carmichael, G.R., Adhikary, B., 2015. Seasonal differences in aerosol abundance and radiative forcing in months of contrasting emissions and rainfall over northern South Asia. Atmos. Environ. 125, 512–523. https://doi.org/10.1016/j.atmosenv.2015.10.092

Samra, J.S., Singh, G., Ramakrishna, Y., 2003. Cold wave of 2002-03: Impact on agriculture. Central Research Institute for Dryland Agriculture, Hyderabad. India.

Sánchez-Triana, E., Enriquez, S., Afzal, J., Nakagawa, A., Khan, A.S., 2014. Cleaning Pakistan's air: policy options to address the cost of outdoor air pollution. https://doi.org/10.1596/978-1-4648-0235-5

Sarkar, S., Chokngamwong, R., Cervone, G., Singh, R.P., Kafatos, M., 2006. Variability of aerosol optical depth and aerosol forcing over India. Adv. Sp. Res. 37, 2153–2159. https://doi.org/10.1016/j.asr.2005.09.043

Sarkar, S., Singh, R.P., Chauhan, A., 2018. Crop residue burning in Northern India: increasing threat to greater India. J. Geophys. Res. Atmos. 123, 6920–6934. https://doi.org/10.1029/2018JD028428

Satheesh, S., Ramanathan, V., 2000. Large differences in tropical aerosol forcing at the top of the atmosphere and Earth's surface. Nature 405, 60–3. https://doi.org/10.1038/35011039

Sathiyamoorthy, V., Arya, R., Kishtawal, C.M., 2016. Radiative characteristics of fog over the Indo-Gangetic Plains during northern winter. Clim. Dyn. 47, 1793–1806. https://doi.org/10.1007/s00382-015-2933-2

Schuster, G.L., Dubovik, O., Holben, B.N., 2006. Angstrom exponent and bimodal aerosol size distributions. J. Geophys. Res. 111, 1–14. https://doi.org/10.1029/2005JD006328

Sehgal, V.K., Singh, M.R., Chaudhary, A., Jain, N., Pathak, H., 2013. Vulnerability of agriculture to climate change: district level assessment in the Indo-Gangetic plains.

Sen, A., Abdelmaksoud, A.S., Nazeer Ahammed, Y., Alghamdi, M.̧., Banerjee, T., Bhat, M.A., Chatterjee, A., Choudhuri, A.K., Das, T., Dhir, A., Dhyani, P.P., Gadi, R., Ghosh, S., Kumar, K., Khan, A.H., Khoder, M., Maharaj Kumari, K., Kuniyal, J.C., Kumar, M., Lakhani, A., Mahapatra, P.S., Naja, M., Pal, D., Pal, S., Rafiq, M., Romshoo, S.A., Rashid, I., Saikia, P., Shenoy, D.M., Sridhar, V., Verma, N., Vyas, B.M., Saxena, M., Sharma, A., Sharma, S.K., Mandal, T.K., 2017. Variations in particulate matter over Indo-Gangetic Plains and Indo-Himalayan Range during four field campaigns in winter monsoon and summer monsoon: Role of pollution pathways. Atmos. Environ. 154, 200–224. https://doi.org/10.1016/j.atmosenv.2016.12.054

Seyyednejad, S.M., Niknejad, M., Koochak, H., 2011. A review of some different effects of air pollution on plants. Res. J. Environ. Sci. 302–309. https://doi.org/10.3923/rjes.2011.302.309

Shahid, M.Z., Hong, L., Yu-lu, Q.I.U., Shahid, I., 2015. Source sector contributions to aerosol levels in Pakistan. Atmos. Ocean. Sci. Lett. 8, 308–313. https://doi.org/10.3878/AOSL20150049.1

Shen, Y., Liu, C., Liu, M., Zeng, Y., Tian, C., 2010. Change in pan evaporation over the past 50 years in the arid region of China. Hydrol. Process. 231, 225–231. https://doi.org/10.1002/hyp

Shrestha, A., Agrawal, N., Alfthan, B., Bajracharya, S., Maréchal, J., van Oort, B., 2015. The Himalayan climate and water atlas. ICIMOD, Kathmandu.

Shrestha, A.B., Aryal, R., 2011. Climate change in Nepal and its impact on Himalayan glaciers. Reg. Environ. Chang. 11, 65–77. https://doi.org/10.1007/s10113-010-0174-9

Shuai, J., Zhang, Z., Liu, X., Shi, Y.C., Wang, P., Shi, P., 2013. Increasing concentrations of aerosols offset the benefits of climate warming on rice yields during 1980–2008 in Jiangsu Province, China. Reg. Environ. Chang. 13, 287–297. https://doi.org/10.1007/s10113-012-0332-3

Siingh, D., Buchunde, P.S., Singh, R.P., Nath, A., Kumar, S., Ghodpage, R.N., 2014. Lightning and convective rain study in different parts of India. Atmos. Res. 137, 35–48. https://doi.org/10.1016/j.atmosres.2013.09.018

Singh, A., Patwardhan, A., 2012. Spatio-temporal distribution of extreme weather events in India, in: APCBEE Procedia. Ajay Singh, pp. 258–262. https://doi.org/http://dx.doi.org/10.1016/j.apcbee.2012.03.042

Singh, A., Rastogi, N., Patel, A., Singh, D., 2016. Seasonality in size-segregated ionic composition of ambient particulate pollutants over the Indo-Gangetic Plain: Source apportionment using PMF. Environ. Pollut. 219, 906–915. https://doi.org/10.1016/j.envpol.2016.09.010

Singh, A., Rastogi, N., Sharma, D., Singh, D., 2015. Inter and Intra-Annual variability in aerosol characteristics over northwestern Indo-Gangetic Plain. Aerosol Air Qual. Res. 15, 376–386. https://doi.org/10.4209/aaqr.2014.04.0080

Singh, A.K., Mondal, G.C., Kumar, S., Singh, K.K., Kamal, K.P., Sinha, A., 2007. Precipitation chemistry and occurrence of acid rain over Dhanbad , coal city of India. Env. Monit Assess 215, 99–110. https://doi.org/10.1007/s10661-006-9243-4

Singh, A.L., Asgher, M.S., 2005. Impact of brick kilns on land use/landcover changes around Aligarh city, India. Habitat Int. 29, 591–602. https://doi.org/10.1016/j.habitatint.2004.04.010

Singh, G., 2015. Agricultural mechanisation development in India. Indian J. Agric. Econ. 70, 64–82.

Singh, J., Bhattacharya, B.K., Kumar, M., 2012. Solar radiation and evaporation trend over India. J. Earth Sci. Eng. 2, 160–165.

Singh, K.P., Singh, V.K., 2007. Hydrochemistry of wet atmospheric precipitation over an urban area in northern Indo-Gangetic plains. Env. Monit Assess 131, 237–254. https://doi.org/10.1007/s10661-006-9472-6

Singh, N., Mhawish, A., Deboudt, K., Singh, R.S., Banerjee, T., 2017a. Organic aerosols over Indo-Gangetic Plain: Sources, distributions and climatic implications. Atmos. Environ. 157, 69–74. https://doi.org/10.1016/j.atmosenv.2017.03.008

Singh, N., Murari, V., Kumar, M., Barman, S.C., Banerjee, T., 2017b. Fine particulates over South Asia: Review and meta-analysis of PM2.5 source apportionment through receptor model. Environ. Pollut. 223, 121–136. https://doi.org/10.1016/j.envpol.2016.12.071

Singh, S., Singh, D., 2010. Recent Fog trends and its impact on wheat productivity in NW plains in India, in: 5th International Conference on Fog, Fog Collection and Dew Münster, Germany, 25–30 July 2010. Münster, Germany.

Singh, S., Soni, K., Bano, T., Tanwar, R.S., Nath, S., Arya, B.C., 2010. Clear-sky direct aerosol radiative forcing variations over mega-city Delhi. Ann. Geophys. 28, 1157–1166. https://doi.org/10.5194/angeo-28-1157-2010

Smith, K.R., Sagar, A., 2014. Making the clean available: Escaping India's Chulha Trap. Energy Policy 75, 410–414. https://doi.org/10.1016/j.enpol.2014.09.024

Soni, K., Parmar, K.S., Kapoor, S., Kumar, N., 2016. Statistical variability comparison in MODIS and AERONET derived aerosol optical depth over Indo-Gangetic Plains using time series modeling. Sci. Total Environ. 553, 258–265. https://doi.org/10.1016/j.scitotenv.2016.02.075

Srivastava, A.K., Dey, S., Tripathi, S.N., 2012a. Aerosol Characteristics over the Indo-Gangetic Basin: Implications to Regional Climate, in: Hayder Abdul-Razzak (Ed.), Atmospheric Aerosols - Regional Characteristics - Chemistry and Physics. InTech, pp. 47–79. https://doi.org/DOI: 10.5772/47782

Srivastava, A.K., Singh, S., Tiwari, S., Bisht, D.S., 2012b. Contribution of anthropogenic aerosols in direct radiative forcing and atmospheric heating rate over Delhi in the Indo-Gangetic Basin. Environ. Sci. Pollut. Res. 19, 1144–1158. https://doi.org/10.1007/s11356-011-0633-y

Srivastava, R., 2016. Trends in aerosol optical properties over South Asia. Int. J. Climatol. n/a-n/a. https://doi.org/10.1002/joc.4710

Srivastava, R., Ramachandran, S., 2013. The mixing state of aerosols over the Indo-Gangetic Plain and its impact on radiative forcing. Q. J. R. Meteorol. Soc. 139, 137–151.

Srivastava, Sanjay Kumar, Sharma, A.R., Sachdeva, K., 2016. Spatial and Temporal Variability of Fog Over the Indo-Gangetic Plains, India. Int. J. Environ. Ecol. Eng. 10, 1042–1057.

Srivastava, S K, Sharma, A.R., Sachdeva, K., 2016. A Ground Observation Based Climatology of Winter Fog: Study over the Indo-Gangetic Plains, India. Int. J. Environ. , Chem. Ecol. Geophys. Eng. 10, 686–697.

Stanhill, G., Cohen, S., 2001. Global dimming: a review of the evidence for a widespread and significant reduction in global radiation with discussion of its probable causes and possible agricultural consequences. Agric. For. Meteorol. 107, 255–278.

Steiner, A.L., Chameides, W.L., 2005. Aerosol-induced thermal effects increase modelled terrestrial photosynthesis and transpiration. Tellus B 57B, 404–411.

Stohl, A., Aamaas, B., Amann, M., Baker, L.H., Bellouin, N., Berntsen, T.K., Boucher, O., Cherian, R., Collins, W., Daskalakis, N., Dusinska, M., Eckhardt, S., Fuglestvedt, J.S., Harju, M., Heyes, C., Hodnebrog, Hao, J., Im, U., Kanakidou, M., Klimont, Z., Kupiainen, K., Law, K.S., Lund, M.T., Maas, R., MacIntosh, C.R., Myhre, G., Myriokefalitakis, S., Olivié, D., Quaas, J., Quennehen, B., Raut, J.C., Rumbold, S.T., Samset, B.H., Schulz, M., Seland, Shine, K.P., Skeie, R.B., Wang, S., Yttri, K.E., Zhu, T., 2015. Evaluating the climate and air quality impacts of short-lived pollutants. Atmos. Chem. Phys. 15, 10529–10566. https://doi.org/10.5194/acp-15-10529-2015

Strada, S., Unger, N., 2016. Potential sensitivity of photosynthesis and isoprene emission to direct radiative effects of atmospheric aerosol pollution. Atmos. Chem. Phys 16, 4213–4234. https://doi.org/10.5194/acp-16-4213-2016

Streets, D.G., Bond, T.C., Carmichael, G.R., Fernandes, S.D., Fu, Q., He, D., Klimont, Z., Nelson, S.M., Tsai, N.Y., Wang, M.Q., Woo, J.-H., Yarber, K.F., 2003. An inventory of gaseous and primary aerosol emissions in Asia in the year 2000. J. Geophys. Res. Atmos. 108. https://doi.org/10.1029/2002JD003093

Streets, D.G., Wu, Y., Chin, M., 2006. Two-decadal aerosol trends as a likely explanation of the global dimming / brightening transition. Geophys. Res. Lett. 33, 1–4. https://doi.org/10.1029/2006GL026471

Sun, H., Zhang, X., Wang, E., Chen, S., Shao, L., Qin, W., 2016. Field Crops Research Assessing the contribution of weather and management to the annual yield variation of summer maize using APSIM in the North China Plain. F. Crop. Res. 194, 94–102. https://doi.org/10.1016/j.fcr.2016.05.007

Syed, F.S., Körnich, H., Tjernström, M., 2012. On the fog variability over south Asia. Clim. Dyn. 39, 2993–3005. https://doi.org/10.1007/s00382-012-1414-0

Taneja, G., Pal, B.D., Joshi, P.K., Aggarwal, P.K., N. K., T., 2014. Farmerss Preferences for Climate-Smart Agriculture: An Assessment in the Indo-Gangetic Plain (No. 01337), Discussion Paper. New Delhi. https://doi.org/10.2139/ssrn.2420547

Taneja, K., Ahmad, S., Ahmad, K., Attri, S.D., 2016. Time series analysis of aerosol optical depth

over New Delhi using Box e Jenkins ARIMA modeling approach. Atmos. Pollut. Res. 7, 585–596. https://doi.org/10.1016/j.apr.2016.02.004

Tao, W., Chen, J., Li, Z., Wang, C., Zhang, C., 2012. Impact of aerosols on convective clouds and precipitation. Rev. Geophys. 50, 1–62. https://doi.org/10.1029/2011RG000369.1.INTRODUCTION

TERI, 2016. Air pollutant emissions scenario for India, The Energy and Resource Institute. TERI, New Delhi.

Tie, X., Huang, R.-J., Dai, W., Cao, J., Long, X., Su, X., Zhao, S., Wang, Q., Li, G., 2016. Effect of heavy haze and aerosol pollution on rice and wheat productions in China, Scientific Reports. Nature Publishing Group. https://doi.org/10.1038/srep29612

Tiwari, S., Dumka, U.C., Kaskaoutis, D.G., Ram, K., Panicker, A.S., Srivastava, M.K., Tiwari, Shani, Attri, S.D., Soni, V.K., Pandey, A.K., 2016a. Aerosol chemical characterization and role of carbonaceous aerosol on radiative effect over Varanasi in central Indo-Gangetic Plain. Atmos. Environ. 125, 437–449. https://doi.org/10.1016/j.atmosenv.2015.07.031

Tiwari, Suresh, Hopke, P.K., Thimmaiah, D., Dumka, U.C., Srivastava, A.K., Bisht, D.S., Rao, P.S.P., Chate, D.M., Srivastava, M.K., Tripathi, S.N., 2016. Nature and sources of ionic species in precipitation across the indo-gangetic plains, India. Aerosol Air Qual. Res. 16, 943–957. https://doi.org/10.4209/aaqr.2015.06.0423

Tiwari, S, Pandithurai, G., Attri, S.D., Srivastava, A.K., Soni, V.K., Bisht, D.S., Kumar, V.A., Srivastava, M.K., 2015. Aerosol optical properties and their relationship with meteorological parameters during wintertime in Delhi, India. Atmos. Res. 153, 465–479. https://doi.org/10.1016/j.atmosres.2014.10.003

Tiwari, S., Payra, S., Mohan, M., Verma, S., Bisht, D.S., 2011. Visibility degradation during foggy period due to anthropogenic urban aerosol at Delhi, India. Atmos. Pollut. Res. 2, 116–120. https://doi.org/10.5094/apr.2011.014

Tiwari, S., Tunved, P., Hopke, P.K., Srivastava, A.K., Bisht, D.S., Pandey, A.K., 2016b. Observations of ambient trace gas and PM10concentrations at Patna, Central Ganga Basin during 2013-2014: The influence of meteorological variables on atmospheric pollutants. Atmos. Res. 180, 138–149. https://doi.org/10.1016/j.atmosres.2016.05.017

Tiwari, Suresh, Hopke, P.K., Pipal, A.S., Srivastava, A.K., Bisht, D.S., Tiwari, Shani, Singh, A.K., Soni, V.K., Attri, S.D., 2015. Intra-urban variability of particulate matter (PM2.5 and PM10) and its relationship with optical properties of aerosols over Delhi, India. Atmos. Res. 166, 223–232. https://doi.org/10.1016/j.atmosres.2015.07.007

Tripathi, S.N., Tare, V., Chinnam, N., Srivastava, A.K., Dey, S., Agarwal, A., Kishore, S., Lal, R.B., Manar, M., Kanawade, V.P., Chauhan, S.S.S., Sharma, M., Reddy, R.R., Gopal, K.R., Narasimhulu, K., Reddy, L.S.S., Gupta, S., Lal, S., 2006. Measurements of atmospheric parameters during Indian Space Research Organization Geosphere Biosphere Programme Land Campaign II at a typical location in the Ganga basin: 1. Physical and optical properties. J. Geophys. Res. Atmos. 111, 1–14. https://doi.org/10.1029/2006JD007278

Tzanis, C., Varotsos, C.A., 2016. Tropospheric aerosol forcing of climate : a case study for the greater area of Greece. Int. J. Remote Sens. 9, 2507–2517. https://doi.org/10.1080/01431160701767575

UNEP & WMO, 2011. Integrated assessment of black carbon and tropospheric ozone, United Nations Environment Programme (UNEP) & World Meteorolocial Organization.

United States Environmental Protection Agency, 2012. Black Carbon and Its Effects on Climate, Report to Congress on Black Carbon.

US Climate Change Science Program, 2009. Atmospheric aerosol properties and climate impacts. Washington DC.

Vadrevu, K.P., Ellicott, E., Badarinath, K.V.S., Vermote, E., 2011. MODIS derived fire characteristics and aerosol optical depth variations during the agricultural residue burning season, north India. Environ. Pollut. 159, 1560–1569. https://doi.org/10.1016/j.envpol.2011.03.001

Venkataraman, C., Brauer, M., Tibrewal, K., Sadavarte, P., Ma, Q., Cohen, A., 2018. Source influence on emission pathways and ambient PM 2 . 5 pollution over India (2015 – 2050). Atmos. Chem. Phys 18, 8017–8039. https://doi.org/https://doi.org/10.5194/acp-18-8017-2018

Villalobos, A.M., Amonov, M.O., Shafer, M.M., Devi, J.J., Gupta, T., Tripathi, S.N., Rana, K.S., Mckenzie, M., Bergin, M.H., Schauer, J.J., 2015. Source apportionment of carbonaceous fine particulate matter (PM2.5) in two contrasting cities across the Indo–Gangetic Plain. Atmos. Pollut. Res. 6, 398–405. https://doi.org/10.5094/APR.2015.044

Wahid, A., Campus, Q., 1995. Effects of air pollution on rice yield in the Pakistan Punjab. Environ. Pollut. 90, 323–329.

Wang, Y., Yang, Y., Zhao, N., Liu, C., Wang, Q., 2012. The magnitude of the effect of air pollution on sunshine hours in China. J. Geophys. Res. 117, 1–9. https://doi.org/10.1029/2011JD016753

Wang, Y.P., Jarvis, P.G., 1990. Description and validation of an array m o d e l - MAESTRO. Agric. For. Meteorol. 51, 257–280.

Wang, Y.W., Yang, Y.H., Zhou, X.Y., Zhao, N., Zhang, J.H., 2014. Air pollution is pushing wind speed into a regulator of surface solar irradiance in China. Environ. Res. Lett. 9, 1–11. https://doi.org/10.1088/1748-9326/9/5/054004

Weerakkody, U., Dover, J.W., Mitchell, P., Reiling, K., 2018. Evaluating the impact of individual leaf traits on atmospheric particulate matter accumulation using natural and synthetic leaves. Urban For. Urban Green. 30, 98–107. https://doi.org/10.1016/j.ufug.2018.01.001

Wester, P., Mishra, A., Mukherji, A., Shrestha, A.B., Change, C., 2019. The Hindu Kush Himalaya assessment : mountains, climate change, sustainability and people. International Center for Integrated Mountain Development (ICIMOD), Hindu Kush Himalayan Monitoring and Assessment Programme (HIMAP) and Springer Open, Kathmandu Nepal.

WHO, 2018. Ambient Air Quality Database, WHO, April 2018 [WWW Document]. URL http://www.who.int/airpollution/en/ (accessed 3.20.19).

WHO, 2015. Reducing global health risks Through mitigation of short-lived climate pollutants. Report.

WHO, 2006. WHO Air quality guidelines for particulate matter, ozone, nitrogen dioxide and sulfur dioxide: global update 2005: summary of risk assessment, Geneva: World Health Organization. https://doi.org/10.1016/0004-6981(88)90109-6

Wild, M., 2012. Enlightening Global Dimming and Brightening. Bull. Am. Meteorol. Soc. 93, 27–37. https://doi.org/10.1175/BAMS-D-11-00074.1

Wild, M., 2009. Global dimming and brightening: A review. J. Geophys. Res. 114, 1–31. https://doi.org/10.1029/2008JD011470

Wild, M., Roesch, A., Ammann, C., 2012. Global dimming and brightening - evidence and agricultural implications. CAB Rev. Perspect. Agric. Vet. Sci. Nutr. Nat. Resour. 7, 1–7. https://doi.org/10.1079/PAVSNNR20127003

Wild, M., Trüssel, B., Ohmura, A., Long, C.N., König-Langlo, G., Dutton, E.G., Tsvetkov, A., 2009. Global dimming and brightening: An update beyond 2000. J. Geophys. Res. 114, D00D13. https://doi.org/10.1029/2008JD011382

WMO, 1975. International Cloud Atlas. Volume I: Manual on the observation of clouds and other meteors, WMO Publication. Geneva, Switzerland.

Xia, X., Li, Z., Wang, P., Chen, H., Cribb, M., 2007. Estimation of aerosol effects on surface irradiance based on measurements and radiative transfer model simulations in northern China. J. Geophys. Res. 112, 1–11. https://doi.org/10.1029/2006JD008337

Xia, Xiangao, Wild, M., Mercado, L.M., Wang, K.C., Dickinson, R.E., Satheesh, S.K., Ramanathan, V., Conant, W.C., Dumka, U.C., Xia, X.A., Li, Z.Q., Chen, H.B., Cribb, M., Huttunen, J., Gueymard, C., Badescu, V., Reno, M.J., Hansen, C.W., Stein, J.S., Gueymard, C.A., Ruiz-Arias, J.A., Conant, W., Allen, R.J., Norris, J.R., Wild, M., Long, C.N., Ackerman, T.P., Xia, X., Levy, R., Ohmura, A., Hinkelman, L.M., Stackhouse, P.W., Wielicki, B.A., Zhang, T.P., Wilson, S.R., Qiu, J.Q., Diermendjian, D., Gueymard, C., Garrison, J., Eck, T., Holben, B.N., Eck, T.F., Dubovik, O., King, M.D., García, O.E., Li, Z., Lee, K., Wang, Y., Xin, J., Hao, W., 2015. Parameterization of clear-sky surface irradiance and its implications for estimation of aerosol direct radiative effect and aerosol optical depth. Sci. Rep. 5, 14376. https://doi.org/10.1038/srep14376

Xiao, D., Tao, F., 2016. Contributions of cultivar shift , management practice and climate change to maize yield in North China Plain in 1981 – 2009. Int. J. Biometeorol. 60, 1111–1122. https://doi.org/10.1007/s00484-015-1104-9

Xiao, D., Tao, F., 2014. Contributions of cultivars , management and climate change to winter wheat yield in the North China Plain in the past three decades. Eur. J. Agron. 52, 112–122. https://doi.org/10.1016/j.eja.2013.09.020

Xu, J., Bergin, M.H., Greenwald, R., Russell, P.B., 2003. Direct aerosol radiative forcing in the Yangtze delta region of China : Observation and model estimation. J. Geophys. Res. 108, 1–12. https://doi.org/10.1029/2002JD002550

Xu, Y., Ramanathan, V., Washington, W.M., 2016. Observed high-altitude warming and snow cover retreat over Tibet and the Himalayas enhanced by black carbon aerosols. Atmos. Chem. Phys. 16, 1303–1315. https://doi.org/10.5194/acp-16-1303-2016

Yang, L., Tulen, I., Kok, L.J. De, Zheng, Y., 2002. SO2 , NO X and acid deposition problems in China - impact on agriculture. Phyt. 42, 255–264.

Yang, X., Asseng, S., Wong, M.T.F., Yu, Q., Li, J., Liu, E., 2013. Quantifying the interactive impacts of global dimming and warming on wheat yield and water use in China. Agric. For. Meteorol. 182–183, 342–351. https://doi.org/10.1016/j.agrformet.2013.07.006

Yasmeen, Z., Rasul, G., Zahid, M., 2012. Impact of aerosols on winter fog of Pakistan. Pakistan J. Meteorol. 8, 21–30.

Yasunari, T.J., Bonasoni, P., Laj, P., Fujita, K., Vuillermoz, E., Marinoni, A., Cristofanelli, P., Duchi, R., Tartari, G., Lau, K.-M., 2010. Estimated impact of black carbon deposition during pre-monsoon season from Nepal Climate Observatory -- Pyramid data and snow albedo changes over Himalayan glaciers. Atmos. Chem. Phys. 10, 6603–6615.

Yue, X., Unger, N., 2017. Aerosol optical depth thresholds as a tool to assess diffuse radiation fertilization of the land carbon uptake in China. Atmos. Chem. Phys 17, 1329–1342. https://doi.org/10.5194/acp-17-1329-2017

Zaman, S., 2009. Solar dimming in Bangladesh and its potential impacts on rice evapotranspiration and production. Bangaladesh University of Engineering and Technology.

Zhang, M., Mcsaveney, M.J., 2018. Is air pollution causing landslides in China ? Earth Planet. Sci. Lett. 481, 284–289. https://doi.org/10.1016/j.epsl.2017.10.045

Zhang, Q., Streets, D.G., Carmichael, G.R., He, K.B., Huo, H., Kannari, A., Klimont, Z., Park, I.S., Reddy, S., Fu, J.S., Chen, D., Duan, L., Lei, Y., Wang, L.T., Yao, Z.L., 2009. Asian emissions in 2006 for the NASA INTEX-B mission. Atmos. Chem. Phys. 9, 5131–5153. https://doi.org/10.5194/acp-9-5131-2009

Zhou, L., Chen, X., Tian, X., 2018. The impact of fi ne particulate matter (PM 2 . 5) on China ' s agricultural production from 2001 to 2010. J. Clean. Prod. 178, 133–141. https://doi.org/10.1016/j.jclepro.2017.12.204

Zhuang, B.L., Li, S., Wang, T.J., Deng, J.J., Xie, M., Yin, C.Q., Zhu, J.L., 2013. Direct radiative forcing and climate effects of anthropogenic aerosols with different mixing states over China. Atmos. Environ. 79, 349–361. https://doi.org/10.1016/j.atmosenv.2013.07.004

Chapter 3

Trends in winter fog events in the Terai region of Nepal

This chapter addresses the research sub-question no 1. This chapter has been published in Agricultural and Forest Meteorology as described in preface.

Agricultural and Forest Meteorology 259 (2018) 118–130

Contents lists available at ScienceDirect

Agricultural and Forest Meteorology

journal homepage: www.elsevier.com/locate/agrformet

Trends in winter fog events in the Terai region of Nepal

Shreemat Shrestha*, Graham A. Moore, Murray C. Peel

Department of Infrastructure Engineering, University of Melbourne, Parkville, Melbourne, Victoria 3010, Australia

ARTICLE INFO

Keywords:
Fog
Trend
Terai
Visibility
Man Kendall
Crop
Nepal

ABSTRACT

Winter fog events of the Indo Gangetic plain (IGP) including the Terai area of Nepal are considered to be one of the important public concerns due to their effect on people's health, transportation, and agriculture. Unlike the IGP area of India, Pakistan and Bangladesh there are only very few fog related studies reported about the Terai region of Nepal. This study is carried out to study the occurrence of fog in the Terai region of Nepal by analysing the historical visibility data from 1980 to 2015 at four airports in the region (Nepalgunj, Bhairahawa, Simara and Biratnagar). It was found that the fog events in the Terai start in the month of November, reach the peak in December/January and end by the end of February. The average number of foggy days ranged from 24 days to 56 days per annum and average number of day-time foggy hours varied from 71 to 169 in the study. Visibility during winter is decreasing at all stations during the study period. The Man Kendall test indicated fog related parameters such as foggy days, foggy hours, dense foggy days, dense foggy hours have increasing trends at least at 0.1 level of statistical significance during the study period. The increasing trend of foggy days and daytime foggy hours may reduce winter crop production and negatively affect the food security of the Terai region of Nepal.

1. Introduction

Winter fog events have been a regular phenomenon in the North Indian Indo-Gangetic Plain (IGP), including the southern Nepalese Terai plain area, since 1990 (Manandhar, 2006). Increased fog events not only reduce Photosynthetically Active Radiation (PAR), but also reduce the air temperature with an observed increase in cold waves, which were found to be statistically significant in the Terai area of Nepal (Manandhar et al., 2011). As the Terai is considered to be the food basket of Nepal, the effect of fog on crop production is not only important for the livelihood of farmers in the Terai, but also the food security of the country. Here we study trends in fog events in the Terai over the last three decades and develop a simple empirical model to estimate fog events based on routinely collected meteorological data.

Fog is defined as a suspension of very small, usually microscopic, water droplets in the air that reduce visibility to less than 1000 m at the Earth's surface (WMO, 1975). Atmospheric pollution has a direct relationship with fog occurrence because particles emitted to the atmosphere act as Cloud Condensation Nuclei (CCN), which are essential for the formation of fog. Air pollution is considered to be a key environmental issue for South Asian countries *viz.* India, Pakistan, Nepal, Bangladesh and Afghanistan (UNEP and DA, 2014). The impact of air pollution has become severe in this region due to very high levels of particulate matter in the atmosphere, resulting in 40 South Asian cities being among the 100 most polluted cities in the world (WHO, 2016). The effects of air pollution is not only limited to urban centres, it has become a regional as well as global problem due to the long range transport of aerosols (Ramanathan and Feng, 2009). MODIS imaging has revealed aerosol loading has a significant impact on fog/low cloud occurrence during winter across the Indo Gangetic Plain (IGP) ranging up to 3000 km in length (spreading from Pakistan in the west to Bangladesh) and 400 km wide, including the plain area of Nepal and Northern India (Gautam et al., 2007).

Fog records at Hisar, India (western IGP), from 1992 to 2008 clearly indicate fog event occurrence is increasing at the rate of 2 days per season during that period (Singh and Singh, 2010). Based upon analysis of observational fog occurrence data in south Asia during 1976–2010, Syed et al. (2012) reported fog frequency increased by 3 times during the last 35 years. Similarly, analysis of fog characteristics over the Indian IGP from 1971 to 2010, found the frequency of fog occurrence increased significantly during December and January over the last four decades (Srivastava et al., 2016). Syed et al. (2012) analysed visibility data from 82 IGP stations across India, Pakistan and Bangladesh for December, January and February during 1976–2000 and found the Western IGP (Punjab, Haryana and Uttar Pradesh) was most affected by fog with more than 18% of winter days being foggy during the study period. Syed et al. (2012) also found the trend in fog occurrence in the region increased in 3 steps: step 1 (1976–1989) with a mean fog

* Corresponding author.
E-mail address: shreemats@student.unimelb.edu.au (S. Shrestha).

https://doi.org/10.1016/j.agrformet.2018.04.018
Received 24 August 2017; Received in revised form 17 April 2018; Accepted 25 April 2018
Available online 03 May 2018

fraction of 6.1%; step 2 (1990–1997) with a mean fog fraction of 10.1%; and step-3 (1998–2010) with a mean fog fraction of 19.5%. By using the Mann-Kendall test, Srivastava et al. (2016) concluded that there is an increasing trend of fog occurrence in the entire IGP with 95% confidence level.

The increasing trend in dense fog events in winter in the IGP has negatively impacted the day-to-day life of millions of people living in the region through frequent flight / train delays due to poor visibility (Jenamani, 2007). Along with reduced visibility, the increased fog events have changed meteorological conditions in winter with a decrease in day-time temperature and an increase in night-time temperature (Aslam, 2012), due to fog reducing solar radiation at the surface during day-time and absorbing night-time long-wave radiation emitted from the surface. Analysing monthly cloud data over the IGP, Sathiyamoorthy et al. (2016) found that fog episodes exerted significant radiative cooling in the IGP, even up to 50 Wm^{-2}. The increase in fog events in the north western plains of India has also been reported to affect the growth and development of the wheat crop due to reduced, or no, photo-synthetically active radiation (PAR), cold stress and congenial conditions for disease and insect pest development (Singh and Singh, 2010).

Although there have been several fog related studies in the Indian and Pakistan sections of the IGP, there are few results reported for the Terai section of the IGP in Nepal. Analysing 36 years of daily temperature records (from 1971 to 2006) in Nepal, Baidya et al. (2008) found that the minimum value of daily maximum temperature trend in the plain area of Nepal is different to that in the hill and mountain regions. In the Terai, the minimum value of maximum temperature and the diurnal temperature range were found to have decreasing trends during winter. In the IGP area of the Koshi basin, the maximum temperature in winter and the pre monsoon season was found to have a statistically significant decreasing trend with an increasing number of cold days in winter between 1975 and 2010 (Shrestha et al., 2016). Baidya et al. (2008) mentioned that decreasing trend of maximum temperature and diurnal temperature in winter in the Terai stations could be due to the increased occurrence of fog events in the Terai region in recent decades. Manandhar (2006) observed that in the Terai continuous fog events with brief openings during winter blocked solar radiation reaching the ground and resulted in the maximum temperature in the afternoon remaining low and near to the minimum temperature, which creates a cold wave situation. Cold waves are one of the important disaster events that occur in Nepal during winter. It is reported that there have been 821 deaths due to cold waves in Nepal since 1990, of which 724 are reported in the Terai region, with the death rate increasing after 2002 (DesInventor, 2015). Similarly, fog is reported as unmeasured weather events in Terai which have considerably affected plant growth during winter over last fifteen years (Smadja et al., 2015). Increased winter fog has become an important issue due to its enormous effect on the health, agriculture, transport and livelihood of the people of the Terai region of Nepal. To better understand the change in meteorological conditions in the Terai during winter, there is a need for a systematic study of fog events in this region. This study aims to analyse past fog events in the Terai region of Nepal and search for a relationship between meteorological conditions and fog events in this region. In Nepal, systematic fog related data have not been collected, so developing a relationship between fog events and meteorological parameters is expected to help assess fog behaviour from more readily available meteorological observations.

2. Methodology

2.1. Study Area

The Terai region of Nepal is a narrow plain area extending from east to west along the foothills of the Himalaya (Fig. 1) and is considered to be an extension of the Gangetic plain of India (GON, 2011). The elevation of the Terai region ranges from 60 m to 200 m and it has a sub-tropical climate. The average monthly maximum temperature, minimum temperature and rainfall of selected stations in the Terai are presented in Fig. 2. Most rainfall (more than 80%) occurs in the monsoon season (June–September) in Nepal. With flat land and the availability of irrigation facilities, agriculture is the major economic activity in the Terai, with rice, wheat, maize, lentil, and sugarcane as the major crops. The 2001 and 2011 census data indicated that the population growth rate in the Terai was higher (1.71%) than in the Hill Districts (1.06%) and Mountain Districts (0.54%) during 2001–2011, which was mainly due to increased migration from the hill and mountain districts to the Terai (CBS, 2016). Even though the Terai region occupies only about 17 percent of the land area of Nepal, it is considered to be a very important region of Nepal as it is home to more than 50 percent of the Nepalese population and is the food basket of the country (CBS, 2015).

2.2. Data and methods

Weather reports in Meteorological Terminal Air Report (METAR) format are recorded in major airports of the Terai and are utilised mainly for aviation purposes. Apart from other regular meteorological information, visibility is also recorded in METAR datasheets. The database of METAR observations is not maintained systematically in Nepal. Historical meteorological and visibility data from METAR datasheets at four representative stations in the Terai, as listed in Table 1, were collected by the lead author from the Nepalese Department of Hydrology and Meteorology (DHM) and transcribed to electronic form for this study. Trained meteorologists are involved in recording and monitoring meteorological data (including visibility data) at airports in Nepal and the METAR report follows a standard protocol to obtain consistent quality data (personal communication with DHM Officials). Transcription of visibility data from each METAR record sheet to electronic form was cross-checked entirely to eliminate mistakes. METAR visibility observations at 3 h intervals (0:0 UTC, 3:0 UTC, 6:0 UTC, 9:0 UTC and 12:0 UTC; local time is UTC + 5:45) were used to study fog events during winter months (November, December, January and February) at these four stations. The time of sun rise and sun set in the study months were calculated based on Meeus (1999). The time of civil dawn (sun 6 degrees below the horizon) and civil dusk (sun 6 degrees below the horizon) was calculated in winter months at each station to discard poor visibility data recorded during night-time hours. Accordingly, the visibility data recorded at 0:0 UTC and 12:0 UTC at each station under study were omitted from the analysis. In the study area the poor visibility during the study period is assumed to be only due to fog because other recorded reason of low visibility such as smoke, dust storm etc. was not found to be reported so far. Based on the visibility data, fog events and dense fog events were identified as occurring when visibility was less than 1000 m and 200 m respectively. The number of foggy hours and dense foggy hours in a day were estimated by assuming that if it was foggy at the observation time, then the fog persisted from 1.5 h before the observation time to 1.5 h after. Therefore a maximum of 9 foggy hours was assigned to the day light hours over the winter period.

The Mann Kendall test, as described by Gilbert (1987), was applied to determine whether statistical trends in visibility/opacity, foggy days and dense foggy days during winter months existed at the four Terai stations. This nonparametric test performs well, even with missing values and outliers, and is widely used in trend analysis of environmental data (Connor et al., 2012, Guerreiro et al., 2014; Salmi et al., 2002) and has been successfully used in trend analysis of fog in India (Srivastava et al., 2016). In the Mann Kendall test the trend is assumed to be monotonic and there should be no seasonal cycle in the data. To avoid the seasonal/monthly cycle, only the opacity, foggy days and dense foggy days in each month during winter and over the whole winter season were analysed. In this test, the null hypothesis (H_o) is that there is no trend in visibility, foggy days, dense foggy days, foggy hours and

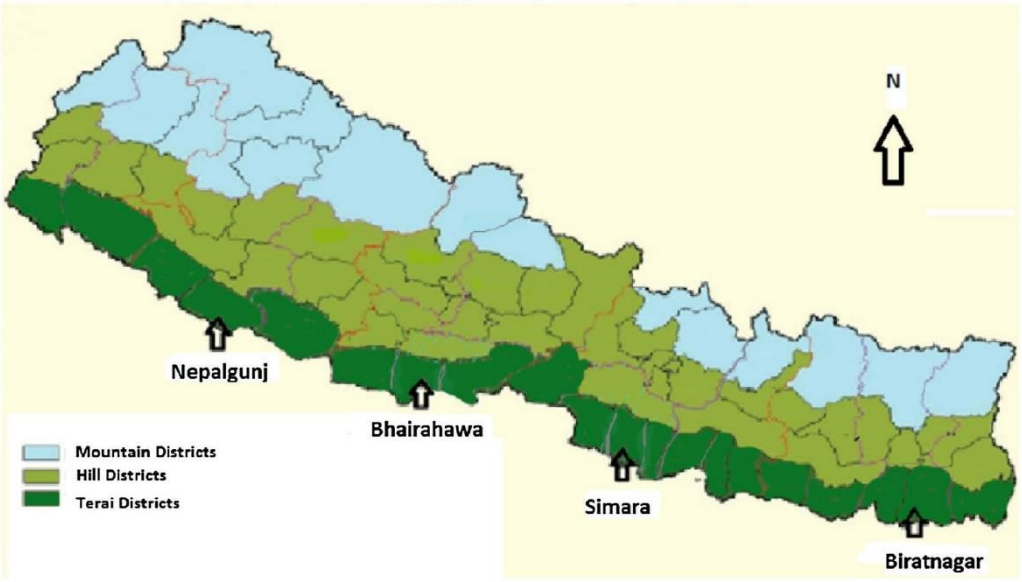

Fig. 1. The study area (Terai region of Nepal) with studied stations.

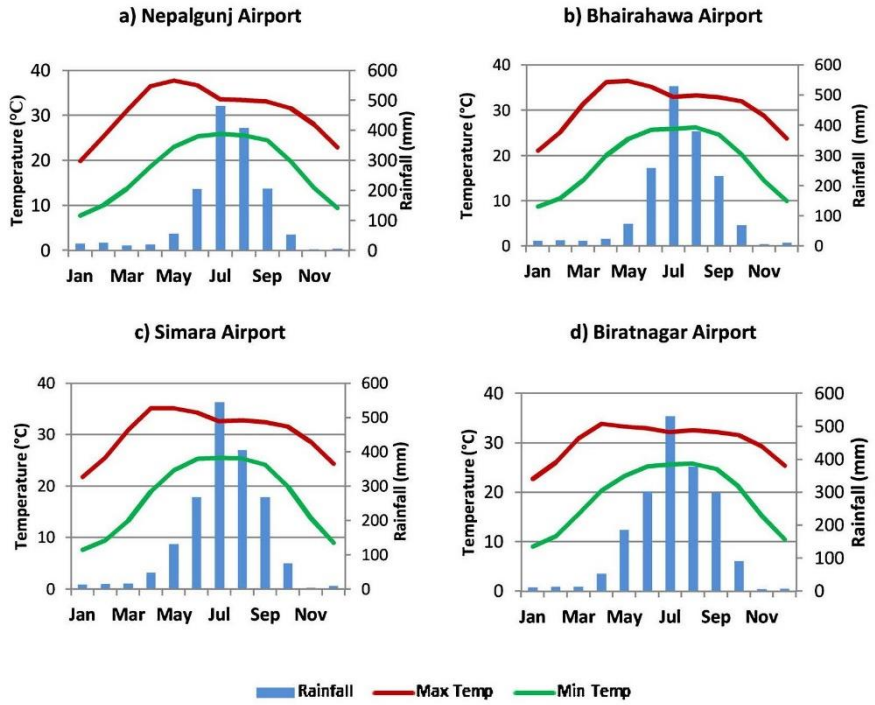

Fig. 2. Average monthly maximum temperature, minimum temperature and rainfall of studied stations.

dense foggy hours in winter months in the Terai. The alternate hypothesis is that there is a trend (increasing or decreasing) over time. The Mann Kendall test statistic (S) is calculated by using the formula below:

$$S = \sum_{i=1}^{n-1} \sum_{j=j+1}^{n} sig\,(X_j - X_i)$$

Table 1
Details of studied stations.

SN	Station	Index No	District	Latitude (degree:min North)	Longitude (degree:min East)	Elevation (m)
1	Nepalgunj Airport	420	Banke	28:06	81:40	165
2	Bhairahawa Airport	705	Rupandehi	27:31	83:26	109
3	Simara Airport	909	Bara	27:10	84:59	130
4	Biratnagar Airport	1319	Morang	26:29	87:16	72

$$sig(X_j - X_i) = \begin{cases} +1 \, if \, (X_j - X_i) > 0 \\ 0 \, if \, (X_j - X_i) = 0 \\ -1 \, if \, (X_j - X_i) < 0 \end{cases}$$

Where X_i and X_j are time series observation in chronological order and n is the length of time series. $sig(X_j - X_i)$ is the indicator function which takes the value of 1, 0 or −1 according to the value of $(X_j - X_i)$.

When the number of observations equal or are greater than 10, then the standard normal distribution can be used to estimate the significance of the S test statistic as described in Gilbert (1987). Standard normal z values are calculated using the value of S and the variance of S and compared against the cumulative standard normal distribution to assess the statistical significance of the trend. In this study the trend is tested at significance levels, $\alpha = 0.001$, 0.01, 0.05 and 0.1.

To estimate the true slope of any trend in opacity/visibility, foggy days, foggy hours, dense foggy days and dense foggy hours during winter months at each station the Sen's slope nonparametric method was adopted (Sen, 1968). The advantage of this method is that missing values are allowed and data need not conform to any particular distribution. In addition, this method is robust to single data errors and outliers (Sen 1968). In this method, the trend is assumed to be linear and the equation is given by:

$$f(t) = Qt + B$$

Where, Q is the slope and B is constant.

To estimate the slope in the previous equation, the slopes of all data value pairs are calculated by using the following equation:

$$Q_i = \frac{x_j - x_k}{j - k}$$

Where, $j > K$

The Sen's slope estimate of Q is obtained by calculating the median value of Q_i and the value of B is calculated subsequently. In addition, the lower and upper confidence levels of the coefficients Q and B at the significance level of 0.05 (Qmin95, Bmin95, Qmax95 and Bmax95) are also calculated. Similarly, to compare the trend in fog parameters against any trends in meteorological data from the studied stations, the Mann Kendall Trend analysis of annual average and foggy season average daily minimum temperature, maximum temperature, precipitation and humidity was also performed.

To develop the statistical model to predict visibility, multiple regressions were performed for different combinations of meteorological parameters. The multiple regression of the log of daily visibility (at a particular time of day) with daily meteorological variables such as maximum temperature, minimum temperature, precipitation, humidity and wind speed provided comparatively better results. Here, the null hypothesis for the statistical test is that there is no relation between the log of daily visibility (at a particular time) with daily meteorological variables. The F test was performed to test the null hypothesis and the models were evaluated based on the adjusted R^2 value. The statistical significance of individual regression coefficients in the following equations were evaluated using a t-test.

$$Y = A + B_1X_1 + B_2X_2 + B_3X_3 + B_4X_4$$

Where, A is an intercept and B_1, B_2, B_3 and B_4 are coefficients of X_1, X_2, X_3 and X_4 respectively.

Y = Log $_{10}$ of Visibility at particular time (3.0, 6.0 and 9.0 UTC)
X_1 = Daily Maximum Temperature, T_{max} (°C)
X_2 = Daily Minimum Temperature, T_{min} (°C)
X_3 = Morning Humidity at 3.0 UTC (%)
X_4 = Daily Rainfall (mm)

3. Results and discussion

3.1. Fog parameters

Results for the fog related parameters: number of foggy days; number of foggy hours; number of dense foggy days; and number of dense foggy hours in the study area over the period 1980–2015 are discussed in the following sub-sections.

3.1.1. Foggy days

The distribution of foggy days is presented as box plots in Fig. 3(a) for the four Terai stations. The whiskers in the box plot extend to the 5th and 95th percentile. Fig. 3(a) indicates that fog events are a regular phenomenon at all stations studied during winter months (i.e. November, December, January and February). There is wide variation of distribution of the number of foggy days spatially, with the average number of monthly foggy days at each station presented in Fig. 4(a). It is found that the foggy days start in November and end in February across the Terai. The months with most foggy days across the study stations were December and January. On average, more foggy days were observed in Biratnagar (54.6 days) compared to other stations Bhairahawa (48.9 Days), Nepalgunj (33.1 days) and Simara (24.0 days). Since fog frequency tends to be high in locations with sufficient moisture (for example, near waterbodies, rivers, lakes, coastal regions, humid tropical *etc.*) (Croft, 2003), the higher number of foggy days in Biratnagar and Bhairahawa airport compared to Nepalgunj and Simara airport could be due to their proximity to the Koshi and Gandaki rivers (major tributaries of the Ganga) and associated extensive irrigation areas from these river systems respectively.

3.1.2. Foggy hours

Box plots of the total number of foggy hours during the daytime at the four Terai stations are shown in Fig. 3(b). The whiskers in the box plot extend to the 5th and 95th percentile. The figure clearly indicates that the total number of foggy hours is highest at Biratnagar, which is consistent with the number of foggy day results (Fig. 3(a)). There is wide variation in the number of foggy hours at different stations in the Terai.

The monthly distribution of the number of foggy hours is presented in Fig. 4(b). The figure shows that on average, most foggy hours occur in December and January compared to November and February. At each station the number of foggy hours in December and January is similar except Simara, where December has much fewer foggy hours than January. The average winter daytime foggy hours at Biratnagar, Nepalgunj, Bhairahawa and Simara are 169, 115, 104 and 71 respectively.

3.1.3. Dense foggy days

The distribution of dense foggy days during winter at the four Terai stations is presented in Fig. 3(c). Unlike the number of foggy days

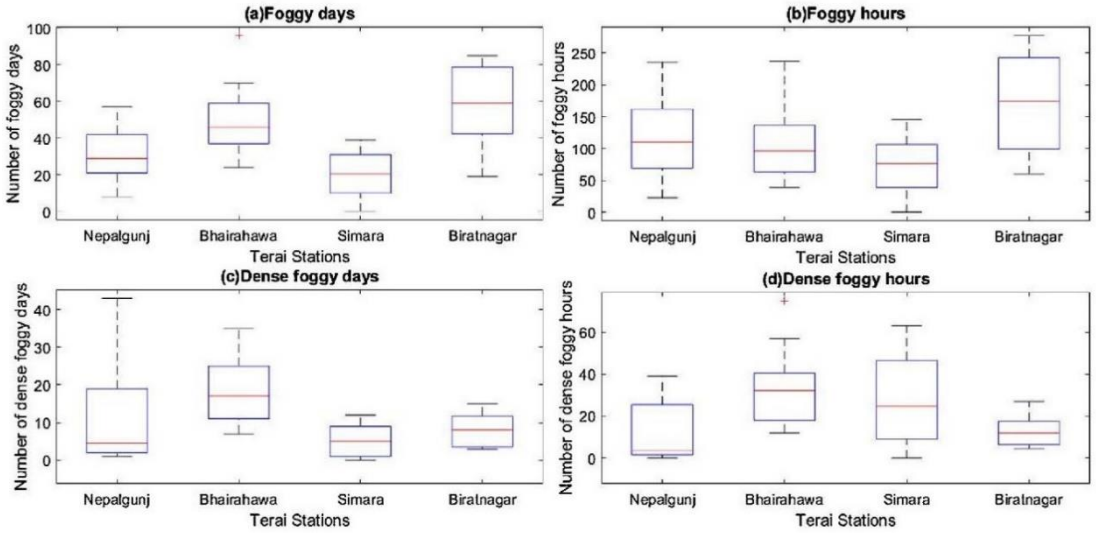

Fig. 3. Box plot of number of foggy days (a), foggy hours (b), dense foggy days (c) and dense foggy hours (d) in the Terai during winter. The box plot whiskers exten to 5th and 95th percentile.

(Fig. 3(a)), on average more dense foggy days are observed at Bhairahawa (18 days) compared to the other stations, Nepalgunj (11 days), Biratnagar (8 days) and Simara (5 days). This indicated that dense fog was observed more in western Terai stations (Nepalgunj and Bhairahawa) compared to the eastern (Biratnagar) and central station (Simara). In addition, a larger variation in the number of dense foggy days was observed at Bhairahawa and Nepalgunj than at Simara and Bir atnagar. The monthly distribution of dense foggy days at the four Tera stations is shown in Fig. 4(c), which indicates that, similar to fogg days, dense foggy days were concentrated in December and January Unlike the other stations, no dense foggy days occurred in November a Simara and the number of dense foggy days in December was low.

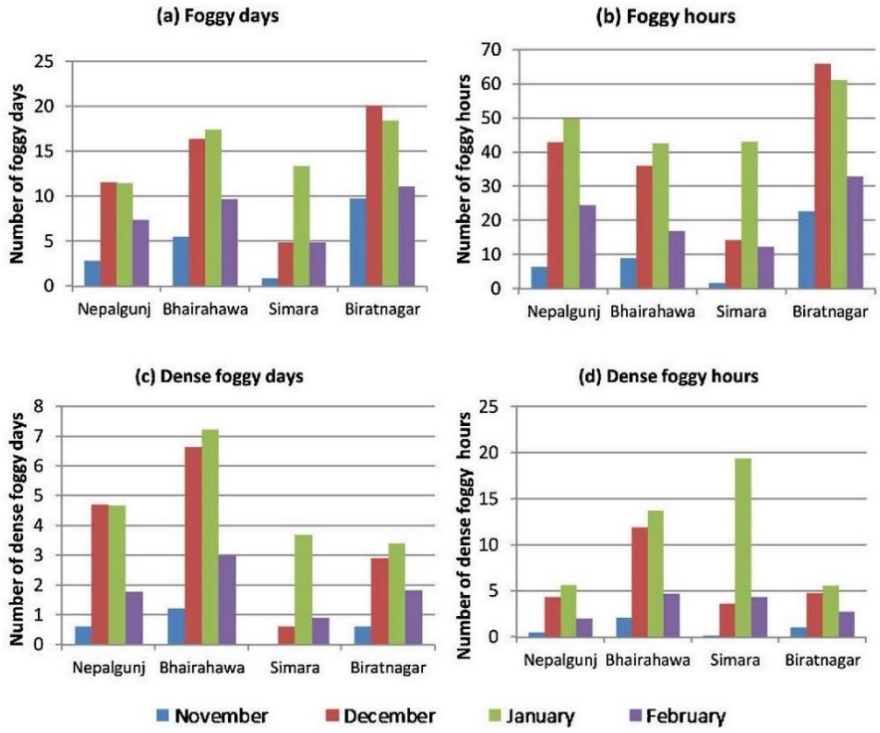

Fig. 4. Monthly distribution of average number of foggy days (a), foggy hours (b), dense foggy days (c) and dense foggy hours in Terai.

3.1.4. Dense foggy hours

The box plot of dense foggy hours in the studied Terai stations during winter is presented in Fig. 3(d). Interestingly, on average more dense foggy hours were observed in Bhairahawa (32 h) and Simara (27 h) compared to Biratnagar (13 h) and Nepalgunj (11 h), which was mainly due to the long duration of dense foggy conditions on foggy days at these two stations. The high number of dense foggy hours at Bhairahawa is supported by the findings of Srivastava et al. (2016), who reported that the highest daily foggy hours in the central IGP was at Gorakhpur (an Indian town about 90 km south of Bhairahawa). The average monthly distribution of dense foggy hours in the four Terai stations during winter is presented in Fig. 4(d). The figure shows that January was the leading month for dense foggy hours at all the stations.

3.2. Trend analysis of meteorological parameters

The trend analysis results for annual and foggy season maximum temperature, minimum temperature, precipitation and humidity are presented in the following sub-sections.

3.2.1. Maximum temperature

Average and trend analysis results of annual and foggy season {January, February, November and December (JFND)} average daily maximum temperature are presented in Table 2. The results indicate a slight increasing gradient in average annual daily maximum temperature from the eastern station Biratnagar (smallest, 30.16 °C) to western Nepalgunj (highest, 30.92 °C) among the four study stations. Regarding the historical trend in annual average daily maximum temperature, all stations except Biratnagar show a non-significant trend. During the foggy season, the trend in average daily maximum temperature was significantly decreasing for Simara and Bhairahawa at the significance level of 0.05, whereas it was non-significant at Biratnagar and Nepalgunj. The declining trend of maximum temperature during winter at Simara and Bhairahawa is found to be consistent with the findings of Shrestha et al., (2016) and Baidya et al. (2008) and it could be due to a reduction of incoming solar radiation due to increased fog events as suggested by them.

3.2.2. Minimum temperature

The average and trend analysis results of annual and foggy season average daily minimum temperature are shown in Table 3. The results indicated that the annual average minimum temperature at Biratnagar, Simara and Bhairahawa had an increasing trend at the significance level of 0.001, 0.05, 0.01 respectively. Similarly, the foggy season average minimum temperatures at these stations were also increasing at the significance level of 0.001, 0.05 and 0.1 respectively. These results were consistent with the study findings of Shrestha et al. (2016) and Baidya et al. (2008), which both indicated that fog and air pollution could be the reason behind the increase in minimum temperature in the plain area. Increasing minimum temperatures during winter could be due to more energy being trapped at the surface as fog reduces losses of long wave radiation at night. In contrast with the results at the other stations, the trend of both annual and foggy season average minimum temperature of Nepalgunj was shown to be non-significant, which may be due to the shorter record length at Nepalgunj compared to the other stations.

3.2.3. Rainfall

The trend analysis results of annual and foggy season rainfall in the studied stations are displayed in Table 4. The results indicated that there was no significant trend in annual or foggy season rainfall at any of the studied stations. The results indicated a decreasing spatial gradient in average annual rainfall from the eastern station Biratnagar (highest, 1867.31 mm) to western Nepalgunj (lowest, 1499.56 mm) among the four study stations, which may be due to the summer monsoon moving from east to west. However, the slight increasing spatial gradient in average foggy season rainfall from eastern station Biratnagar (lowest, 37.7 mm) to western Nepalgunj (highest, 53.54 mm) among the four study stations may be due to western disturbance (Dimri et al., 2015) moving from west to east direction responsible for winter rain (Chand and Singh, 2015; Dimri and Chevuturi, 2016). Interestingly, the foggy season rainfall is only 2–3 percent of the annual rainfall at the studied stations.

3.2.4. Humidity

The results of trend analysis of annual and foggy season average humidity readings at 5:45 a.m. in the studied stations are given in Table 5. The results clearly indicated that the annual and foggy season average humidity was increasing at least at the 0.01 level of significance at all the stations except Nepalgunj. The increasing trend of humidity agreed with the findings of Dai (2006) who described the high increase (0.5–2.0% per decade) in humidity in India, the United States and Western China during 1976–2004. The non-significant humidity trend results at Nepalgunj were similar to the temperature trend at the same station and may be due to less data being available (only recent 20 years data) compared to the other stations. Apart from the global warming reasons as described by Dai (2006), the increasing trend of humidity in the studied stations could also be due to the increasing irrigation area in the Terai region. In 1981, the irrigation area in the Terai was 449,000 ha and this area was almost doubled by 2011 (985,000 ha) (Goverment of Nepal, 2016). The increasing trend in humidity during winter season in Terai area of Nepal may also create a conducive environment for more fog events.

3.3. Trend analysis

The results of trend analysis of visibility and fog parameters, number of foggy days, foggy hours, dense foggy days and dense foggy hours, are discussed in the following sub-sections.

3.3.1. Opacity trend

It is observed that the trend in visibility is the opposite to that of fog related parameters. To simplify the discussion of results a new variable 'opacity' is introduced which is defined as the reciprocal of visibility and measured in kilometre^{-1}. Time series of average opacity for winter months (January, February, November and December) at the four Terai

Table 2
Trend analysis of annual and foggy season average daily maximum temperature in studied stations.

	Biratnagar	Simara	Bhairahawa	Nepalgunj
Number of years Data (n)	45 (1971 –2015)	39 (1976– 2015)	45 (1971–2015)	20 (1996–2015)
Annual Average Maximum Daily Temperature (Deg. Celsius)	30.16	30.45	30.74	30.92
Z value of MK Test on Annual Average Daily Maximum Temperature	2.67**	1.35^{ns}	1.32^{ns}	1.00^{ns}
Rate of Increase on Annual Average Maximum Daily Temperature (Deg. Celsius/Decade)	0.26	–	–	–
Foggy Season (JFND) Average Daily Maximum Temperature (Deg. Celsius)	25.81	25.11	24.70	24.17
Z value of MK Test on Foggy Season Average Daily Max Temperature	1.20^{ns}	−2.30*	−2.16*	-0.74^{ns}
Rate of Decrease on Foggy Season Average Maximum Daily Temperature (Deg. Celsius/Decade)	–	0.49	0.21	–

+ Significant at 0.1 level, * Significant at 0.05 level, ** Significant at 0.01 level, *** Significant at 0.001 level, ns non-significant.

Table 3
Trend analysis of annual and foggy season average daily minimum temperature in studied stations.

	Biratnagar	Simara	Bhairahawa	Nepalgunj
Number of years Data (n)	45 (1971–2015)	39 (1976–2015)	45 (1971–2015)	20 (1996–2015)
Annual Average Minimum Daily Temperature (Deg. Celsius)	18.80	18.00	18.65	18.16
Z value of MK Test on Annual Average Daily Minimum Temperature	3.93^{***}	3.19^{**}	2.59^{**}	-0.22^{ns}
Rate of increase of Annual Average Minimum Daily Temperature (Degree Celsius / Decade)	0.26	0.23	0.22	–
Foggy Season (JFND) Average Daily Min Temperature (Deg. Celsius)	11.22	10.09	10.94	10.30
Z value of MK Test on Foggy Season Average Daily Min Temperature	4.04^{***}	2.80^{**}	1.91^{+}	$.09^{ns}$
Rate of increase of Foggy Season Average Minimum Daily Temperature (Degree Celsius / Decade)	0.45	0.32	0.17	–

$^{+}$ Significant at 0.1 level, * Significant at 0.05 level, ** Significant at 0.01 level, ***Significant at 0.001 level, ns non-significant.

Table 4
Trend analysis of annual and foggy season rainfall in studied stations.

	Biratnagar	Simara	Bhairahawa	Nepalgunj
Number of years Data (n)	46 (1970–2015)	46 (1970–2015)	46 (1970–2015)	20 (1996–2015)
Annual Average Rainfall (mm)	1867.31	1752.29	1643.63	1499.56
Z value of MK Test on Annual Rainfall	0.91^{ns}	0.13^{ns}	-0.68^{ns}	-0.16^{ns}
Average Foggy Season (JFND) rainfall (mm)	37.7	40.97	52.8	53.54
Z value of MK Test on Foggy Season Rainfall	-0.86^{ns}	2.33^{ns}	3.21^{ns}	3.57^{ns}

^{ns} non-significant.

stations are presented in Fig. 5. In this plot, Sen's slope of opacity is also plotted. Clearly the average opacity during winter months was increasing at all four stations. These results were in line with the findings of Jaswal et al., 2013, who described the declining visibility and increasing trend of the poor visibility days in India. The increasing trend of average opacity at Bhairahawa was steeper than that at Simara, Biratnagar and Nepalgunj. The different levels of average opacity and trend at the four Terai stations may be due to differences in the level of atmospheric aerosols present in the atmosphere as well as the frequency and intensity of fog events. The population of the Terai in 2011 increased by 103% from the population of 1981, whereas the total population of Nepal increased by 76% over the same period (CBS, 2016). One of the major reasons of faster growth of population in the Terai during that period was reported to be high internal migration. The decline of visibility may be associated with increased population and associated economic activity in the Terai leading to increasing levels of air pollution during the study period. In addition to this, the increased emissions from the adjacent IGP area of India, as described by Gautam (2014), as well as high precipitation in the eastern IGP and increased surface and ground water extraction for irrigation in the western IGP (due to flat tariff rate in Punjab, Haryana and Western Uttar Pradesh as described by Sharma et al. (2010), might also have contributed to the increased opacity in the study area.

Table 6 provides the significance level of the trend and the values of slope, Q, and constant, B, of the Sen's slope trend line. It is shown in Table 6 that average opacity is increasing at all stations, with all trends significant at either the 0.05 level (Nepalgunj and Biratnagar), 0.01 level (Simara) or 0.001 level (Bhairahawa). The value of Sen's slope at Simara and Biratnagar was the same and close to that of Nepalgunj. Whereas Sen's slope at Bhairahawa was almost double that of the other

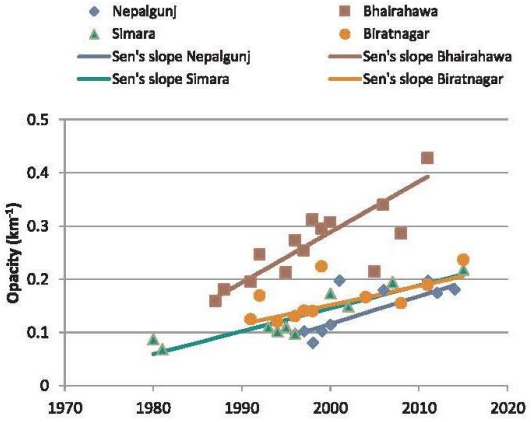

Fig. 5. Average opacity trend during winter in Terai region of Nepal.

three stations, which indicated that the rate of increase of opacity at Bhairahawa was two times that of the other stations during the study period. The increasing trend in opacity (decline in visibility) not only affects the air/surface traffic and tourism industry, but also affects surface solar radiation that is vital for winter crop production.

3.3.2. Trend in number of foggy days

Time series of the number of foggy days each year are plotted for the four Terai stations in Fig. 6. At all four stations the number of foggy

Table 5
Trend analysis of annual and foggy season average daily humidity at 5:45 in studied stations.

	Biratnagar	Simara	Bhairahawa	Nepalgunj
Number of years Data (n)	40 (1976–2015)	40 (1976–2015)	40 (1976–2015)	19 (1997–2015)
Annual Average Daily Humidity at 5:45 (%)	81.57	79.62	81.73	86.15
Z value of MK Test on Annual Average Daily Humidity at 5:45	5.30^{***}	3.62^{***}	6.35^{***}	-1.32^{ns}
Rate of increase of Annual Average Daily Humidity at 5:45 (% per Decade)	2.4	1.8	2.9	–
Foggy Season (JFND) Average Daily Humidity (%)	88.26	88.01	92.26	95.61
Z value of MK Test on Average Foggy Season Daily Humidity at 5: 45	4.71^{***}	3.09^{**}	6.75^{**}	0.41^{ns}
Rate of increase of Foggy Seasonal Average Daily Humidity at 5:45 (% per Decade)	2.9	1.6	2.6	–

$^{+}$ Significant at 0.1 level, * Significant at 0.05 level, ** Significant at 0.01 level, ***Significant at 0.001 level, ns non-significant.

Table 6
Sen's slope of opacity trend at the stations in Terai during winter months.

Stations	Test Z	Q	Qmin95	Qmax95	B	Bmin95	Bmax95
Nepalgunj	2.326*	0.005	0.001	0.010	0.013	0.117	−0.084
Bhairahawa	3.394***	0.009	0.005	0.012	0.099	0.174	0.063
Simara	2.862**	0.004	0.002	0.006	0.060	0.087	0.022
Biratnagar	2.335*	0.004	0.001	0.006	0.079	0.124	0.041

* Significant at 0.05 level, ** Significant at 0.01 level, ***Significant at 0.001 level.

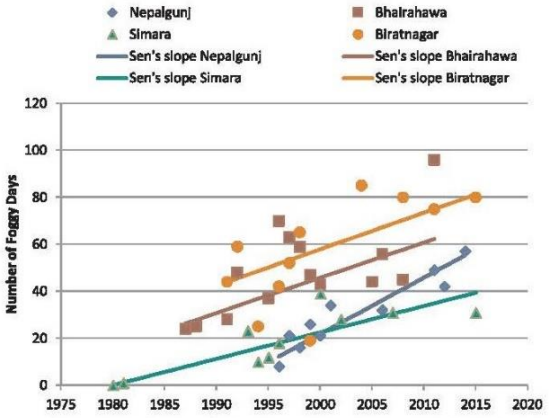

Fig. 6. Foggy days trend during winter in Terai region of Nepal.

days was increasing over time. Results for Sen's slope test statistics, slope and constant of trend line for the number of foggy days are presented in Table 7. At Nepalgunj and Simara the increasing trend in number of foggy days was statistically significant at the 0.01 level, while at Bhairahawa and Biratnagar the increasing trend was significant at the level of 0.05 and 0.1 respectively. The significant decreasing trend of maximum temperature, increasing trend of minimum temperature and humidity during the foggy season in the majority of studied stations were consistent with the increasing trend of fog at the studied stations. The value of Sen's slope at Bhairahawa was almost the same as that at Biratnagar, while the slope at Nepalgunj is higher than the other stations (Table 7). The results are also similar to the findings of Srivastava et al. (2016), who also reported a positive trend in foggy days during winter months in the entire Indian side of the IGP at the 95% confidence level during 1971–2010.

3.3.3. Trend in number of foggy hours

Time series of the number of daytime total foggy hours during the winter months are plotted for the four Terai stations in Fig. 7. The figure clearly indicates that the total daytime foggy hours trend was increasing at all four Terai stations. The statistical significance of the trends in the number of foggy hours during winter, as well as slope and constant of Sen's slope are given in Table 8. The increasing trend in the number of foggy hours during winter was found to be statistically significant at the level of 0.01 in Nepalgunj and Bhairahawa. In Simara and Biratnagar the increasing trend of foggy hours during winter was found to be significant at the level of 0.05. The table also indicates that Sen's slope at Nepalgunj and Biratnagar is higher (almost double) than that at Simara and Bhairahawa.

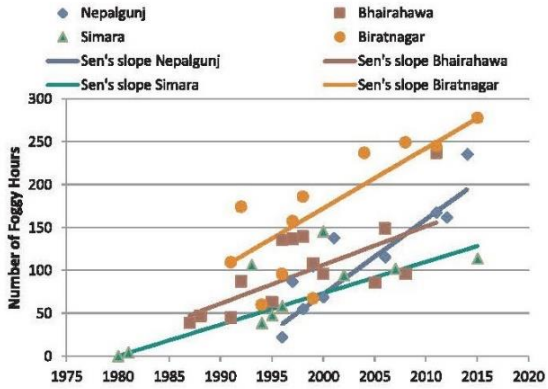

Fig. 7. Foggy hours trend during winter in Terai region of Nepal.

3.3.4. Trend in number of dense foggy days

The number of dense foggy days in winter months at the four Terai stations over time is plotted in Fig. 8. This figure indicates an increasing trend in dense foggy days at all the stations. Sen's slope for dense foggy days was steeper at Nepalgunj and Bhairahawa compared to Simara and Biratnagar. The test statistics for Sen's slope and values of slope and constant for the four stations is presented in Table 9. Increasing trends in the number of dense foggy days at Simara and Biratnagar were found to be significant at the 0.05 level. While the increasing trend in dense foggy days at Nepalgunj and Bhairahawa were significant at the 0.001 level and 0.01 level respectively. The increasing trend in dense foggy days is expected to affect agriculture in the Terai in the future.

3.3.5. Trend in number of dense foggy hours

The observed dense foggy hours in different years in the studied stations in Terai is shown in Fig. 9 along with Sen's slope. It is evident that dense foggy hours were increasing at all stations and this increasing trend was found to be statistically significant at the 0.05 level (Table 10). Sen's slope for dense foggy hours was lowest at Biratnagar and highest at Bhairahawa.

3.3.6. Mann Kendall trend analysis

The Mann Kendall trend analysis results for opacity and fog related variables (number of foggy days, foggy hours, dense foggy days and dense foggy hours) at the four selected Terai stations during winter months are presented in Table 11. These results complement the Sens analysis by examining monthly as well as winter season trends. Overall winter season opacity was increasing over time at all four stations at least at the 0.05 level of significance. Similarly, overall winter season trends in foggy days, foggy hours, dense foggy days and dense foggy hours were also increasing at all stations at least at the 0.05 level of significance.

Table 7
Sen's slope of the number of foggy days at the stations in Terai during winter months.

Stations	Test Z	Q	Qmin95	Qmax95	B	Bmin95	Bmax95
Nepalgunj	3.143**	2.400	1.598	3.250	−26.200	−7.648	−44.000
Bhairahawa	1.971*	1.500	0.062	2.908	15.750	44.533	−1.125
Simara	2.784**	1.125	0.588	1.881	0.000	9.501	−12.748
Biratnagar	1.796+	1.556	−0.403	3.818	26.778	63.833	−19.093

+Significant at 0.1 level, * Significant at 0.05 level, ** Significant at 0.01 level.

Table 8
Sen's slope of the number of foggy hours at the stations in Terai during winter months.

Stations	Test Z	Q	Qmin95	Qmax95	B	Bmin95	Bmax95
Nepalgunj	3.041**	8.719	5.136	13.778	−101.859	−1.328	−202.248
Bhairahawa	2.687**	4.500	1.500	8.750	16.500	67.500	−42.750
Simara	2.504*	3.656	1.500	6.777	0.422	48.000	−51.800
Biratnagar	2.491*	7.000	2.912	12.783	32.500	133.590	−108.530

* Significant at 0.05 level, ** Significant at 0.01 level.

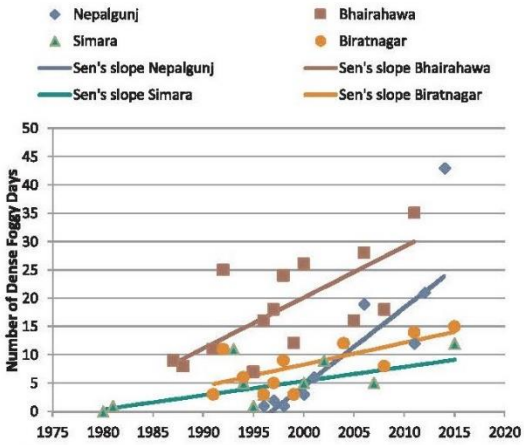

Fig. 8. Dense foggy days trend during winter in Terai region of Nepal.

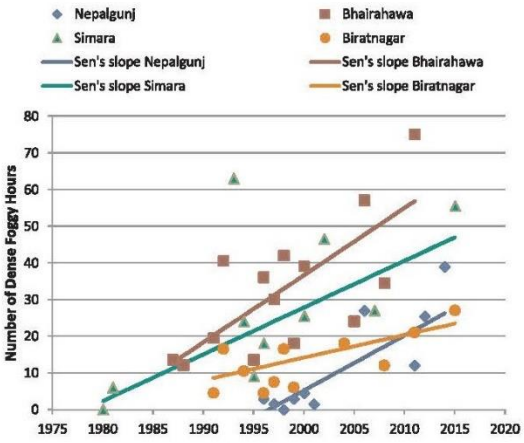

Fig. 9. Dense foggy hours trend during winter in Terai region of Nepal.

Individual monthly trends in opacity show clear increasing trends at least at the 0.1 level of significance in all stations and all months, except for February at Nepalgunj, and November and February at Biratnagar. Similarly, trends in monthly foggy days were increasing at least at the 0.1 level of significance in all months, except for November at Nepalgunj; December, January and February at Bhairahawa and November and January at Biratnagar. Regarding the monthly trend in foggy hours, it was found that there is increasing trend at least at the 0.1 level of significance in all the months except November and February of Nepalgunj and November and January of Biratnagar. Monthly trends in dense foggy hours was found to be significant in all months of the studied stations at least at 0.1 level of significance except November of Nepalgunj; January of Bhairahawa and November and January of Biratnagar. Regarding the monthly trend of dense foggy hours, December and January of Bhairahawa; November, December and February of Simara and November and January of Biratnager did not show any trend. However, the remaining winter months of the studied stations indicated increasing trend at least at the 0.1 level of significance. From the results of Mann Kendall's trend it was evident that the overall trend of opacity foggy days, foggy hours, dense foggy days and dense foggy hours in winter season was found to be at increasing trend at least at 0.1 level of significance in all the studied stations in Terai. The results agrees with the main climatic variation expressed by the people in Terai during winter reported as "more intense cold periods" and "fog more frequent and denser" (Smadja et al., 2015). Similarly, in general the monthly trend of opacity, foggy days, foggy hours and dense foggy days were found to be increasing at least at 0.1 level of significance in the studied stations.

To analyse the reasons behind the increasing trend of fog events, various literature were reviewed and discussed. It was considered that the reduction of atmospheric aerosol load or improvement in air quality in Europe was the major reason behind the decline of fog frequency over the past 30 years in Europe (Vautard et al., 2009; Van Oldenborgh et al., 2010). Similarly the decrease in suspended particulate matter in the atmosphere was indicated as a primary reason for the decline of dense fog in Los Angeles over the past 40 years (Witiw and LaDochy, 2008). However, the decline of foggy days in many inland stations in Japan during 1965–2005 was reported due to an increase of global warming and urbanization (Akimoto and Kusaka, 2015). Hence, atmospheric air quality, urbanization and global warming could be considered as major factors for declining trend of fog.

In contrast to the declining trend of fog in Europe, America and Japan, there is an increasing trend in fog reported in IGP, Indian subcontinent and in the overall South Asian region (Syed et al., 2012; Muslehuddin et al., 2004; Srivastava et al., 2016; Ghude et al., 2017). In this study, an increasing trend in fog over the Terai region of Nepal is observed, which is consistent with fog trends in the IGP region. The

Table 9
Sen's slope of the number of dense foggy hours at the stations in Terai during winter months.

Stations	Test Z	Q	Qmin95	Qmax95	B	Bmin95	Bmax95
Nepalgunj	3.426***	1.385	0.726	2.481	−23.192	−10.431	−44.826
Bhairahawa	2.636**	0.900	0.304	1.281	2.150	10.304	−4.135
Simara	2.006*	0.250	0.000	0.500	0.375	5.000	−3.500
Biratnagar	1.968*	0.385	0.000	0.731	0.615	8.000	−7.430

* Significant at 0.05 level, ** Significant at 0.01 level, *** Significant at 0.001 level.

Table 10
Sen's slope of the number of dense foggy hours at the stations in Terai during winter months.

Stations	Test Z	Q	Qmin95	Qmax95	B	Bmin95	Bmax95
Nepalgunj	2.344*	1.500	0.454	2.447	−24.750	−4.420	−44.132
Bhairahawa	2.358*	1.833	0.355	3.000	0.000	24.264	−19.500
Simara	2.147*	1.275	0.214	2.210	2.363	21.107	−12.153
Biratnagar	2.193*	0.618	0.106	1.251	1.853	9.035	−13.763

* Significant at 0.05 level.

increasing trend in fog is supported by the declining trend of maximum temperature, increasing trend of minimum temperature and increasing trend of humidity in the foggy season at the studied stations in Terai area of Nepal. The increasing trend in fog events could also be due to the increasing trend in air pollution in the region (Yasmeen et al., 2012; Srivastava et al., 2012; Kaskaoutis et al., 2012; Ramanathan, 2006). Similarly, the increase in irrigation area in Terai region, as well as in the IGP, might also be responsible for the increasing humidity as suggested by Syed et al. (2012). Since a fog event is the result of complex interactions among various local microphysical, dynamical, radiative and chemical processes, boundary layer conditions, and large-scale meteorological processes (Gultepe et al., 2007), there is need for further research to identify definitively the particular reason behind the observed fog trends at the studied stations.

3.4. Multiple regressions

Multiple linear regression was used to develop empirical models to estimate visibility using daily measured meteorological variables. The rationale for attempting this analysis was to find a means of predicting fog to years and locations other than the airports that did not have visibility records. After several attempts, it was found that a multiple linear regression of the Log_{10} value of visibility at 3:00, 6:00 and 9:00 UTC with daily maximum temperature, daily minimum temperature, precipitation, and humidity provided comparatively better results. The regression coefficients and adjusted R^2 values for each regression and station are presented in Table 12. The maximum adjusted R^2 value obtained was 0.432 at Bhairahawa Airport for 3:00 UTC. The variance explained by the empirical models developed to predict visibility is low as seen in the low adjusted R^2 values in Table 12. The low explained variance of the regression models may be due to the exclusion of atmospheric aerosols in these models, which are not commonly available in meteorological data sets.

3.5. Implication of fog on crop production

Results from the analysis of fog data in the previous sub-sections has shown that the Terai region is experiencing fog for between 1/3 and 2/3 of the 120 days during winter. In addition, the trends in the number of foggy days, foggy hours, dense foggy days and dense foggy hours are found to be increasing over the past 20–30 years. As the Terai region of Nepal is considered to be the food basket of the country, it is important to analyse the effect of fog on crop production. The crop calendar of important crops in the Terai is presented in Table 13.

Rice is the major crop grown in summer that is not affected by fog during its growing season because fog starts around the 2nd week of November. However, farmers leave the harvested rice plant in the field for sun drying and the onset of fog events may delay drying and threshing of harvested rice (Shrestha, 2011). A delay in drying rice in the field before threshing may also delay land preparation and sowing

Table 11
Mann Kendall's trend probability of selected parameters in the station during winter months.

Stations	Months	Trend of Studied Parameters				
		Opacity	Foggy Days	Foggy Hours	Dense Foggy Days	Dense Foggy Hours
Nepalgunj	November	0.9963[b]	0.2877[e]	0.1562[e]	0.6554[e]	0.9850[c]
	December	0.9750[c]	0.9846[c]	0.9699[c]	0.9836[c]	0.9826[c]
	January	0.9100[d]	0.9971[b]	0.9880[c]	0.9830[c]	0.9510[c]
	February	0.8210[e]	0.9780[c]	0.8700[c]	0.9780[c]	0.9510[c]
	Overall	0.9898[c]	0.9992[b]	0.9988[b]	0.9997[a]	0.9901[b]
Bhairahawa	November	0.9984[b]	0.9699[c]	0.9919[b]	0.9099[d]	0.9505[c]
	December	0.9968[b]	0.8749[e]	0.9783[c]	0.9265[d]	0.8531[e]
	January	0.9222[d]	0.8643[e]	0.9424[c]	0.8962[e]	0.8888[e]
	February	0.9812[c]	0.8998[e]	0.9959[b]	0.9817[c]	0.9911[b]
	Overall	0.9997[a]	0.9756[c]	0.9963[b]	0.9957[b]	0.9906[b]
Simara	November	0.9963[b]	0.9251[d]	0.9251[d]	0.9177[d]	0.6331[e]
	December	0.9988[b]	0.9854[c]	0.9946[b]	0.9834[c]	0.8888[e]
	January	0.9625[c]	0.9868[c]	0.9554[c]	0.9474[d]	0.9099[d]
	February	0.9938[c]	0.9649[c]	0.9554[c]	0.9608[c]	0.8212
	Overall	0.9979[b]	0.9973[b]	0.9938[b]	0.9812[c]	0.9838[c]
Biratnagar	November	0.8577[e]	0.8363[e]	0.7324[e]	0.0618[e]	0.0606[e]
	December	0.9963[b]	0.9992[b]	0.9993[a]	0.9940[b]	0.9940[b]
	January	0.9236[d]	0.6406[e]	0.8770[e]	0.6064[e]	0.6737[e]
	February	0.8925[e]	0.9693[c]	0.9906[b]	0.9452[d]	0.9452[d]
	Overall	0.9901[b]	0.9633[c]	0.9936[b]	0.9750[c]	0.9857[c]

Index.
[a] Increasing Trend at 0.001 level of significance.
[b] Increasing Trend at 0.01 level of Significance.
[c] Increasing Trend at 0.05 level of Significance.
[d] Increasing Trend at 0.1 level of Significance.
[e] No trend.

Table 12
Results of multiple regression of visibility reading with meteorological variables.

SN	Station	For Log_{10} visibility at time	A	B_1	B_2	B_3	B_4	Adjusted R^2
1	Simara Airport	8:45 (3:00 UTC)	0.491	**0.089**	**−0.026**	**−0.022**	**0.027**	0.410
		11:45 (6:00 UTC)	0.322	**30.066**	**−0.019**	**−0.012**	**0.023**	0.412
		14:45 (9:00 UTC)	**0.613**	**0.046**	**−0.017**	**−0.009**	**0.019**	0.332
2	Nepalgunj Airport	8:45 (3:00 UTC)	**1.956**	**0.056**	0.009	**0.034**	**−0.031**	0.350
		11:45 (6:00 UTC)	**0.850**	**0.047**	−0.002	**0.030**	**−0.013**	0.358
		14:45 (9:00 UTC)	**0.593**	**0.033**	**−0.005**	**0.020**	**−0.005**	0.266
3	Bhairahawa airport	8:45 (3:00 UTC)	**3.636**	**0.030**	0.000	**−0.047**	**0.026**	0.432
		11:45 (6:00 UTC)	**0.958**	**0.042**	**0.000**	**−0.016**	**0.023**	0.424
		14:45 (9:00 UTC)	**0.678**	**0.032**	**0.000**	**−0.009**	**0.020**	0.417
4	Biratnagar airport	8:45 (3:00 UTC)	0.086	**0.035**	**0.027**	**−0.013**	**0.028**	0.250
		11:45 (6:00 UTC)	0.222	**0.050**	**−0.010**	**−0.007**	**0.017**	0.305
		14:45 (9:00 UTC)	**0.296**	**0.041**	**−0.006**	**−0.005**	**0.017**	0.248

The bold coefficients indicate significant coefficients at the 95 percent confidence level.

of winter crops such as wheat. Since, a delay in sowing of wheat from November 14th decreases the grain yield significantly (Marasini et al., 2016), there may be a decrease in wheat yield due to increased fog events. In addition, the reduction in Photosynthetically Active Radiation (PAR), increased cold stress, and more favourable conditions for insects and pests during fog events in the region (Singh and Singh, 2010) may also contribute to a reduction of winter crop (wheat, lentil *etc.*) yield due to increased fog frequency in the Terai. Because of increased events of fog, the temperature drops in the daytime due to reduced solar radiation. The persistent low temperature over longer periods may reduce the vegetative growth which may damage and negatively affect the productivity of sub-tropical horticultural and agricultural crops (Salinger et al., 2000). From Table 13, it is anticipated that the germination as well as vegetative growth of winter crops *viz.* lentil, wheat and winter maize could be negatively affected by reduced PAR and low temperature due to the fog events in Terai. Lentils are an important legume crop in the Terai and disease is one of the major problems of grain legume (including lentil) cultivation in the Terai area of Nepal (Gharti et al., 2014). *Stemphylium* blight is an important disease of lentils, which occurs under high humidity and low solar radiation conditions (Subedi et al., 2015), like the foggy conditions increasingly being experienced in the Terai. In addition to lentils, potatoes, brinjal, and tomatoes are also reported to be susceptible to disease in the foggy conditions (Samra et al., 2003). Apart from negative effects of fog, there are also some positive effects of fog events found to be reported, such as fog water harvesting in the hills of Nepal (Bignell and Makepeace, 2016) and use of fog water for irrigation in Ethiopia (KHM and El Enin MM et al., 2016). However, these positive effects of fog events are not found to be reported in the Terai. In this context, the increasing duration and intensity of fog events in the Terai may have further negative effects on winter crops and may cause a threat to food security in the region. To address this, there is need of in-depth study to understand the dynamics of occurrences of fog events in Terai. In addition, the development of an effective model to understand as well as predict fog events and their impact on agricultural production in Terai will support effective adaptation as well as mitigation measures in future.

4. Summary and conclusions

In this study, historical visibility data at four airport stations in the Terai region of Nepal (Nepalgunj, Bhairahawa, Simara and Biratnagar) were analysed to study changes in fog events over time. The fog variables investigated included the number of foggy days, foggy hours, dense foggy days and dense foggy hours. In addition, we searched for a simple empirical model to estimate visibility based on daily meteorological parameters. The major findings and conclusion of this study are listed below.

- The fog events start in the month of November, reach their peak in the months of December/January and end by the end of February in the Terai region of Nepal. There is a wide variation of the number of foggy days in the Terai spatially as well as temporarily. During the period 1980–2015, the average number of foggy days during winter in the Terai ranged from 24 days to 56 days across the different stations. The average total foggy hours in day-time during winter varied from 71 h to 169 h.
- Opacity (reciprocal of visibility) during winter is increasing at all the stations in the Terai during the study period of 1980–2015. Overall the fog related parameters *viz.* foggy days, foggy hours, dense foggy days and dense foggy hours have increasing trends at least at the 0.1 level of statistical significance. The decreasing trend of maximum temperature and increasing trend of minimum temperature and humidity during winter in the majority of the studied stations also support the results of increasing trend of fog related parameters.
- A simple empirical model to estimate visibility based on the daily meteorological parameters was formulated. The formulated model is

Table 13
Crop calendar and months with foggy days in Terai.

	Jan	Feb	Mar	Apr	May	Jun	Jul	Aug	Sep	Oct	Nov	Dec
Months with Foggy Days												
Early Rice			TP	TP		H	H					
Normal Rice						TP	TP			H	H	
Later Summer Rice							TP	TP			H	H
Lentil		H	H							P	P	
Wheat			H								P	
Winter Maize		H	H							P	P	
Spring Maize	P	P			H	H						

(TP = Transplanting; H = Harvesting; P = Sowing), Source: (FAO, 2007).

not found to be impressive due to low adjusted R^2 value. The model could be further improved by including atmospheric aerosol data, where available, along with meteorological parameters.

- As the increasing trend in fog events in the Terai may curtail the winter crop production and negatively affect the livelihood, as well as the food security, of the Terai region of Nepal, there is need of better understanding regarding the dynamics of the fog episodes in the Terai region of Nepal for adaptation and mitigation measures for the future.

Acknowledgments

The lead author (S Shrestha) is thankful to the Australian Centre for International Agricultural Research (ACIAR) for providing the John Alright Fellowship (JAF) to pursue his Ph.D. at the University of Melbourne. Murray Peel is the recipient of an Australian Research Council Future Fellowship (FT120100130). We acknowledge the Department of Hydrology and Meteorology (DHM) for providing access to the METAR datasheets of Terai stations. Similarly, we would like to thank Er. Sanjeet Kumar Jha, Er. Bikash KC, and Er. Mukti Nath Jha of the Agricultural Engineering Division, Nepal Agriculture Research Council (NARC) for assisting the first author in transcribing the fog data. Thanks also to Dr. Anne Verhoef, Associate Editor, and the anonymous reviewers for their valuable suggestions in improving the manuscript.

References

Akimoto, Y., Kusaka, H., 2015. A climatological study of fog in Japan based on event data. Atmos. Res. 151, 200–211. http://dx.doi.org/10.1016/j.atmosres.2014.04.003.
Aslam, M., 2012. Fog hazards in Punjab. Pak. J. Meteorol. 8, 1–9.
Baidya, S.K., Shrestha, M.L., Sheikh, M.M., 2008. Trends in daily climatic extremes of temperature and precipitaton in Nepal. J. Hydrol. Meteorol. 5, 38–51.
Bignell, B., Makepeace, T., 2016. Fog collection projects in Nepal : 1997–2016. In: 7th International Conference on Fog, Fog Collection and Dew Wroclaw. Poland 24–29 July 2016. pp. 3–6.
CBS, 2016. Statistical Year Book Nepal-2015, 15th ed. Central Bureau of Statistics, National Planning Commission Secretariat, Government of Nepal, Kathmandu, Nepal.
CBS, 2015. Nepal In Figure- 2015. Central Bureau of Statistics, National Planning Commission Secretariat, Government of Nepal, Kathmandu, Nepal.
Chand, R., Singh, C., 2015. Movements of western disturbance and associated cloud convection. J. Indian Geophys. Union 19, 62–70.
Connor, J.A., Farhat, S.K., Vanderford, M., 2012. GSI Mann-Kendall Toolkit For Constituent Trend Analysis- User's Manual. Groundwater Services, Inc., Houston, Texas, USA.
Croft, P.J., 2003. Fog. In: In: Holton, J.R., Curry, J.A., Pyle, J.A. (Eds.), Encyclopedia of Atmospheric Sciences, vol. 1–6. Elsevier, pp. 777–792.
Dai, A., 2006. Recent climatology, variaility, and trends in global surface humidity. J. Clim. 19, 3589–3606. http://dx.doi.org/10.1175/JCLI3816.1.
DesInventor, 2015. Nepal - historic inventory of disaster [WWW document]. Disaster Inf. Manag. Syst URL https://online.desinventar.org/desinventar/#NPL-DISASTER (Accessed 2.July.17).
Dimri, A.P., Chevuturi, A., 2016. Western disturbances - an Indian meteorological perspective. Springerhttp://dx.doi.org/10.1007/978-3-319-26737-1.
Dimri, A.P., Niyogi, D., Barros, A.P., Ridley, J., Mohanty, U.C., Yasunari, T., Sikka, D.R., 2015. Western disturbances: a review. Rev. Geophys. 53, 225–246. http://dx.doi.org/10.1002/2014RG000460.
FAO, 2007. Special Report Nepal: FAO Global Information and Early Warning System on Food and Agriculture - World Food Programme.
Gautam, R., 2014. Challenges in early warning of the persistent and widespread winter fog over the Indo- Gangetic plains: a satellite perspective. In: Singh, Ashbindu, Zommers, Zinta (Eds.), Reducing Disaster: Early Warning Systems for Climate Change. Springer Science+Business Media Dordrecht, pp. 51–61. http://dx.doi.org/10.1007/978-94-017-8598-3.
Gautam, R., Hsu, N.C., Kafatos, M., Tsay, S.C., 2007. Influences of winter haze on fog/low cloud over the Indo-Gangetic plains. J. Geophys. Res. Atmos. 112, 1–11. http://dx.doi.org/10.1029/2005JD007036.
Gharti, D.B., Darai, R., Subedi, S., Sarker, A., Kumar, S., 2014. Grain legumes in Nepal: present scenario and future prospects. World J. Agric. Res. 2, 216–222. http://dx.doi.org/10.12691/wjar-2-5-3.
Ghude, S.D., Bhat, G.S., Prabhakaran, T., Jenamani, R.K., Chate, D.M., Safai, P.D., Karipot, A.K., Konwar, M., Pithani, P., Sinha, V., Rao, P.S.P., Dixit, S.A., Tiwari, S., Todekar, K., Varpe, S., Srivastava, A.K., Bisht, D.S., Murugavel, P., Ali, K., Mina, U., Dharua, M., Rao, J., Padmakumari, B., Hazra, A., Nigam, N., Shende, U., Chandra, B.P., Mishra, A.K., Kumar, A., Hakkim, H., Pawar, H., Acharga, P., Kulkarni, R., Subharthi, C., Balaji, B., Varghese, M., Bera, S., Rajeevan, M., 2017. Winter fog experiment over the Indo-Gangetic plains of India. Curr. Sci. 112, 767–784. http://dx.doi.org/10.18520/cs/v112/i04/767-784.
Gilbert, R.O., 1987. Statistical Methods for Environmental Pollution Monitoring. Van Nostrand Reinhold Company, New York. http://dx.doi.org/10.2307/1270090.
GON, 2011. The Population and Socio-Economic Atlas of Nepal 2011. Government of Nepal, NGIIP, Survey Department and Central Bureau of Statistics, Kathmandu, Nepal.
Goverment of Nepal, 2016. Compendium of Environment Statistics, Nepal 2015. Central Bureau of Statistics, National Planning Commission Secretariat, Governemnt of Nepal, Kathmandu, Nepal.
Guerreiro, C.B.B., Foltescu, V., de Leeuw, F., 2014. Air quality status and trends in Europe. Atmos. Environ. 98, 376–384. http://dx.doi.org/10.1016/j.atmosenv.2014.09.017.
Gultepe, I., Tardif, R., Michaelides, S.C., Cermak, J., Bott, A., Bendix, J., Mullar, M.D., Pagwoski, M., Hansen, B., Ellrod, G., Jacobs, W., Toth, G., Cober, S.G., 2007. Fog research : a review of past achievements and future perspectives. Pure Appl. Geophys. 164, 1121–1159. http://dx.doi.org/10.1007/s00024-007-0211-x.
Jaswal, A., Kumar, N., Prasad, A., Kafatos, M., 2013. Decline in horizontal surface visibility over India (1961-2008) and its association with meteorological variables. Nat. Hazards 68, 929–954.
Jenamani, R.K., 2007. Alarming rise in fog and pollution causing a fall in maximum temperature over Delhi. Curr. Sci. 93, 313–322.
Kaskaoutis, D.G., Singh, R.P., Gautam, R., Sharma, M., Kosmopoulos, P.G., Tripathi, S.N., 2012. Variability and trends of aerosol properties over Kanpur, northern India using AERONET data (2001–10). Environ. Res. Lett. 7, 24003. http://dx.doi.org/10.1088/1748-9326/7/2/024003.
KHM, M., El Enin MM, A., 2016. Fog water collection for agriculture use (peanut irrigation) under semi- arid region conditions in North Coast of Egypt. Adv. Crop Sci. Technol. 4. http://dx.doi.org/10.4172/2329-8863.1000219.
Manandhar, K.B., 2006. The fog episode in Southern Terai Plains of Nepal: some observations and concepts. J. Hydrol. Meteorol. 3, 95–99.
Manandhar, S., Vogt, D.S., Perret, S.R., Kazama, F., 2011. Adapting cropping systems to climate change in Nepal: a cross-regional study of farmers' perception and practices. Reg. Environ. Chang. 11, 335–348. http://dx.doi.org/10.1007/s10113-010-0137-1.
Marasini, D., Marahatta, S., Dhungana, S.M., Acharya, R., 2016. Effect of date of sowing on yield and yield attributes of different wheat varieties under conventional tillage in sub-humid condition of Chitwan District of Nepal. Int. J. Appl. Sci. Biotechnol. 4, 27. http://dx.doi.org/10.3126/ijasbt.v4i1.14335.
Meeus, J., 1999. Astronomical Algorithms, 2nd ed. Willmann-Bell, Richmond Virginia 23235, USA.
Musleheddin, B.M., Mir, H., Faisal, N., 2004. Recent occurence of fog over Pakistan (1997–2000). Pak. J. Meteorol. 1, 3–18.
Ramanathan, V., 2006. Atmospheric brown clouds: health, climate and agriculture impacts. Scr. Var. 47.
Ramanathan, V., Feng, Y., 2009. Air pollution, greenhouse gases and climate change: global and regional perspectives. Atmos. Environ. 43, 37–50. http://dx.doi.org/10.1016/j.atmosenv.2008.09.063.
Salinger, M.J., Stigter, C.J., Das, H.P., 2000. Agrometeorological adaptation strategies to increasing climate variability and climate change. Agric. For. Meteorol. 103, 167–184.
Salmi, T., Maatta, A., Anttila, P., Ruoho-Airola, T., Amnell, T., 2002. Detecting Trends of Annual Values of Atmospheric Pollutants by the Mann-Kendall Test and Sen's Slope Estimates the Excel Template Application MAKESENS, Finnish Meteorological Institute, Air Quality Research. Finnish Meteorological Institute, Helsinki, Finnland.
Samra, J.S., Singh, G., Ramakrishna, Y., 2003. Cold Wave of 2002-03: Impact on Agriculture. Central Research Institute for Dryland Agriculture, Hyderabad. India.
Sathiyamoorthy, V., Arya, R., Kishtawal, C.M., 2016. Radiative characteristics of fog over the Indo-Gangetic Plains during northern winter. Clim. Dyn. 47, 1793–1806. http://dx.doi.org/10.1007/s00382-015-2933-2.
Sen, P.K., 1968. Estimates of the regression coefficient based on Kendall's Tau. J. Am. Stat. Assoc. 63, 1379–1389.
Sharma, B., Amarasinghe, U., Xueliang, C., de Condappa, D., Shah, T., Mukherji, A., Bharati, L., Ambili, G., Qureshi, A., Pant, D., Xenarios, S., Singh, R., Smakhtin, V., 2010. The Indus and the Ganges: River basins under extreme pressure. Water Int. 35, 493–521. http://dx.doi.org/10.1080/02508060.2010.512996.
Shrestha, A.B., Bajracharya, S.R., Sharma, A.R., Duo, C., Kulkarni, A., 2016. Observed trends and changes in daily temperature and precipitation extremes over the Koshi River Basin 1975–2010. Int. J. Climatol. 37, 1067–1083. http://dx.doi.org/10.1002/joc.4761.
Shrestha, S., 2011. Status of agricultural mechanization in Nepal. In: Proceedings of Sustainable Agricultural Mechanization Roundtable: Moving Forward on the Sustainable Intensification of Agriculture 8–9 December 2011, Bangkok Thailand. Centre for Sustainable Agricultural Mechanization, Bangkok, Thailand. pp. 1–4.
Singh, S., Singh, D., 2010. Recent fog trends and its impact on wheat productivity in NW plains in India. In: 5th International Conference on Fog, Fog Collection and Dew Münster, Germany. 25–30 July 2010. Münster, Germany.
Smadja, J., Aubriot, O., Puschiasis, O., Duplan, T., Grimaldi, J., Hugonnet, M., Buchheit, P., 2015. Climate change and water resources in the Himalayas. J. Alp. Res. Rev. Géogr. Alp. 0–25. http://dx.doi.org/10.4000/rga.2910.
Srivastava, A.K., Dey, S., Tripathi, S.N., 2012. Aerosol characteristics over the Indo-Gangetic Basin: implications to regional climate. In: Abdul-Razzak, Hayder (Ed.), Atmospheric Aerosols - Regional Characteristics - Chemistry and Physics. InTech, pp. 47–79. http://dx.doi.org/10.5772/47782.
Srivastava, S.K., Sharma, A.R., Sachdeva, K., 2016. A ground observation based climatology of winter fog: study over the Indo-Gangetic plains, India. Int. J. Environ. Chem. Ecol. Geophys. Eng. 10, 686–697.
Subedi, S., Shrestha, S., KC, G.B., Thapa, R.B., Ghimire, S.K., Neupane, S., 2015. Effect of

meteorological factors on the development of lentil stemphylium blight at different sowing dates in Rampur, Chitwan, Nepal. Azarian J. Agric. 3, 142–146.
Syed, F.S., Körnich, H., Tjernström, M., 2012. On the fog variability over south Asia. Clim. Dyn. 39, 2993–3005. http://dx.doi.org/10.1007/s00382-012-1414-0.
UNEP, DA, 2014. South Asia Environment Outlook 2014. United Nations Environment Programme (UNEP) South Asian Association for Regional Cooperation (SAARC) and Development Alternatives (DA).
Van Oldenborgh, G.J., Yiou, P., Vautard, R., 2010. On the roles of circulation and aerosols in the decline of mist and dense fog in Europe over the last 30 years. Atmos. Chem. Phys. 10, 4597–4609. http://dx.doi.org/10.5194/acp-10-4597-2010.
Vautard, R., Yiou, P., Van Oldenborgh, G.J., 2009. Decline of fog, mist and haze in Europe over the past 30 years. Nat. Geosci. 2, 115–119. http://dx.doi.org/10.1038/ngeo414.
WHO, 2016. Ambient Air Pollution Database, WHO, May 2016. URL http://www.who.int/phe/health_topics/outdoorair/databases/cities/en/ (Accessed 2.July.17).
Witiw, M.R., LaDochy, S., 2008. Trends in fog frequencies in the Los Angeles Basin. Atmos. Res. 87, 293–300. http://dx.doi.org/10.1016/j.atmosres.2007.11.010.
WMO, 1975. International Cloud Atlas. Volume I: Manual on the Observation of Clouds and Other Meteors. WMO Publication, Geneva, Switzerland.
Yasmeen, Z., Rasul, G., Zahid, M., 2012. Impact of aerosols on winter fog of Pakistan. Pak. J. Meteorol. 8, 21–30.

Chapter 4

Cold waves in Terai region of Nepal and farmer's perception of the effect of fog events and cold waves on agriculture

This chapter addresses the research sub-question no 2 and 3. This chapter has been submitted to Theoretical and Applied Climatology and is currently under review as described in the preface.

Cold waves in Terai region of Nepal and farmer's perception of the effect of fog events and cold waves on agriculture

Shreemat Shrestha [1]*, Murray C. Peel and Graham A. Moore

Department of Infrastructure Engineering, University of Melbourne, Parkville, Melbourne, VIC 3010, Australia; mpeel@unimelb.edu.au (M.C.P.); grahamam@unimelb.edu.au (G.A.M.)

* Correspondence: shreemats@student.unimelb.edu.au or shreematshrestha@yahoo.com

Abstract: Cold waves are considered one of the important extreme weather events affecting winter crop production in the Indo Gangetic plain (IGP). In spite of media coverage of extreme cold events in the Terai area of Nepal (Nepal section of IGP) in recent years, few studies on this topic were found. This study investigates cold waves and their impact on agriculture during winter in the Terai region of Nepal. Historical daily maximum and minimum temperature data from six stations in the Terai (Dhangadhi, Nepalgunj, Bhairahawa, Simara, Janakpur and Biratnagar) during 1971- 2015 were analyzed to study the occurrence of cold days, cold nights, extreme cold days, extreme cold nights, cold wave days and extreme cold wave days in the Terai. The average number of cold days per annum ranges from 15.6 days to 17.9 days and the extreme cold days per annum ranges from 3.2 days to 3.6 days in the Terai. Except for Nepalgunj, all the Terai stations show statistically significant increasing trends in the frequency of cold days and extreme cold days over the last four decades. Similarly, the average number of cold wave days varies from 9.2 to 13.8 per annum and the average number of extreme cold wave days varies from 1.4 to 3.8 days in the Terai region of Nepal. By comparing the co-occurrence of foggy days and cold and extreme cold wave days at Biratnagar, Simara, Bhairahawa and Nepalgunj airport, it is also observed that most of the cold and extreme cold wave days are also foggy days. The perception of farmers regarding the effect of fog and cold wave events was explored through focus group discussions at Dhanusha and Sunsari districts of Nepal and found that the fog and cold events have significantly affected their winter crops, livestock and their day to day life.

Keywords: cold wave; cold days; Terai; fog; farmer's perception; Nepal

1. Introduction

Large areas of south Asia, extending west from Pakistan to Bangladesh, including the Indo Gangetic Plain (IGP), are usually covered by a thick blanket of fog during winter (Syed et al., 2012). Similarly, cold wave and severe cold wave conditions are regularly experienced in north India, northwest India and central India during winter (Bhan, 2016). In north India, these extreme weather events are due to "western disturbances" during winter (Dimri and Chevuturi, 2016). Significant impacts on agriculture due to these extreme events (cold wave and fog) are reported in several studies in India (Samra et al., 2003; Singh and Singh, 2010; Mahdi et al., 2015). In spite of being part of the IGP, only limited information is reported on the agricultural impact of cold wave and fog events in the Terai area of Nepal. In this context, this paper aims to study cold wave events through analysis of historical daily temperature data from stations in the Terai region of Nepal and investigate any relationship between temperature and fog events during winter. In addition, the impact of cold wave and fog events on agriculture in the Terai region of Nepal, along with farmer's perception of these impacts, will also be explored.

Cold waves are a regular episode during winter in the northern part of the Indian sub-continent. After analysis of daily temperature data from 103 stations in India during 1961-2010, Pai et al. (2017) concluded that cold waves are a regular phenomenon of most areas of India, except the southern Peninsula and north-east India. Similarly, Singh and Patwardhan (2012) studied extreme weather events in India during 1978-2006 and found that cold waves are the 4th most important event with respect to impact (mortality) in that period. Singh and Patwardhan (2012) also reported that among the states of India, Bihar (a neighbouring state of the Terai area of Nepal) is a leading state affected by cold waves with a high number of events and mortality during that period. For example, during the 1st to 3rd weeks of January 2003, the northern states of India were severely affected by several cold wave events, resulting in more than 900 reported deaths, of which 813 were from Uttar Pradesh alone (De et al., 2005).

The Indian Meteorological Department (IMD) uses a threshold value of daily minimum temperature to declare a cold wave event in India as described in Table 1. This definition is adopted in many cold wave event studies in India. Pai et al. (2004) studied heat wave and cold wave events for the meteorological sub-divisions of India from 1971-2000 and indicated a significant increase in the frequency, persistence and spatial coverage of cold wave events in the decade 1991-2000 compared to the previous two decades. Bhatla et al. (2016) studied the cold wave in the six stations of eastern Uttar Pradesh, India (Allahabad, Varanasi, Gorakhpur, Lucknow, Baharaich and Khiri) and found that in all the stations except Varanasi, the cold wave days during winter increased in the decade 2001-2010 compared to previous decade. Similarly, Mahdi and Dhekale (2016) studied heat wave and cold wave events in southern Bihar using temperature data from 1969-2013 and found that January, February, and December were the months with most

cold events in southern Bihar, with average duration of 3.98, 3.5 and 3 consecutive days respectively. In contrast to the findings of Pai et al. (2004), Mahdi and Dhekale (2016) found a declining trend in cold waves in the study area. Revadekar et al. (2012) studied Indian weather extremes during 1970-2003, at 121 stations, and found 75 percent of stations showed a declining trend in the number of cold events. Similarly, Jaswal et al. (2013) studied extreme events at Indian stations using daily maximum and minimum temperature during 1969-2012. Their trend analysis of cold, very cold and extremely cold nights indicated a significant decreasing trend of cold events in December, a mixed trend in January, while in February there was a significant decreasing trend in North India.

Table 1: Definition of cold wave adopted by IMD (IMD, n.d.)

Cold wave condition is considered when the wind chill effective minimum temperature (WCTn) is ≤10 ˚C. The WCTn is derived from daily minimum temperature and wind speed as described in WMO (1972). Cold wave and severe cold wave are declared in the following conditions.		
Condition	**Departure of T_{min} from normal**	**Declared Event**
Normal minimum Temperature ≥10 ˚C	-5 ˚C to -6 ˚C	Cold Wave
	≤ -7 ˚C	Severe Cold Wave
Normal minimum Temperature <10 ˚C	-4 ˚C to -5 ˚C	Cold Wave
	≤-6 ˚C	Severe Cold Wave
When WCTn ≤ 0 ˚C	Any Value	Cold Wave in all stations except in those station whose normal minimum temperature is < 0 ˚C

The entire IGP area of Punjab, Haryana, Delhi, Uttar Pradesh, Bihar and west Bengal area can be engulfed by dense fog during winter (Badarinath et al., 2009; Syed et al., 2012; Jenamani, 2012; Sathiyamoorthy et al., 2016). Syed et al. (2012) suggested that moisture available from western disturbances and from vast irrigated agricultural land in the western IGP region could be the reason behind high fog frequency in the region. In addition, their study also found an increasing occurrence of fog events in the foot hills of the Himalaya, with a trend of more than 8% increase per decade in mean frequency of fog occurrence during winter. By analysing Indian weather satellite, INSAT-3D fog data, International Satellite Cloud Climatology Project (ISCCP) cloud data, and Clouds and the Earths Radiant Energy System (CERES) cloud radiative forcing data, Sathiyamoorthy et al. (2016) showed that a foggy winter is colder than a non-foggy winter in the IGP and cooling of the entire IGP occurs at a rate of -0.6˚C for every 10 Wm^{-2} decrease in radiative forcing due to fog. Following a western disturbance, fog is normally observed, due to nocturnal cooling, which blocks solar radiation and further reduces the temperature to make the cold wave more intense (Bedekar et al., 1974). Similarly, Gautam, (2014) explained that cold waves, in combination with moist air and atmospheric aerosols, help the formation of fog and dense fog, which reduces solar insolation and results in lower temperatures, which provides a positive feedback to the persistence of foggy and cold conditions. During foggy days in winter, the

maximum temperature is below normal, which results in prolonged cold periods (Samra et al., 2003). However, the IMD definition of cold wave only considers the minimum temperature (which occurs during night) and does not consider the reduction in maximum temperature (which occurs during day time). Even though, people's health is affected by both prolonged series of cold nights (low minimum temperature) and cold days (low maximum temperature) (Hassi, 2005), it is expected that people are more exposed to outdoor temperature in the day time compared to night due to their increased daytime activities. So, in contrast to the absolute threshold of minimum daily temperature used by IMD, Radinović and Ćurić (2012) used a statistical threshold of daily temperature to define cold and hot waves. Labajo et al. (2014) defined the occurrence of a cold wave event when the daily maximum and minimum temperature are both less than the 10^{th} percentile value for more than two days. Similarly, if the daily maximum temperature and minimum temperature are both less than the 5^{th} percentile value for two days, it is called an extreme cold wave event. A similar definition, but based on three consecutive days, was adopted by Capozzi and Budillon (2017) during analysis of cold waves in Montevergine during 1984-2015. Similarly, Spinoni et al. (2015), used 10^{th} percentile maximum temperature and minimum temperature for five consecutive days for cold wave days and cold wave nights respectively in the Carpathian region from 1961-2010.

The Terai region of Nepal in the foot hills of the Himalaya is also reported to be severely affected by cold wave during winter, but there is a lack of systematic study of cold waves and their effect in this region. Some cold wave related studies for the Terai region of Nepal are discussed below.

Baidya et al. (2008) studied temperature extremes during 1971-2006 for Nepal and found an increasing trend in minimum temperature, decreasing trend in maximum temperature and decreasing trend in daily temperature range in the Terai region during winter. Similarly, Shrestha et al. (2016) analysed daily temperature data from the Koshi basin between 1975 and 2010 and found daily maximum temperature was increasing by $0.1^{o}C$ per decade and minimum temperature by $0.3^{o}C$ per decade. Their study also found in the IGP area that maximum temperature in winter and the pre-monsoon season was decreasing (statistically significant) and the number of cold days in winter was increasing.

The cold wave is reported to be a comparatively new weather phenomena in the Terai and well covered in local media in recent years and it has become a major health hazard to the people of this region (WHO, 2016). Cold waves have not only resulted in the death of 797 people during 2000-2013, but also damaged 22,000 ha of crops and caused the death of 732 cattle in Nepal (DesInventor, 2015). Manandhar (2006) analysed the 1997/98 and 2002/3 winter fog episodes in the Terai and suggested that the maximum temperature dropped close to the minimum temperature, due to the thick and continuous foggy weather, which resulted in cold wave events in the region. Manandhar et al., (2011) reported that the frequency of cold wave days increased

at Bhairahawa (Western Terai in Nepal) during 1992-2005 and the combination of a cold wave event with dense fog had adverse effects on agriculture in the Terai region.

Assessing the impact on farmers of extreme events, like cold waves, is important to understand the impact on their livelihood and the economy. Manandhar et al. (2011) reported that the majority of farmers (56 out of 74) in Bhairahawa experienced an increase in cold wave days over the last 14 years, which adversely affected people's lives and agriculture. Yang et al. (2014) found that, contrary to people's perception of decreasing cold wave frequency in the hills and mountains, the farmers of the Terai region of the Koshi basin experienced increasing cold wave frequency, which resulted in loss of crops and adverse effects on both human and animal health. Ojha et al. (2014) studied the perception of the farmers regarding climate change in the IGP covering Nepal, Bangladesh and Indian state of Punjab and found that 78% of the respondents felt that summer days are getting hotter and 66 % agreed that winter is getting colder. Similarly, Haque et al. (2012) studied people's perception of climate change and subsequent human risks in Bangladesh and found that almost all participants perceived that cold wave and dense fog events increased in recent years compared to the previous 5 to 10 years and the impact of those events on Boro rice, beetle leaf, potato, and mango crops was negative. Samra et al. (2003) documented the effect of cold waves on agriculture during 2002-03 in North India and found that winter crops, vegetables and fruits were seriously affected. For example, around Agra there was 100% damage of brinjal, 80% for tomato and 25% for potato due to cold wave during that period, and it was estimated that there was reduction of wheat, gram and mustard by 10-40%, 25-30% and 50-70% respectively that year.

Although cold waves are important weather events in the Terai, very few studies have been conducted. In this paper we seek to understand cold wave events in the Terai region of Nepal and their effect on agriculture. To do this we analyzed historical daily temperature data to investigate cold wave occurrence in the Terai region of Nepal via trend analysis of annual cold wave days and extreme cold wave days. We also investigated farmer's perception of the effect of fog and cold wave events on agriculture in the eastern Terai.

2. Material and methods

2.1. Study area

The Terai region is a flat plain in southern Nepal with elevation ranging from 60 to 200 m (Figure 1). Compared to hilly and mountainous regions of the country, the Terai only occupies 17% of the land area of Nepal. However, this region is very important as it accommodates 50.27% of the population of the country (CBS, 2016). The population of the Terai has increased due to recent migration of people from the mountainous and hilly regions of Nepal (CBS, 2014a). Due to the availability of agricultural land and irrigation facilities in the Terai, most of the countries crop production of paddy rice, maize, wheat, lentil, sugarcane, vegetable etc. comes from the Terai, which is considered the food basket of the country. Based on the Köppen climatic classification (Peel et al., 2007), the Terai region of Nepal has a humid subtropical climate (Cwa) with distinctly dry winters (CBS/GON, 2016). Karki et al. (2016) using a larger dataset of local data also found the Terai region to have a Cwa climate type using the Köppen climate classification. However, they argue that the Köppen rules should be changed for this region, to ensure the climate of the Terai is tropical savanna (Aw) with a distinct dry season in winter (Karki et al., 2016).

To investigate cold wave events in the Terai region, historical daily temperature data from six stations listed in Table 2 were analysed. The six selected stations are evenly spread across the Terai region (see Figure 1), which stretches ~885 km from east to west and is 26 to 32 km wide (CBS, 2016), and they are considered to be representative of the region.

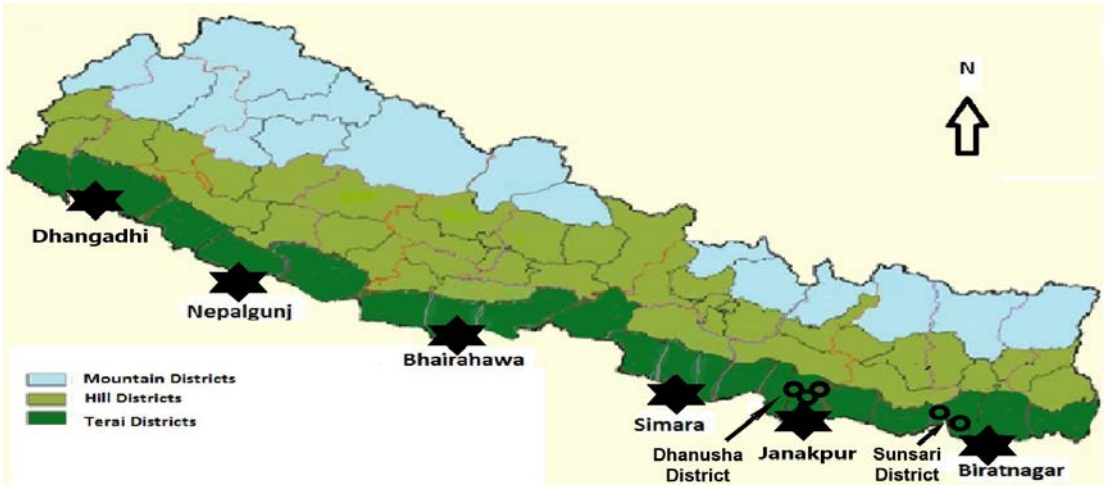

Figure 1: Study area -Terai region of Nepal (dark green colored area) and studied stations (stars) and focus group discussion locations (circles). Adapted from Shrestha et al. (2018)

Table 2: Details of studied temperature stations

SN	Station	Index No	District	Latitude (° North)	Longitude (° East)	Elevation (m)
1	Dhangadhi	209	Kailali	28.800°	80.550°	187
2	Nepalgunj Airport	420	Banke	28.100°	81.667°	165
3	Bhairahawa Airport	705	Rupandehi	27.517°	83.433°	109
4	Simara Airport	909	Bara	27.167°	84.983°	130
5	Janakpur Airport	1111	Dhanusha	26.717°	85.967°	90
6	Biratnagar Airport	1319	Morang	26.483°	87.267°	72

The Sunsari and Dhanusha districts are representative of the eastern Terai and these two districts were selected to explore farmer's perceptions of the effect of fog and cold wave on agriculture. In both districts, diverse and mixed ethnic groups are found due to internal migration of people from the hill and mountain districts (Figure 1). Based on 2011 census data, the four major ethnic groups in Dhanusha are Yadav, Koiri, Musalman and Teli and in Sunsari are Tharu, Musalman, Chettri and Bramin (Hill) (CBS, 2016). The farmer's perception study was conducted in five randomly selected villages, listed in Table 3, from the Sunsari and Dhanusha districts.

Table 3: Villages included in farmer's perception of the effect of fog / cold wave on agriculture

SN	Study Village	District	Location	Major Feature
1	Batteswor	Dhanusha	26.883˚N 85.925˚E 120 m Elevation	Village with mixed Terai communities and farmers are involved in both cereal and vegetable cultivation.
2	Naktajhijh, Mithila	Dhanusha	26.880˚N 85.960˚E 150 m Elevation	Village with major ethnic group Koiri (Mahato) and farmers are mainly involved in vegetable cultivation.
3	Sinnorjoda	Dhanusha	26.780˚N 85.925˚E 80 m Elevation	Village with major ethnic group Yadav and mainly cereal crop is cultivated.
4	Saalbandi	Sunsari	26.715˚N 87.107˚E 95 m Elevation	Village with mainly migrated communities from the hills and farmers are involved in both cereal and vegetable cultivation.
5	Simariya	Sunsari	26.576˚N 87.237˚E 85 m Elevation	Village with indigenous Tharu (Chaudhari) community and farmers are involved in both vegetable and cereal cultivation.

2.2. Methods

The methods adopted in this study are discussed in following subsections.

2.2.1. Cold days, cold night and cold wave analysis

The daily maximum and minimum temperature data of the selected meteorological stations were collected from the Department of Hydrology and Meteorology (DHM). In this study, quality control of the temperature data was performed by removing the outliers and error values (for example,

maximum and minimum temperature greater than 70^{o} C, minimum temperature greater than maximum temperature etc.). Time series plots and histogram were also compared with neighbouring stations, and validation against external sources was performed to ensure the quality of the data. In addition, we also tested the homogeneity of daily maximum and minimum temperature data at each study site using the RHtestsV4 software package (Wang and Feng, 2013), which is based on the algorithms described by Wang (2008a) and Wang (2008b), to identify any non-climatic variability within each time series. This package is widely used to check the homogeneity of daily temperature data in different parts of the world, for example China (Xu et al., 2013), Israel (Yosef et al., 2018), Bulgaria (Malcheva, 2018), Canada (Fortin et al., 2017), and South Africa (Kruger and Nxumalo, 2017).

In this study we used percentile threshold values of daily maximum temperature and minimum temperature, as suggested by the Expert Team on Climate Change Detection and Indices (ETCCDI) (ETCCDI, n.d.), Fang et al. (2016) and Acar et al. (2018), to define cold day and cold night respectively. The cold day and extreme cold day are defined as a day in which the daily maximum temperature is equal to or less than the 5th and 1st percentiles respectively. Similarly, cold night and extreme cold night is declared when the minimum temperature is equal or less than the 5th and 1st percentile respectively. The number of cold days, extreme cold days, cold nights and extreme cold nights per annum are used to analyse extreme cold scenario in the six Terai stations of Nepal.

There is no standard definition of a cold wave adopted in Nepal and various researchers have explained cold wave from different perspectives. Cold waves in the Terai area of Nepal are portrayed as foggy days with low temperature due to the absence of sunshine, high humidity and low visibility (Gum et al., 2009). However, Manandhar et al. (2011) defined cold wave in the Terai area as a sudden drop of temperature within 24 hours, often accompanied by fog for many days. Similarly, Sharma (2015) explained cold wave in the Terai as a cold condition in winter created by thick fog throughout the day, and even subsequent days, in which the maximum temperature significantly drops. From this review it seems that cold wave is found to be closely related with fog events during winter in the Terai. The meteorological department in India only considers a minimum temperature threshold to declare a cold wave. After discussion with farmers in the Terai, consultation with experts, and a brief review of the literature, it is considered that the deviation of both maximum and minimum temperature, in combination with persistence of that deviation, is important for identification of cold wave. In this study, cold wave and extreme cold wave is defined as when both the maximum and minimum temperature are less than the 10th and 5th percentile respectively for two or more consecutive day.

The Mann Kendall test, as described by Gilbert (1987), is used to determine whether statistical trends in annual cold days, extreme cold days, cold nights, extreme cold nights, cold wave days,

and extreme cold wave days exist at the six Terai stations. Standard normal z values are used to test the trend significance at significance levels, α=0.001, 0.01, 0.05 and 0.1. To estimate the slope of any trend in the annual number of cold days, extreme cold days, cold nights, extreme cold nights at each station the Sen's slope nonparametric method is adopted (Sen, 1968). In this method, the trend is assumed to be linear and the equation is given by:

$$f(t)=Qt + B \quad (1)$$

Where, Q is the slope and B is constant.

To investigate fog events and cold wave, visibility observation data from Meteorological Terminal Air Report (METAR) visibility observations at four Terai airports, Biratnagar, Simara, Bhairahawa and Nepalgunj, during 1994-2015 were used. A foggy day is defined to occur when the visibility is less than 1000 m in that day (WMO, 1975).

2.2.2 Field Work

To explore the perception of the farmers on the effect of fog and cold wave on agriculture, the methodologies adopted in this study were key informant survey, transect walk, field observations and focus group discussion (FGD). For each village, a key informant survey was conducted to acquire general information about the village, agricultural scenario and potential participants based on the study criteria for the focus group discussion. Potential participants were representative farmers of the selected village who were directly involved in farming with 20 years of experience. Key informants for a village were either a local agricultural technician, social worker, teacher, etc. A transect walk, along with the key informants and participating farmers, was also performed to observe the crops cultivated, visually observe the effect of fog and cold wave on agriculture and observe the adaptive measures adopted by the farmers to minimize the effect of fog and cold wave on agriculture and their livelihood. This study (Ethics ID 1750778) was conducted after approval by Engineering Human Ethics Advisory Group, University of Melbourne as a minimum risk project. This study was conducted in the study area during the foggy season of December 2017.

Since focus group discussion (FGD) is considered an appropriate methodology for exploratory qualitative research (Stewart et al., 2007), it was adopted in this study to explore farmer's perceptions of the effect of fog on agriculture and their livelihood in the Terai region of Nepal. Regarding the number and size of each FGD, a wide range of approaches have been found. It is recommended that more than one FGD be conducted to increase the reliability of the collected data (Vaughn et al., 1996). It is also reported that more than 80 percent of themes were discoverable within 2-3 FGDs (Carlsen and Glenton, 2011; Guest et al., 2017). In this study it was planned to conduct a FGD in each of the randomly selected five villages in Sunsari and Dhanusha districts. About six to eight experienced farmers were included in each FGD, which aligns with the

advice of Guest et al. (2017). The aim in selecting participants for the FGD was to include representative farmers cultivating major crops in that area as well as farmers from different ethnic groups and gender to capture a diverse perspective on the effect of fog on agriculture and adopted adaptation measures. In Dhanusha, it was noticed that women members of the FGD did not actively participant in the discussion with the male participants. In this case, a separate FGD for only women participants was conducted in Naktajhijh, Mithila in Dhanusha to capture women's perspective on the issue. The lead author of this paper moderated all FGDs and audio from each FGD was recorded. To capture verbal and non-verbal communication expressed during the FGDs, three trained note takers were also involved in data collection during the FGDs. An open check list was used by the moderator to run the FGD and the methodology adopted to moderate the FGDs in this study were as described and suggested by Morgan (1996), Stewart et al. (2007) and Gill et al. (2008).

3.0 Results and discussions

The results and discussion of this study are described in three sections. The first section deals with farmers' perception of cold wave and fog at Dhanush and Sunsari district of the eastern Terai region of Nepal. The second section explains the results of analysis of the daily temperature in relation to cold wave and fog events during winter in the Terai region of Nepal. The third section describes the farmers' perceptions of the effect of cold waves and fog events on agriculture and the livelihood of people of Dhanusha and Sunsari Districts.

3.1 Farmers' perception of fog events and cold waves

The perception of the farmers on the effect of fog events and cold waves on agriculture was assessed during field study through FGDs conducted at Dhanusha and Sunsari districts of the Terai region of Nepal and the results are described in this section.

3.1.1 Characteristics of farmers participated in FGD

The characteristics of the participants of the six FGDs conducted in the villages of Dhanusha and Sunsari are presented in Table 4. In general, the average age of the participants is above 46 years, except that of the women's FGD at Naktajhijh, Mithila, which is the lowest at 39.3 years. The oldest participant of age 70 participated at Naktajhijh, Mithila (Male) FGD. Regarding land ownership of the FGD participants, the average land holding of the participants at Batteswor, Dhanusha is the lowest (0.53 ha), whereas the participants at Simariya Sunsari had the highest (1.67 ha). The average land holding in the Terai region is 0.75 ha (CBS, 2014b) and the average land holding of the participants of FGDs are found to be near to this figure.

Table 4: Participants of FGD and their characteristics

SN	FGD Locations	Gender			Age			Land Ownership (Ha)		
		Male	Female	Total	Min	Max	Average	Min	Max	Average
1	Batteswor, Dhanusha	8		8	28	60	46.7	0.17	0.67	0.53
2	Sinorjoda, Dhanusha	7		7	35	62	46.4	0.66	1.5	0.96
3	Naktajhijh, Mithila (Male), Dhanusha	7		7	34	70	58.2	0.50	2.00	1.20
4	Naktajhijh, Mithila (Female), Dhanusha		6	6	28	55	39.3	0.50	1.00	0.74
5	Simariya, Sunsari	3	3	6	35	60	47.3	0.67	2.00	1.67
6	Saalbani, Sunsari	4	2	6	50	64	57	0.67	1.32	1.02

Source: FGDs (2017)

3.1.2 Perceptions of fog and cold wave occurrence

In all FGDs conducted in this study, the participants unanimously agreed that fog events are regular events that occur almost every year in their area. The participants all also agreed that the fog starts in the month of 'Mangshir' (the eighth month in 'Bikram Sambat' (Official calendar of Nepal)), which coincides with mid-November to mid-December of the Gregorian Calendar, during winter in their area. As almost all participants of FGDs recalled and agreed that the fog starts around the 'Bibaha Panchami' festival which occurs on the 5th day of 'Mangshir Shukla' month. In summary, it can be said from the FGD findings that the fog event generally starts in mid-November. Similarly, the participants agreed that the fog events generally end after the end of 'Magh' (10th month of Bikram Sambat) or beginning of 'Phalgun' (11th month of Bikram Sambat). Hence, FGD results clearly indicated that fog events generally end by the second week of February. The farmers also indicated that generally they experience 30 foggy days during winter every year (FGD Batteswor).

The participants of all the FGDs conducted in Sunsari and Dhanusha agreed that continuous and dense fog events bring a cold wave. According to the farmers, a cold wave starts when the Terai area is engulfed by a blanket of thick fog for several days during winter. The cold wave could be due to the blockage of solar radiation reaching the ground surface by fog, which results in a significant reduction in temperature as described by Bedekar et al. (1974). The participants also mentioned that due to a lack of solar radiation, it is very cold even during the day time, like "Mutu Samaune Jando" (very cold catching the heart) in the Terai. Regarding the cold, the FGD at Saalbani (migrated communities from hills) explained a local proverb "Pahad ko jando lato, Madhesh ko jando tikho" (the cold at the hills is blunt whereas the cold in the Terai is sharp). They explained that people and animals in the hills can face more cold than those of the plain area because of their body structure and preparedness. In addition, they explained that during winter in the hills, it is cold at night and morning but in the day time it is warm due to sunny day. In the Terai, during

cold day in winter it remains cold throughout the day because they won't be able to see the sun for several days due to dense fog.

Regarding recent extreme fog events, the FGD at Mithila (Male) recalled the fog event six years ago that was continuous foggy for more than a week. Similarly, the FGD at Batteswor, Dhanusha recalled an extreme fog event that occurred six years ago (2011 AD) in which 13 people from Batteswor and Kalipur village died due to the cold wave during that period. Similarly, the FGD of Sinorjoda, Dhanusha recalled an extreme fog event in the Terai six years before, in which eight villagers died due to cold and they could not see the sun for about one month during that winter. The extreme cold event mentioned by the farmers aligns with the cold wave death reported in the DesInventer database, which reports that in 2010, 59 people died due to cold wave in the Terai region of Nepal and 150 died in 2011 (DesInventor, 2015). Similarly, the extreme cold wave events of 2010/2011 also align with the extreme cold wave events observed in daily maximum and minimum temperature at Biratnagar and Janakpur airport, where three and two extreme cold wave events were identified respectively in the year 2011.

During field study, it was noticed that all FGDs (5 out of 6), except the women FGD at Mithila, Dhanusha, unanimously agreed that there is an increasing trend in fog compared to the past. Among those five FGDs, four FGDs agreed that fog events are increasing over the past 15 to 20 years. To support this statement, most FGDs explained that only in the last 15-20 years have people in their area started using clothes "Jhul"/ "Chaddi" on their animals to prevent animals from cold during fog events. The participants from Saalbani FGD said that their relatives in the hill areas used to descend to the Terai during winter to escape from cold weather in the hills, but they feel that some of their old people are going to the hills to avoid cold wave in the Terai in recent years. Similarly, the participants from Simariya and Batteswor said that it is warmer in the nearby hilly area (Dhankuta and Sindhuli respectively) than their area (Terai) during winter. However, the women's FGD at Mithila, Dhanusha were not sure about the definitive trend of fog events in Terai because they feel that fog events are erratic.

Regarding the reason behind the increasing trend of fog events in the Terai, FGD Batteswor, Dhanusha suggested that it could be due to increasing population. Similarly, the FGD at Sinorjoda suggested that it could be due to deforestation and the FGD at Saalbani, Sunsari suggested it could be due to increasing industrialization, air pollution and increased irrigation area.

In summary, the key perceptions related to fog and cold wave events perceived by the farmers during FGD conducted at Sunsari and Dhanusha in this study are:

- Fog events are regular events during winter and generally start by mid-November and end by mid-February.

- Farmers believe that cold wave conditions are generally brought by continuous dense fog events.
- The farmers experienced an extreme cold wave six years before (2010/11 winter).
- Almost all the participants of the all the FGDs, except the women's FGD at Mithila, agreed that fog events, and associated cold wave events, are increasing over time.

3.2 Temperature and fog data analysis

Temperature and fog data are analyzed in this sub-section to study extreme cold days, cold wave days and compare fog events with cold wave days.

3.2.1 Maximum and Minimum Temperature of Terai Region

The homogeneity test results indicated that the maximum temperature series at all the stations, except Janakpur, are homogeneous at the 5% level of significance (Table 5). At Janakpur, three change point inhomogeneities within the maximum daily temperature were detected, with step size less than 1◦C (-0.16, 0.5 and 0.14◦C). Compared to the maximum temperature results, more inhomogeneities were detected within the minimum temperature series. The number of inhomogeneities within minimum temperature series ranged from 1 step change at Bhairahawa to 7 steps at Janakpur. Since the same instrument (maximum-minimum thermometer) is used to measure maximum and minimum temperature and none of these stations are reported to have shifted, the inhomogeneities in the minimum temperature data could be due to changes in the observer recording the observations and or the surrounding environment. Moreover, the difference in homogeneity results may be due to the change point detection algorithm being more sensitive to changes in minimum temperature than maximum temperature as suggested by Qingxiang and Wenjie (2009). Adopting the step by step procedure suggested by Wang and Feng (2013), to assess the homogeneity of maximum and minimum temperature, any section of the time series with a significant step size, beyond the 95% confidence interval, was set to missing. The percentage of total missing data for maximum temperature ranges from 0.44% at Biratnagar to 10.35% at Dhangadhi and that for minimum temperature ranges from 0.69% at Biratnagar to 17.71% at Dhangadhi during the study period (Table 5).

Based upon the homogenized historical daily maximum and minimum temperature of six representative stations in the Terai; Biratnagar, Janakpur, Simara, Bhairahawa, Nepalgunj and Dhangadhi, the key summary statistics are presented in Table 5. There is little difference in the average daily maximum temperature of the stations in Terai, but the daily maximum temperature observed in the western stations of Bhairahawa, Nepalgunj and Dhangadhi is slightly higher than in the eastern stations of Biratnagar, Janakpur and Simara. The standard deviation of maximum temperature in the Terai stations ranged from 4.2 at Biratnagar to 6.16 at Nepalgunj. Among the

six stations, Nepalgunj has the lowest and Biratnagar has the highest 1st, 5th as well as 10th percentile daily maximum temperature. The highest average minimum temperature is recorded at Janakpur, while the lowest average minimum temperature is recorded in far western Dhangadhi. Among these six stations, the maximum daily minimum temperature is recorded at Dhangadhi and Bhairahawa (34.3˚C) in contrast to the minimum daily minimum temperature at eastern station Biratnagar (29˚C). Unlike the maximum temperature, the lowest of 1st, 5th and 10th percentile of minimum temperature is recorded at Dhangadhi. The highest of 1st percentile of minimum temperature is recorded at Biratnagar, highest of 5th percentile at Biratnagar and Janakpur and that of 10th percentile at Janakpur.

The distribution of the daily maximum and minimum temperatures at all the stations were tested for normality using the skewness test suggested by D'agostino et al. (1990) and found that the maximum and minimum temperature data at all stations are not normally distributed. Using the Kruskal-Wallis test and Mann Whitney test (Hollander et al., 2014), it was found that the maximum and minimum temperature data of those six stations are not from the same distribution.

Table 5: Key summary statistics of historical daily maximum and minimum temperature of the Terai stations

	Biratnagar	**Janakpur**	**Simara**	**Bhairahawa**	**Nepalgunj**	**Dhangadhi**
Duration	45 years (1971-2015)	45 years (1971-2015)	45 years (1971-2015)	45 years (1971-2015)	20 years (1996-2015)	45 years (1971-2015)
Maximum Temperature						
Number of inhomogeneities	0	3	0	0	0	0
Percentage of missing data (%)	0.44	4.42	3.46	1.55	0.77	10.35
Average (˚C)	30.15	30.54	30.42	30.76	30.89	30.88
Minimum (˚C)	10.00	10.00	9.00	9.50	9.60	7.50
Maximum (˚C)	42.00	42.40	42.80	45.20	45.00	45.00
Standard Deviation (˚C)	4.20	4.76	4.96	5.59	6.16	5.80
1st Percentile (˚C)	18.6	17.0	15.6	14.5	13.2	15.4
5th Percentile (˚C)	22.50	22.00	21.70	21.00	19.70	21.00
10th percentile (˚C)	24.20	24.00	23.70	23.00	22.60	23.00
Minimum Temperature						
Number of inhomogeneities	2	7	4	1	2	5
Percentage of missing data (%)	0.69	11.81	3.88	1.61	2.06	17.71
Average (˚C)	18.83	19.36	18.03	18.66	18.43	17.86
Minimum (˚C)	2.00	0.50	0.60	2.00	-0.30	0.00
Maximum (˚C)	29.00	31.00	30.50	34.30	31.50	34.30
Standard Deviation (˚C)	6.50	6.73	7.08	6.82	6.96	7.47
1st Percentile (˚C)	6.00	6.00	4.00	5.50	4.20	3.50
5th Percentile (˚C)	8.00	8.00	6.40	7.60	6.80	5.60
10th percentile (˚C)	9.20	9.50	7.80	9.00	8.50	7.40

3.2.2 Cold Days and Cold Nights in the Terai

Figure 2 shows the monthly share of average cold days, extreme cold days, cold nights and extreme cold nights per annum in the studied stations of the Terai. The figure clearly indicates that January, December and February are the months with cold days and cold nights in a year. On average the number of cold days per annum ranges from 15.6 days at Dhangadhi to 17.9 days at Nepalgunj. Similarly, the number of extreme cold days per annum ranges from 3.2 days at Dhangadhi to 3.6 days at Biratnagar and Nepalgunj. The average number of cold nights per annum ranges from 13 days at Janakpur to 17.6 days at Bhairahawa. Likewise, average number of extreme cold nights per year varies from 2.6 days at Janakpur to 3.4 days at Nepalgunj and Biratnagar.

Box plots of the annual number of cold and extreme cold days in the Terai stations of Nepal are presented in Figure 3. Historical data of daily maximum temperature during 1971-2015, except at Nepalgunj (where data are from 1996-2015), were used to analyze annual number of cold / extreme cold days. The highest median number of cold days per annum is observed at Nepalgunj (21) followed by Biratnagar (17 days), Simara (16 days), Janakpur (16 days), Bhairahawa (14 days), and Dhangadhi (13 days). Regarding extreme cold days Nepalgunj (3 days) and Biratnagar (3 days) have highest median compared to Janakpur (2 days), Simara (2 days), Bhairahawa (2 days) and Dhangadhi (1 day).

Box plots of the annual number of cold and extreme cold nights in the Terai stations of Nepal are presented in Figure 4. In the box plots, 45 years (from 1971-2015) of daily minimum temperature, except at Nepalgunj (where data are from 1996-2015), were used to analyze annual number of cold / extreme cold nights. The highest median number of cold nights per annum is observed in Nepalgunj (19 nights), followed by Bhairahawa (18 nights), Simara (17 nights), Biratnagar (17 nights), Janakpur (11 nights), and Dhangadhi (11 nights). Regarding extreme cold nights Biratnagar (2 nights), Bhairahawa (2 nights), and Dhangadhi (2 nights) have the highest median cold nights compared to Nepalgunj (1.5 night), Simara (1 night) and Janakpur (1 night). From the box plots of cold and extreme cold days and nights it is observed that there are slightly more cold days and extreme cold days compared to cold nights / extreme cold nights in the stations in the Terai region of Nepal.

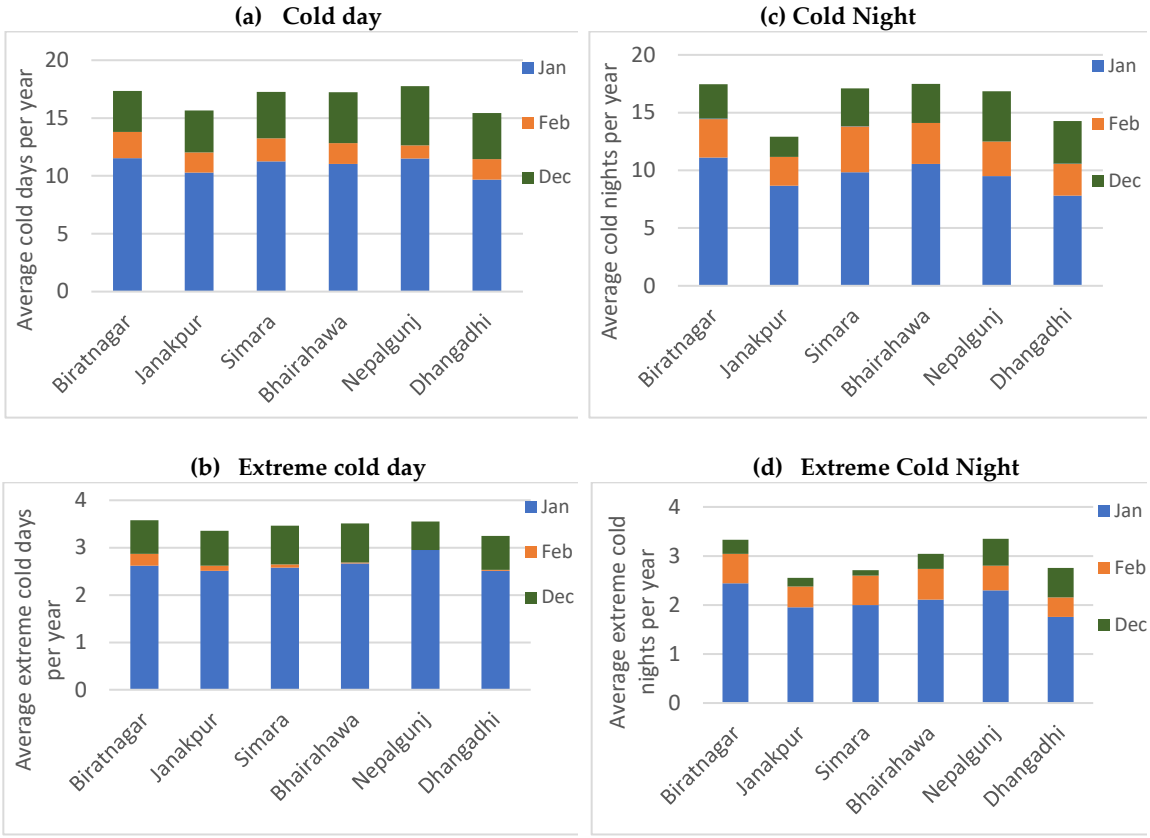

Figure 2: Monthly share of average number of (a) cold days (b) extreme cold days (c) cold nights and (d) extreme cold nights per annum in the study area

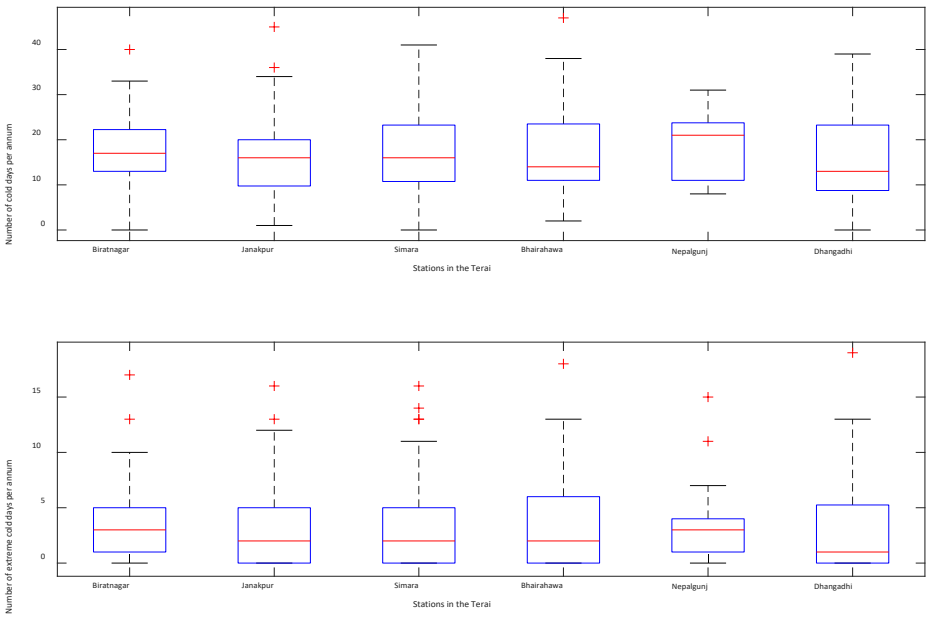

Figure 3: Box plots of number of cold days and extreme cold days per annum during 1971 and 2015 in the Terai stations. The box plot whiskers extend to the 5th and 95th percentiles.

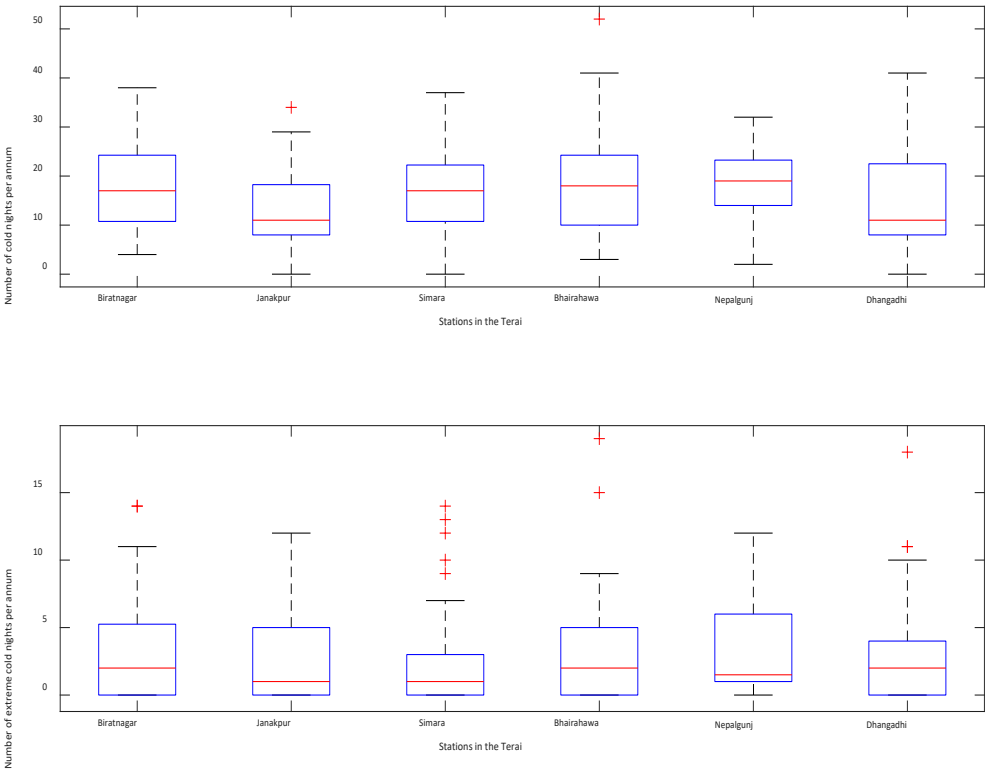

Figure 4: Box plots of number of cold nights and extreme cold nights per annum during 1971 and 2015 in the Terai stations. The box plot whiskers extend to the 5th and 95th percentiles.

The presence of annual trends in cold days and extreme cold days during 1971-2015 at the six studied Terai stations is investigated in Figure 5. From the figure it is clear that the annual number of cold days and extreme cold days are increasing at all the Terai stations, except Nepalgunj. Compared to the time series of cold days per annum, more variance is observed in the occurrence of extreme cold days in the Terai stations. The Mann Kendall (MK) test results for trend in annual number of cold days and extreme cold days are presented in Table 6. The results clearly indicate that the annual number of cold days is increasing at all stations, except Nepalgunj, at the statistical significance level of at least 0.05. The rate of increase of annual number of cold days varies from 0.21 days per annum at Biratnagar to 0.46 days per annum at Bhairahawa. The MK test also clearly indicates that the annual number of extreme cold days is increasing at all stations, again except Nepalgunj, at the statistical significant level of 0.001. The increasing trend in annual number of cold days and extreme cold days at all Terai stations, except Nepalgunj, may be due to the increasing trend in fog at Terai stations (Shrestha et al., 2018). The non-significant trend in the annual number of cold and extreme cold days at Nepalgunj may be due to the short data range (20 years) compared to the other stations (45 years). The rate of increase in the annual number of extreme cold days varies from 0.10 days per annum at the eastern station Biratnagar to 0.15 days per annum at the western stations of Dhangadhi. The analysis of increasing trend in the

annual number of cold days and extreme cold days agrees with the perception of the farmers on increasing trend of fog events and cold days in the Dhanusha and Sunsari districts.

Table 6: Results of MK trend test on the annual number of cold and extreme cold days in the Terai stations of Nepal.

SN	Stations	First year	Last Year	n	Cold Day			Extreme Cold Day		
					Test Z	Q	B	Test Z	Q	B
1	Biratnagar	1971	2015	45	2..47*	0.21	12.00	3.31***	0.10	0.81
2	Janakpur	1971	2015	45	4.54***	0.39	5.64	4.75***	0.13	-0.50
3	Simara	1971	2015	45	4.39***	0.44	6.55	4.18***	0.14	-0.11
4	Bhairahawa	1971	2015	45	4.52***	0.46	9.20	4.79***	0.13	-0.67
5	Nepalgunj	1996	2015	20	1.20ns	0.42	4.42	0.07ns	0.00	3.00
6	Dhangadhi	1971	2015	45	3.26**	0.39	6.96	4.11***	0.15	-0.58

** Significant at 0.05 level, ** Significant at 0.01 level, *** Significant at 0.001 level, ns non-significant*

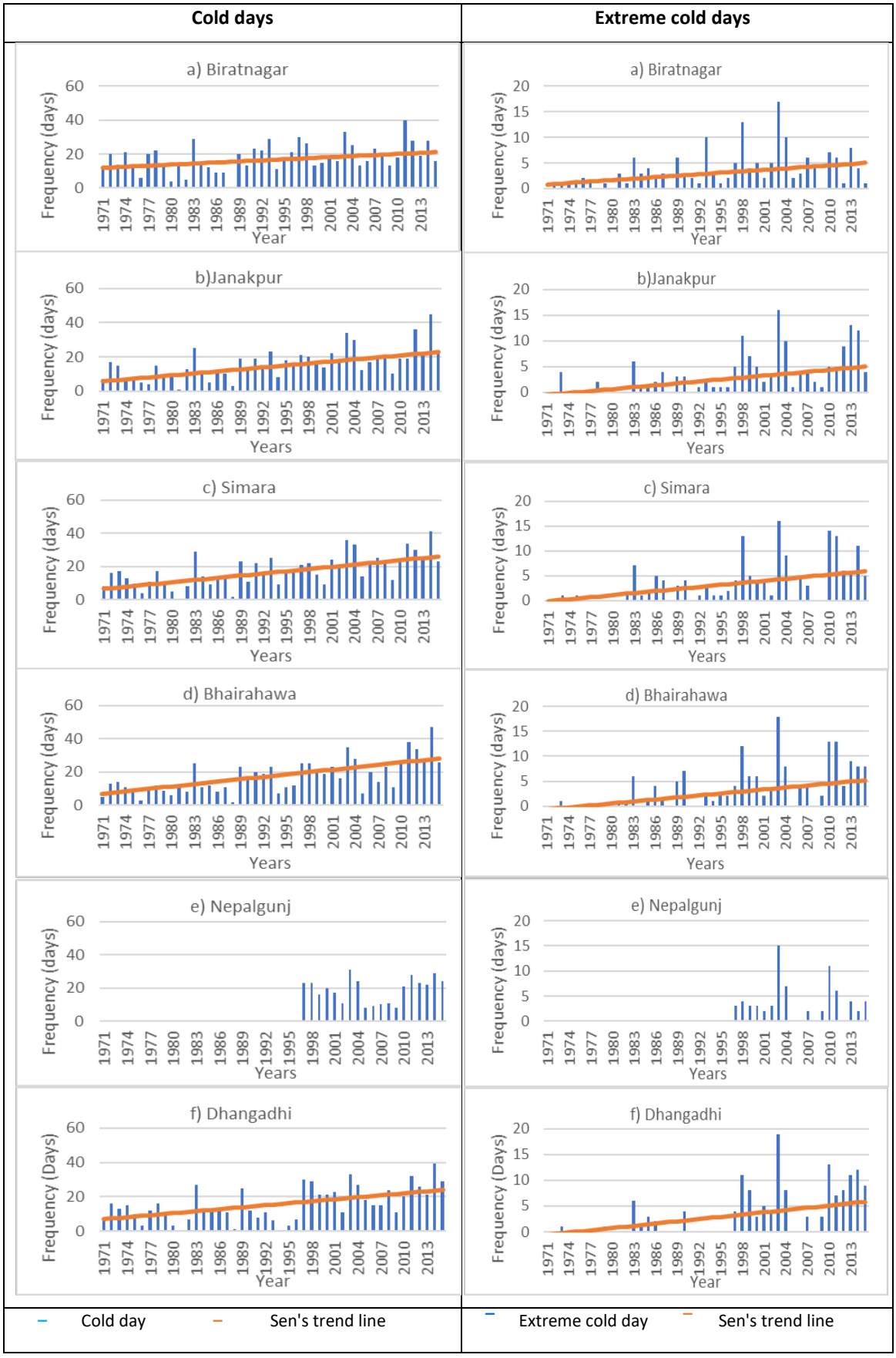

Figure 5: Time series of annual number of cold days and extreme cold days in the Terai stations with associated trend line.

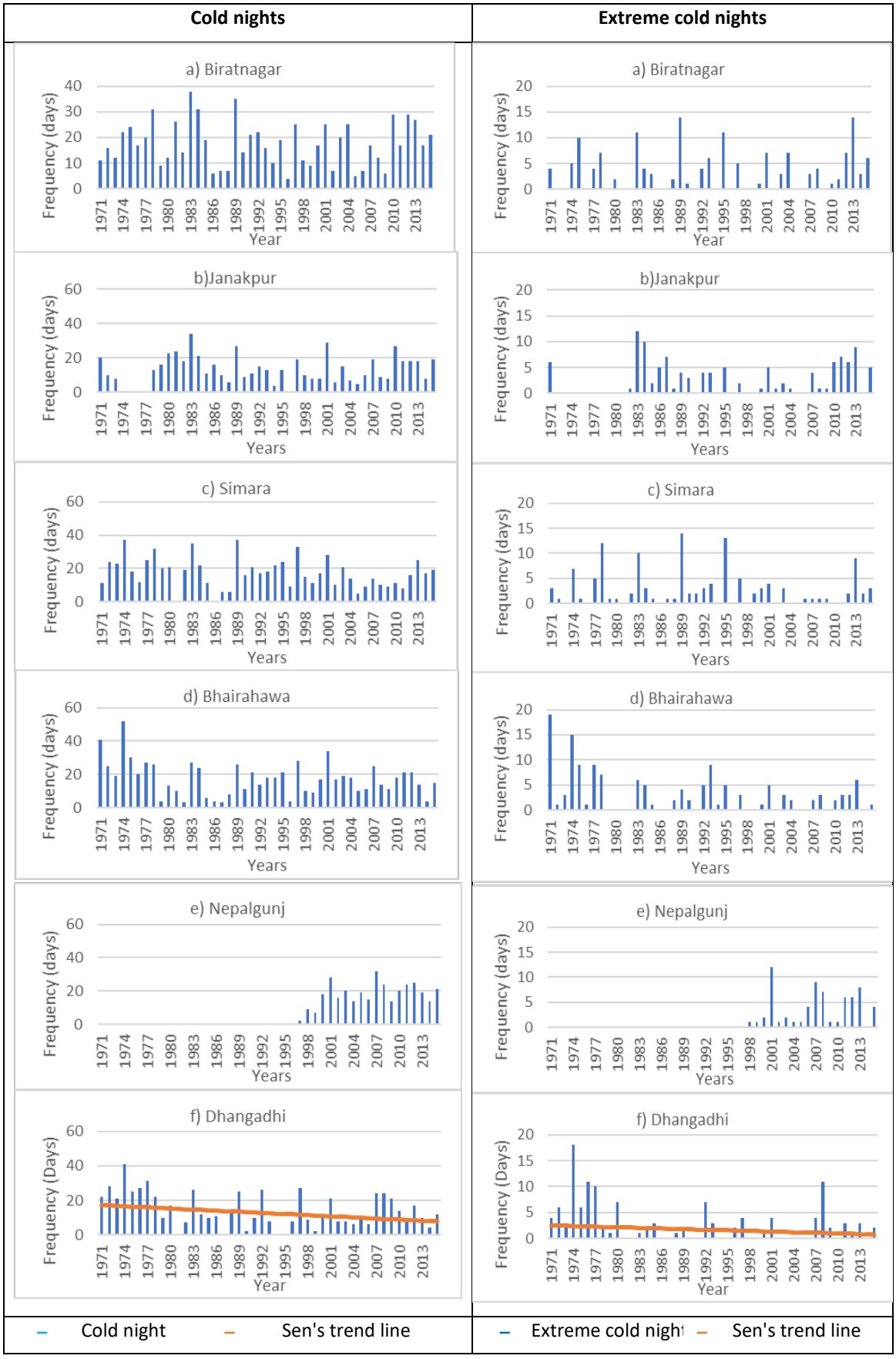

Figure 6: Time series of annual number of cold nights and extreme cold nights in the Terai stations with associated trend line.

The time series of the annual number of cold nights and extreme cold nights at the Terai stations are presented in Figure 6. The figure indicates the declining trend on the annual number of cold nights and extreme cold nights at Dhangadhi and no definite trend at all other stations of Terai. The MK test results for trend in the annual number of cold nights and extreme cold nights are presented in Table 7. The results indicate that the majority of stations in Terai have no definite trend in the annual number of cold nights or extreme cold nights over the past 45 years. At Simara the number of cold nights is decreasing whereas at Nepalgunj it is increasing at the statistical significance level of 0.1. At Janakpur the number of extreme cold nights is increasing at the statistical significance level of 0.05. However, at Dhangadhi both cold nights and extreme cold nights are decreasing at the statistical significant level of 0.05.

Table 7: Results of MK trend test on the annual number of cold and extreme cold nights in the Terai stations of Nepal.

SN	Stations	First year	Last Year	Cold Night			Extreme Cold Night		
				Test Z	Q	B	Test Z	Q	B
1	Biratnagar	1971	2015	-0.02ns	0.00	17.00	0.72ns	0.00	2.00
2	Janakpur	1971	2015	0.52ns	0.06	10.18	2.03*	0.03	0.18
3	Simara	1971	2015	-1.73+	-0.17	20.83	-0.42ns	0.00	1.00
4	Bhairahawa	1971	2015	-1.31ns	-0.17	21.83	-1.40ns	0.00	2.00
5	Nepalgunj	1996	2015	1.83+	0.67	-6.00	1.73+	0.19	-4.33
6	Dhangadhi	1971	2015	-2.09*	-0.22	17.24	-2.09*	-0.04	2.51

*+ Significant at 0.1 level, * Significant at 0.05 level, ns non-significant*

3.2.3 Cold wave in Terai

The decadal number of cold wave days are presented in Figure 7, based on analysis of the daily maximum and minimum temperature at the six studied Terai stations. The number of cold wave days range from 72 to 198 days per decade across the Terai stations. Compared to other stations, less cold wave days are experienced at Dhangadhi. The decade 1986-1995 is the decade with the least cold wave days in the western Terai stations (Bhairahawa and Dhangadhi). In Biratnagar, Janakpur, Nepalgunj and Dhangadhi the number of cold waves days has increased in the recent decade (2006-2015) compared to previous decade (1996-2015) which agrees with the FGD findings. To obtain the annual trend in cold wave events and days at those stations, the MK trend test was performed. No statistically significant trend in annual number of cold wave days was found at those stations during 1971 to 2015 (Table 8).

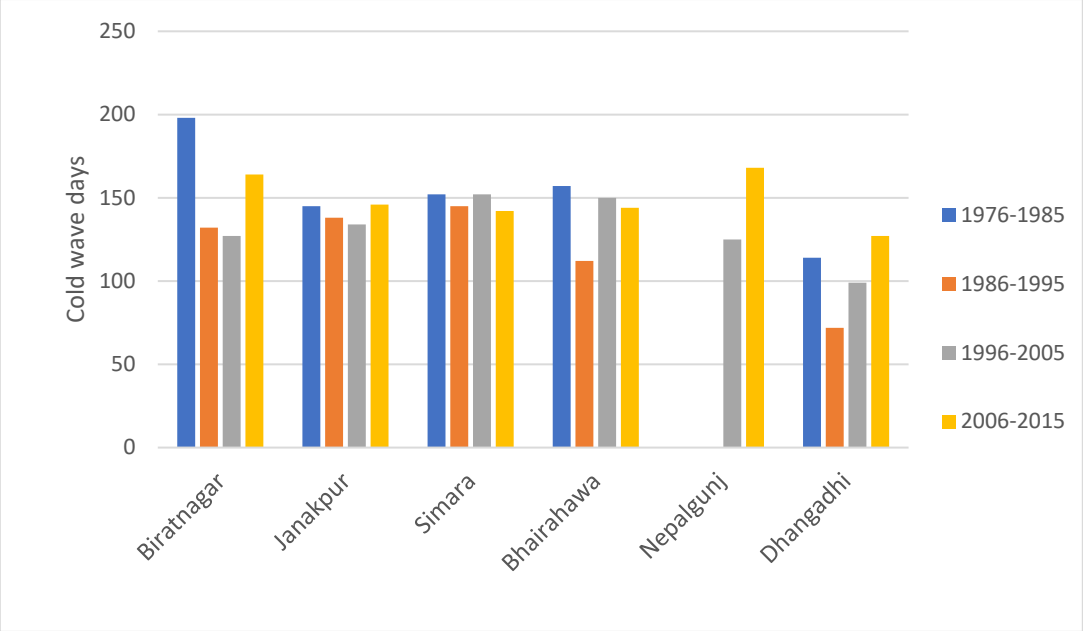

Figure 7: Decadal cold wave days in Terai region

Table 8: Results of MK trend test on the annual number of cold wave days and extreme cold wave days in the Terai stations of Nepal.

SN	Stations	First year	Last Year	Cold Wave Days			Extreme Cold Wave Days		
				Test Z	Q	B	Test Z	Q	B
1	Biratnagar	1971	2015	-0.85ns	-0.11	18.89	0.21 ns	0.00	2.00
2	Janakpur	1971	2015	0.14 ns	0.00	14.00	0.35 ns	0.00	2.00
3	Simara	1971	2015	-0.29 ns	-0.01	15.33	0.77 ns	0.00	4.00
4	Bhairahawa	1971	2015	-1.29 ns	-0.12	17.68	0.05 ns	0.00	2.00
5	Nepalgunj	1996	2015	1.49 ns	0.35	2.71	0.99 ns	0.00	1.00
6	Dhangadhi	1971	2015	-0.28 ns	-0.01	10.39	-1.40 ns	0.00	0.00

ns non-significant

The average number of cold wave days per month are presented in Figure 8. The figure indicates that cold waves occur only in the months of January, February and December. At all the stations, January is the month with the highest number of cold wave days. On average, about 68.2%, 19.3% and 12.5% of the cold wave days occur in the months of January, December and February respectively in the Terai region. The average number of cold wave days per annum ranges from 11.3 days at Dhangadhi to 16.1 days at Biratnagar.

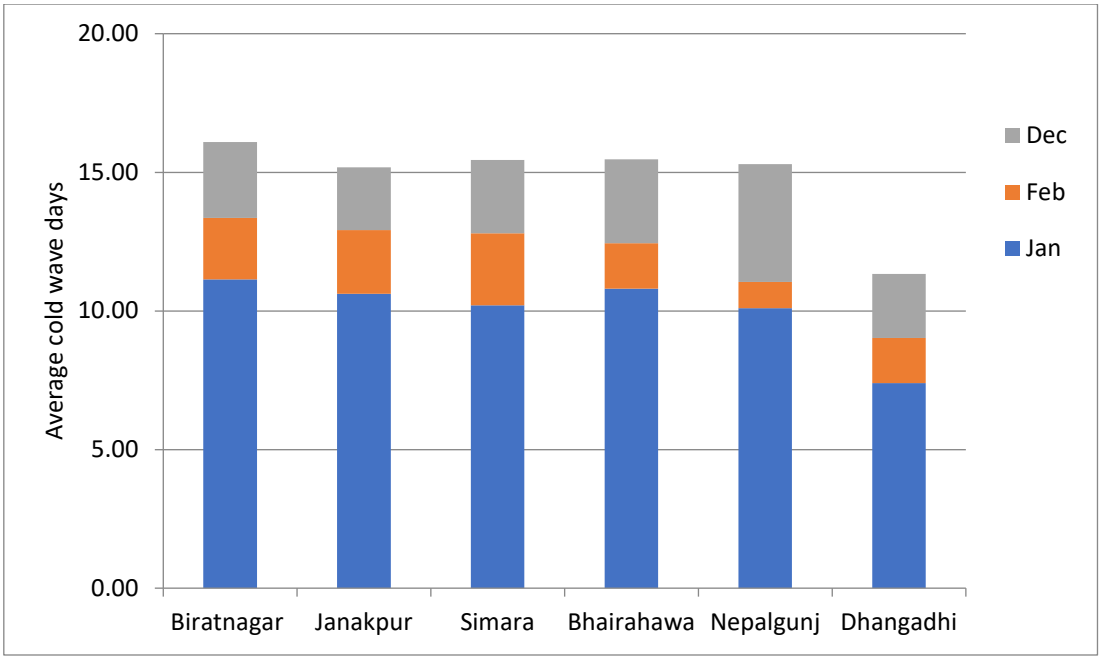

Figure 8: Monthly share of average number of cold wave days per annum in Terai region

Box plots of the annual number of cold wave days at the Terai stations are presented in Figure 9. The historical data from 1975-2015 are used for the box plots at all stations, except Nepalgunj where data from 1996-2015 are used. Even though the median value of annual number of cold wave days at Biratnagar, Janakpur, Simara, Bhairahawa and Nepalgunj are similar, there is less variation in Nepalgunj compared to other stations (Figure 9), possibly due to the shorter record length.

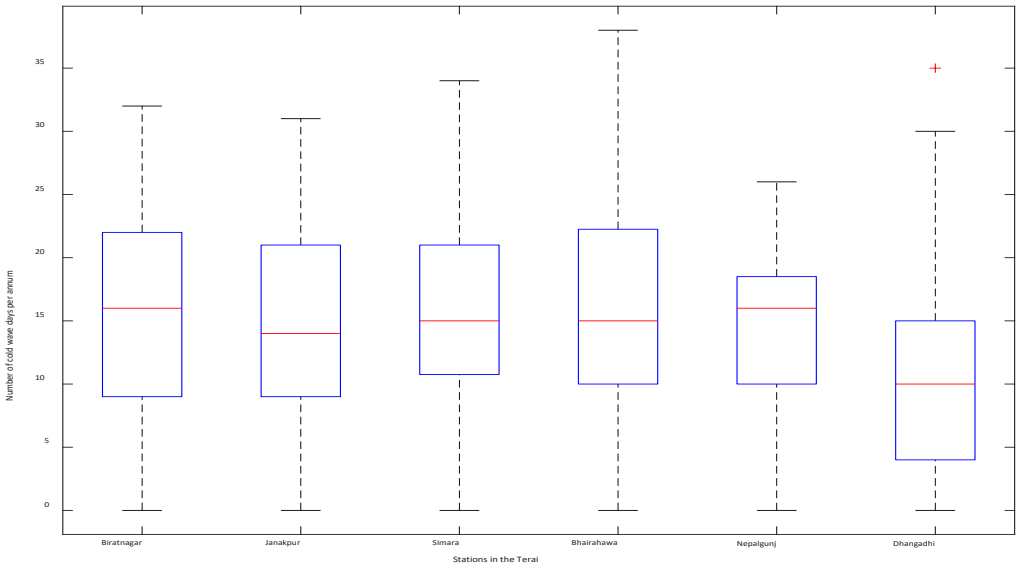

Figure 9: Box plots of the annual number of cold wave days at Terai stations. The box plot whiskers extend to the 5th and 95th percentiles.

3.2.4 Extreme cold wave in Terai

The number of extreme cold wave days are analyzed based on historical daily maximum and minimum temperature from the selected six Terai stations. The decadal distributions of extreme cold wave days at the studied stations are presented in Figure 10. The total number of extreme cold wave days per decade vary from 13 to 50 days per decade. The number of extreme cold wave days at Nepalgunj and Dhangadhi is less than the other Terai stations. Regarding any trend in the annual number of extreme cold wave days, there is no general trend (statistically significant) across the Terai stations during 1975-2015 (Table 8). However, from Figure 10, it can be said that at the Terai stations except Dhangadhi, the extreme cold wave days of the recent decade (2006-2015) is increased relative to the previous decade (1996-2005) and this increment is stronger at eastern Terai stations (Biratnagar and Janakpur). This observation agrees with the farmer's perception in the majority of the FGDs. Moreover, it is also aligning with the findings of Oxfam (Gum et al., 2009), which indicated that there are more intense cold waves in the eastern Terai plains in recent years.

The monthly distribution of annual average extreme cold wave days at the Terai stations is shown in Figure 11. Among the Terai stations, on average the lowest number of extreme cold wave days was observed at Nepalgunj (1.8 days/annum), whereas the highest number of cold wave days was observed at Simara (4.4 days/annum).

To study the distribution of annual extreme cold wave days at the Terai stations during 1976-2015, box plots of extreme cold wave days are presented in Figure 12. The highest median annual number of extreme cold events was found at Simara (4) and the lowest median at Dhangadhi (0). In spite of large variation in the distribution of extreme cold wave days over the last four decades at Biratnagar, Janakpur, and Bhairahawa, the median was found to be same (equal to 2) at these stations.

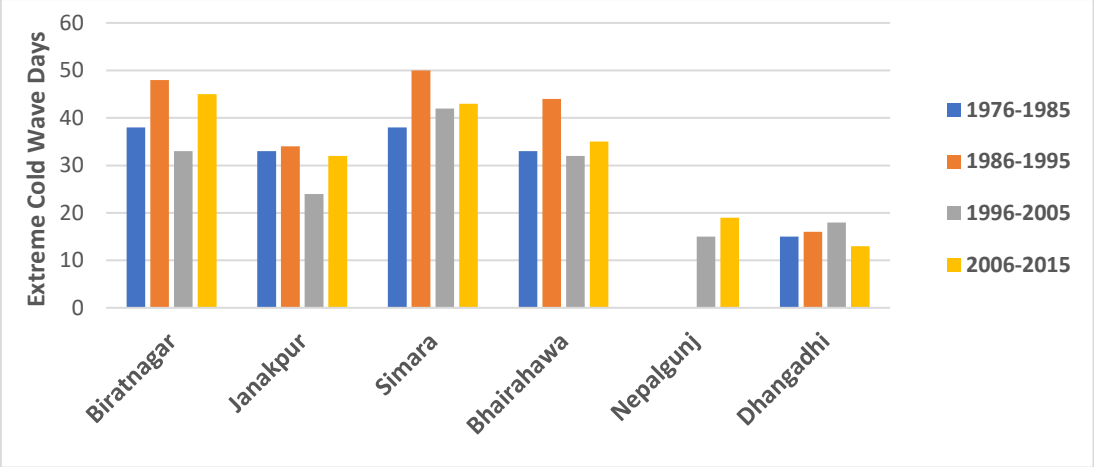

Ffigure 10: Decadal extreme cold wave days in the Terai

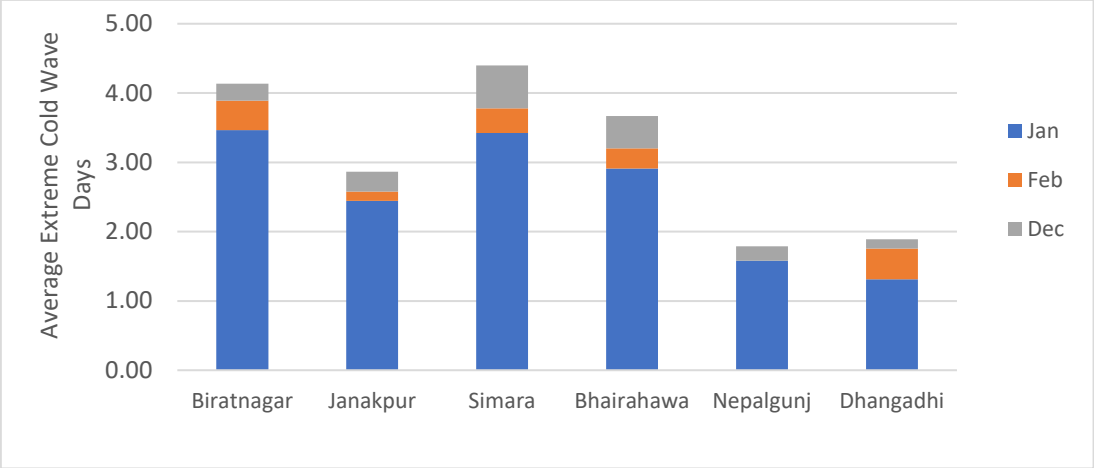

Figure 11: Monthly share of average number of extreme cold wave days per annum in Terai region

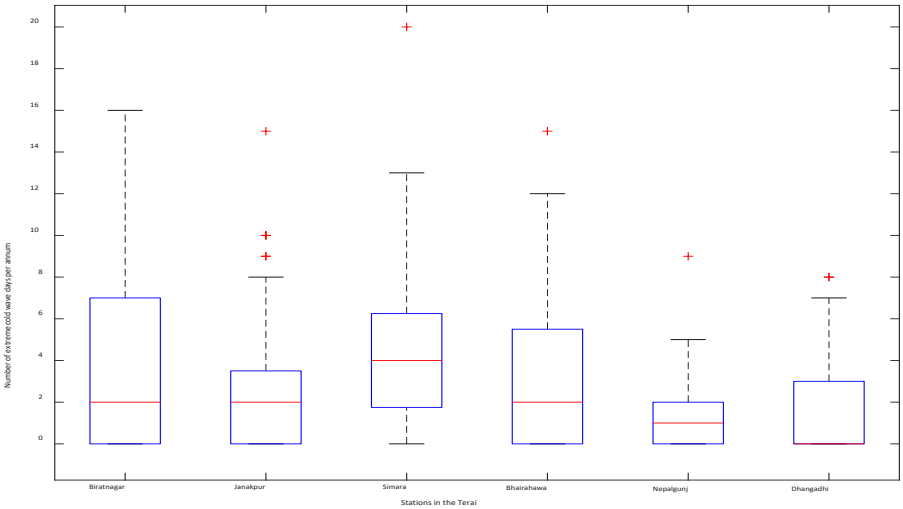

Figure 12: Box plots of annual number of extreme cold wave days in the Terai. The box plot whiskers extend to the 5th and 95th percentiles.

3.2.5 Fog events and cold wave

Shrestha et al. (2018) studied winter fog events in the Terai region of Nepal using visibility data from four Terai stations and found that fog events start in November, reach their peak in December / January and end in February. This finding exactly matched with the farmer's FGD findings in this study. Moreover, Shrestha et al. (2018)'s findings of an increasing trend in the number of foggy days per annum, at statistically significant levels, in the studied Terai stations also agrees with the FGD findings at Sunsari and Janakpur. The increased fog events reduce solar insolation and provide a positive feedback for the persistence of foggy and cold conditions during winter (Gautam, 2014).

The cold wave events and fog events at four Terai stations during 1994-2015 were compared and presented in Table 9. From the table it is observed that most (more than three quarters) of the cold wave days and extreme cold wave days co-occur with foggy days at Biratnagar and Bhairahawa. Whereas, at Simara and Nepalgunj about half of the cold wave days co-occur with foggy days. Similarly, more than 86 percent of cold wave days co-occur with foggy days on the same day or the previous day at Biratnagar and Bhairahawa. Whereas, at Simara and Nepalgunj this condition occurs more than 60 percent of the cold days. For the condition of a cold wave day preceded by a foggy day anywhere within the previous two days, more than 90 percent of the cold wave days at Biratnagar and Bhairahawa experience this condition, whereas only two thirds of cold wave days at Nepalgunj and Simara experience this condition. Generally, the percentage of extreme cold wave days associated with a co-occurring, or preceding, foggy day, is higher than the percentage for cold wave days. Hence, from the table it is evident that the majority of cold wave days and extreme cold wave days occur close to foggy days. This is mainly due to the obstruction of solar radiation by the fog during the day time, which reduces the temperature (mainly maximum temperature) (Bedekar et al., 1974; Gautam, 2014). It also supports the farmer's perception regarding cold wave events, that they are closely related with fog events.

Table 9: Comparison of Cold event and fog events at Biratnagar, Simara, Bhairahawa and Nepalgunj

SN	Conditions	Biratnagar	Simara	Bhairahawa	Nepalgunj
1	Percentage of cold wave day with same day foggy day	77.97	48.46	79.17	58.67
2	Percentage of cold wave day with same day or 1 day after foggy day	87.57	60.77	86.11	70.24
3	Percentage of cold wave day with same day or 1 or 2 days after foggy day	91.53	67.69	93.06	75.20
4	Percentage of Extreme cold wave day with same day foggy day	77.78	76.92	96.55	75.00
5	Percentage of Extreme cold wave day with same day or 1 day after foggy day	91.67	79.49	100.00	75.00
6	Percentage of Extreme cold wave day with same day or 1 or 2 days after foggy day	97.22	82.05	100.00	75.00

3.3 Effect of fog and cold waves and adaptations

The results of the FGDs on the effects of fog and cold wave on agriculture are discussed in four subsections. In the first subsection, the effect on crop production is elaborated and in the second subsection the effect on livestock is discussed. Similarly, in the third subsection other effects are explained and in the fourth subsection, the adaptation measures adopted by the farmers are discussed.

3.3.1 Effect of fog on crop production

The major crops affected by fog identified by the FGDs conducted during this study are presented in Table 10. All FGDs conducted in this study identified potato and vegetables (including tomato, brinjal, beans, chilly, etc.) as the number one and number two crops affected by fog in prioritized order respectively. Regarding the third most affected crop due to fog, this varied across FGD locations. Wheat was identified as the third most important crop affected by fog by all the FGDs, except that of Saalbani, Sunsari where Kidney bean was considered to be the third most important crop affected. Along with wheat, pigeon pea and lentil crops were also considered the third most important crop affected by fog by the FGDs at Batteswor and Sinorjoda respectively.

According to the FGDs in Dhanusha and Sunsari, fog events bring a conducive environment (humid and cool without sunlight) for late blight disease for potato. This agrees with the findings of Samra et al. (2003) and Bhat et al. (2010), who noted total crop failure is experienced when timely spraying is not performed. According to the farmers, the effect of fog on potato also depends upon the potato planting date. November planted potato is more damaged due to late blight than October planted potato. In general, late blight reduces potato production by about 50 percent. In extreme foggy condition, 100% damage is also observed. A farmer at Simariya, Sunsari experienced total failure of her potato crop by late blight during the foggy season four years ago. To minimize damage due to late blight, various chemicals are used viz. Endophyl, Clear axyel,

Dythenium 45. On average, potato is sprayed 6.33 times (minimum 5 and maximum 8 times across all FGD locations) to minimize damage due to late blight during the foggy season. On average, the spraying against late blight increases the cost of cultivation of potato by about 473 AUD (Rs. 37,887) per ha in the study area (equivalent to 18% of the production cost) (FGD, 2017). For potato, more than 95 percent of agricultural pesticides used are fungicides, which indicates farmers are trying to reduce the severity of late blight in Nepal (PRMS, 2014).

Table 10: Important crops effected by fog

SN	Location of FGDs	Important Crop Effected by Fog in Prioritised Order		
		First	Second	Third
1	Batteswor, Dhanusha	Potato	Vegetables (tomato, brinjal, beans etc.)	Pigeon pea /wheat
2	Sinorjoda, Dhanusha	Potato	Vegetables (tomato, brinjal, beans etc.)	Wheat /Lentil
3	Naktajhijh, Mithila (Male), Dhanusha	Potato	Vegetables (onion, tomato, brinjal, chilly etc.)	Wheat
4	Naktajhijh, Mithila (Female), Dhanusha	Potato	Vegetables (tomato, onion, brinjal etc.)	Wheat
5	Simariya, Sunsari	Potato	Mustard (used as leafy vegetable as well as oilseed)	Wheat
6	Saalbani, Sunsari	Potato	Vegetables (Mustard leafy vegetable, beans, onion, tomato, chilly etc.)	Kidney Bean

Source: FGDs (2017)

Vegetable crops (tomato, brinjal, onion, chilly, leafy vegetables, green beans etc.) are identified as the second most important crop affected by fog during FGDs in the study area. In all the FGDs the farmers unanimously agreed that infestation of fungal disease increases in these crops during fog events. In addition, the farmers also observed increased infestation of aphids on vegetables (specially on beans, pigeon pea, mustard etc.) during the foggy season, which is similar to the findings of Samra et al. (2003) and Ali and Rijvi (2008) for mustard crop. A farmer at Simariya FGD noticed that increased fungal infestation in cauliflower is observed in the foggy season, resulting in black spots on the cauliflower curd, which significantly reduced the market value of the cauliflower. To get rid of fungal attack and aphid infestation, farmers are spraying chemicals which has increased the cost of cultivation.

Wheat is also considered to be an important crop affected by fog events in the Terai (Table 10). If there is early fog during November, the harvested paddy left in the field does not dry and it delays wheat cultivation (FGD Sinorjoda & Batteswor, 2017). Since there is linear decline of wheat productivity at the rate of 1 to 1.5 % per day at Ludhiana (agro-ecology similar to the Terai region of Nepal) due to delay in planting after the end of November (Ortiz-Monasterio R. et al., 1994), the resultant delay due to fog may also cause reduction in wheat yield in the Terai.

According to the farmers, the fog period lies in the vegetative growth period of wheat and its vegetative growth rate is reduced during foggy period. Moreover, all FGD participants agreed that delay in maturity of wheat makes it more susceptible to being affected by dry western wind, which may significantly reduce the wheat yield due to shrivelled grain (FGD, 2017). The effect of dry western wind and shrivelled wheat grains in the Terai explained by the farmers exactly matches with the shrivelled grain scenario due to dry wind during maturity of wheat in the Punjab explained by (Luthra and Chima, 1941).

The participating FGD farmers at Saalbani described increased infestation of fungal attack on Kidney bean during the foggy season. Similarly, the participating farmers at Sinorjoda described increased blight infestation of their lentil crop during fog events. The farmer's observations match with the findings of Subedi et al. (2015) regarding favourable conditions for the occurrence of Stemphylium blight in lentil as high humidity and low solar radiation (similar to foggy day condition). To address the blight and fungal attack on lentil and kidney bean the farmers are spraying pesticides (mainly fungicides).

Pesticide consumption is reported to be increasing in the Terai area and the accessible Hilly areas of Nepal (Joshi et al., 2012). The share of agricultural pesticide use in the Terai area is reported to be 59 percent of the total use in Nepal. Similarly, vegetable crops are the main consumer of agricultural pesticides, with about 79 percent share on total agricultural pesticides used in Nepal. Among the vegetable crops, brinjal, tomato, potato and cole crops are the major consumer of agricultural pesticides in Nepal (PRMS, 2014).

A six-fold increase in import and formulation of agricultural pesticides in the year 2011/12 relative to 1997/98 clearly indicates a rapid increase in consumption of agricultural pesticides in Nepal (Sushma et al., 2015). Among the pesticides used in agriculture, fungicides have a major share of about 60% in the total used in Nepal (PRMS, 2014). The increased pesticides use in the Terai could be due to the conducive environment for disease and pests during increasing fog events, as mentioned in FGDs in the study area. During field observations, farmers were not found adopting of safe method of chemical applications by using mask, apron, & gloves. Due to low level of awareness of Nepalese farmers on the safe use of pesticides (Giri et al., 2008), the increasing, pesticides consumption trend not only threaten the farmer's health and the consumer's health, but also negatively affected the natural environment (Diwakar et al., 2010). Apart from the negative effect of fog on the crops, a women farmer in the Simariya FGD observed that in foggy conditions, mushroom grows well, which may be due to high humidity during fog events.

3.3.2 Effect on livestock production

The participating farmers of all the FGDs in the study area unanimously agreed that fog events and resulting cold waves have significantly affected their livestock during winter. Cattle, goat and

buffalo are the major livestock affected by fog in the study area. The FGDs conducted in the study area agreed that milk production from cows and buffalos were significantly reduced. The farmers of Batteswor FGD estimated about 25 percent reduction in milk production where as those of Sinorjoda, Naktajhijh, Simariya and Saalbani estimated about 33% reduction of milk production during fog induced cold wave. The reduction in milk production reported by the farmers agrees with the findings of Upadhyay et al. (2014), who reported that milk production of bovines was reduced during cold wave at the rate of 10 to 30% in first lactation and 5 to 20% in second and third lactation. Upadhyay et al. (2014) also reported that the cold wave not only has an immediate effect on milk production, but also short to long term cumulative effects on milk yield and production in cattle and buffalos that depend upon the extent and severity of cold wave. The reduction in milk production estimated by the farmers in the study area was higher than the 20% reduction of milk production due to 2002-03 cold wave in Agra reported by Samra et al. (2003).

The FGD farmers also indicated that calves are more susceptible to cold stress than the cows and mature heifers. The reason behind this could be due to larger surface area to body mass ratio of calves than that of more mature animals, resulting in more body heat loss. In addition, it could also be due to less fat availability in calves compared to mature animals (Singh et al., 2015). The farmers also noticed that goats are also affected with respiratory disease during foggy season in winter. Similarly, they also agreed that compared to adult goats, kids are more effected by cold wave in the study area. These farmer's observations align with the findings of Paudyal et al. (2012).

To minimize the effect of fog & cold wave on the animals, it was observed that the farmers of the study area use coats made of jute bag or old cloths to cover their animals. Similarly, the animal sheds were improved with better roof and wall to make it warmer. Even poor farmers are using thatched roof and straw mat to cover the side wall of their animal sheds. On the extreme cold days, it was observed that the farmers are also burning agricultural residue near their animal shed to make it warm. The farmers also mentioned that they also started to provide warm water and cooked feed during winter to increase water intake of their cattle during the winter foggy season.

3.3.3 Other effects

According to the participating FGD farmers, children and old people are more affected by cold, pneumonia and respiratory disease during the foggy season (Women FGD Naktajhijh, 2017). All the FDG participants agreed that they do not prefer to work in the field due to cold and that farm labours are not easily available during the foggy season. Moreover, all agreed that farm labour productivity was significantly reduced, even by more than 50 percent during the foggy season (FGD Saalbani, 2017). Because of a reduction in labour productivity, the cost of cultivation is increased, and the farm operation is delayed. These farmer's observations are supported by CBS (2017) findings, which reported that in the Terai 23.36% of households are affected due to cold

wave and Terai households have missed an average of 4.1 working days due to cold wave in the last five years.

The FGD participants at Batteswor and Naktajhijh recalled the death of several villagers during the extreme cold event in 2011. According to them, the old people from poor families died due to a lack of enough clothes to make them warm during those extreme cold events. They also realized that this was due to a lack of preparedness for the cold event. Similarly, the Saalbani FGD agreed that compared to people from migrated hill communities, people from indigenous Terai communities were more affected by the fog and cold wave due to a lack of preparedness and poor economic condition.

During dense foggy days children cannot go to school and schools are generally closed during those periods. Due to poor visibility during fog events the road transportation is also affected. Similarly, the participants of the FGD noticed that road accidents increased during fog events. One of the tractor drivers at Naktajhijh died due to a road accident during fog events four years ago (FGD Naktajhijh, 2017).

3.3.4 Adaptation measures:

To minimize the effect of fog and cold wave on crop and livestock production in the study area the following adaptation measures were found to be successfully adopted by the farmers.

- To minimize the effect of late blight, aphids and other fungal disease on potato, vegetable other crops, farmers are spraying chemicals during the foggy season. (FGD, 2017)
- The farmers also realized that early planting of potato (October planting) may escape fog (FGD Simariya, 2017),
- To minimize the effect of delay in cultivation of the winter crop and labor unavailability due to fog, farmers are adopting more agricultural mechanization technologies for timely accomplishment of agricultural operations (FGD, Sinorjoda, 2017).
- The farmers also realized that groundwater irrigation during winter (foggy season) is beneficial due to water being warmer relative to the colder surface water (FGD Naktajhijh, 2017).
- Farmers have improved their animal sheds to minimize the effect of fog and cold wave on their livestock (Field observations and FGD, 2017).

- Use of coat (made from jute bag / old clothes) for animals to minimize the effect of cold during foggy season (Field observations and FGD, 2017).
- Making the animals and people warm by burning agricultural residue near the animal shed (Field Observations).
- Providing warm water and even cooked feed to increase water intake of animals (FGD, 2017)

4.0 Summary and conclusions:

Historical daily maximum and minimum temperature were analyzed to investigate the occurrence of cold days, cold nights, extreme cold days, extreme cold nights, cold wave days and extreme cold wave days in the Terai region of Nepal for the first time. Similarly, the perception of farmers regarding the effect of fog and cold wave events were explored through focus group discussion in Dhanusha and Sunsari districts of the Terai. The major findings of the study are listed below.

January, February and December are the months when cold / extreme cold days/nights occur in the Terai region of Nepal. The average number of cold days per annum ranges from 15.6 days to 17.9 days and the average number of cold nights per annum ranges from 13 to 17.6 days in the Terai region. Similarly, the average number of extreme cold days per annum ranges from 3.2 days to 3.6 days and average number of extreme cold nights per annum ranges from 2.6 to 3.4 days in the Terai. Except for Nepalgunj, all the Terai stations show statistically significant increasing trends in the frequency of cold days and extreme cold days over the last four decades. However, statistically significant trends in the frequency of cold nights and extreme cold nights over last four decades was not observed in the majority of stations in Terai.

Cold wave and extreme cold wave days occur during winter in January, February and December in the Terai region of Nepal. Based on historical data, the average number of cold wave days varies from 9.2 to 13.8 per annum and the average number of extreme cold wave days varies from 1.4 to 3.8 days in the Terai region of Nepal. By comparing the co-occurrence of foggy days and cold and extreme cold wave days at Biratnagar, Simara, Bhairahawa and Nepalgunj airport, it is also observed that most of the cold and extreme cold wave days are also foggy days.

Through an exploratory study of the farmer's perception of the effect of fog events and cold wave on agriculture, it was found that there is a significant effect on winter crop cultivation and livestock farming. Potato, tomato, brinjal, wheat, chilly, onion, beans etc. are the major crops affected by fog and cold wave in the Terai. The major effect of cold wave and fog events is to create a conducive environment for fungal infection / late blight and poor vegetative growth. Up to 100% damage of crops, especially potato, tomato, brinjal, is reported during fog / cold wave events in the Terai due to late blight. All the farmers are spraying more chemicals to prevent late blight

during the foggy season. On average 6.3 times spraying events are done to prevent potato crop from late blight and the increased chemical spraying of fungicide increased the cost of cultivation by about 18%. Livestock are also affected by cold events in the Terai. Milk production is reduced by 25% to 50% due to cold wave. Similarly, goats are affected by respiratory disease and cold during a cold wave. During cold wave days, farmers prefer not to work on the farm and they have noticed that labor productivity is significantly reduced on cold wave days.

5.0 Recommendations:

- This exploratory study clearly indicates that there are significant effects of fog and cold wave on agriculture in the Terai region of Nepal. To obtain more in-depth information on the effect of fog on the agriculture sector in the Terai, there needs to be more detailed study, including crop modelling.
- Considering the higher risk to farmers of reduced winter crop yield due to the negative effects of fog and cold waves, there needs to be an effective crop insurance program to minimize the risk of fog to their crops in the Terai region of Nepal.
- There is a need for disease and insect / pest resistant winter crop varieties (specially, potato, vegetables (tomato, brinjal, cauliflower, chilly, onion etc.), mustard, legumes etc.) for the Terai region of Nepal.
- There is also need of improving the awareness about the fog events and cold waves and support for the preparedness for specially resource poor farmers can significantly reduce the negative effects on humans, animals and crops from these disasters in Terai region of Nepal.
- Forecasting of fog events and cold wave events in advance could help farmers and other stakeholders to minimize the effect on agriculture, transport and other sectors.

Acknowledgments: The lead author (S.S.) is thankful to Australian Centre for International Agricultural Research (ACIAR) for providing John Allwright Fellowship (JAF) to pursue his PhD in the University of Melbourne. we would like to acknowledge the farmers participated in the focus group discussion (FGD) conducted at Dhanusha and Sunsari. We also would like to thank Er. Sanjeet Kumar Jha, Er. Mukti Nath Jha and Mr. Pankaj Gyawaly of Nepal Agriculture Research Council (NARC) for assisting the first author in conducting FGD.

References

Acar, Z., Gonencgil, B., Gumusoglu, N.K., 2018. Long-Term Changes in Hot and Cold Extremes in Turkey. J. Geog. 37, 57–67. https://doi.org/10.26650/JGEOG2018-0002

Ali, A., Rijvi, P.Q., 2008. Effect of Varying Temperature on the Survival and Fecundity of Coccinella septempuncta (Coleoptera: Coccinellidae) Fed on Lipaphis ersimi (Hemiptera: Aphididae). J. Entomol. 5, 133–137.

Badarinath, K.V.S., Kharol, S.K., Sharma, A.R., Roy, P.S., 2009. Fog over Indo-Gangetic Plains - A study using multisatellite data and ground observations. IEEE J. Sel. Top. Appl. Earth Obs. Remote Sens. 2, 185–195. https://doi.org/10.1109/JSTARS.2009.2019830

Baidya, S.K., Shrestha, M.L., Sheikh, M.M., 2008. Trends in Daily Climatic Extremes of Temperature and Precipitaton in Nepal. J. Hydrol. Meteorol. 5, 38–51.

Bedekar, V.C., Dekate, M. V, Banerjee, A.K., 1974. Heat and cold waves in India forcasting manual part IV (FMU Rep. No. IV-6). Poona< India.

Bhan, S.C., 2016. Weather Extremes : A spatio temporal perspective. Mausam 67, 27–52.

Bhat, J.N., Singh, B.P., R.K., A., Ra, R.P., Garg, I.D., Trehan, S.P., 2010. Assessment of crop losses in potato due to late blight disease during 2006-2007. Potato J. 37, 37–43.

Bhatla, R., Gupta, P., Mall, R.K., 2016. Cold Wave / Severe Cold Wave Events during Post-Monsoon and Winter Season over Some Stations of Eastern Uttar Pradesh , India. J. Clim. Chang. 2, 27–34. https://doi.org/10.3233/JCC-160003

Capozzi, V., Budillon, G., 2017. Detection of heat and cold waves in Montevergine time series (1884-2015). Adv. Geosci. 44, 35–51. https://doi.org/10.5194/adgeo-44-35-2017

Carlsen, B., Glenton, C., 2011. What about N? A methodological study of sample-size reporting in focus group studies. BMC Med. Res. Methodol. 11, 26. https://doi.org/10.1186/1471-2288-11-26

CBS/GON, 2016. Compendium of environment statistics, Nepal 2015. Central Bureau of Statistics, National Planning Commission Secretariat, Governemnt of Nepal, Kathmandu, Nepal.

CBS, 2017. National Climate Change Impact Survey 2016. A Statistical Report. Central Bureau of Statistics, Kathmandu, Nepal.

CBS, 2016. Statistical Year Book Nepal-2015, 15th ed. Central Bureau of Statistics, National Planning Commission Secretariat, Government of Nepal, Kathmandu, Nepal.

CBS, 2014a. Population monograph of Nepal, Volume II. Central Bureau of Statistics, National Planning Commission Secretariat, Government of Nepal, Kathmandu, Nepal.

CBS, 2014b. Statistical pocket book of Nepal 2014. Central Bureau of Statistics, National Planning

Commission Secretariat, Government of Nepal, Kathmandu, Nepal. https://doi.org/10.2833/77358

D'agostino, R.B., Belanger, A., D'Agostino Jr, R.B., 1990. A Suggestion for Using Powerful and Informative Tests of Normality. Am. Stat. 44, 316–321.

De, U.S., Dube, R.K., Rao, G.S.P., 2005. Extreme weather events over India in the last 100 years. J. Indian Geophys. Union 9, 173–187.

DesInventor, 2015. Nepal - Historic Inventory of Disaster [WWW Document]. Disaster Inf. Manag. Syst. URL https://online.desinventar.org/desinventar/#NPL-DISASTER (accessed 2.7.17).

Dimri, A.P., Chevuturi, A., 2016. Western disturbances - An Indian meteorological perspective, Western Disturbances - An Indian Meteorological Perspective. Springer. https://doi.org/10.1007/978-3-319-26737-1

Diwakar, J., Prasai, T., Pant, S.R., Jayana, B.L., 2010. Study on Major Pesticides and Fertilizers used in Nepal. Sci. World 6. https://doi.org/10.3126/sw.v6i6.2638

ETCCDI, n.d. Climate change indices [WWW Document]. ETCCDI/CRD Cliamte Chang. Indices. URL http://etccdi.pacificclimate.org/list_27_indices.shtml (accessed 1.24.17).

Fang, S., Qi, Y., Han, G., Li, Q., Zhou, G., 2016. Changing Trends and Abrupt Features of Extreme Temperature in Mainland China from 1960 to 2010. Atmosphere (Basel). 7, 1–13. https://doi.org/10.3390/atmos7020022

Fortin, G., Acquaotta, F., Simona Fratianni, 2017. The evolution of temperature extremes in the Gaspé Peninsula , Quebec , Canada (1974 – 2013). Theor Appl Clim. 130, 163–172. https://doi.org/10.1007/s00704-016-1859-x

Gautam, R., 2014. Challenges in early warning of the persistent and widespread winter fog over the Indo- Gangetic plains: a satellite perspective, in: Singh, Z.Z. and A. (Ed.), Reducing Disaster: Early Warning Systems for Climate Change. Springer Science+Business Media Dordrecht, pp. 51–61. https://doi.org/10.1007/978-94-017-8598-3

Gilbert, R.O., 1987. Statistical Methods for Environmental Pollution Monitoring. Van Nostrand Reinhold Company, New York. https://doi.org/10.2307/1270090

Gill, P., Stewart, K., Treasure, E., Chadwick, B., 2008. Methods of data collection in qualitative research: interviews and focus groups. Br. Dent. J. 204, 291–295. https://doi.org/10.1038/bdj.2008.192

Giri, Y.P., Maharjan, R., Sporleder, M., Kroschel, J., 2008. Pesticide use practices and awareness among potato growers in Nepal, in: 15th Triennial ISTRC Symposium. pp. 34–43.

Guest, G., Namey, E., McKenna, K., 2017. How Many Focus Groups Are Enough? Building an Evidence Base for Nonprobability Sample Sizes. Field methods 29, 3–22. https://doi.org/10.1177/1525822X16639015

Gum, W., Singh, P.M., Emmett, B., 2009. Even the Himalayas have stopped smiling: Climate Change, Poverty and Adaptation in Nepal. Kathmandu, Nepal.

Haque, M.A., Yamamoto, S.S., Malik, A.A., Sauerborn, R., 2012. Households' perception of climate change and human health risks: A community perspective. Environ. Heal. 11, 1. https://doi.org/10.1186/1476-069X-11-1

Hassi, J., 2005. Cold Extremes and Impacts on Health, in: Extreme Weather Events and Public Health Responses. Springer Berlin Heidelberg, Berlin and Hidelberg, Germany, pp. 59–67.

Hollander, M., Chicken, E., Wolfe, D.A., 2014. Nonparametric statistical methods., Wiley series in probability and statistics. Hoboken, New Jersey : John Wiley & Sons, Inc., [2014].

IMD, n.d. Terminologies and Glossary [WWW Document]. Terms and Glosary. URL http://imd.gov.in/section/nhac/termglossary.pdf (accessed 2.3.18).

Jaswal, A.K., Tyagi, A., Bhan, S.C., 2013. Trends in extreme temperature events over india during 1969-2012, in: High-Impact Weather Events over the SAARC Region. pp. 365–382. https://doi.org/10.1007/978-3-319-10217-7_26

Jenamani, R.K., 2012. Micro-climatic study and trend analysis of fog characteristics at IGI airport New Delhi using hourly data (1981-2005). Mausam 63, 203–218.

Joshi, K.D., Conroy, C., Witcombe, J.R., 2012. Agriculture, seed, and innovation in Nepal: Industry and policy issues for the future, International Food Policy Research Institute.

Karki, R., Talchabhadel, R., Aalto, J., Baidya, S.K., 2016. New climatic classification of Nepal. Theor. Appl. Climatol. 125, 799–808. https://doi.org/10.1007/s00704-015-1549-0

Kruger, A.C., Nxumalo, M., 2017. Surface temperature trends from homogenized time series in South Africa : 1931 – 2015. Int. J. Climatol. 2377, 2364–2377. https://doi.org/10.1002/joc.4851

Labajo, Á.L., Egido, M., Martín, Q., Labajo, J., Labajo, J.L., 2014. Definition and temporal evolution of the heat and cold waves over the Spanish Central Plateau from 1961 to 2010. Atmosfera 27, 273–286. https://doi.org/10.1016/S0187-6236(14)71116-6

Luthra, J.C., Chima, I.S., 1941. Some studies on the potentiality of shrivelled wheat grains, in: Proceedings of the Indian Academy of Sciences - Section B. pp. 47–67. https://doi.org/10.1007/BF03049638

Mahdi, S.S., Dhekale, B.S., 2016. Long term climatology and trends of heat and cold waves over southern Bihar, India. J. Earth Syst. Sci. 125, 1557–1567. https://doi.org/10.1007/s12040-016-0762-2

Mahdi, S.S., Dhekale, B.S., Choudhury, S.R., Bangroo, S.A., 2015. On the climate risks in crop production and management in India : A review. Aust. J. Crop Sci. 9, 585–595.

Malcheva, K., 2018. Cold waves on the territory of Bulgaria in the period 1952-2011. Bulg. J. Meteorol. Hydrol. 22, 16–31.

Manandhar, K.B., 2006. The Fog Episode in Southern Terai Plains of Nepal: Some Observations and Concepts. J. Hydrol. Meteorol. 3, 95–99.

Manandhar, S., Vogt, D.S., Perret, S.R., Kazama, F., 2011. Adapting cropping systems to climate change in Nepal: A cross-regional study of farmers' perception and practices. Reg. Environ. Chang. 11, 335–348. https://doi.org/10.1007/s10113-010-0137-1

Morgan, D.L., 1996. Focus groups. Annu. Rev. Sociol 22, 12952. https://doi.org/10.1146/annurev.soc.22.1.129

Ojha, H.R., Sulaiman V, R., Sultana, P., Dahal, K., Thapa, D., Mittal, N., Thompson, P., Bhatta, G.D., Ghimire, L., Aggarwal, P., 2014. Is South Asian Agriculture Adapting to Climate Change? Evidence from the Indo-Gangetic Plains. Agroecol. Sustain. Food Syst. 38, 505–531. https://doi.org/10.1080/21683565.2013.841607

Ortiz-Monasterio R., J.I., Dhillon, S.S., Fischer, R.A., 1994. Date of sowing effects on grain yield and yield components of irrigated spring wheat cultivars and relationships with radiation and temperature in Ludhiana, India. F. Crop. Res. 37, 169–184. https://doi.org/10.1016/0378-4290(94)90096-5

Pai, D.S., Srivastava, A.K., Nair, S.A., 2017. Heat and cold waves over India, in: Rajeevan, M.N., Nayak, S. (Eds.), Observed Climate Variability and Change over the Indian Region. Springer

Geology, pp. 51–72. https://doi.org/10.1007/978-981-10-2531-0

Pai, D.S., Thapliyal, V., Kokate, P.D., 2004. Decadal variation in the heat and cold waves over India during 1971-2000. Mausam 2, 281–292.

Paudyal, N., GC, C., Banjade, J., Chaudhary, D., 2012. Retrospective Analysis of Goat Disease in a Government Research Farm, in: Gurung, T.B., Joshi, B.R., Singh, U.M., Paudel, K.P., Shrestha, B.S., Rijal, K.P., Khanal, D.R. (Eds.), National Workshop on Research & Development Strategies for Goat Enterprises in Nepal. Nepal Agricultural Research Council. https://doi.org/10.13140/RG.2.1.1024.4006

Peel, M.C., Finlayson, B.L., McMahon, T.A., 2007. Updated world map of the Köppen-Geiger climate classification. Hydrol. Earth Syst. Sci. 11, 1633–1644. https://doi.org/10.5194/hess-11-1633-2007

PRMS, 2014. Study on national pesticide consumption statistics in Nepal. Lalitpur, Nepal.

Qingxiang, L.I., Wenjie, D., 2009. Detection and Adjustment of Undocumented Discontinuities þ. Adv. Atmos. Sci. 26, 143–153. https://doi.org/10.1007/s00376-009-0143-8.1.Introduction

Radinović, D., Ćurić, M., 2012. Criteria for heat and cold wave duration indexes. Theor. Appl. Climatol. 107, 505–510. https://doi.org/10.1007/s00704-011-0495-8

Revadekar, J. V., Kothawale, D.R., Patwardhan, S.K., Pant, G.B., Rupa Kumar, K., 2012. About the observed and future changes in temperature extremes over India, in: Natural Hazards. pp. 1133–1155. https://doi.org/10.1007/s11069-011-9895-4

Samra, J.S., Singh, G., Ramakrishna, Y., 2003. Cold wave of 2002-03: Impact on agriculture. Central Research Institute for Dryland Agriculture, Hyderabad. India.

Sathiyamoorthy, V., Arya, R., Kishtawal, C.M., 2016. Radiative characteristics of fog over the Indo-Gangetic Plains during northern winter. Clim. Dyn. 47, 1793–1806. https://doi.org/10.1007/s00382-015-2933-2

Sen, P.K., 1968. Estimates of the Regression Coefficient Based on Kendall's Tau. J. Am. Stat. Assoc. 63, 1379–1389.

Sharma, R.R., 2015. Nepalma sheetlahar ra prabhav. Gorkhapatra (January 12, 2015).

Shrestha, A.B., Bajracharya, S.R., Sharma, A.R., Duo, C., Kulkarni, A., 2016. Observed Trends and Changes in Daily Temperature and Precipitation Extremes over the Koshi River Basin 1975–2010. Int. J. Climatol. 37, 1067–1083. https://doi.org/10.1002/joc.4761

Shrestha, S., Moore, G.A., Peel, M.C., 2018. Trends in winter fog events in the Terai region of Nepal. Agric. For. Meteorol. 259, 118–130. https://doi.org/10.1016/j.agrformet.2018.04.018

Singh, A., Patwardhan, A., 2012. Spatio-temporal distribution of extreme weather events in India, in: APCBEE Procedia. Ajay Singh, pp. 258–262. https://doi.org/http://dx.doi.org/10.1016/j.apcbee.2012.03.042

Singh, D.N., Sirohi, R., Singh, Y., Ajay, 2015. Neonatal managements during adverse climatic conditions, in: Yadav, S., Yadav, B. (Eds.), Effect of Climate Change on Productive and Reproductive Performance of Dairy Animals. Directorate of Extension and Department of Veterinary Physiology on behalf of UP Pt. Deen Dayal Upadhyaya Pashu Chikitsa Vigyan Vishwavidyalaya Evam Go-Anusandhan Sansthan (DUVASU), Mathura, India, p. 228.

Singh, S., Singh, D., 2010. Recent Fog trends and its impact on wheat productivity in NW plains in India, in: 5th International Conference on Fog, Fog Collection and Dew Münster, Germany, 25–30 July 2010. Münster, Germany.

Spinoni, J., Lakatos, M., Szentimrey, T., Bihari, Z., Szalai, S., Vogt, J., Antofie, T., 2015. Heat and

cold waves trends in the Carpathian Region from 1961 to 2010. Int. J. Climatol. 35, 4197–4209. https://doi.org/10.1002/joc.4279

Stewart, D.W., Shamdasani, P.N., W., D.R., 2007. Focus Groups: Theory and Practice, Second. ed, SAGE. Sage Publications, Ltd., California, USA. https://doi.org/http://dx.doi.org/10.4135/9781412991841

Subedi, S., Shrestha, S., KC, G.B., Thapa, R.B., Ghimire, S.K., Neupane, S., 2015. Effect of meteorological factors on the development of lentil stemphylium blight at different sowing dates in Rampur, Chitwan, Nepal. Azarian J. Agric. 3, 142–146.

Sushma, D., Dipesh, R., Lekhendra, T., Shalik Ram, S., 2015. A Review on Status of Pesticides Use in Nepal. Res. J. Agric. For. Sci. Res. J. Agric. For. Sci 3, 2320–6063.

Syed, F.S., Körnich, H., Tjernström, M., 2012. On the fog variability over south Asia. Clim. Dyn. 39, 2993–3005. https://doi.org/10.1007/s00382-012-1414-0

Upadhyay, R.C., Hooda, O.K., Aggarwal, A., Singh, S.V., Chakravarty, R., Sirohi, S., 2014. Indian Livestock Production has Resilience for Climate Change R.C., in: Singh, S.V., Upadhyay, R.C., Sirohi, S., Singh, A.K. (Eds.), Climate Resilient Livestock & Production System. Division of Dairy Cattle Physiology National Dairy Research Institute, Indian Council of Agriculture Research, Karnal, INDIA.

Vaughn, S., Schumm, J.S., Sinagub, J., 1996. Focus group interviews in education and psychology. Sage Publication, Thousand Oaks, California. https://doi.org/10.4135/9781452243641

Wang, X.L., 2008a. Penalized maximal F test for detecting undocumented mean shift without trend change. J. Atmos. Ocean. Technol. 25, 368–384. https://doi.org/10.1175/2007JTECHA982.1

Wang, X.L., 2008b. Accounting for autocorrelation in detecting mean shifts in climate data series using the penalized maximal t or F test. J. Appl. Meteorol. Climatol. 47, 2423–2444. https://doi.org/10.1175/2008JAMC1741.1

Wang, X.L., Feng, Y., 2013. RHtestsV4 user Manual. Climate Research Divsion, Atmospheric Science and Technology Directorate, Toronto, Canada.

WHO, 2016. Climate and Health Country Profile – 2015 Nepal [WWW Document]. URL http://www.searo.who.int/entity/water_sanitation/nep_c_h_profile.pdf?ua=1 (accessed 3.14.18).

WMO, 1975. International Cloud Atlas. Volume I: Manual on the observation of clouds and other meteors, WMO Publication. Geneva, Switzerland.

WMO, 1972. The assessment of human bioclimate: A Limited Review of Physical Parameters. WMO no 331/ Technical Note Number 123. Geneva, Switzerland.

Xu, W., Li, Q., Wang, X.L., Yang, S., Cao, L., Feng, Y., 2013. Homogenization of Chinese daily surface air temperatures and analysis of trends in the extreme temperature indices. J. Geophys. Res. Atmos. 118, 9708–9720. https://doi.org/10.1002/jgrd.50791

Yang, X., Khanal, N.R., Koirala, H.L., Nepal, P., 2014. People's Perceptions of and Adaptation Strategies to Climate Change in the Koshi River Basin, Nepal, in: Vaidya, R.A., Sharma, E. (Eds.), Research Insights on Climate and Water in the HinduKush Himalayas. ICIMOD, Kathmandu Nepal, pp. 145–160.

Yosef, Y., Aguilar, E., Alpert, P., 2018. Detecting and adjusting artificial biases of long-term temperature records in Israel. Int. J. Climatol. 38, 3273–3289. https://doi.org/10.1002/joc.5500

Chapter 5

Development of a Regression Model for Estimating Daily Radiative Forcing Due to Atmospheric Aerosols from Moderate Resolution Imaging Spectrometers (MODIS) Data in the Indo Gangetic Plain (IGP)

This chapter addresses the research sub-question no 4. This chapter has been published in Atmosphere as described in preface. The supplementary material of this paper i.e. the Comparison of MODIS and AERONET data are presented in Annex 1.

atmosphere

MDPI

Article

Development of a Regression Model for Estimating Daily Radiative Forcing Due to Atmospheric Aerosols from Moderate Resolution Imaging Spectrometers (MODIS) Data in the Indo Gangetic Plain (IGP)

Shreemat Shrestha *, Murray C. Peel and Graham A. Moore

Department of Infrastructure Engineering, University of Melbourne, Parkville, Melbourne, VIC 3010, Australia; mpeel@unimelb.edu.au (M.C.P.); grahamam@unimelb.edu.au (G.A.M.)

* Correspondence: shreemats@student.unimelb.edu.au or shreematshrestha@yahoo.com

Received: 31 July 2018; Accepted: 29 September 2018; Published: 16 October 2018

Abstract: The assessment of direct radiative forcing due to atmospheric aerosols (ADRF) in the Indo Gangetic Plain (IGP), which is a food basket of south Asia, is important for measuring the effect of atmospheric aerosols on the terrestrial ecosystem and for assessing the effect of aerosols on crop production in the region. Existing comprehensive analytical models to estimate ADRF require a large number of input parameters and high processing time. In this context, here, we develop a simple model to estimate daily ADRF at any location on the surface of the IGP through multiple regressions of AErosol RObotic NETwork (AERONET) aerosol optical depth (AOD) and atmospheric water vapour using data from 2002 to 2015 at 10 stations in the IGP. The goodness of fit of the model is indicated by an adjusted R^2 value of 0.834. The Jackknife method of deleting one group (station data) was employed to cross validate and study the stability of the regression model. It was found to be robust with an adjusted R^2 fluctuating between 0.813 and 0.842. In order to use the year-round ADRF model for locations beyond the AERONET stations in the IGP, AOD, and atmospheric water vapour products from MODIS Aqua and Terra were compared against AERONET station data and they were found to be similar. Using MODIS Aqua and Terra products as input, the year-round ADRF regression was evaluated at the IGP AERONET stations and found to perform well with Pearson correlation coefficients of 0.66 and 0.65, respectively. Using ADRF regression model with MODIS inputs allows for the estimation of ADRF across the IGP for assessing the aerosol impact on ecosystem and crop production.

Keywords: radiative forcing; IGP; multiple regression; MODIS; AERONET; Jackknife method

1. Introduction

The Indo Gangetic Plain (IGP) is considered to be one of the most highly polluted regions of the world due to persistent heavy aerosol loading in its atmosphere [1,2]. Due to the high level of air pollution, premature mortality as a result of exposure to $PM_{2.5}$ in the Indian section of IGP alone is estimated to be 240,000 per annum [3]. Krishna Moorthy et al. [4] analysed the historical data from aerosol observatories in India and found that the aerosol optical depth (AOD) had increased at a rate of 2.3% (relative to 1985) per annum and the increasing trend was further increased (to 4%) in the last decade. High atmospheric pollution in this region is not only due to emissions from an increased use of fossil fuel in transportation and the industrial sector, but also due to a high dependence on biomass being used mainly for cooking in the residential sector [5,6]. In addition, the burning of crop residue (rice and wheat) in the field has significantly contributed to the high level of aerosols during the post monsoon and pre monsoon seasons in the IGP [7–11]. Furthermore, the unique topographic

features of the IGP with the Hindu Kush Himalayan range to the north, moderate hills in the south, Thar desert and Arabian sea to the west, and the Bay of Bengal to the east, in combination with rapidly increasing anthropogenic aerosol loading in the region and mineral dust from the Thar desert, has resulted in an alarming increase in aerosol loading in this region [1]. Based upon the annual mean $PM_{2.5}$ concentration, 17 cities of the IGP were included in the 20 most polluted cities of the world [12]. Given that all the representative concentration pathway (RCP) scenarios indicate that the air quality in this region is likely to degrade further. It is expected that severe negative effects on public health and the ecosystem will continue into the future [13].

Along with the negative effects on public health, it is reported that the high level of atmospheric aerosols in the IGP has also affected natural systems significantly. Unlike other parts of the world, solar dimming is found to be continued in India even after 2000 [14]. Similarly, while analyzing net downward shortwave radiation (NDSWR) over south Asia for the period of 1979–2004, it was found that solar dimming continues in south Asia with a trend of -0.54 W/m^2/year [15]. Singh et al. [16] analyzed the solar radiation and evaporation trends at four metrological stations in India during 1975–1995 and found solar diming in the range of 1.5% to 3.4% per decade across the stations. Similarly, it is reported that the net incoming radiation reduced by about 19% in the Indo Gangetic basin due to aerosols, which is expected to effect the regional climate significantly [17]. The atmospheric brown cloud (ABC) over the north Indian Ocean and south Asia, due to anthropogenic atmospheric aerosols, was documented after the Indian Ocean Experiment (INDOEX) and several studies into its possible effects on regional and global climate [18–22]. In the study of the IGP region using remote sensing techniques, Devara and Manoj [23] concluded that there is strong association between atmospheric aerosol content and monsoon precipitation. Since the summer monsoon provides 75–90% of the annual rainfall in the IGP, the agricultural performance of this region is also expected to be affected by the high level of atmospheric aerosols.

Aerosols also have a significant effect on fog formation in the IGP region [24]. Every winter, the whole IGP region is engulfed by dense fog with a significant increasing trend in the number of foggy days during the past 35 years [25,26]. The increasing trend of winter fog has not only affected day-to-day life of millions of people living in this region, through frequent flight/train delay due to poor visibility [27], but it also negatively affected the production of several winter crops [28,29]. A statistical model of historical rice harvest in India, coupled with a regional climate scenario, indicated that there has been a slowdown in the increase in production over the last two decades due to increased brown cloud and greenhouse gas [30]. Similarly, Latha et al. [31] compared the radiative forcing of atmospheric black carbon at two locations in IGP, Varanasi and Ranchi by using Santa Barbara DISTORT Atmospheric Radiative Transfer (SBDART) model and concluded that the incoming radiation is reduced by about 5% due to black carbon (BC) during any time of day at Varanasi and 4% at Ranchi. This study also estimated the loss of wheat crop at Varanasi and Ranchi while using the empirical model that was developed by Ahmed and Hassen [32] as -149 kg/ha and -141 kg/ha, respectively, due to the reduction of solar radiation because of atmospheric black carbon. Moreover, a crop response simulation model has shown that there is a direct relationship between the increase (decrease) in solar irradiance and increase (decrease) in rice and wheat yield in China and that due to atmospheric aerosols and regional haze there has been a reduction in wheat and rice yields in China by 5 to 30% [33]. In this context, information on the effect of aerosols on solar radiation in the IGP is important not only to study the effect on the climate and ecosystem in the long run, but also to study the immediate effects of atmospheric aerosols on solar radiation availability for agricultural production in the region.

The effect of atmospheric aerosols on climate is generally measured in terms of aerosol radiative forcing, which is defined as the effect of anthropogenic aerosols on the radiative fluxes [34]. The radiative forcing is estimated at the top of atmosphere (TOA), bottom of atmosphere (BOA), and in the atmosphere. Ramanathan & Ramana [19] studied the direct radiative forcing of atmospheric brown clouds in the Himalayan foot hills and Indo Gangetic Plains (IGPs) by using MODIS Terra satellite data during 2001 to 2003 and found the average surface radiative forcing during the dry season

(October to May) in the region is about -32 ± 5 Wm^{-2}. Similarly, Dey and Tripathi [35] studied the direct radiative effect of aerosols in the IGP during 2001 to 2005 by using an aerosol optical model and found the annual average radiative forcing at the surface at Kanpur was -31.8 ± 10.9 Wm^{-2}. Their study also concluded that anthropogenic aerosols contributed 80% of the radiative forcing at Kanpur during October to February. Similarly, Ramachandran and Kedia [36] investigated the seasonal variation of aerosol radiative forcing at Kanpur and Gandhi college during January 2006 to December 2007 by using AERONET data and the Santa Barbara DISORT Atmospheric Radiative Transfer (SBDART) model, which provided very similar results. The maximum radiative forcing in the atmosphere and at the surface was in the pre-monsoon season at both stations. Das et al. [37] studied winter haze in the eastern Indo Gangetic Basin through ground measurements during December 2013 to February 2014 and the radiative effect of haze by using SBDART and found the radiative forcing at the BOA in Silguri, Kolkata and Sunderban was -39.3, -70.3 and -38 Wm^{-2} respectively. In addition, Latha et al. [31] studied the radiative forcing of atmospheric black carbon at Varanasi and Ranchi using SBDART and concluded that the radiative forcing due to atmospheric black carbon is significantly increased from February to March (i.e., from -30 Wm^{-2} to -50 Wm^{-2}) at Varanasi due to an increased BC concentration and mixing layer height. The radiative forcing due to atmospheric aerosols at IGP stations has been studied at the annual, seasonal, and in some cases, monthly time scale by using radiative transfer models [36,38–44].

The Santa Barbara DISTORT Atmospheric Radiative Transfer (SBDART) model was developed to model the plane parallel radiative transfer within the atmosphere and at the earth surface [45]. SBDART is a comprehensive model that consists of six standard atmospheric profiles, five basic surface types and four standard aerosol types, SBDART is widely used to study direct radiative forcing due to atmospheric aerosols at the earth surface, within the atmosphere and at the top of atmosphere [38,46–48]. However, it requires a large number of input parameters (and therefore assumptions) and high processing time, making it unrealistic for use with large amounts of data across spatial and temporal scales [49]. In this context, there is a need for a simple model to determine radiative forcing across the IGP at daily time scale. Determination of the daily radiative forcing across the IGP may also help to determine the change in radiative flux due to atmospheric aerosols loading, and this could help to assess the effect of atmospheric aerosols on terrestrial ecosystems at the regional scale. In turn, this will help to investigate the effects of atmospheric aerosols on the crop production system at the regional level, as suggested by Huntingford et al. [50].

We aimed to develop a simple regression model to determine daily radiative forcing from high quality station data in the IGP, which can then be driven by remotely sensed data (which has wide temporal and spatial coverage). Within the IGP, there are several AERONET (AErosol RObotic NETwork) stations that are part of the global network of ground based remote sensing aerosol stations initiated by National Aeronautics and Space Administration (NASA) [51]. These stations provide continuous high-quality point observations of aerosol loading and radiative forcing due to atmospheric aerosols. Garcia et al. [52] validated the AERONET estimated radiative forcing against ground based broad band measurements from the Baseline Surface Radiation (BSRN) and the Solar Radiation Networks (SolRad-Net), and found that AERONET estimated radiative forcing is very close to ground measurements with uncertainty less than 15 Wm^{-2} for all stations, which is within the uncertainty of BSRN and SolRad-Net observed data. AERONET ground observation data are extensively used to study the optical properties of atmospheric aerosols and their radiative effects [48,53–55]. In addition, AERONET observations are also considered to be the benchmark for the validation of aerosol properties obtained from other indirect methods, such as models and satellite imagery. But, these point data on aerosol optical properties and radiative forcing due to atmospheric aerosols at the surface and top of atmosphere are limited to the location of the AERONET stations.

In this context, it is planned to develop and evaluate a multiple regression model to estimate daily radiative forcing at the bottom of the atmosphere in the IGP by using the quality AERONET station point data and spatially distributed satellite remotely sensed data in the region. Remer et al. [56]

extensively validated the Moderate Resolution Imaging Spectrometers (MODIS) retrieved AOD with AERONET measured AOD at the global scale and found that MODIS products are accurate within prelaunch expectations and they are sufficiently accurate for a variety of applications, including improved estimates of observationally based aerosol radiative effects. For the wide scale application of this simple regression model, it is evaluated by using MODIS derived aerosol properties at the AERONET stations located in IGP. After successful evaluation of the model with MODIS derived aerosol properties at AERONET stations in the IGP, this model can be used to estimate the radiative forcing due to atmospheric aerosols at the surface on any day at any location of the IGP because MODIS sensors on the Terra and Aqua earth observing system (EOS) satellites provide continuous and near real time aerosol properties of the earth at higher temporal and spatial resolutions. This model will help to estimate the reduction of solar radiation at the surface of the IGP, which may be utilised to study the immediate effects of aerosols in the IGP on, for example, crop production, evapotranspiration, etc., along with the long-term effects of aerosols on climate change and the natural systems of the IGP.

The important feature of this study is the development and evaluation of a simple regression model to estimate direct daily radiative forcing due to atmospheric aerosol (ADRF) in the IGP region by using point AERONET data. Once established, the model will be evaluated while using MODIS inputs at the AERONET stations, where AERONET ADRF is available. Using MODIS products of daily average AOD and precipitable water vapour in this model will allow, ADRF to be estimated at any location across the IGP. This simple model may be used to assess the effect of atmospheric aerosols on solar radiation, and consequently environmental effects at daily time scale in the IGP region.

2. Study Area and Data Sets

2.1. Study Area

The Indo-Gangetic basin is the combination of two neighbouring river basins—the Indus and the Ganga in south Asia. The origin of both rivers is the Hindu Kush Himalaya, which strongly influences and controls the atmospheric circulation around the region [57]. Both of these rivers have fertile alluvium plains that are intensely cultivated and are known as the Indo Gangetic Plain (IGP). The IGP is the study area, which encompasses the eastern plain area of Pakistan, most of northern and eastern India, the southern plain area of Nepal and almost all of Bangladesh (Figure 1). The IGP is 250 to 450 km wide and extends from the delta of the Indus river at the Arabian sea to the delta of the Ganga at the Bay of Bengal and it separates the Himalaya from the Indian peninsula [58]. Agriculture is one of the major economic activities of the population in the IGP. Rice and wheat are the major crops that are cultivated in the IGP covering 13.5 M ha of Pakistan, India, Nepal and Bangladesh [59]. The IGP is also known as the 'food basket' of the region because it produces 53% of rice and 93% of wheat in these countries [60]. The IGP is home to about 800 M people with high population density in the range of 400–600 people per square kilometre [61,62]. The IGP is a densely populated region with five mega cities (New Delhi, Karachi, Dhaka, Kolkata, and Lahore) and dozens of cities with population of more than one-million [63]. Due to rapid urbanization, industrialization and lack of effective monitoring and control on pollution, there is persistent heavy aerosol loading in the atmosphere of the Indo Gangetic Plain (IGP), which is considered to be one of the most highly polluted regions of the world [1,2].

The climate of the IGP varies from semi-arid in the Punjab region of Pakistan, hot sub-humid in Haryana, Uttar Pradesh and Bihar of India and Terai region of Nepal and sub-humid to humid climate in West Bengal of India and the plain area of Bangladesh [59]. There is a clear gradient in annual average precipitation in the IGP with 654 mm in the Punjab (western IGP) to 1462 mm in West Bengal (eastern IGP) [64]. The monsoon season (June to September) is the rainy season and about 85% of the total precipitation occurs during this period.

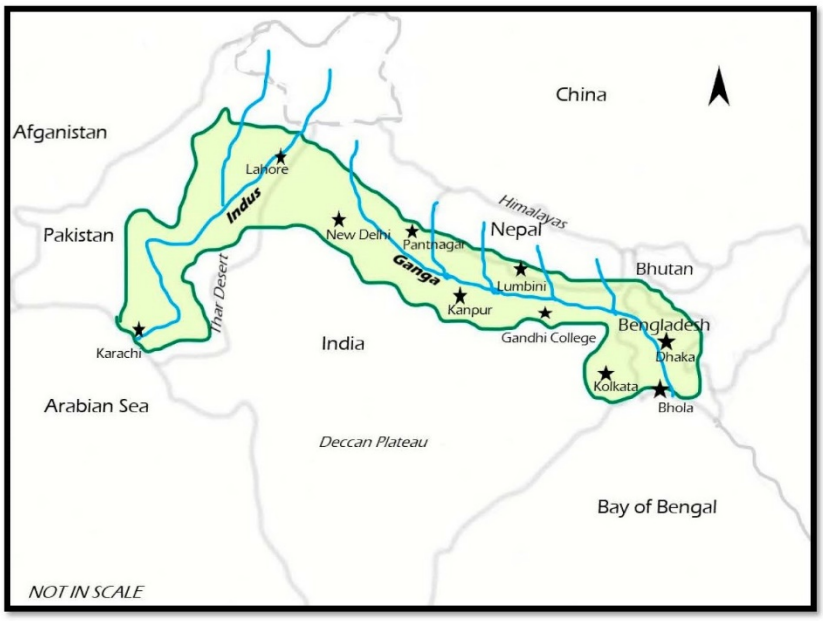

Figure 1. Study area—Indo Gangetic Plain (IGP) and the location of AErosol RObotic NETwork (AERONET) stations (starred).

2.2. Ground Station Instrumentation and Data

The AERONET network provides, long-term continuous monitoring and characterisation of aerosols, at a regional and global scale, as well as aerosol information from spectral data of direct sun radiation extinction and angular measurement of sky radiance [51,65]. In addition, the inversion AERONET products provide aerosol parameters (e.g., size distribution, complex refractive index, partition of spherical, and non-spherical particles) and properties (e.g., phase function, refractive index, spectral and broad band fluxes, etc.), including radiative forcing at the top of atmosphere and bottom of atmosphere [66]. The AERONET data for daily aerosol optical depth (AOD) at 500 nm, atmospheric water vapour, and daily direct radiative forcing at the bottom of the atmosphere (BOA) from the AERONET stations in the IGP (listed in Table 1) are used in this study. Out of those 10 AERONET stations in the IGP, two stations are from Pakistan, five are from India, one from Nepal, and two from Bangladesh.

Table 1. AERONET Stations in the IGP.

SN	Site Name	Country	Longitude (Decimal Degrees)	Latitude (Decimal Degrees)	Elevation (Metres)
1	Bhola	Bangladesh	90.756	22.227	7
2	Dhaka University	Bangladesh	90.398	23.728	34
3	Gandhi College	India	84.128	25.871	60
4	IIT KGP EXT Kolkata	India	88.418	22.574	10
5	Kanpur	India	80.232	26.513	123
6	Karachi	Pakistan	67.136	24.946	49
7	Lahore	Pakistan	74.264	31.480	209
8	Lumbini	Nepal	83.280	27.490	110
9	New Delhi	India	77.222	28.589	241
10	Pantnagar	India	79.521	29.046	241

2.3. Satellite Data

Two Moderate Resolution Imaging Spectroradiometer (MODIS) sensors, Aqua and Terra of the Earth observing system (EOS) satellites are considered to be the most comprehensive sensors

continuously providing electromagnetic images of land, ocean, and atmosphere environment for a wide range of applications. EOS with MODIS Terra sensor (10:30 p.m. local solar equatorial crossing time) was launched in late 1999 and the MODIS Aqua sensor (1:30 p.m. local solar Equatorial crossing time) was launched in 2002 [67]. The MODIS deep blue (DB) algorithm was originally developed to retrieve AOD over bright surfaces by using deep blue wave length and similarly the MODIS dark target (DT) algorithm was originally developed for dark vegetated surface areas. The merged DT-DB product combines and it merges the results of both algorithms and is considered to be the "best-of" combined aerosol product available [68]. In addition, Mhawish et al. [51] found that the merged DT-DB product showed less bias across IGP sites and performed as good as DT and DB products, except over the upper IGP. The MODIS Aqua and MODIS Terra merged DT and DB AOD products are used in this study. At each of the AERONET stations in the IGP listed in Table 1, the area averaged time series of daily merged DT and DB AOD product from MODIS Aqua and Terra was extracted for pixel lying in a $\pm 0.1^{\circ}$ longitude and latitude box around each station. Similarly, time series data of mean daily precipitable water vapour from MODIS Aqua and Terra products at those selected AERONET stations were also obtained.

2.4. Data Quality

The accuracy of the Cimel radiometers, used at the AERIONET stations, is within ± 0.01 to ± 0.02 for measured columnar AOD [51,69]. Based upon the results of extensive sensitivity studies on AERONET data by Dubovik et al. [70], Dubovik et al. [71] recommended a set of quality control criteria for high accuracy in the retrieval of aerosol parameters. These recommended quality control criteria were used to produce quality assured version 2.0 AERONET inversion products (National Aeronautics and Space Administration, Washington, DC, USA) [72]. Similarly, Pérez-Ramírez, D. et al. [73] demonstrated the ability of AERONET to retrieve precipitable water vapour (average bias less than 6% and total uncertainty less than 15%) by comparing it with radio sonde, Global Positioning System (GPS), and microwave radiometry methods. The AERONET data used in this study are taken from the highest quality version under clear-sky conditions, i.e., Version 2.0 at level 2.0. Hence, the AERONET data are considered to be standard data and are used to validate atmospheric properties from satellite data. The MODIS Aqua and Terra products are validated by using AERONET data at the regional and global scale in many studies [74–79]. The uncertainty in the MODIS retrieved aerosol optical depth (AOD) over land and ocean are reported to be in the range of $\pm(0.05 + 0.2 \times \text{AOD})$ and $\pm(0.03 + 0.15 \times \text{AOD})$, which is also considered to be the expected error (EE) [74]. Similarly, Sayer et al. [80] compared the MODIS Aqua data products with AERONET data at global and regional scales and found that MODIS merged AOD at 550 nm has the correlation coefficient and root mean square error of 0.86 and 0.16, respectively, for the Indian subcontinent.

3. Methodology

This section is sub-divided in to 3 sub-sections. The first sub-section describes the regression modelling of the ADRF using AERONET data. In the second sub-section, the method adopted to compare the MODIS products (AOD and precipitable water vapour) with the corresponding AERONET product is presented. Finally, in the third sub-section, the method employed to evaluate the developed model is described.

3.1. Multiple Regressions

To develop a statistical model to predict daily direct radiative forcing due to atmospheric aerosols (ADRF) at the bottom of atmosphere (BOA), multiple regressions were performed for different combinations of parameters, including AOD, atmospheric water vapour, elevation, Angstrom coefficient, etc. A multiple regression of ADRF with daily mean AOD and daily mean atmospheric water vapour provided a simple model with good results (see Equation (1)) and significant improvement was not obtained with the inclusion of other variables in the model. Russel et al. [81]

showed that AOD is the important factor that is responsible for the local radiative forcing among other several factors. Bilbao et al. [82] also showed that direct short wave irradiance is a function of AOD at 550 nm. Obviously, AOD is an important parameter related to the radiative forcing at the surface because it measures the optical extinction due to scattering and absorption in the vertical column. Moreover, it is also reported that the optical properties of hygroscopic aerosols are significantly affected by atmospheric water vapour [83]. Furthermore, Bilbao et al. [82] showed that there is statistically significant negative correlation between direct short wave irradiance and column atmospheric water vapour.

The null hypothesis for the statistical test of this multiple regression is that there is no relationship between daily ADRF and daily aerosol optical depth and daily mean atmospheric water vapour at any particular location in the IGP. The F test was performed, as described by Cohen [84], to test the hypothesis and the model was evaluated while using the adjusted R^2 value. The statistical significance of the individual atmospheric parameters (viz. AOD and atmospheric water vapour) in the following linear model was evaluated using the *t* test, as described by Cohen [84].

$$ADRF = A + B_1\, AOD_{550} + B_2\, AWV \quad (1)$$

where, A is an intercept and B_1 and B_2 are the coefficients for AOD and atmospheric water vapour respectively.

$ADRF$ = Daily direct radiative forcing due to atmospheric aerosols (Wm^{-2}).

AOD_{550} = Daily average atmospheric aerosol optical depth at wavelength 550 nm.

AWV = Daily mean atmospheric water vapour (m).

After pooling the data sets from all the stations together, a year-round radiative model for the IGP region is developed. Similarly, after pooling the seasonal data (winter, pre-monsoon, monsoon, and post monsoon seasons) of all stations seasonal models for the IGP region are also developed.

3.2. Comparison of AERONET and MODIS Products

As the AERONET measured AOD and precipitable water vapour are only available at a few stations in the IGP, this limits the applicability of the derived model. Unlike point products of AERONET, MODIS provides continuous spatial as well as the temporal distribution of AOD and precipitable water vapour over the earth. Since MODIS provide the AOD at 550 nm and AERONET provides the AOD at 500 nm, the AOD at 500 nm wavelength, is transformed to 550 nm by using the following equation, as suggested by Prasad and Singh [85] and Bibi et al. [44].

$$AOD_{550} = AOD_{500}\,(500/550)^{-\alpha} \quad (2)$$

where,

AOD_{550} = Daily average atmospheric aerosol optical depth at wavelength 550 nm.

AOD_{500} = Daily average atmospheric aerosol optical depth at wavelength 500 nm.

α = Angstrom Exponent in the wavelength range of 440 to 870 nm.

Before using MODIS derived AOD and precipitable water vapour for the IGP in the developed model, the MODIS derived AOD and mean precipitable water vapour are compared against the AERONET station based AOD and mean atmospheric water in the IGP. The comparison was performed using a scatterplot, calculating mean error (ME), mean absolute error (MAE), root mean square error (RMSE), and Pearson correlation coefficient (r).

3.3. Evaluation of the Model

The ADRF predicted by the model is compared with the AERONET observed ADRF for all the AERONET stations in the IGP. The model predicted results are evaluated by calculating the mean error, mean absolute error, root mean square error, Nash-Sutcliffe coefficient of efficiency [86], and Pearson correlation coefficient. Since it is reported that Jackknife validation is unbiased when compared to

validation with data splitting [87], the model is evaluated and the stability of the model is tested by adopting a delete one group (station) Jackknife method, as described by [88,89]. The ADRF predicted by the model when using MODIS Aqua and Terra derived AOD and mean precipitable water vapour is compared against the AERONET measured ADRF.

4. Results and Discussions

This section is sub-divided in to six sub-sections. In the first sub-section, the year round and seasonal ADRF models that were developed through multiple regression using AERONET data at 10 stations in the IGP region are presented. In the second sub-section, the overall and station wise evaluation of the performance of the models are discussed. Moreover, the results of the cross-validation Jackknife method are also discussed in this sub-section. To use the developed year-round ADRF model beyond the AERONET stations in the IGP, two model input parameters AOD and precipitable water vapour retrieved from MODIS Aqua and Terra are compared against AERONET values in the third sub-section. In the fourth sub-section, the developed ADRF is evaluated by using MODIS Aqua and Terra products. In the fifth sub-section, the performance of the model with MODIS Aqua input parameters is compared with that of the MODIS Terra products. Finally, in the sixth sub-section, the results of the ADRF model is compared against the published values from SBDART at two AERONET stations.

4.1. Development of Regression Model for ADRF

Multiple linear regressions are developed for year-round and seasonal empirical models to estimate daily ADRF at the surface using AOD and mean atmospheric water vapour from the AERONET stations in the IGP listed in Table 1. The results of the regressions are presented in Table 2. The intercept (A) and coefficients (B_1 and B_2) of the year-round model, which is developed using 5138 daily data points from the IGP, are found to be significant ($p < 0.01$). The adjusted R^2 of the year-round model is 0.834, which indicates the year-round model provides a good fit to the ADRF in the IGP. All of the seasonal models, except winter, have significant ($p < 0.01$) intercept and coefficients. In the winter model the coefficient of mean atmospheric water vapour in the atmosphere is not significant, which may be due to the dry atmospheric condition during this time with nil to very little rainfall in the IGP [90]. The adjusted R^2 values of the seasonal models are similar to that of the year-round model, ranging from 0.825 for the monsoon model to 0.862 for the post monsoon model. The standard error is a measure of model prediction accuracy and it is defined as the square root of the ratio of the sum of squared residuals and the degree of freedom. The standard error of the year-round model is 14.39 Wm^{-2} where as that of the seasonal models range from 11.364 Wm^{-2} for the Monsoon model to 14.970 Wm^{-2} for the post monsoon model. From the results of the regression using AERONET data, it appears that the proposed models could be promising models for estimating daily ADRF in the IGP.

Table 2. Regression results of year-round and seasonal models to predict atmospheric aerosol (ADRF).

Model	Number of Observations	*A* (Sig.) (Wm^{-2})	B_1 (Sig.) (Wm^{-2})	B_2 (Sig.) (Wm^{-3})	Adjusted R^2	Standard Error (Wm^{-2})
Year-round Model	5138	−32.464 (0.00)	−119.446 (0.00)	4.471×10^2 (0.00)	0.834	14.390
Season Models						
Winter	884	−23.895 (0.00)	−117.876 (0.00)	-4.89×10^2 (0.62)	0.846	14.724
Pre-monsoon	1854	−24.256 (0.00)	−129.979 (0.00)	2.232×10^2 (0.00)	0.828	13.184
Monsoon	812	−40.510 (0.00)	−97.921 (0.00)	4.093×10^2 (0.00)	0.825	11.364
Post monsoon	1588	−35.872 (0.00)	−118.795 (0.00)	5.458×10^2 (0.00)	0.862	14.970

Note: *A* is the intercept and B_1 and B_2 are the coefficients shown in Equation (1). Significance was tested using a *t*-test and *p* values are in brackets.

4.2. Evaluation of the Performance of the ADRF Model

The performance of the developed year-round ADRF regression model is evaluated through station wise scatterplots of AERONET ADRF and estimated ADRF using AERONET AOD and precipitable atmospheric water vapour, as shown in Figure 2. The total number of daily observations across all 10 stations in the IGP during 2002 to 2015 is 5138 and the station wise observations vary from 27 at Kolkata to 1581 at Kanpur. From Figure 2, it is evident that most of the observed and estimated ADRF points follow the 1:1 line, indicating agreement between the estimated ADRF and the AERONET ADRF at all ten stations of the IGP.

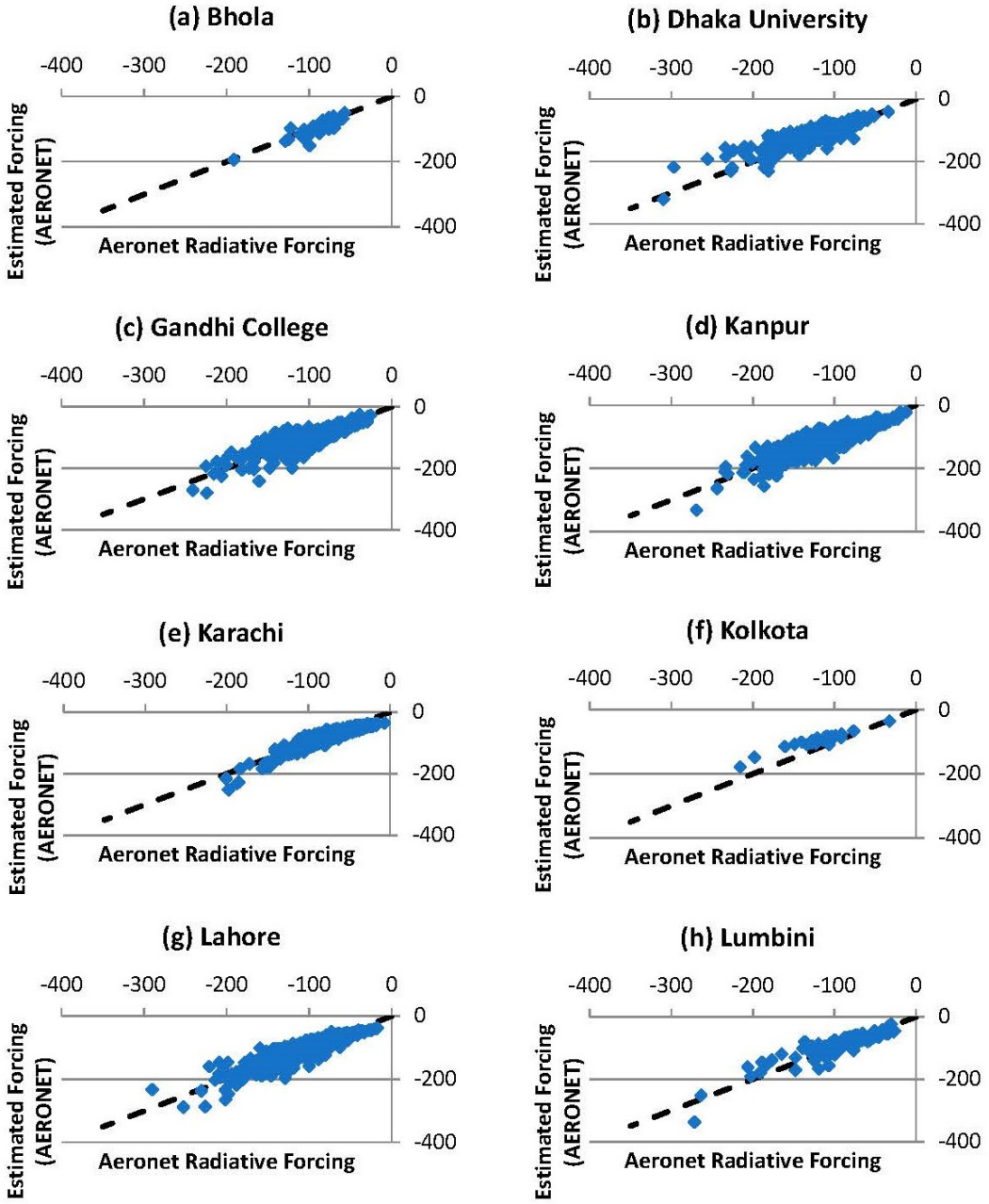

Figure 2. *Cont.*

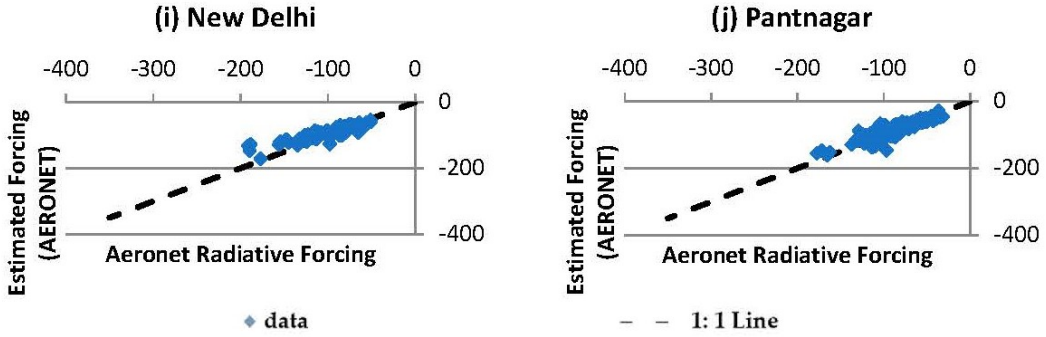

Figure 2. Evaluation of estimated radiative forcing with that of AERONET radiative forcing (Wm^{-2}) in the IGP stations. (**a**) Bhola (**b**) Dhaka University (**c**) Gandhi College (**d**) Kanpur (**e**) Karachi (**f**) Kolkata (**g**) Lahore (**h**) Lumbini (**i**) New Delhi (**j**) Pantnagar.

The results of applying the year-round model to estimate daily ADRF by using AERONET AOD and daily mean atmospheric moisture at each station is presented in Table 3. The mean error (ME) in the estimation of daily ADRF varies from −7.689 Wm^{-2} at Bhola to 22.946 Wm^{-2} at Kolkata. Both of those stations have very few observations i.e., 37 and 27 at Bhola and Kolkata, respectively, out of a total of 5138 data points. The mean absolute error (MAE) ranges from 8.607 Wm^{-2} at Karachi to 23.338 Wm^{-2} at Kolkata and the MAE across all stations is 10.490 Wm^{-2}. The root mean square error (RMSE) in estimated ADRF across all the stations in IGP is 14.390 Wm^{-2}. The RMSE of Kolkata is highest (26.284 Wm^{-2}) and that of Karachi is lowest (10.592 Wm^{-2}) among the stations in the IGP.

Table 3. Results of the ADRF model using all AERONET stations in the IGP by using AERONET aerosol optical depth (AOD) and atmospheric water vapour at each station.

SN	Stations	Number of Observations	Mean Error (Wm^{-2})	Mean Absolute Error (Wm^{-2})	Root Mean Square Error (RMSE) (Wm^{-2})	Nash-Sutcliffe Efficiency (NSE)	Correlation Coefficient, r
1	Bhola	37	−7.689	11.760	15.428	0.608	0.870
2	Dhaka University	253	10.158	16.997	22.914	0.723	0.882
3	Gandhi College	833	0.419	10.924	15.144	0.782	0.886
4	Kanpur	1581	−0.405	9.780	13.522	0.831	0.912
5	Karachi	1028	−5.255	8.607	10.592	0.827	0.932
6	Kolkata	27	22.946	23.338	26.284	0.402	0.954
7	Lahore	1017	1.289	10.646	14.436	0.822	0.909
8	Lumbini	106	3.679	16.702	20.912	0.802	0.900
9	New Delhi	67	7.828	12.962	18.301	0.695	0.888
10	Pantnagar	189	2.984	8.816	11.911	0.790	0.896
	All Stations	5138	0.000	10.490	14.390	0.830	0.910

Even though the acceptability of the performance of a model depends upon the application of the model [91], for practical application Ritter and Muñoz-Carpena [92] adopted Nash–Sutcliffe efficiency of between 0.65 and 0.8 as an acceptable range and 0.81 to 0.9 as a good range for the goodness of fit when evaluating a model. The Nash–Sutcliffe efficiency of the year-round model for all station data is 0.830, indicating that the model is a good fit to the data. The station wise Nash–Sutcliffe efficiency of the year-round model at all stations in the IGP, except that of Kolkata (0.402) and Bhola (0.608) is within the acceptable range. The Pearson correlation coefficient (r) between the year-round model estimated ADRF and the AERONET ADRF at all stations in the IGP is 0.91. The Pearson correlation coefficient of the station wise estimated values of the ADRF range from 0.87 at Bhola to 0.95 at Kolkata. Test results of the year-round ADRF model at the station level indicate that the year round ADRF model is acceptable.

To test the consistency and stability of the year-round model for prediction of ADRF, the model is tested by adopting a delete one group (station) Jackknife method. The results of the multiple regressions from the delete one group (station data) Jackknife method are shown in Table 4. From the table, it is observed that the adjust R^2 value ranged from 0.813 to 0.842 and the standard error varied from

13.791 Wm^{-2} to 15.098 Wm^{-2} in the 10 Jackknife cases, which indicates consistency in the performance of the model, even when one of the stations is removed from the analysis. The intercept (A) of the year-round model in the Jackknife cases ranged from −36.43 to −30.21. The coefficients B_1 and B_2 values fluctuated from −121.390 to −116.116 and 3.843 to 5.113, respectively. Interestingly, it is also observed that the mean value of intercept, coefficients, adjusted R^2, and standard error from the Jackknife cases is very close to the values that are generated by the regression with all station data. The limited variation in the distribution of the coefficients, the intercepts, adjusted R^2, and standard error values in the Jackknife cases indicates that the year-round model is a stable model for the prediction of the ADRF in the IGP.

Table 4. Results of multiple regression of ADRF using AERONET AOD and atmospheric water vapour in the IGP by adopting a delete one group (station data) Jackknife method.

SN	All Stations of IGP Except	Number of Observations N	Intercept, A (Wm^{-2})	AOD Coefficient, B_1 (Wm^{-2})	Atmospheric Moisture Coefficient, B_2 (Wm^{-3})	Adjusted R Square	Standard Error (Wm^{-2})
1	Bhola	5101	−32.388	−119.608	4.451×10^2	0.834	14.382
2	Dhaka University	4885	−32.355	−118.039	4.301×10^2	0.835	13.791
3	Gandhi College	4305	−32.846	−120.940	5.113×10^2	0.842	14.224
4	Kanpur	3557	−31.758	−121.390	4.552×10^2	0.834	14.749
5	Karachi	4110	−36.430	−116.116	4.775×10^2	0.813	15.098
6	Kolkata	5111	−32.424	−119.215	4.448×10^2	0.835	14.300
7	Lahore	4121	−30.218	−120.602	3.843×10^2	0.835	14.352
8	Lumbini	5032	−32.409	−119.616	4.527×10^2	0.835	14.220
9	New Delhi	5071	−32.420	−119.184	4.429×10^2	0.835	14.331
10	Pantnagar	4949	−32.205	−119.537	4.426×10^2	0.834	14.476
	Min	3557	−36.430	−121.390	3.843×10^2	0.813	13.791
	Max	5111	−30.218	−116.116	5.113×10^2	0.842	15.098
	Average	4624.20	−32.545	−119.425	4.487×10^2	0.833	14.392
	Standard Deviation	553.99	1.543	1.513	0.323×10^2	0.008	0.344
	All Stations	5138	−32.464	−119.446	4.471×10^2	0.834	14.390

Note: ADRF = Daily direct radiative forcing due to atmospheric aerosols (Wm^{-2}); AERONET = Aerosol Robotic Network; AOD = Aerosol Optical Depth; IGP = Indo Gangetic Plain.

4.3. Comparison of MODIS and AERONET Products

To extend the applicability of the developed year-round and seasonal ADRF models throughout the IGP, it is necessary to obtain AOD and atmospheric water vapour data for any location within the IGP. In this context, MODIS products are considered to be very useful for this application, because they provide high spatial resolution atmospheric aerosol data with observations twice a day covering most of the planet and easy access to near real-time data [78]. Before applying MODIS data in this model, it is necessary to compare the MODIS and AERONET products in the IGP. The comparison of MODIS Aqua and MODIS Terra products is performed separately against the AERONET AOD and atmospheric water vapour. The results of comparison of MODIS and AERONET data are presented in the supplement section.

4.3.1. Comparison of MODIS Aqua and AERONET Products

The station wise comparison of MODIS Aqua retrieved AOD_{550} against transformed AERONET AOD at 550 nm from measured AOD at 500 nm at the IGP stations is performed through scatterplots in Figure S1. The plots indicate that the MODIS Aqua AOD is similar to the transformed AERONET AOD measured at each station in the IGP, because the majority of the scatter points are near to the 1:1 line. The uncertainty in the MODIS retrieved aerosol optical depth (AOD) over land and ocean are reported to be in the range of $\pm(0.05 + 0.2 \times AOD)$ and $\pm(0.03 + 0.15 \times AOD)$, which is also considered to be the expected error (EE) [74]. Figure S2 provides the share of the MODIS Aqua AOD values that lie within, above and below the expected error range where AERONET AOD is assumed to be actual AOD. The figure indicates that in all the stations except Kolkata, more than 60% of MODIS

Aqua retrieved AOD data lie within the expected error range for the IGP stations. Since more than 70% of MODIS Aqua retrieved AOD at Kanpur is within the expected error range, MODIS retrieved AOD is well matched with AERONET data, which is similar to the findings of Choudhary et al. [93]. As 64.4% of MODIS Aqua retrieved AOD is within the expected error range at Gandhi college in this study, the correlation of the MODIS Aqua retrieved AOD at Gandhi College in this study is higher than the findings of Choudhary et al. [93], which may be due to the extended data period of this study (2002 to 2015) as compared to the previous study (2002 to 2010). Similarly, more than two-thirds of the MODIS Aqua AOD data across all IGP stations are within the expected error range.

The statistical comparison of the MODIS Aqua retrieved AOD and atmospheric water vapour with the AERONET measured AOD and atmospheric water vapour is presented in Table 5. It is observed that the station wise mean error (ME) of the MODIS Aqua retrieved AOD ranges from −0.107 to 0.079 with an all station ME of −0.004. Similarly, the station wise MAE of MODIS Aqua retrieved AOD ranges from 0.11 to 0.175 with an all station MAE of 0.144. The station wise root mean square error (RMSE) of MODIS Aqua AOD varies from 0.156 at Kanpur to 0.255 at Lahore and the all station RMSE is 0.210. Station wise Pearson correlation coefficient (r) of the MODIS Aqua retrieved daily AOD with AERONET measured daily AOD ranges from a minimum of 0.538 at New Delhi to a maximum of 0.898 at Lumbini. The Pearson Correlation coefficient of MODIS Aqua retrieved AOD with AERONET AOD across all stations in the IGP is 0.778. In summary, the MODIS Aqua retrieved daily AOD at the IGP stations is found to be similar to the AERONET measured AOD.

Table 5. Evaluation of Moderate Resolution Imaging Spectroradiometer (MODIS) Aqua derived AOD and atmospheric water vapour against AERONET measured AOD and atmospheric water vapour for the IGP stations.

SN	Row Labels	Number of Observations N	MODIS Aqua Retrieved AOD				MODIS Aqua Retrieved Atmospheric Water Vapour			
			ME	MAE	RMSE	r	ME (cm)	MAE (cm)	RMSE (cm)	r
1	Bhola	37	0.052	0.124	0.182	0.811	−0.264	0.493	0.617	0.838
2	Dhaka University	253	−0.072	0.156	0.218	0.785	0.445	0.559	0.674	0.865
3	Gandhi College	833	−0.060	0.159	0.223	0.732	0.210	0.500	0.669	0.899
4	Kolkata	1581	0.029	0.140	0.207	0.767	0.348	0.481	0.645	0.882
5	Kanpur	1028	−0.078	0.110	0.156	0.785	0.313	0.460	0.592	0.847
6	Karachi	27	−0.107	0.175	0.206	0.686	0.383	0.501	0.651	0.839
7	Lahore	1017	0.079	0.175	0.255	0.776	0.246	0.450	0.631	0.929
8	Lumbini	106	−0.083	0.133	0.183	0.898	−0.436	0.602	0.705	0.906
9	New Delhi	67	0.023	0.167	0.240	0.538	0.518	0.623	0.819	0.930
10	Pantnagar	189	0.046	0.124	0.164	0.749	0.152	0.394	0.556	0.871
	All Stations	5138	−0.004	0.144	0.210	0.778	0.278	0.479	0.638	0.887

Note: ME = Mean Error; MAE = Mean Absolute Error; RMSE = Root Mean Square Error; r = Pearson Correlation Coefficient.

Scatterplots of the station wise MODIS Aqua retrieved daily mean precipitable water vapour and AERONET measured daily mean atmospheric water vapour are presented in Figure S3. The figure indicates that the MODIS Aqua derived precipitable water vapour is very similar to that of AERONET, because most the points are close to the 1:1 line at all stations in the IGP. The station wise ME of MODIS Aqua derived precipitable water vapour ranges from −0.436 cm at Lumbini to 0.518 cm at New Delhi and across all of the stations ME in the IGP is 0.278 cm (Table 5). The station wise MAE ranges from 0.394 cm at Pantnagar to 0.623 cm at New Delhi and across all the stations the MAE is 0.479 cm. The RMSE of the MODIS Aqua derived precipitable water vapour across all of the stations in the IGP is limited to 0.638 cm. The correlation coefficient of the MODIS Aqua derived precipitable water vapour with AERONET measured atmospheric water vapour across all the stations in the IGP is 0.887, which indicates a good correlation.

At the seasonal scale (winter, pre-monsoon, monsoon, and post monsoon), MODIS Aqua derived AOD at all stations of the IGP is plotted against AERONET measured AOD in Figure S4. It is observed that there is more variation of MODIS Aqua AOD and AERONET AOD in the monsoon season when

compared to other seasons, which may be due to the effect of clouds on MODIS Aqua retrieved AOD because AERONET Version 2 AOD is quality assured and cloud screened data [94]. Season wise evaluation of the MODIS Aqua retrieved AOD and water vapour is presented in Table 6. The table indicates that the ME of MODIS Aqua retrieved AOD vary from −0.059 during the pre-monsoon to 0.093 in the monsoon season. The MAE and RMSE value of MODIS Aqua retrieved AOD is found to be least (0.118 and 0.180, respectively) during winter and maximum (0.249 and 0.336, respectively) during the monsoon season. With respect to seasonal performance of MODIS Aqua derived daily mean precipitable water vapour, the least value of ME, MAE, and RMSE is found during the post monsoon as 0.175, 0.397, and 0.519, respectively, and the maximum value is found during monsoon season as 0.642, 0.813, and 1.015, respectively. Comparatively higher ME, MAE, and RMSE of MODIS Aqua retrieved AOD and precipitable water vapour during the monsoon season is possibly due to the effect of clouds in this season. The correlation between AERONET and MODIS Aqua retrieved AOD and atmospheric water vapour ranges from 0.702 to 0.84 and 0.655 to 0.853, respectively, indicating good seasonal correlations.

Table 6. Evaluation of MODIS Aqua derived AOD and precipitable water vapour against AERONET measured AOD and atmospheric water vapour in four seasons in the IGP.

SN	Row Labels	Number of Observations N	MODIS Aqua Retrieved AOD				MODIS Aqua Retrieved Atmospheric Water Vapour			
			ME	MAE	RMSE	r	ME (cm)	MAE (cm)	RMSE (cm)	r
1	Winter	884	0.020	0.118	0.180	0.840	0.297	0.417	0.523	0.655
2	Pre monsoon	1854	−0.059	0.130	0.185	0.702	0.197	0.432	0.562	0.820
3	Monsoon	558	0.093	0.249	0.336	0.703	0.642	0.813	1.015	0.853
4	Post monsoon	1842	0.011	0.139	0.197	0.824	0.175	0.397	0.519	0.780
	All Stations	5138	−0.004	0.144	0.210	0.778	0.278	0.479	0.638	0.887

4.3.2. Comparison of MODIS Terra Products

The station wise comparison of MODIS Terra retrieved AOD_{550} against transformed AERONET AOD at 550 nm from measured AOD at 500 nm at the IGP stations is performed through scatterplots in Figure S5. The figure also consists of two lines indicating expected error (EE) range of MODIS Terra retrieved AOD as $\pm(0.05 + 0.2 \times \text{AOD})$, as explained by Chu [74]. It is observed that at Bhola, Dhaka University, Gandhi College, Kanpur, Lahore and New Delhi a significant portion of the points lie above the upper limit of expected error line. Similarly, at Karachi, Lumbini, and Pantnagar a significant portion of the points lie below the lower limit of expected error line. The figures indicate that in general the majority of MODIS Terra retrieved AOD are within the expected error limits. Figure S6 presents the share of the MODIS Terra AOD values that lie within, above and below the expected error range where AERONET AOD is assumed to be actual AOD. The figure indicates that in all of the stations, except Bhola, Pantnagar, and Lumbini, more than 60% of MODIS Terra AOD data lie within the expected error range for the IGP stations. The figure also shows that more than 65% of the MODIS Terra AOD data across IGP stations are within the expected error range.

The station wise statistical comparison of the MODIS Terra AOD and precipitable water vapour with the AERONET measured AOD and atmospheric water vapour is presented in Table 7. It is observed that the station wise ME of the MODIS Terra AOD ranges from −0.178 at Pantnagar to 0.115 at Bhola with an all station ME of 0.035. Similarly, the station wise MAE of MODIS Terra retrieved AOD ranges from 0.106 at Kanpur to 0.197 at Pantnagar with an all station MAE of 0.152. The station wise RMSE of MODIS Terra retrieved AOD vary from 0.162 at Kanpur to 0.262 at Dhaka University and the all station RMSE is 0.230. Station wise Pearson correlation coefficient of the MODIS Terra retrieved daily AOD with AERONET measured daily AOD vary from 0.572 at New Delhi to 0.907 at Lumbini. The Pearson Correlation coefficient of MODIS Terra retrieved AOD with AERONET AOD across all the stations in the IGP is 0.781. In summary, the MODIS Terra retrieved daily AOD at the IGP stations is also found to be similar to the AERONET measured AOD.

Scatterplots of the station wise MODIS Terra retrieved atmospheric water vapour and AERONET measured atmospheric water vapour are shown in Figure S7. Even though MODIS Terra somewhat overestimated the atmospheric water vapour at Karachi, Kanpur, and New Delhi and somewhat underestimated at Bhola, Lumbini, and Pantnagar; overall MODIS Terra derived daily atmospheric water vapour is very similar to that of AERONET measured atmospheric water vapour because most the points are close to the 1:1 line at all stations in the IGP (Figure S7). The station wise ME of MODIS Terra derived atmospheric water vapour vary from −0.651 cm at Lumbini to 0.543 cm at New Delhi and across all of the stations in the IGP the ME is 0.212 cm (Table 7). The station wise MAE ranges from 0.425 cm at Lahore to 0.690 cm at Lumbini and across all the stations the MAE is 0.483 cm. The RMSE of the MODIS Terra derived atmospheric water vapour across all the stations in the IGP is 0.646 cm. The correlation coefficient of the MODIS derived atmospheric water vapour with AERONET measured atmospheric water vapour across all of the stations in the IGP is 0.880, which indicates a good correlation.

Table 7. Evaluation of MODIS Terra derived AOD and atmospheric water vapour against AERONET measured AOD and atmospheric water vapour for the IGP stations.

SN	Row Labels	Number of Observations N	MODIS Terra Retrieved AOD				MODIS Terra Retrieved Atmospheric Water Vapour			
			ME	MAE	RMSE	r	ME (cm)	MAE (cm)	RMSE (cm)	r
1	Bhola	41	0.115	0.162	0.218	0.744	−0.317	0.527	0.658	0.876
2	Dhaka University	232	0.014	0.166	0.262	0.768	0.262	0.492	0.604	0.819
3	Gandhi College	823	0.000	0.143	0.220	0.729	0.186	0.513	0.709	0.893
4	Kolkata	1773	0.087	0.149	0.225	0.793	0.301	0.474	0.655	0.895
5	Kanpur	918	−0.062	0.106	0.162	0.748	0.381	0.484	0.616	0.845
6	Karachi	25	−0.037	0.163	0.225	0.613	0.369	0.528	0.638	0.849
7	Lahore	1005	0.112	0.195	0.289	0.768	0.118	0.425	0.582	0.918
8	Lumbini	104	−0.067	0.114	0.166	0.907	−0.651	0.690	0.781	0.884
9	New Delhi	69	0.082	0.189	0.256	0.572	0.543	0.611	0.776	0.947
10	Pantnagar	190	−0.178	0.197	0.235	0.690	−0.453	0.543	0.670	0.825
	All Stations	5180	0.035	0.152	0.230	0.781	0.212	0.483	0.646	0.880

For the season wise comparison, the scatterplots of MODIS Terra retrieved AOD with AERONET AOD in four seasons (winter, pre-monsoon, monsoon, and post monsoon) at all stations of the IGP are plotted in Figure S8. Like MODIS Aqua seasonal plot, in this figure, also, there is more variation in the monsoon season when compared to other seasons, which may be also due to the effects of clouds in MODIS Terra retrieved AOD. However, the majority of points are near to the 1:1 line, indicating that the MODIS Terra retrieved AOD is similar to AERONET measured AOD.

The statistical results of season wise evaluation of MODIS Terra retrieved AOD and precipitable water vapour with the AERONET AOD and atmospheric water vapour is presented in Table 8. The ME of the MODIS Terra retrieved AOD vary from −0.016 cm during the pre-monsoon to 1.508 cm during the monsoon season. Comparatively small MAE and RMSE on seasonal MODIS Terra derived AOD is obtained during the pre-monsoon season with values 0.126 cm and 0.181 cm, respectively, and larger MAE and RMSE during the monsoon season with values 1.100 and 0.673, respectively. The seasonal Pearson correlation coefficient of MODIS Terra derived AOD and AERONET AOD vary from 0.713 in the monsoon season to 0.834 in the post monsoon season, which indicates good seasonal correlations. The ME of the MODIS Terra retrieved atmospheric water vapour ranges from 0.079 cm during post monsoon season to 0.573 cm during monsoon season. Similarly, comparatively higher MAE and RMSE on MODIS Terra derived atmospheric water vapour is obtained during the monsoon season with values 0.799 cm and 1.015 cm, respectively. The seasonal Pearson correlation coefficient of MODIS Terra derived precipitable water vapour and the AERONET water vapour ranges from 0.598 during winter to 0.820 during monsoon season. It is observed that comparatively more error on the MODIS Terra products is observed during monsoon season than other seasons, which may be due to the effect

of clouds. After comparing the seasonal and station wise errors and correlation coefficients, it is found that the MODIS Terra retrieved products in general are found to be close to the AERONET products.

Table 8. Evaluation of MODIS Terra derived AOD and atmospheric water vapour against AERONET measured AOD and atmospheric water vapour in four seasons in the IGP.

SN	Row Labels	Number of Observations N	MODIS Terra Retrieved AOD				MODIS Terra Retrieved Atmospheric Water Vapour			
			ME	MAE	RMSE	r	ME (cm)	MAE (cm)	RMSE (cm)	r
1	Winter	886	0.065	0.142	0.226	0.821	0.175	0.388	0.492	0.598
2	Pre monsoon	1848	−0.016	0.126	0.181	0.725	0.182	0.445	0.579	0.813
3	Monsoon	833	1.508	1.100	0.673	0.713	0.573	0.799	1.015	0.820
4	Post monsoon	1613	0.035	0.149	0.222	0.834	0.079	0.415	0.541	0.750
	All Stations	5180	0.035	0.152	0.230	0.781	0.212	0.483	0.646	0.880

4.4. Evaluation of Model with MODIS Products

The developed year-round ADRF model is evaluated by using the MODIS Aqua and MODIS Terra retrieved AOD and atmospheric water vapour in the following sections.

4.4.1. Evaluation of the Model with MODIS Aqua Products

By using the MODIS Aqua derived AOD and daily mean atmospheric water vapour in the developed year-round ADRF model, the daily ADRF is estimated and it is plotted against AERONET ADRF in Figure 3. Since the majority of the points are clustered near to the 1:1 line in almost all stations, the estimated ADRF are similar to the AERONET ADRF. However, in the stations like Kolkata, New Delhi and Bhola the estimated ADRF showed more deviation from the AERONET observation when compared to other stations, which may be due to less number of data points compared to other stations. The test results of the year-round model estimated ADRF by using the MODIS Aqua AOD and atmospheric water vapour is presented in Table 9. It is observed that the average error ranged from −15.070 Wm^{-2} at Bhola to 37.429 Wm^{-2} at Kolkata and the average error of the model with all the stations in IGP is only 1.739 Wm^{-2}. The MAE varies from 15.083 Wm^{-2} at Karachi to 40.715 Wm^{-2} at Kolkata and the MAE of all stations of IGP is limited to 21.822 Wm^{-2}. Similarly, the station wise RMSE value fluctuated from 20.810 Wm^{-2} at Karachi to 45.397 Wm^{-2} at Kolkata and the RMSE value across all of stations in the IGP of the model with MODIS Aqua AOD and atmospheric water vapour is 30.700 Wm^{-2}. Except New Delhi, Pantnagar, and Lahore, the station wise Pearson correlation coefficient of the year-round model estimated ADRF from MODIS Aqua AOD and precipitable water vapour is found to be above 0.6 in all stations of IGP and the correlation coefficient of the model across all the stations in the IGP is found to be 0.66. These data indicate that the year round ADRF model at the surface using inputs of MODIS Aqua AOD and precipitable water vapour provided fairly reliable estimates of daily ADRF in the IGP region.

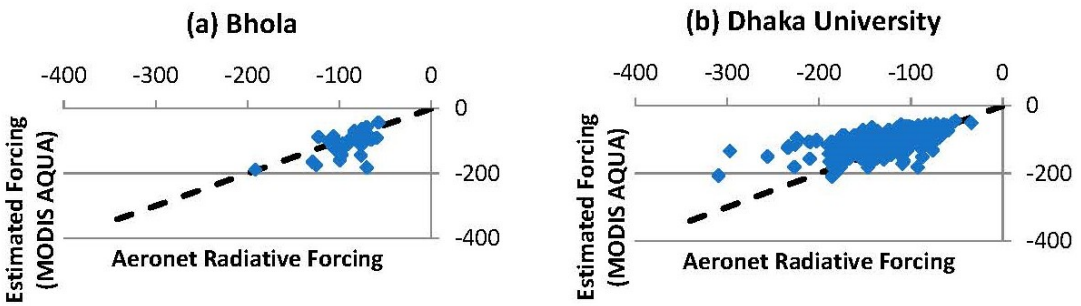

Figure 3. *Cont.*

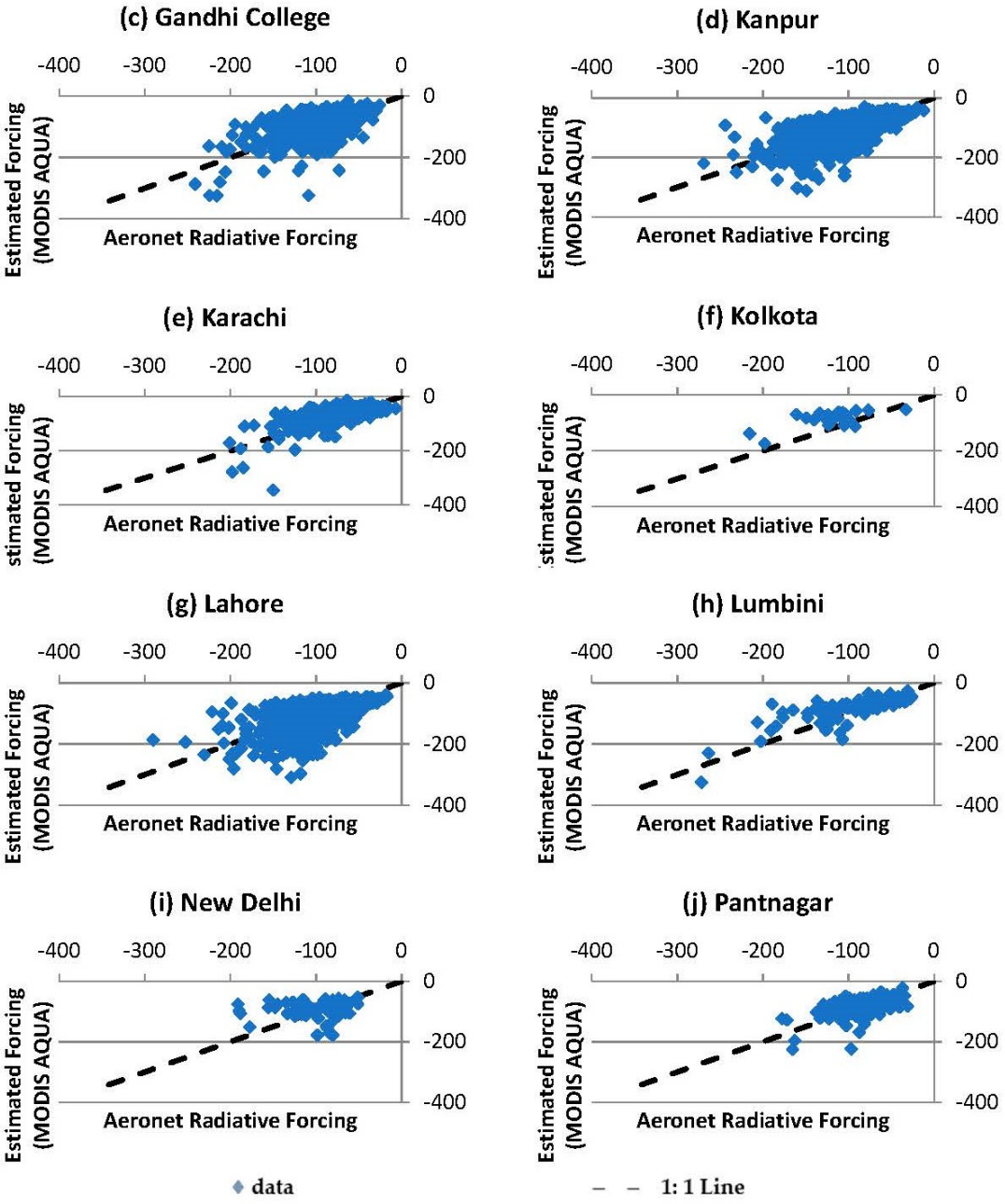

Figure 3. Comparison of estimated radiative forcing by using MODIS Aqua derived AOD and atmospheric water vapour with AERONET radiative forcing in the stations of IGP. (**a**) Bhola (**b**) Dhaka University (**c**) Gandhi College (**d**) Kanpur (**e**) Karachi (**f**) Kolkata (**g**) Lahore (**h**) Lumbini (**i**) New Delhi (**j**) Pantnagar.

Table 9. Evaluation of the model with AOD and Atmospheric water vapour retrieved from MODIS Aqua in the IGP.

SN	Row Labels	Number of Observations	Mean Error (Wm^{-2})	Mean Absolute Error (Wm^{-2})	RMSE (Wm^{-2})	Correlation Coefficient, r
1	Bhola	37	−15.070	22.611	31.371	0.610
2	Dhaka University	253	20.767	29.357	40.322	0.619
3	Gandhi College	833	8.478	23.676	32.359	0.603
4	Kanpur	1581	−2.349	20.921	29.095	0.672
5	Karachi	1028	5.466	15.083	20.810	0.661

Table 9. *Cont.*

SN	Row Labels	Number of Observations	Mean Error (Wm^{-2})	Mean Absolute Error (Wm^{-2})	RMSE (Wm^{-2})	Correlation Coefficient, r
6	Kolkata	27	37.429	40.715	45.397	0.664
7	Lahore	1017	−6.989	25.954	36.337	0.586
8	Lumbini	106	11.589	24.624	31.964	0.779
9	New Delhi	67	7.410	29.878	41.419	0.138
10	Pantnagar	189	−1.876	18.234	24.768	0.587
	All Stations	5138	1.739	21.822	30.700	0.660

4.4.2. Evaluation of the Model with MODIS Terra Products

The estimated ADRF by using inputs of MODIS Terra AOD and daily mean precipitable water vapour in the year-round model is compared with AERONET ADRF in the IGP stations through scatterplots in Figure 4. Except Bhola, Kolkata, and New Delhi, the station wise scatterplots in the stations of IGP tend to follow the 1:1 line, indicating an agreement of the estimation with the AERONET ADRF. More deviation of estimated ADRF in Kolkata, New Delhi, and Bhola may be due to the low number of data points at those stations. The test results for the evaluation of the estimated ADRF from the year-round model whileusing MODIS TERRA AOD and atmospheric water vapour inputs is given in Table 10. The table indicates that the station wise average error varies from -21.532 Wm^{-2} at Bhola to 28.748 Wm^{-2} at Kolkata and the average error using all the stations in the IGP is -2.818 Wm^{-2}. The MAE and RMSE of the model for all stations in the IGP while using MODIS Terra AOD and precipitable water vapour is 22.668 Wm^{-2} and 33.08 Wm^{-2} respectively. The Pearson correlation coefficient of the estimated value of the model for all stations of the IGP with MODIS Terra AOD and precipitable water vapour is 0.654, indicating good correlation between estimated ADRF and AERONET ADRF in the IGP region.

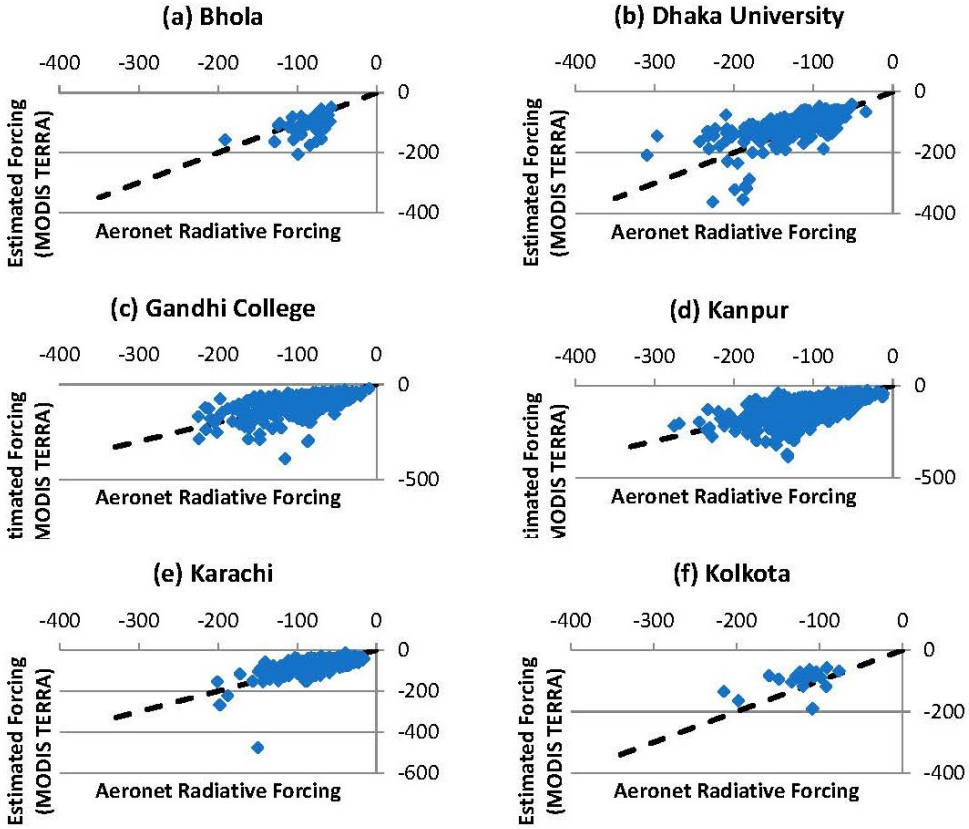

Figure 4. *Cont.*

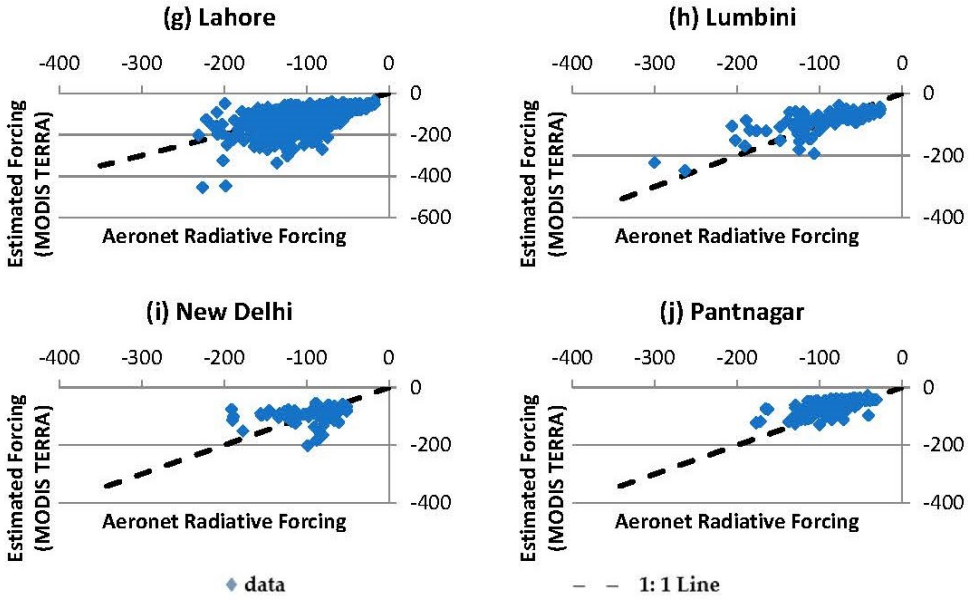

Figure 4. Comparison of estimated radiative forcing by using MODIS Terra derived AOD and atmospheric water vapour with AERONET radiative forcing in the stations of IGP. (**a**) Bhola (**b**) Dhaka University (**c**) Gandgi Colleague (**d**) Kanpur (**e**) Karachi (**f**) Kolkata (**g**) Lahore (**h**) Lumbini (**i**) New Delgi (**j**) Pantnagar.

Table 10. Evaluation of the model with AOD and precipitable water vapour retrieved from MODIS Terra in the IGP.

SN	Row Labels	Number of Observations	Mean Error (Wm^{-2})	Mean Absolute Error (Wm^{-2})	RMSE (Wm^{-2})	Correlation Coefficient, r
1	Bhola	41	−21.532	28.316	37.577	0.452
2	Dhaka University	232	10.634	30.945	42.617	0.610
3	Gandhi College	823	1.574	22.494	33.057	0.576
4	Kanpur	1773	−8.722	21.861	31.624	0.675
5	Karachi	918	4.114	14.923	22.069	0.625
6	Kolkata	25	28.748	37.405	42.506	0.462
7	Lahore	1005	−11.536	27.854	40.269	0.573
8	Lumbini	104	9.137	23.826	32.175	0.762
9	New Delhi	69	−0.385	29.929	41.748	0.144
10	Pantnagar	190	21.894	24.394	29.638	0.649
	All Stations	5180	−2.818	22.668	33.080	0.654

4.5. Comparison of the Model Estimation from MODIS Aqua and Terra Products

While comparing the evaluation results of ADRF estimated from MODIS Aqua and MODIS Terra in Tables 9 and 10, respectively, it is observed that the ADRF estimated from both the products provided almost similar results. It is found that the results from the MODIS Aqua is slightly superior than MODIS Terra, because of low average error (1.739 Wm^{-2} against −2.818 Wm^{-2}), MAE (21.822 Wm^{-2} against 22.668 Wm^{-2}), and RMSE (30.700 Wm^{-2} against 33.080 Wm^{-2}) in all the stations of the IGP. Moreover, the Pearson correlation coefficient of the ADRF estimated from MODIS Aqua AOD and atmospheric water vapour in all stations of the IGP is marginally higher than that from MODIS Terra (0.660 against 0.654). In summary, the results of the ADRF model with MODIS Aqua products is almost similar to that from MODIS Terra products in the IGP, but MODIS Aqua products provided a slightly better estimate of ADRF when compared to that of MODIS Terra products in the IGP.

4.6. Comparison of Model Estimated ADRF with Published SBDART Results

The SBDART model is considered to be a comprehensive reliable model to estimate radiative forcing due to the atmospheric aerosols. In Table 11, the performance of the ADRF model is compared against published SBDART model results at Lahore and Karachi from Alam et al. [95,96]. The ADRF model estimated monthly ADRF at the surface for Karachi during July 2006 and November 2010 and Lahore during November 2010 to be consistent with the published SBDART results. It is shown that the ME of year-round model is less in both the periods July 2006 and November 2010 than that of SBDART model. Since MAE and RMSE from the SBDART model are less than from the year-round model at both stations, SBDART is found to be a better model than the year round ADRF model to estimate ADRF at Lahore and Karachi. Similarly, the SBDART model performed better than the year round ADRF model with respect to Pearson correlation coefficient at both stations. In spite of the comparatively better performance of SBDART than the year round ADRF model at Lahore and Karachi, the results of the year round ADRF model are comparable to the complex SBDART model. Moreover, with respect to the input requirement (only two input parameters for the year round ADRF model against more than 60 input parameters for SBDART [48] and simplicity the ADRF model is an attractive alternative to SBDART and other complex models to estimate radiative forcing at the surface across the IGP region.

Regarding the limitations of this model, the performance of the model is mainly dependent upon the accuracy of those two input parameters that are derived from satellite data. Moreover, other limitation is that the accuracy of this model is only moderate. Moreover, the output of the model is limited to only daily radiative forcing. In spite of these limitations, because of simplicity and moderate accuracy, this could be used to study the effect of atmospheric aerosols on the natural systems in the IGP.

Table 11. Comparative statistical evaluation of ADRF model and Santa Barbara DISTORT Atmospheric Radiative Transfer (SBDART) model estimated monthly ADRF at Karachi and Lahore in the IGP.

Station	Duration	Mean Error (Wm^{-2})		Mean Absolute Error (Wm^{-2})		Root Mean Square Error (Wm^{-2})		Pearson Correlation Coefficient	
		SBDART	ADRF MODEL	SBDART	ADRF MODEL	SBDART	ADRF MODEL	SBDART	ADRF MODEL
Karachi	August 2006 to July 2007	4.64	0.21	5.18	11.28	8.11	13.46	0.91	0.74
Karachi	April 2010 to February 2011	2.68	1.49	3.92	3.89	4.97	6.64	0.91	0.79
Karachi	Combined	2.05	0.39	4.74	8.67	7.16	11.52	0.92	0.82
Lahore	April 2010 to Feb 2011	−6.77	−3.35	6.77	14.37	8.86	15.67	0.98	0.71

5. Summary and Conclusions

The IGP region is considered to have an extremely high loading of atmospheric aerosols in the south Asian region [97]. The high loading of atmospheric aerosols has not only negatively affected the public health and day to day life of people, but also the natural systems in the IGP. The ADRF is a measure to estimate the effect of atmospheric aerosols on the regional and global natural systems. Various studies indicate that there is a significant effect of atmospheric aerosols on solar radiation in the IGP. To estimate the ADRF at the BOA and TOA, radiative transfer models are used, and, among them, SBDART is found to be comprehensive and widely used. However, the complexity of SBDART, which requires more than 60 input parameters [48] and high processing time, are limitations to wider use. To address these limitations, here we developed a simple year-round model to estimate the daily radiative forcing due to atmospheric aerosols (ADRF) at the surface of the IGP through multiple regressions of AERONET AOD, atmospheric water vapour, and the radiative forcing at the surface using data from 2002 to 2015 at 10 stations in the IGP. The goodness of fit of the developed ADRF model is indicated by the adjusted R^2 value of 0.834. The Jackknife method of delete one group (station data) was employed to study the stability of the model and the model was found to be robust because adjusted R^2 fluctuated between 0.813 and 0.842 and the standard error varied from 13.791 to 15.098. Station wise and season wise evaluations of the model were performed and found that the model performed well in all seasons and stations.

In order to use the year-round ADRF model beyond the AERONET stations, AOD and atmospheric water vapour products from MODIS Aqua and Terra (daily mean AOD at 550 nm and daily mean precipitable water vapour) were compared against AERONET AOD and atmospheric water vapour. Since the RMSE of MODIS Aqua derived daily mean AOD and precipitable water vapour in IGP stations is 0.210 and 0.638 cm with correlation coefficients 0.778 and 0.887, MODIS Aqua product is found to be similar to the AERONET product. Similarly, MODIS Terra product is also found to be similar to the AERONET products because RMSE of MODIS Terra retrieved daily mean AOD and precipitable water vapour is 0.230 and 0.646 cm, respectively, with Pearson correlation coefficients of 0.781 and 0.880, respectively.

By using the MODIS Aqua and MODIS Terra products, the year round ADRF is evaluated in the IGP stations and found that the model performed well with both MODIS products with RMSE 30.700 Wm^{-2} and 33.080 Wm^{-2} respectively with Pearson correlation coefficient 0.660 and 0.654 respectively. The ADRF model performed slightly better with MODIS Aqua products than MODIS Terra products. The ADRF model was also compared against the published SBDART results at Karachi and Lahore. The results indicate the ADRF model is comparable with the complex SBDART results. Even though SBDART is found to be better than the year round ADRF model, with respect to RMSE (7.16 Wm^{-2} against 11.52 Wm^{-2} at Karachi and 8.86 Wm^{-2} against 15.67 Wm^{-2} at Lahore) and correlation coefficients (0.92 against 0.82 at Karachi and 0.98 against 0.71 at Lahore), the developed year round model is much simpler and it requires less input parameters (two compared to more than 60 in SBDART) to estimate radiative forcing at the surface in the IGP.

Supplementary Materials: The following are available online at http://www.mdpi.com/2073-4433/9/10/405/s1, Figure S1: Comparison of MODIS Aqua Derived AOD with AERONET AOD at the IGP stations, Figure S2: Station wise comparison of MODIS Aqua AOD with AERONET AOD in terms of expected error (EE) for the IGP stations, Figure S3: Comparison of MODIS Aqua and AERONET derived Atmospheric Water vapour (in cm) at the IGP Stations, Figure S4: Comparison of MODIS Aqua derived AOD with AERONET AOD in four seasons in the IGP, Figure S5: Comparison of MODIS Terra derived AOD with AERONET AOD at the IGP stations, Figure S6: Station wise comparison of MODIS Terra AOD with AERONET AOD in terms of expected error (EE) in the IGP stations, Figure S7: Comparison of MODIS Terra derived atmospheric water vapour with AERONET atmospheric water vapour at the IGP stations, Figure S8: Comparison of MODIS Terra derived AOD with AERONET AOD in four seasons in the IGP.

Author Contributions: Conceptualization, S.S.; Formal analysis, S.S.; Supervision, M.C.P. and G.A.M.; Writing–Original draft, S.S.; Writing–Review & editing, M.C.P. and G.A.M.

Funding: This research received no external funding.

Acknowledgments: The lead author (S.S.) is thankful to Australian Centre for International Agricultural Research (ACIAR) for providing John Alright Fellowship (JAF) to pursue his PhD in the University of Melbourne. We thank the principal investigators and their staff for establishing and maintaining the AERONET sites used in this study. Also, thanks are owed to Brent N. Holben and AERONET team for their effort in making the data available. We also acknowledge the MODIS mission scientists and associated NASA personnel for the production of the data used in this research effort. We also would like to express our gratitude to three anonymous reviewers for their valuable suggestions in improving the manuscript.

Conflicts of Interest: The authors declare no conflicts of interest.

References

1. Srivastava, A.K.; Dey, S.; Tripathi, S.N. Aerosol Characteristics over the Indo-Gangetic Basin: Implications to Regional Climate. In *Atmospheric Aerosols—Regional Characteristics—Chemistry and Physics*; Abdul-Razzak, H., Ed.; InTech: London, UK, 2012; pp. 47–79.
2. Kumar, M.; Parmar, K.S.; Kumar, D.B.; Mhawish, A.; Broday, D.M.; Mall, R.K.; Banerjee, T. Long-Term Aerosol Climatology over Indo-Gangetic Plain: Trend, Prediction and Potential Source Fields. *Atmos. Environ.* **2018**, *180*, 37–50. [CrossRef]
3. Ghude, S.D.; Chate, D.M.; Jena, C.; Beig, G.; Kumar, R.; Barth, M.C.; Pfister, G.G.; Fadnavis, S.; Pithani, P. Premature Mortality in India Due to PM2.5 and Ozone Exposure. *Geophys. Res. Lett.* **2016**, *43*, 4650–4658. [CrossRef]
4. Krishna Moorthy, K.; Suresh Babu, S.; Manoj, M.R.; Satheesh, S.K. Buildup of Aerosols over the Indian Region. *Geophys. Res. Lett.* **2013**, *40*, 1011–1014. [CrossRef]
5. Streets, D.G.; Bond, T.C.; Carmichael, G.R.; Fernandes, S.D.; Fu, Q.; He, D.; Klimont, Z.; Nelson, S.M.; Tsai, N.Y.; Wang, M.Q.; et al. An Inventory of Gaseous and Primary Aerosol Emissions in Asia in the Year 2000. *J. Geophys. Res. Atmos.* **2003**, *108*. [CrossRef]
6. Venkataraman, C.; Habib, G.; Eiguren-Fernandez, A.; Miguel, A.H.; Friedlander, S.K. Residential Biofuels in South Asia: Carbonaceous Aerosol Emissions and Climate Impacts. *Science* **2005**, *307*, 1454–1456. [CrossRef] [PubMed]
7. Mishra, A.K.; Shibata, T.; Srivastava, A. Synergistic Approach for the Aerosol Monitoring and Identification of Types over Indo-Gangetic Basin in Pre-Monsoon Season. *Aerosol Air Qual. Res.* **2014**, *14*, 767–782. [CrossRef]
8. Kaskaoutis, D.G.; Kumar, S.; Sharma, D.; Singh, R.P.; Kharol, S.K.; Sharma, M.; Singh, A.K.; Singh, S.; Singh, A.; Singh, D. Effects of Crop Residue Burning on Aerosol Properties, Plume Characteristics, and Long-Range Transport over Northern India. *J. Geophys. Res. Atmos.* **2014**, *119*, 5424–5444. [CrossRef]
9. Singh, R.P.; Kaskaoutis, D.G. Crop Residue Burning: A Threat to South Asian Air Quality. *EOS* **2014**, *95*, 333–334. [CrossRef]
10. Rajput, P.; Sarin, M.; Sharma, D.; Singh, D. Characteristics and Emission Budget of Carbonaceous Species from Post-Harvest Agricultural-Waste Burning in Source Region of the Indo-Gangetic Plain. *Tellus Ser. B Chem. Phys. Meteorol.* **2014**, *66*, 1–12. [CrossRef]
11. Rastogi, N.; Singh, A.; Sarin, M.M.; Singh, D. Temporal Variability of Primary and Secondary Aerosols over Northern India: Impact of Biomass Burning Emissions. *Atmos. Environ.* **2016**, *125*, 396–403. [CrossRef]
12. WHO. Ambient Air Quality Database, WHO. April 2018. Available online: http://www.who.int/airpollution/en/ (accessed on 3 May 2018).
13. Kumar, R.; Barth, M.C.; Pfister, G.G.; Delle Monache, L.; Lamarque, J.F.; Archer-Nicholls, S.; Tilmes, S.; Ghude, S.D.; Wiedinmyer, C.; Naja, M.; et al. How Will Air Quality Change in South Asia by 2050? *J. Geophys. Res. Atmos.* **2018**, *123*, 1840–1864. [CrossRef]
14. Wild, M. Global Dimming and Brightening: A Review. *J. Geophys. Res.* **2009**, *114*, 1–31. [CrossRef]
15. Kambezidis, H.D.; Kaskaoutis, D.G.; Kharol, S.K.; Moorthy, K.K.; Satheesh, S.K.; Kalapureddy, M.C.R.; Badarinath, K.V.S.; Sharma, A.R.; Wild, M. Multi-Decadal Variation of the Net Downward Shortwave Radiation over South Asia: The Solar Dimming Effect. *Atmos. Environ.* **2012**, *50*, 360–372. [CrossRef]
16. Singh, J.; Bhattacharya, B.K.; Kumar, M. Solar Radiation and Evaporation Trend over India. *J. Earth Sci. Eng.* **2012**, *2*, 160–165.
17. Dey, S.; Tripathi, S.N. Estimation of Aerosol Optical Properties and Radiative Effects in the Ganga Basin, Northern India, during the Wintertime. *J. Geophys. Res.* **2007**, *112*, D03203. [CrossRef]

18. Ramanathan, V.; Crutzen, P.J.; Lelieveld, J.; Mitra, A.P.; Althausen, D.; Anderson, J.; Andreae, M.O.; Cantrell, W.; Cass, G.R.; Chung, C.E.; et al. Indian Ocean Experiment: An Integrated Analysis of the Climate Forcing and Effects of the Great Indo-Asian Haze. *J. Geophys. Res.* **2001**, *106*, 28371. [CrossRef]
19. Ramanathan, V.; Ramana, M.V. Persistent, Widespread, and Strongly Absorbing Haze over the Himalayan Foothills and the Indo-Gangetic Plains. *Pure Appl. Geophys.* **2005**, *162*, 1609–1626. [CrossRef]
20. Ramanathan, V. Atmospheric Brown Clouds: Health, Climate and Agriculture Impacts. Scripta Varia. 2006. Available online: http://www.academyofsciences.va/content/dam/accademia/pdf/sv106/sv106-ramanathan.pdf (accessed on 29 September 2018).
21. Ramanathan, V.; Ramana, M.V.; Roberts, G.; Kim, D.; Corrigan, C.; Chung, C.; Winker, D. Warming Trends in Asia Amplified by Brown Cloud Solar Absorption. *Nature* **2007**, *448*, 575–578. [CrossRef] [PubMed]
22. Bonasoni, P.; Laj, P.; Marinoni, A.; Sprenger, M.; Angelini, F.; Arduini, J. Atmospheric Brown Clouds in the Himalayas: First Two Years of Continuous Observations at the Nepal-Climate Observatory at Pyramid (5079 M). *Atmos. Chem. Phys.* **2010**, *10*, 7515–7531. [CrossRef]
23. Devara, P.C.S.; Manoj, M.G. Aerosol–cloud–precipitation Interactions: A Challenging Problem in Regional Environment and Climate Research. *Particuology* **2013**, *11*, 25–33. [CrossRef]
24. Gautam, R.; Hsu, N.C.; Kafatos, M.; Tsay, S.C. Influences of Winter Haze on Fog/Low Cloud over the Indo-Gangetic Plains. *J. Geophys. Res. Atmos.* **2007**, *112*, 1–11. [CrossRef]
25. Syed, F.S.; Körnich, H.; Tjernström, M. On the Fog Variability over South Asia. *Clim. Dyn.* **2012**, *39*, 2993–3005. [CrossRef]
26. Shrestha, S.; Moore, G.A.; Peel, M.C. Trends in Winter Fog Events in the Terai Region of Nepal. *Agric. For. Meteorol.* **2018**, *259*, 118–130. [CrossRef]
27. Jenamani, R.K. Alarming Rise in Fog and Pollution Causing a Fall in Maximum Temperature over Delhi. *Curr. Sci.* **2007**, *93*, 313–322.
28. Samra, J.S.; Singh, G.; Ramakrishna, Y. *Cold Wave of 2002–03: Impact on Agriculture*; Central Research Institute for Dryland Agriculture: Hyderabad, India, 2003.
29. Singh, S.; Singh, D. Recent Fog Trends and Its Impact on Wheat Productivity in NW Plains in India. In Proceedings of the 5th International Conference on Fog, Fog Collection and Dew, Münster, Germany, 25–30 July 2010.
30. Auffhammer, M.; Ramanathan, V.; Vincent, J.R. Integrated Model Shows That Atmospheric Brown Clouds and Greenhouse Gases Have Reduced Rice Harvests in India. *Proc. Natl. Acad. Sci. USA* **2006**, *103*, 19668–19672. [CrossRef] [PubMed]
31. Latha, R.; Murthy, B.S.; Lipi, K.; Srivastava, M.K.; Kumar, M. Absorbing Aerosols, Possible Implication to Crop Yield—A Comparison between IGB Stations. *Aerosol. Air Qual. Res.* **2017**, *17*, 693–705. [CrossRef]
32. Ahmed, M.; Hassan, F. Cumulative Effect of Temperature and Solar Radiation on Wheat Yield. *Not. Bot. Horti Agrobot. Cluj-Napoca* **2011**, *39*, 146–152. [CrossRef]
33. Chameides, W.L.; Yu, H.; Liu, S.C.; Bergin, M.; Zhou, X.; Mearns, L.; Wang, G.; Kiang, C.S.; Saylor, R.D.; Luo, C.; et al. Case Study of the Effects of Atmospheric Aerosols and Regional Haze on Agriculture: An Opportunity to Enhance Crop Yields in China through Emission Controls? *Proc. Natl. Acad. Sci. USA* **1999**, *96*, 13626–13633. [CrossRef] [PubMed]
34. Chung, C.E. Aerosol Direct Radiative Forcing: A Review. In *Atmospheric Aerosols—Regional Characteristics—Chemistry and Physics*; Abdul-Razzak, H., Ed.; InTech: London, UK, 2012; pp. 379–394.
35. Dey, S.; Tripathi, S.N. Aerosol Direct Radiative Effects over Kanpur in the Indo-Gangetic Basin, Northern India: Long-Term (2001–2005) Observations and Implications to Regional Climate. *J. Geophys. Res. Atmos.* **2008**, *113*, 1–20. [CrossRef]
36. Ramachandran, S.; Kedia, S. Radiative Effects of Aerosols over Indo-Gangetic Plain: Environmental (Urban vs. Rural) and Seasonal Variations. *Environ. Sci. Pollut. Res.* **2012**, *19*, 2159–2171. [CrossRef] [PubMed]
37. Das, S.K.; Chatterjee, A.; Ghosh, S.K.; Raha, S. An Integrated Campaign for Investigation of Winter-Time Continental Haze over Indo-Gangetic Basin and Its Radiative Effects. *Sci. Total Environ.* **2015**, *533*, 370–382. [CrossRef] [PubMed]
38. Kaskaoutis, D.G.; Sinha, P.R.; Vinoj, V.; Kosmopoulos, P.G.; Tripathi, S.N.; Misra, A.; Sharma, M.; Singh, R.P. Aerosol Properties and Radiative Forcing over Kanpur during Severe Aerosol Loading Conditions. *Atmos. Environ.* **2013**, *79*, 7–19. [CrossRef]

39. Srivastava, R.; Ramachandran, S. The Mixing State of Aerosols over the Indo-Gangetic Plain and Its Impact on Radiative Forcing. *Q. J. R. Meteorol. Soc.* **2013**, *139*, 137–151. [CrossRef]
40. Praveen, P.S.; Ahmed, T.; Kar, A.; Rehman, I.H.; Ramanathan, V. Link between Local Scale BC Emissions in the Indo-Gangetic Plains and Large Scale Atmospheric Solar Absorption. *Atmos. Chem. Phys.* **2012**, *12*, 1173–1187. [CrossRef]
41. Patel, P.N.; Kumar, R. Estimation of Aerosol Characteristics and Radiative Forcing during Dust Events over Dehradun. *Aerosol. Air Qual. Res.* **2015**, *15*, 2082–2093. [CrossRef]
42. Sadavarte, P.; Venkataraman, C.; Cherian, R.; Patil, N.; Madhavan, B.L.; Gupta, T.; Kulkarni, S.; Carmichael, G.R.; Adhikary, B. Seasonal Differences in Aerosol Abundance and Radiative Forcing in Months of Contrasting Emissions and Rainfall over Northern South Asia. *Atmos. Environ.* **2015**, *125*, 512–523. [CrossRef]
43. Sathiyamoorthy, V.; Arya, R.; Kishtawal, C.M. Radiative Characteristics of Fog over the Indo-Gangetic Plains during Northern Winter. *Clim. Dyn.* **2016**, *47*, 1793–1806. [CrossRef]
44. Bibi, H.; Alam, K.; Bibi, S. Estimation of Shortwave Direct Aerosol Radiative Forcing at Four Locations on the Indo-Gangetic Plains: Model Results and Ground Measurement. *Atmos. Environ.* **2017**, *163*, 166–181. [CrossRef]
45. Ricchiazzi, P.; Yang, S.; Gautier, C.; Sowle, D. SBDART: A Research and Teaching Software Tool for Plane-Parallel Radiative Transfer in the Earth's Atmosphere. *Bull. Am. Meteorol. Soc.* **1998**, *79*, 2101–2114. [CrossRef]
46. Singh, S.; Soni, K.; Bano, T.; Tanwar, R.S.; Nath, S.; Arya, B.C. Clear-Sky Direct Aerosol Radiative Forcing Variations over Mega-City Delhi. *Ann. Geophys.* **2010**, *28*, 1157–1166. [CrossRef]
47. Tiwari, S.; Dumka, U.C.; Kaskaoutis, D.G.; Ram, K.; Panicker, A.S.; Srivastava, M.K.; Tiwari, S.; Attri, S.D.; Soni, V.K.; Pandey, A.K. Aerosol Chemical Characterization and Role of Carbonaceous Aerosol on Radiative Effect over Varanasi in Central Indo-Gangetic Plain. *Atmos. Environ.* **2016**, *125*, 437–449. [CrossRef]
48. Fu, Y.; Zhu, J.; Yang, Y.; Yuan, R.; Liu, G.; Xian, T.; Liu, P. Grid-Cell Aerosol Direct Shortwave Radiative Forcing Calculated Using the SBDART Model with MODIS and AERONET Observations: An Application in Winter and Summer in Eastern China. *Adv. Atmos. Sci.* **2017**, *34*, 952–964. [CrossRef]
49. Gautier, C.; Landsfeld, M. Surface Solar Radiation Flux and Cloud Radiative Forcing for the Atmospheric Radiation Measurement (ARM) Southern Great Plains (SGP): A Satellite, Surface Observations, and Radiative Transfer Model Study. *J. Atmos. Sci.* **1997**, *54*, 1289–1307. [CrossRef]
50. Huntingford, C.; Cox, P.M.; Mercado, L.M.; Sitch, S.; Bellouin, N.; Boucher, O.; Gedney, N. Highly Contrasting Effects of Different Climate Forcing Agents on Terrestrial Ecosystem Services. *Philos. Trans. R. Soc. A Math. Phys. Eng. Sci.* **2011**, *369*, 2026–2037. [CrossRef] [PubMed]
51. Holben, B.N.; Eck, T.F.; Slutsker, I.; Tanré, D.; Buis, J.P.; Setzer, A.; Vermote, E.; Reagan, J.A.; Kaufman, Y.J.; Nakajima, T.; et al. AERONET—A Federated Instrument Network and Data Archive for Aerosol Characterization. *Remote Sens. Environ.* **1998**, *66*, 1–16. [CrossRef]
52. García, O.E.; Díez, A.M.; Expósito, F.J.; Díaz, J.P.; Dubovik, O.; Dubuisson, P.; Roger, J.C.; Eck, T.F.; Sinyuk, A.; Derimian, Y.; et al. Validation of AERONET Estimates of Atmospheric Solar Fluxes and Aerosol Radiative Forcing by Ground-Based Broadband Measurements. *J. Geophys. Res. Atmos.* **2008**, *113*, 1–16. [CrossRef]
53. Kaskaoutis, D.G.; Houssos, E.E.; Houssos, E.E.; Bartzokas, Á.A.; Goto, D.; Nastos, P.T.; Sinha, P.R.; Kharol, S.K.; Kosmopoulos, P.G.; Singh, R.P.; et al. Synoptic Weather Conditions and Aerosol Episodes over Indo-Gangetic Plains, India. *Clim. Dyn.* **2014**, *43*, 2313–2331. [CrossRef]
54. Srivastava, A.K.; Tripathi, S.N.; Dey, S.; Kanawade, V.P.; Tiwari, S. Inferring Aerosol Types over the Indo-Gangetic Basin from Ground Based Sunphotometer Measurements. *Atmos. Res.* **2012**, *109–110*, 64–75. [CrossRef]
55. Zhuang, B.L.; Li, S.; Wang, T.J.; Deng, J.J.; Xie, M.; Yin, C.Q.; Zhu, J.L. Direct Radiative Forcing and Climate Effects of Anthropogenic Aerosols with Different Mixing States over China. *Atmos. Environ.* **2013**, *79*, 349–361. [CrossRef]
56. Remer, L.A.; Kaufman, Y.J.; Tanré, D.; Mattoo, S.; Chu, D.A.; Martins, J.V.; Li, R.-R.; Ichoku, C.; Levy, R.C.; Kleidman, R.G.; et al. The MODIS Aerosol Algorithm, Products, and Validation. *J. Atmos. Sci.* **2005**, *62*, 947–973. [CrossRef]

57. Shrestha, A.; Agrawal, N.; Alfthan, B.; Bajracharya, S.; Maréchal, J.; van Oort, B. (Eds.) *The Himalayan Climate and Water Atlas: Impact of Climate Change on Water Resources in Five of Asia's Major River Basins*; ICIMOD, GRID-Arendal and CICERO: Kathmandu, Nepal, 2015.
58. Mani, M.S. Biogeography of the Indo-Gangetic Plain. In *Ecology and Biogeography in India*; Mani, M.S., Ed.; Springer: Dordrecht, The Netherlands, 1974; pp. 689–697.
59. Gupta, R.; Seth, A. A Review of Resource Conserving Technologies for Sustainable Management of the Rice-Wheat Cropping Systems of the Indo-Gangetic Plains (IGP). *Crop Prot.* **2007**, *26*, 436–447. [CrossRef]
60. Sharma, B.; Amarasinghe, U.; Xueliang, C.; de Condappa, D.; Shah, T.; Mukherji, A.; Bharati, L.; Ambili, G.; Qureshi, A.; Pant, D.; et al. The Indus and the Ganges: River Basins under Extreme Pressure. *Water Int.* **2010**, *35*, 493–521. [CrossRef]
61. Taneja, G.; Pal, B.D.; Joshi, P.K.; Aggarwal, P.K.; Tyagi, N.K. *Farmerss Preferences for Climate-Smart Agriculture: An Assessment in the Indo-Gangetic Plain*; International Food Policy Research Institute (IFPRI): Washington, DC, USA, 2014.
62. Lal, D.M.; Ghude, S.D.; Patil, S.D.; Kulkarni, S.H.; Jena, C.; Tiwari, S.; Srivastava, M.K. Tropospheric Ozone and Aerosol Long-Term Trends over the Indo-Gangetic Plain (IGP), India. *Atmos. Res.* **2012**, *116*, 82–92. [CrossRef]
63. Department of Economic and Social Affairs Population Division. *World Urbanization Prospects, 2014 Revisions (ST/ESA/SER.A/366)*; Department of Economic and Social Affairs Population Division: New York, NY, USA, 2015.
64. Erenstein, O.; Thorpe, W.; Singh, J.; Varma, A. *Crop–Livestock Interactions and Livelihoods in the Trans-Gangetic Plains, India*; International Livestock Research Institute: Nairobi, Kenya, 2007.
65. Dubovikl, O.; King, M.D. A Flexible Inversion Algorithm for Retrieval of Aerosol Optical Properties from Sun and Sky Radiance Measurements. *J. Geophys. Res.* **2000**, *105*, 20673–20696. [CrossRef]
66. NASA. AERONET Inversion Products. Available online: https://aeronet.gsfc.nasa.gov/new_web/Documents/Inversion_products_V2.pdf (accessed on 5 July 2016).
67. NASA. MODIS (Moderate Resolution Imaging Spectroradiometer). Available online: http://modis.gsfc.nasa.gov/about/media/modis_brochure.pdf (accessed on 26 September 2016).
68. Levy, R.C.; Mattoo, S.; Munchak, L.A.; Remer, L.A.; Sayer, A.M.; Patadia, F.; Hsu, N.C. The Collection 6 MODIS Aerosol Products over Land and Ocean. *Atmos. Meas. Tech.* **2013**, *6*, 2989–3034. [CrossRef]
69. Eck, T.F.; Holben, B.N.; Reid, J.S.; Dubovik, O.; Smirnov, A.; O'Neill, N.T.; Slutsker, I.; Kinne, S. Wavelength Dependence of the Optical Depth of Biomass Burning, Urban, and Desert Dust Aerosols. *J. Geophys. Res.* **1999**. [CrossRef]
70. Dubovik, O.; Smirnov, A.; Holben, B.N.; King, M.D.; Kaufman, Y.J.; Eck, T.F.; Slutsker, I. Accuracy Assessments of Aerosol Optical Properties Retrieved from Aerosol Robotic Network (AERONET) Sun and Sky Radiance Measurements. *J. Geophys. Res.* **2000**, *105*, 9791–9806. [CrossRef]
71. Dubovik, O.; Holben, B.; Eck, T.F.; Smirnov, A.; Kaufman, Y.J.; King, M.D.; Tanré, D.; Slutsker, I. Variability of Absorption and Optical Properties of Key Aerosol Types Observed in Worldwide Locations. *J. Atmos. Sci.* **2002**, *59*, 590–608. [CrossRef]
72. Holben, B.N.; Eck, T.F.; Slutsker, I.; Smirnov, A.; Sinyuk, A.; Schafer, J.; Giles, D.; Dubovik, O. AERONET's Version 2.0 Quality Assurance Criteria. *Remote Sens. Atmos. Clouds* **2006**. [CrossRef]
73. Pérez-ramírez, D.; Whiteman, D.N.; Smirnov, A.; Lyamani, H.; Holben, B.N.; Pinker, R.; Andrade, M.; Alados-Arboledas, L.; Whiteman, D.N.; Smirnov, A.; et al. Evaluation of AERONET Precipitable Water Vapor versus Microwave Radiometry, GPS, and Radiosondes at ARM Sites. *J. Geophys. Res. Atmos.* **2014**, *119*, 9596–9613. [CrossRef]
74. Chu, D.A. Validation of MODIS Aerosol Optical Depth Retrieval over Land. *Geophys. Res. Lett.* **2002**, *29*. [CrossRef]
75. Remer, L.A.; Kleidman, R.G.; Levy, R.C.; Kaufman, Y.J.; Tanré, D.; Mattoo, S.; Martins, J.V.; Ichoku, C.; Koren, I.; Yu, H.; et al. Global Aerosol Climatology from the MODIS Satellite Sensors. *J. Geophys. Res. Atmos.* **2008**, *113*, 1–18. [CrossRef]
76. Hyer, E.J.; Reid, J.S.; Zhang, J. An Over-Land Aerosol Optical Depth Data Set for Data Assimilation by Filtering, Correction, and Aggregation of MODIS Collection 5 Optical Depth Retrievals. *Atmos. Meas. Tech.* **2011**, *4*, 379–408. [CrossRef]
77. Mao, K.B.; Ma, Y.; Xia, L.; Chen, W.Y.; Shen, X.Y.; He, T.J.; Xu, T.R. Global Aerosol Change in the Last Decade: An Analysis Based on MODIS Data. *Atmos. Environ.* **2014**, *94*, 680–686. [CrossRef]

78. Shi, Y.; Zhang, J.; Reid, J.S.; Holben, B.; Hyer, E.J.; Curtis, C. An Analysis of the Collection 5 MODIS Over-Ocean Aerosol Optical Depth Product for Its Implication in Aerosol Assimilation. *Atmos. Chem. Phys.* **2011**, *11*, 557–565. [CrossRef]
79. Soni, K.; Parmar, K.S.; Kapoor, S.; Kumar, N. Statistical Variability Comparison in MODIS and AERONET Derived Aerosol Optical Depth over Indo-Gangetic Plains Using Time Series Modeling. *Sci. Total Environ.* **2016**, *553*, 258–265. [CrossRef] [PubMed]
80. Sayer, A.M.; Munchak, L.A.; Hsu, N.C.; Levy, R.C.; Bettenhausen, C.; Jeong, M. MODIS Collection 6 Aerosol Products: Comparison between Aqua's e-Deep Blue, Dark Target, and "Merged" Data Sets, and Usage Recommendations. *J. Geo-Phys. Res. Atmos.* **2014**, *119*, 13965–13989. [CrossRef]
81. Russell, P.B.; Kinne, S.A.; Bergstrom, R.W. Aerosol Climate Effects: Local Radiative Forcing and Column Closure Experiments. *J. Geophys. Res.* **1997**, *102*, 9397–9407. [CrossRef]
82. Bilbao, J.; Román, R.; Yousif, C.; Mateos, D.; de Miguel, A. Total Ozone Column, Water Vapour and Aerosol Effects on Erythemal and Global Solar Irradiance in Marsaxlokk, Malta. *Atmos. Environ.* **2014**, *99*, 508–518. [CrossRef]
83. Yu, H.; Kaufman, Y.J.; Chin, M.; Feingold, G.; Remer, L.A.; Anderson, T.L.; Balkanski, Y.; Bellouin, N.; Boucher, O.; Christopher, S.; et al. A Review of Measurement-Based Assessments of the Aerosol Direct Radiative Effect and Forcing. *Atmos. Chem. Phys.* **2006**, *6*, 613–666. [CrossRef]
84. Cohen, J. Multiple Regression as a General Data Analytic System. *Psychol. Bull.* **1968**, *70*, 426–443. [CrossRef]
85. Prasad, A.K.; Singh, R.P. Comparison of MISR-MODIS Aerosol Optical Depth over the Indo-Gangetic Basin during the Winter and Summer Seasons (2000–2005). *Remote Sens. Environ.* **2007**, *107*, 109–119. [CrossRef]
86. Nash, J.E.; Sutcliffe, J.V. River Flow Forecasting Through Conceptual Models Part I—A Discussion of Principles*. *J. Hydrol.* **1970**, *10*, 282–290. [CrossRef]
87. Olden, J.D.; Jackson, D.A. Torturing Data for the Sake of Generality: How Valid Are Our Regression Models? *Ecoscience* **2000**, *7*, 501–510. [CrossRef]
88. Shao, J.; Rao, J.N.K. Jackknife Inference for Heteroscedastic Linear Regression Models. *Can. J. Stat.* **1993**, *21*, 377–395. [CrossRef]
89. Garren, S.T.; Kott, P.S. Evaluating the Effective Degrees of Freedom of the Delete-a-Group Jackknife. *Commun. Stat. Simul. Comput.* **2014**, *43*, 2649–2660. [CrossRef]
90. Nair, V.S.; Moorthy, K.K.; Alappattu, D.P.; Kunhikrishnan, P.K.; George, S.; Nair, P.R.; Babu, S.S.; Abish, B.; Satheesh, S.K.; Tripathi, S.N.; et al. Wintertime Aerosol Characteristics over the Indo-Gangetic Plain (IGP): Impacts of Local Boundary Layer Processes and Long-Range Transport. *J. Geophys. Res. Atmos.* **2007**, *112*, 1–15. [CrossRef]
91. Beven, K. A Manifesto for the Equifinality Thesis. *J. Hydrol.* **2006**, *320*, 18–36. [CrossRef]
92. Ritter, A.; Muñoz-Carpena, R. Performance Evaluation of Hydrological Models: Statistical Significance for Reducing Subjectivity in Goodness-of-Fit Assessments. *J. Hydrol.* **2013**, *480*, 33–45. [CrossRef]
93. Choudhry, P.; Misra, A.; Tripathi, S.N. Study of MODIS Derived AOD at Three Different Locations in the Indo Gangetic Plain: Kanpur, Gandhi College and Nainital. *Ann. Geophys.* **2012**, *30*, 1479–1493. [CrossRef]
94. García, O.E.; Díaz, J.P.; Expósito, F.J.; Díaz, A.M.; Dubovik, O.; Derimian, Y. Aerosol Radiative Forcing: AERONET-Based Estimates. In *Climate Models*; Druyan, L., Ed.; InTech: London, UK, 2012; p. 336.
95. Alam, K.; Trautmann, T.; Blaschke, T. Aerosol Optical Properties and Radiative Forcing over Mega-City Karachi. *Atmos. Res.* **2011**, *101*, 773–782. [CrossRef]
96. Alam, K.; Trautmann, T.; Blaschke, T.; Majid, H. Aerosol Optical and Radiative Properties during Summer and Winter Seasons over Lahore and Karachi. *Atmos. Environ.* **2012**, *50*, 234–245. [CrossRef]
97. Sen, A.; Abdelmaksoud, A.S.; Nazeer Ahammed, Y.; Alghamdi, M.; Banerjee, T.; Bhat, M.A.; Chatterjee, A.; Choudhuri, A.K.; Das, T.; Dhir, A.; et al. Variations in Particulate Matter over Indo-Gangetic Plains and Indo-Himalayan Range during Four Field Campaigns in Winter Monsoon and Summer Monsoon: Role of Pollution Pathways. *Atmos. Environ.* **2017**, *154*, 200–224. [CrossRef]

Chapter 6

Effect of anthropogenic aerosols on wheat production in the eastern Indo Gangetic Plain

This chapter addresses the research sub-question no 5. This chapter is submitted to Agricultural and Forest Meteorology for publication as described in preface. The supplementary tables of this paper are presented in Annex 2.

Effect of anthropogenic aerosols on wheat production in the eastern Indo Gangetic Plain

Shreemat Shrestha*[a], Murray C. Peel[a], Graham A. Moore[a], Donald S Gaydon[b], Perry Poulton[b] and Swaraj Kumar Dutta.[c]

[a] *Department of Infrastructure Engineering, University of Melbourne, Parkville, Melbourne, Victoria 3010, Australia*

[b] *CSIRO Agriculture and Food, Queensland BioScience Precinct, St. Lucia Q 4067, Australia*

[c] *Bihar Agriculture University, Bhāgalpur, India*

Abstract

The Indo Gangetic Plain (IGP) is a food basket of South Asia and is considered a hot spot of air pollution due to persistent and high emissions of anthropogenic aerosols. High levels of aerosols in the IGP not only affect the health of people but also the health of the natural system and climate of the region. Aerosol effects on crop production in the IGP is an emerging area of interest of policymakers and the scientific community due to their possible effect on food security and livelihood of millions of people in the region. To investigate the effect of anthropogenic aerosols on wheat production in the eastern IGP, we used a calibrated Agricultural Production System Simulator (APSIM) model at the Sustainable Resilient Farming Systems Intensifications (SRFSI) project nodes in the Bangladesh, India and Nepal components of the eastern IGP during 2015-2017. The effects of anthropogenic aerosols on wheat production were examined by running the APSIM model in three conditions: firstly, in the condition with anthropogenic aerosols by using the observed meteorological data; secondly, in the condition without anthropogenic aerosols by considering only the radiative effect of anthropogenic aerosols; and thirdly, in the condition without anthropogenic aerosols by considering the radiation as well as temperature effects of anthropogenic aerosols. The study revealed that on average anthropogenic aerosols have reduced the wheat grain yield, biomass yield, and crop evapotranspiration by 11.2-13.5%, 21.2-22%, and 13.5-15% respectively during 2015-2017 at the SRSFI nodes of the eastern IGP. The study also showed a reduction of more than 3.2 kg per capita per annum of wheat production in the eastern IGP due to anthropogenic aerosols, which represents a substantial effect on food security in the region. Moreover, the loss of wheat grain yield due to anthropogenic aerosols in the eastern IGP is estimated to be more than 300 million USD per annum during the study period, which indicates a significant effect of anthropogenic aerosols on wheat production in the eastern IGP.

Key words: APSIM, Eastern IGP, wheat, aerosols, SRSFI, crop model

* Corresponding author, Email: shreemats@student.unimelb.edu.au

1.0 Introduction

The Indo Gangetic Plain (IGP) region of South Asia has become a hotspot for emissions of anthropogenic aerosols resulting in adverse impacts on the health and environment of the region (Sen et al., 2017; Wester et al., 2019). Several studies based on satellite data and ground observations have depicted the IGP region as one of the most polluted regions of the world due to persistent high levels of atmospheric aerosols (Mehta et al., 2016; Singh et al., 2017; Kumar et al., 2018; David et al., 2018). The high level of atmospheric aerosols in the IGP is not only due to anthropogenic emissions from one of the most densely populated regions of the world, but also due to conducive conditions for concentrating aerosols created by the local topography and meteorology (Srivastava et al., 2012a). Spatial and seasonal variation of aerosols within the IGP is governed by aerosol sources, vertical and horizontal transport, and local and regional meteorology (Kumar et al., 2017). The average aerosol optical depth (AOD), a measure of the proportion of sunlight extinguished before reaching the ground, of the entire IGP during 2006-2015 was 0.503, which is more than 4 times that of the global average (Mao et al., 2014). In the eastern IGP, mainly eastern Uttar Pradesh, north and central Bihar, there were persistent periods of high AOD greater than 0.8 (Kumar et al., 2018). The major anthropogenic emissions in the IGP are from fossil fuel combustions (vehicular and industrial emissions) and biomass burning (residential cooking and space heating and crop residue burning in the field) (TERI, 2016; Paliwal et al., 2016; Sarkar et al., 2018). Whereas, the major natural aerosols in the IGP are mineral dust transported from the Thar Desert and west Asian dry regions during pre-monsoon seasons and the sea salt brought from the Arabian sea and the Bay of Bengal (Pandey et al., 2017; Tiwari et al., 2016). The increasing trend of aerosols over the past decades in the IGP region is mainly due to increased emissions of anthropogenic aerosols due to increased urbanization and industrialization (Kaskaoutis et al., 2012; Babu et al., 2013; Krishna Moorthy et al., 2013). Recently, in 2018, 16 cities of the IGP were listed in the 20 most polluted cities in the world based on mean annual particulate matter $PM_{2.5}$ concentration (WHO, 2018).

Cities across the IGP experience very high annual ambient $PM_{2.5}$ concentration of up to 173 μgm^{-3} (WHO, 2018), which is more than 17 times the WHO guideline (WHO, 2006). Air pollution remained a leading risk factor for death and disease burden in India in 2017 (Balakrishnan et al., 2019). Exposure to particulate matter increases the risk factor for early death due to heart disease and stroke, lung cancer, chronic lung disease and respiratory infections (Health Effects Institute, 2018). In addition, exposure to air pollution also impedes the cognitive performance of people (Chen et al., 2018). Total premature mortality due to exposure to ambient $PM_{2.5}$ in India is estimated to be 999,000 per year, with 24,606,000 years of life lost (YLL), of which the IGP region contributes 71 percent of the Indian total (Conibear et al., 2018a). In the future, the risk due to air pollution is very severe, even with no emissions growth in India. The disease burden due to exposure of $PM_{2.5}$ in 2050 is estimated to increase by 75% relative to 2015, due to population ageing and growth increases in the number of people susceptible to air pollution (Conibear et al., 2018b).

Along with the negative effects of atmospheric aerosols on the health of people in the IGP, serious effects are also reported on the natural systems of the region, which are mainly driven by changes in radiative forcing. Ramanathan and Ramana (2005) studied radiative forcing due to atmospheric

aerosols in the IGP during the dry season (October to May) from 2001 to 2003 and found that the average reduction of surface radiation was 32±5 Wm^{-2}. Similarly, Ramachandran and Kedia, (2012) estimated the average annual radiative forcing at Kanpur (urban) and Gandhi College (rural) in the IGP during 2006 to 2008 as -35.46 and -36.24 Wm^{-2} respectively. The radiative forcing due to aerosols at the eastern IGP stations of Silguri, Kolkata and Sunderban during winter in 2014/15 was -39.3, -70.3 and -38 Wm^{-2} respectively (Das et al., 2015). Similarly, Kumar et al. (2018) estimated the radiative forcing due to atmospheric aerosols at Varanasi during winter (2014/15) in the range of -51 to -80 Wm^{-2}. These studies clearly indicate that atmospheric aerosols significantly reduce solar radiation in the IGP, which may affect the natural environment of the IGP.

The global decline of surface solar radiation (SSR) due to atmospheric aerosols, termed 'surface dimming', which occurred during 1950 to 1990 (Gilgen et al., 1998), reversed (or brightened) in most places by the end of 20th century, except in India where surface dimming is still occurring at the rate of -8 Wm^{-2} $decade^{-1}$ (Wild, 2009). Singh et al. (2012) analysed trends in solar radiation at 4 meteorological stations in central and northern India during 1960-2003 and found all stations showed surface dimming at the range of 1.5% to 3.4% per decade. By analysing pan evaporation data of 58 widely distributed stations over India during 1971 and 2010, Padmakumari et al. (2013) concluded there was a decreasing trend in pan evaporation at the rate of 9.24 mm per $annum^2$ with a statistically significant confidence level of 99.9 percent.

The expected impact of continued surface dimming on the Indian monsoon remains unclear. For example, reduced evaporation from the ocean, due to reduced solar radiation, may also reduce the moisture inflow to south Asia and weaken monsoon precipitation (Ramanathan et al., 2005). In addition to this, surface dimming in the IGP is claimed to be responsible for the weakening of the land-sea temperature gradient and resulting the shift of the Asian monsoon circulation southward and decrease its intensity (Ramanathan et al., 2005). Conversely, by using the elevated heat pump (EHP) hypothesis, the increased loading of aerosols in the IGP during the pre-monsoon season may be responsible for increased heating of the upper troposphere with the formation of an upper level warm core anticyclone over the Tibetan Plateau in April to May, which may result in the advance of the monsoon into northern India and subsequent increase of rainfall in the Indian sub-continent (Lau and Kim 2006, Meehl, Arblaster, and Collins 2008). Recently, Freychet et al. (2019) analysed the effect of local aerosols by using numerical simulations (1982-2016) at the regional scale and found that the maximum temperature during winter is reduced by 0.5 °C in north-eastern India (eastern IGP) and precipitation is locally decreased by 0.5 mm day^{-1} over north Indian due to anthropogenic aerosols. In spite of these different theories on the effect of aerosols on the summer monsoon, all these studies recognized that the occurrence and pattern of the monsoon is affected by high levels of atmospheric aerosols in the IGP region. Since the summer monsoon provides 75 to 90 percent of precipitation in the IGP, the agricultural performance of the IGP is largely affected by the monsoon pattern and performance. High aerosol levels are also expected to affect other agriculturally relevant meteorological features in the region. Wide areas of the IGP, from Pakistan to Bangladesh, are engulfed by fog/low cloud during winter due to fine aerosols contributing to fog formation as cloud condensation nuclei (Gautam et al., 2007). Fog frequency in the IGP increased by 118.4% during 1971 - 2015 in the winter months of December

and January (Srivastava et al., 2016). Fog events negatively affect the growth and development of wheat due to a reduction in solar radiation availability, increased cold stress and favourable conditions for disease and pest (Singh and Singh, 2010). It is believed that the increased aerosols in the IGP also affect crop production in the region indirectly through the change in natural systems viz. change in monsoon precipitation, disease, pest population, water availability, etc. Along with those indirect effects, the reduced solar radiation, due to high levels of atmospheric aerosols, may also directly affect crop production in the IGP. In this context, studies related to the direct effect of atmospheric aerosols on crop production are discussed below.

Assessments of the effect of atmospheric aerosols on crop production are mainly performed via three types of studies viz. experimental, statistical model and process-based model studies. Experimental studies, using open top field chambers, are conducted mainly to study the effect of air pollutants in gaseous form viz. O_3, SO_2, NO_2, etc. (Agrawal et al., 2003; Heagle et al., 1987; Maggs et al., 1995; Wahid and Campus, 1995). In a chamber study, Hirano et al. (1995) studied the effect of particulate matter deposition on the leaf surface and found that it affects the stomatal conductance, photosynthesis, and transpiration by shading, plugging the stomata and increasing the leaf temperature. Similarly, the accumulation of particulate matter and trace elements on vegetation is reported to be affected by air pollution level, rainfall and the passage of time (Przybysz et al., 2014). Weerakkody et al. (2018), using natural and synthetic leaves in experiments on the accumulation of particulate matter, found that all three characteristics of leaves viz. leaf size, leaf shapes and leaf surface characteristics are influential in the capture and retention of particulate matter. In a recent experimental study on the effect of deposition of aerosols on rice leaves at New Delhi in the IGP by Mina et al. (2018), they found that aerosols reduced the yield of rice (Basmati varieties). Experimental studies on the effect of aerosols on crop production mainly focus on the effect of gaseous aerosols and deposition of particulate matter on leaves, not on the effect on crop production of atmospheric aerosols reducing surface solar radiation.

Statistical modelling has also been used to study the effect of atmospheric aerosols on crop production in India and China. Auffhammer et al. (2006) used a statistical model of historical rice harvest in India coupled with a regional climate scenario to suggest that increased brown cloud and greenhouse gases reduced harvest growth over the last two decades. Similarly, by using a statistical model, Burney and Ramanathan (2014) concluded that the combined effect of climate change and short-lived climate pollutants (SLCPs) from 1980 to 2010 reduced wheat yield up to 36% in India. Gupta et al. (2017) analysed the impact of temperature and solar radiation (due to atmospheric aerosols) on wheat production through a regression analysis of data from 208 districts in India during 1981 to 2009 and found that every 1 ◦C increase in average daily maximum and minimum temperature tends to lower yield by 2-4% and a 1% increase in solar radiation increases yield by 1%. By using historical MODIS AOD data during 2001- 2013, their study also indicated that a one standard deviation decrease of AOD is estimated to increase wheat yield by about 4.8% in India. Likewise in China, various statistical modelling results have shown that reduced solar radiation due to increased atmospheric aerosols has resulted in a decline in rice, wheat and maize production (Shuai et al., 2013; Zhou et al., 2018).

Process-based crop simulation models are also widely used to study the effects of atmospheric aerosols on crop production and to investigate different scenarios. Using the Crop Environment Resource Synthesis (CERES) 3.1 model, Chameides et al. (1999) presented a 1:1 relationship between change in solar irradiance and change in rice and wheat yield in China, they suggested that the yield of 70% of crop grown are reduced by 5 to 30% due to the regional haze in China. Greenwald et al. (2006) used a modified CERES crop model to study the influence of aerosols on rice, wheat and maize production under various atmospheric conditions. They also found that aerosols tend to decrease plant water stress by reducing soil evaporation and transpiration when crops are grown under rainfed conditions.

Along with the CERES crop model, the Agriculture Production System Simulator (APSIM) model is also used to study the effect of atmospheric aerosols on crop production. Liu et al. (2016) used a calibrated APSIM model to study the impact of air pollution on wheat yield in the North China Plain and found that the reduction in incoming solar radiation due to air pollution affects wheat yield significantly. Similarly, Xiao and Tao (2014) studied detailed field experiment data from four stations in the North China Plain during 1980 to 2009 and used the APSIM to investigate the impact of changes in climate on winter wheat yield and found that the significant decline in solar radiation (at the rate ranging from 0.06 to 0.15 MJm^{-2} $decade^{-1}$) over the past 3 decades reduced wheat yield by 3-12 % across the stations. Likewise, Zhang et al. (2013) also found that declining average daily sunshine hours (at the rate of 0.0239 hour/season) in the North China Plain, due to increasing air pollution, resulted in a decline in wheat yield during 1979 to 2012.

APSIM has also been used in the North China Plain to investigate the impact of aerosols on maize production. Sun et al. (2016) indicated a positive linear correlation between maize yield and sunshine hours (from silking to harvest stage) and the important role of radiation during grain filling stage for the final yield of maize. Similarly, by using a calibrated APSIM model, Xiao and Tao (2016) found that change in climate variables during 1981 to 2009 in the North China Plain reduced maize yield by 15 to 30%. They also found that among the changing climate variables, the highest reduction in maize yield 12-24% was due to the reduction in solar radiation (caused by increased atmospheric aerosols) during that period. Crop simulation modelling is an important tool for quantify the effect of atmospheric aerosols on wheat and maize production in China.

The impact of aerosols on the natural system and crop production in the IGP is an emerging area of interest for policymakers and the scientific community. Study on the effects of atmospheric aerosols on crop production in IGP is very important with respect to food security of this region as this region produces 53% of rice and 93% of wheat produced in the IGP countries (Pakistan, India, Nepal, and Bangladesh) (Sharma et al., 2010). The IGP is home to about 800 million people spread across four countries (Taneja et al., 2014) and the negative effects of atmospheric aerosols on crop production could threaten the livelihoods of many people in this region. In the eastern IGP, the effect could be more serious because of the comparatively higher atmospheric aerosol levels and dominance of agriculture by smallholders (with low risk-bearing capacity). Of particular interest is the impact of relatively high levels of aerosols during winter in the eastern IGP (Kar et al., 2010; Kumar et al., 2018; Mamun et al., 2014) and their effect on the performance of the major winter crop, wheat. Already some studies based on statistical models (Auffhammer et al., 2006; Burney and Ramanathan, 2014; Gupta et al., 2017) have shown a significant negative effect of

atmospheric aerosols on crop production (rice and wheat) in India. However, studies on the effects of atmospheric aerosols in the IGP using process-based models in the IGP are lacking. In this context, this study is aimed to investigate the effect of atmospheric aerosols on winter wheat production in the eastern IGP by using a calibrated APSIM model. This study is also intended to quantify the economic implications of the impact of air pollution on winter wheat production in the IGP to inform policymakers about potential benefits of pollution control programs in the region.

2.0 Study Area and Methods

2.1 Study area

The IGP is one of the largest fertile plains in the world formed by the Indus and Ganges river systems and it encompasses the eastern plain area of Pakistan, most of northern and eastern India, the southern plain area of Nepal and almost all of Bangladesh. The IGP is home to 1 billion people and it is also the 'food basket' of the region producing 53% of rice and 93% of wheat of those countries (Sharma et al., 2010). Considering biophysical condition and socioeconomic development, the IGP can be divided into two broad categories: western IGP and eastern IGP (Taneja et al., 2014). Our study area is the eastern IGP which encompasses eastern Uttar Pradesh, Bihar and West Bengal of India, the eastern Terai area of Nepal and the plain area of Bangladesh (Figure 1).

The biophysical and socio-economic characteristics of the eastern IGP are different from the western IGP. There is a clear gradient in annual average precipitation in the IGP with 654 mm in Punjab (western IGP) to 1462 mm in West Bengal (eastern IGP) (Erenstein et al., 2007). The climate of the eastern IGP is hot and sub-humid with a monsoon season (June to September) in which about 85% of total precipitation occurs (Gupta and Seth, 2007). In spite of higher precipitation in the eastern IGP, compared to western IGP, crop productivity in the eastern IGP is lower due to a lack of assured irrigation facilities, low level of agricultural inputs, traditional agriculture systems and climate extremes (flood and droughts) (Taneja et al., 2014). A major characteristic of the eastern IGP is low lying flood prone land, formed by alluvium deposit from the Ganga river system (Pal et al., 2009). The average land holding in the eastern IGP is small (only 0.59 ha/household) and less mechanized compared to the western IGP (3.55 ha/household) (Balasubramanian et al., 2013). The IGP is considered to be one of the most densely populated regions of the world with a population of more than 800 M (Taneja et al., 2014) and a clear gradient (ascending) of population density from west to east (Erenstein et al., 2007). Census data from 2011 indicates a total population of eastern IGP of more than 360 million with an average population density of 991 people per square kilometre.

Increasing urbanization and high population density, industrialization and the dominance of biomass in domestic energy use has resulted in high levels of atmospheric aerosol loading in the IGP (Sen et al., 2017). The persistence of exceptionally high AOD (greater than 0.8) in eastern Uttar Pradesh, north and central Bihar is an important feature of aerosols in the eastern IGP, which are mainly due to emissions from households and industries as well as local topography and meteorology acting to concentrate aerosols (Kumar et al., 2018).

Rice is the important crop of the eastern IGP and the major seasonal cropping patterns of this region are rice-rice, rice-maize, and rice-wheat. Wheat is an important winter crop in Bihar covering 2.1 M ha (47% of the net cropped area), whereas only 0.32 M ha (only 6 % of the cropped area) is cultivated in West Bengal (https://www.indiaagristat.com). Similarly, wheat is also an important winter crop of the Terai area of Nepal cultivated in 0.43 M ha (about 33% of the cropped area)(CBS, 2014). In Bangladesh, rice covers more than 75% of the major cropping area cultivated in all three seasons – Kharif 1 (Aus rice), Kharif (Aman rice) and Rabi (Boro rice). Wheat and maize are the important Rabi crop after Boro rice in Bangladesh. In Bangladesh, wheat cultivated area declined significantly after 1998/99 as farmers preferred to cultivate maize due to the increased economic return of maize due to higher productivity of hybrid maize (5.3 t/ha) compared to wheat (1.6 t/ha) and increasing demand for maize from the expanding poultry industry (Monlruzzaman et al., 2009).

The Sustainable and Resilient Farming Systems Intensification (SRFSI) project is an Australian Centre for International Agricultural Research (ACIAR) and Australian Department of Foreign

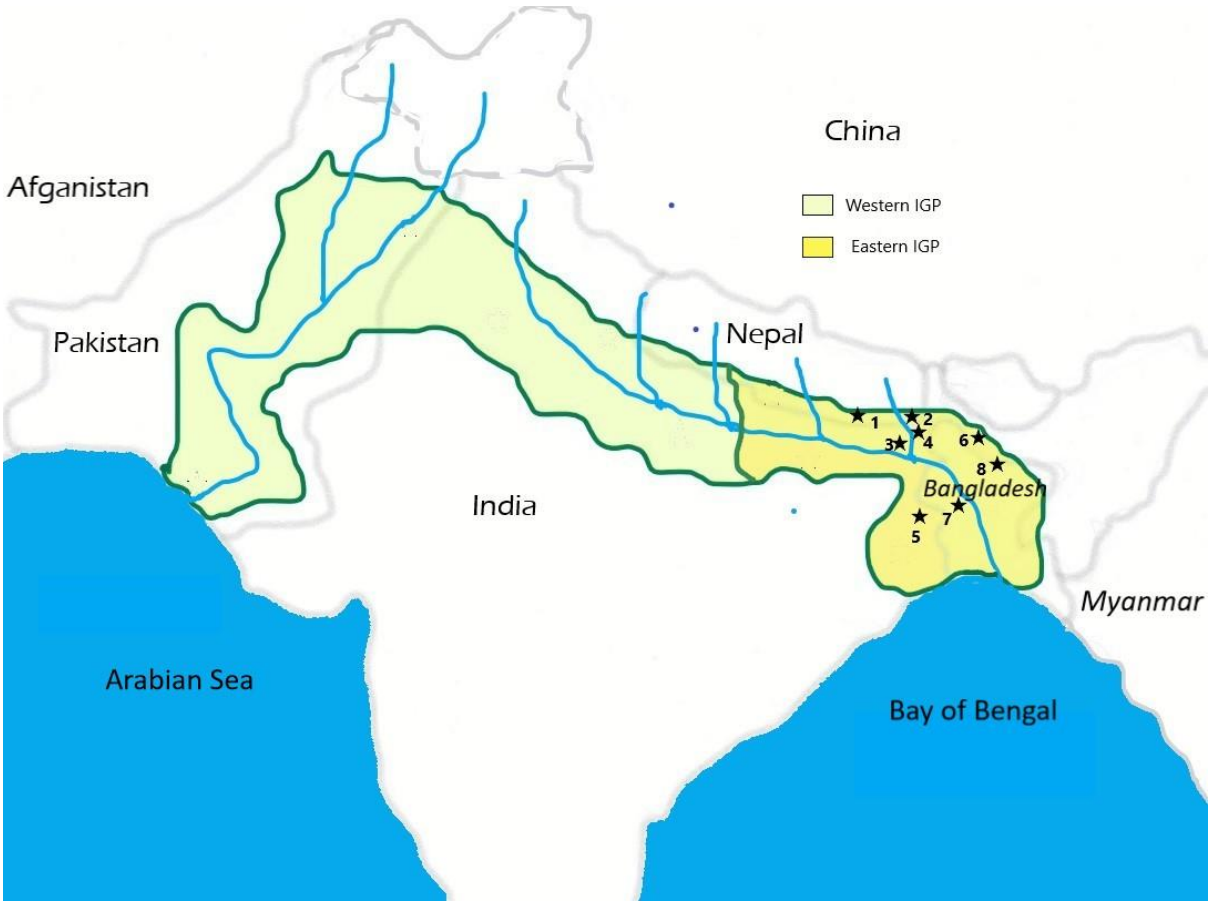

Figure 1: Study area, the eastern IGP and the Sustainable and Resilient Farming Systems Intensification (SRSFI) project districts (1- Dhanusha & 2- Sunsari of Nepal; 3 –Madhubani & 4– Purnea of Bihar, India; 5- Cooch Behar & 6- Malda of West Bengal, India; and 7- Rajshahi & 8- Rangapur of Bangladesh)

Affairs and Trade (DFAT) funded regional project implemented during 2014 to 2018 in the eastern IGP has an aim to reduce poverty by improving productivity, profitability and sustainability of small farmers while safeguarding the environment (Gathala et al., 2018). The SRFSI Project focusses on

the eastern IGP of Bangladesh, India, and Nepal and has established 40 nodes/villages across 8 districts (Figure 1) to implement project activities. One project activity conducted at these 40 nodes is on-farm trials to compare conservation agriculture technologies with conventional tillage practice. After checking data quality, on-farm trials at two nodes at each district of Rajshahi, Rangapur, Purnea, and Sunsari were selected for SRFSI on-farm calibration and evaluation of the APSIM crop simulation model. The details of those nodes are presented in Table 1. In all nodes, APSIM is set up to simulate the rice-wheat cropping system, but in this study only the winter wheat crop is analysed.

The monthly mean maximum and minimum temperature and the precipitation of the study districts are shown in Figures 2 and 3 respectively. The monthly maximum and minimum temperature indicate that the study district Rajshahi is comparatively warmer and Sunsari is comparatively cooler. All the 4 study districts show a similar precipitation pattern with precipitation mainly concentrated in the monsoon period and only nominal winter precipitation during the wheat growing period.

Table 1: Details of nodes in which the SRFSI on-farm APSIM calibration and validation was conducted based on on-farm experimental trials (Gaydon et al., 2018).

Country	District	Nodes	Latitude	Longitude	Cropping system simulated
Nepal	Sunsari	Simariaya	26.570	87.239	Rice-wheat
		Bhaluwa	26.547	87.249	Rice-wheat
India	Purnea	Dogachi	25.516	87.334	Rice-wheat
		Tikapatti	25.312	87.124	Rice-wheat
Bangladesh	Rajshahi	Baduria	24.337	88.717	Rice-wheat-mung bean
		Premtoli	24.406	88.434	Rice-wheat
	Rangapur	Kolkondo	25.875	89.199	Rice-wheat-jute
		Mohonpur	25.375	88.875	Rice-wheat-jute

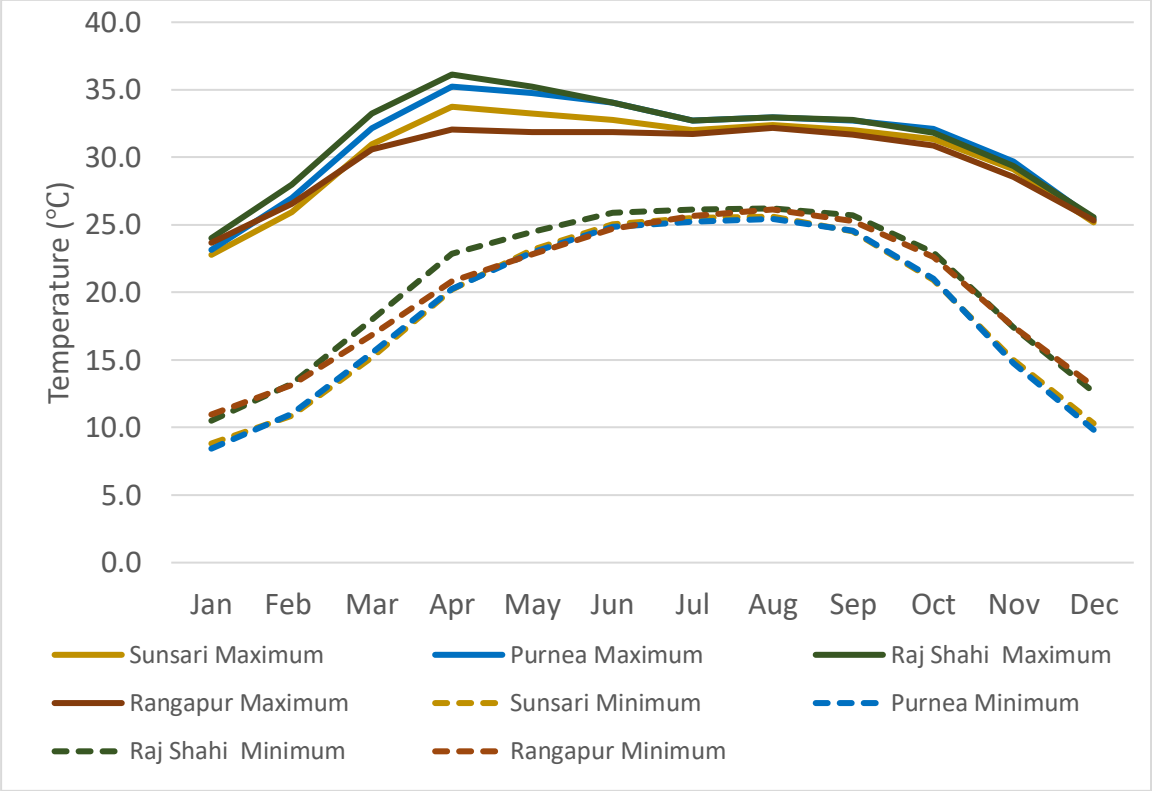

Figure 2: Monthly mean maximum and minimum temperature of the study districts

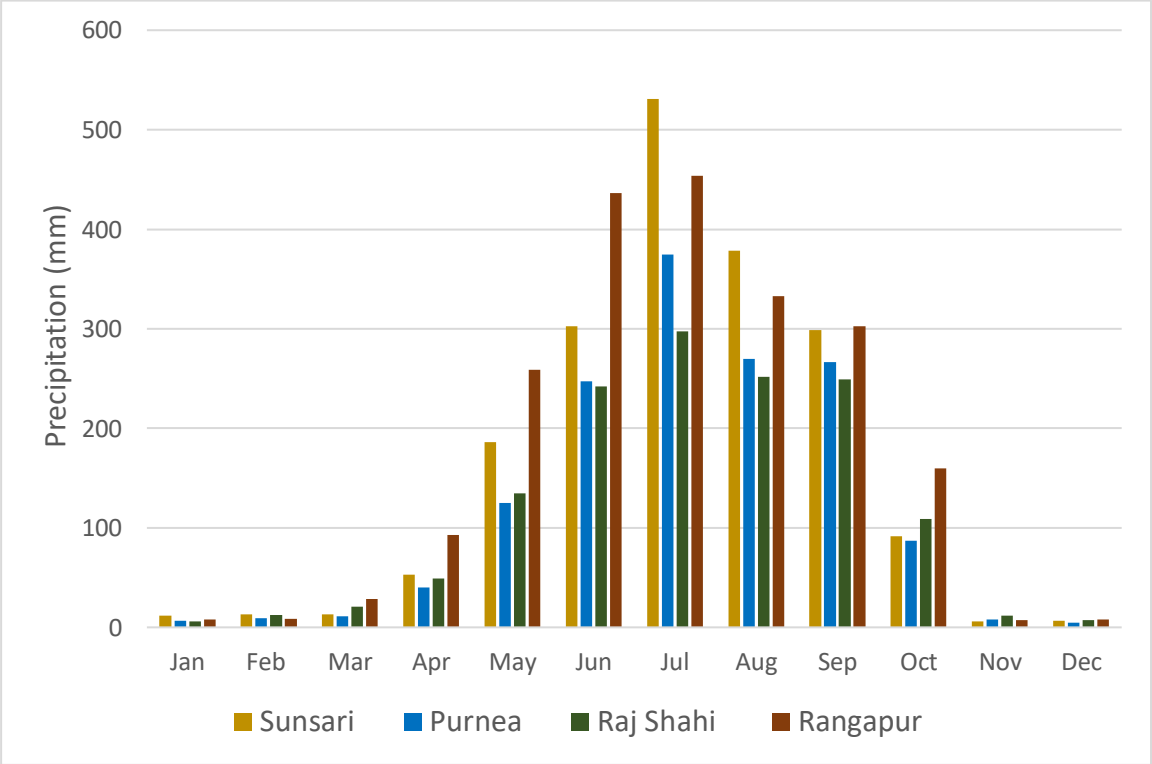

Figure 3: Monthly mean precipitation of the study districts

2.2 Methods

2.2.1 Atmospheric aerosols in the eastern IGP

Atmospheric aerosols in the eastern IGP are studied by using AOD at 500 nm and Angstrom exponent data from 2003 to 2017 at four AErosol RObotic NETwork (AERONET) stations (Lumbini, Gandhi college, Dhaka, and Bhola) located in the eastern IGP. The average monthly AOD and Angstrom exponent is calculated at each station to study the overall seasonal status of aerosols at those stations. To obtain historical data of AOD at the SRFSI nodes listed in Table 1, area average daily MODIS Aqua AOD at 550 nm is extracted for pixels lying within ±0.1° co-ordinates of each node during 2003 to 2017. The trend analysis of AOD at the SRFSI nodes is performed using a Mann-Kendall test (Gilbert, 1987). A positive aspect of this method is that missing values are allowed, and data need not belong to any specific distribution. In addition, this method is robust to single data errors and outliers (Sen 1968). In this method, the trend is assumed to be monotonic and the equation for AOD as a function of time (years) is given by,

$$f(t)= Qt+B \qquad (1)$$

where *Q* is the slope and *B* is a constant.

2.2.2 Estimation of radiative forcing due to aerosols at SRFSI nodes in eastern IGP

There are direct and indirect effects of atmospheric aerosols on the energy balance of the earth-atmosphere system. The direct effects are through scattering and absorption of solar radiation by aerosols in the atmosphere and the indirect effects are by aerosols acting as cloud condensation nuclei and modifying cloud properties (viz. albedo, lifetime, precipitation efficiency, etc.) (Lohmann and Feichter, 2004). The effect of the aerosols is measured in terms of radiative forcing, which is defined as the net radiative flux either at the bottom (surface of the earth) or top of the atmosphere with and without aerosols in the atmosphere (Russell et al., 1999). Here, we are interested in the direct effect of atmospheric aerosols on incoming solar radiation at the surface of the earth. The direct radiative forcing at the surface ($ADRF_{clr}$) under clear sky conditions is expressed as equation (2).

$$ADRF_{clr} = F_{clr}^{a\downarrow} - F_{clr}^{o\downarrow} \qquad (2)$$

Where,

$F_{clr}^{a\downarrow}$ = Net downward flux with aerosol under clear sky conditions

$F_{clr}^{o\downarrow}$ = Net downward flux without aerosol under clear sky conditions

Clouds in the atmosphere also affect the energy balance of the earth-atmosphere system. Cloud radiative forcing is used to measure the impact of clouds on radiation and is defined as the difference between the clear sky and all sky radiation (Coakley and Baldwin, 1984). Liu et al. (2011) derived a simple relationship for cloud radiative forcing with cloud albedo (α) and cloud fraction (*f*). By using this relationship, the incoming solar radiation at the bottom of the atmosphere without atmospheric aerosol ($F_{all}^{o\downarrow}$) can be expressed in terms of incoming radiation under clear sky conditions by equation (3).

$$F_{all}^{o\downarrow} = (1 - \alpha f)F_{clr}^{0\downarrow} \qquad (3)$$

Where,

$F_{all}^{o\downarrow}$ = Net downward flux without aerosol under the all-sky condition.

If we assume no interaction between the clouds and aerosols in the atmosphere, the incoming solar radiation at the bottom of the atmosphere with atmospheric aerosols ($F_{all}^{a\downarrow}$) can also be expressed as analogous to the Liu et al. (2011) relationship, as in equation (4).

$$F_{all}^{a\downarrow} = (1 - \alpha f) F_{clr}^{a\downarrow} \qquad (4)$$

The radiative forcing at the surface (*ARF$_{all}$*) in the all-sky condition is the difference between the net downward radiative flux all-sky condition with aerosols in the atmosphere ($F_{all}^{a\downarrow}$) and that without aerosols ($F_{all}^{o\downarrow}$). From equations 2 – 4, the relationship between the all-sky radiative forcing (*ARF$_{all}$*) and clear sky radiative forcing $ADRF_{clr}$ can be expressed as in equation (5).

$$ARF_{all} = (1 - \alpha f) ADRF_{clr} \qquad (5)$$

In this study, the clear sky daily radiative forcing at the surface of the SRFSI nodes in the eastern IGP is estimated from a regression model (Equation 6) developed by Shrestha et al. (2018). The input parameters of this model are the daily average atmospheric aerosol optical depth at wavelength 550 nm (*AOD$_{550}$*) and daily mean atmospheric water vapor (*AWV*). Daily merged dark target (DT) and deep blue (DB) AOD products and daily mean atmospheric water vapor from MODIS Aqua were extracted for pixels lying within ±0.1° of the SRFSI nodes listed in Table 1 for the years 2014 to 2017.

$$ADRF_{clr} = -32.464 - 119.446 * AOD_{550} + 4.471 * AWV \qquad (6)$$

The area-averaged cloud albedos at pixels within ±0.1◦ of the SRFSI nodes listed in Table 1 were extracted from the Modern-Era Retrospective analysis for Research and Applications, version 2 (MERRA-2) for the same duration. Similarly, the area-averaged mean daily cloud fraction at pixels within ±0.1◦ of the SRFSI nodes were obtained from MODIS Aqua for the years 2014 to 2017. The daily direct radiative forcing at the surface under all-sky conditions (*ARF$_{all}$*) for the SRFSI nodes listed in Table 1 during 2014 and 2017 was computed using equation 5.

The radiative forcing estimated from equation 5, provides the radiative forcing at the surface by aerosols from both natural and anthropogenic sources. Here, we are interested in the radiative forcing due to anthropogenic aerosols. In the IGP region, anthropogenic and natural aerosols exhibit distinct seasonal characteristics and mixing (Dey et al., 2004; Jethva et al., 2005; Srivastava et al., 2012; Ramachandran and Kedia, 2012; Kumar et al., 2018). Dey and Tripathi (2008) studied radiative forcing due to atmospheric aerosols and the anthropogenic contribution on a monthly basis at Kanpur in the IGP and found that anthropogenic aerosols contributed 90.5% in winter, 83.7% in the post monsoon season and 47.6% in summer. Similarly, Srivastava et al. (2012b) chemically analysed aerosols over Delhi in the IGP to identify their source and estimated the contribution of anthropogenic aerosols using the SBDART model in the year 2007 and found that the radiative forcing due to anthropogenic aerosols in winter was 90.7% followed by post-monsoon season (84.3%) and summer (53.6%). Hence, based upon study results on seasonal variation of the contribution of anthropogenic aerosols in the IGP, the radiative forcing due to anthropogenic aerosols in winter, post-monsoon and summer (pre-monsoon and monsoon) is approximately 90%, 80% and 50% respectively that of radiative forcing due to aerosols under all-sky conditions (*ARF$_{all}$*) at the surface of the IGP. Therefore, seasonal radiative forcing due to anthropogenic aerosols under all-sky conditions (*AARF$_{all}$*) is given by,

$$AARF_{all} = ARF_{all}.\ \mu \qquad (7)$$

where,

μ= seasonal coefficient (value of μ for winter 0.9, post-monsoon 0.8, summer 0.5)

2.2.3 Crop modelling

The crop model and the methodology adopted to simulate the effect of atmospheric aerosols on wheat production at the nodes of the study districts listed in Table 1 is described in the following subsections.

2.2.3.1. Crop Model

Crop growth models simulate crop growth and the crops response to management and the surrounding environment. Crop models were developed with an aim for scientific understanding of the system and to assist decision making and policy support (Sto et al., 2003). Specifically, the major applications of crop models are to: synthesize research understanding about genetics, physiology and the environment; assist management decisions on inputs and crop management practices; and assist policy makers to predict leaching of agro-chemicals, the effect of climate change, large area yield forecasts, environment management, etc. (Boote et al., 1996). APSIM, DSSAT, CROPSYST, ORYZA, EPIC are examples of well recognized dynamic models used in agricultural system modelling (Jones et al., 2016). APSIM (Agricultural Production Systems Simulator) which is developed by the Agricultural Production Systems Research Unit in Australia is a widely used model for modelling agricultural systems (Keating et al., 2003). The primary focus of APSIM on simulating crop resource supply (soil as a central simulation component), rather than crop resource demand, makes it distinct from other crop models (McCown et al., 1996). Along with farming system research, APSIM is also widely used in climate change, ecological and environmental research at both farm and catchment level (Asseng et al., 1998; Huth and Possingham, 2007; Paydar and Gallant, 2008; Hunt and Norton, 2011; Li-li et al., 2015). Since APSIM is adopting an open and transparent 'open source framework', it is widely applied in Asia, Africa, Europe, America and Australia (Gaydon et al., 2017; Whitbread et al., 2010; Sus et al., 2010; Archontoulis et al., 2014). Of relevance to this study, Yang et al. (2013), Liu et al. (2016) and Zhang et al. (2018) have already used APSIM to study the effect of atmospheric aerosols on wheat and maize production in China. In this study, the calibrated and validated APSIM model for SRFSI sites (Gaydon et al., 2018) is used to quantify the effect of atmospheric aerosols on crop production in the eastern IGP.

2.2.3.2. Crop Simulation by APSIM

As crop simulation modelling represents processes of crop growth and development as a function of weather conditions, soil conditions, and crop management, it is applied in research, education and to support decision-making process (Ittersum et al., 2003). The SRFSI project uses APSIM to evaluate the long-term sustainability of different technological options in the eastern IGP, for which on-farm trial datasets were used to calibrate and validate APSIM (Gathala et al., 2018). To quantify the effect of atmospheric aerosols on crop production we use the already calibrated and validated APSIM rice-wheat cropping system (Gaydon et al., 2018). This model was calibrated and validated using the SRFSI field trials data at the nodes listed in Table 1 from 2014 to 2017 in the eastern IGP (Gaydon et al., 2018). Even though, this calibrated and validated model is set up to evaluate conservation agriculture (CA) technologies across a range of cropping systems and

locations in the eastern IGP, here we have used only one treatment of the model for the rice-wheat system with conventionally tilled puddled transplanted rice followed by conventionally tilled wheat, which is practiced by the majority of farmers in the eastern IGP.

In this study, we study the impact of anthropogenic atmospheric aerosols on winter wheat in the eastern IGP. The amount of reduced radiation due to anthropogenic aerosols from 2014 to 2017 at the SRFSI nodes listed in Table 1 is estimated by equation (7). The solar radiation without anthropogenic aerosols is estimated by adding this reduced solar radiation to the observed solar radiation for each day.

The alteration of the energy balance due to anthropogenic aerosols also affects the ambient temperature globally (Shindell et al., 2013). Global models are used to study the implication of change in temperature due to atmospheric aerosols, in this context Freychet et al. (2019) used UK HadGEM Unified Model to study the local aerosol emission effect in North America, Europe, India and China during 1982 to 2016 and found that in northeast India (i.e. eastern IGP) the maximum temperature is reduced by 0.5 ◦C during winter (December, January, and February). Here it is assumed that the anthropogenic aerosols reduced the maximum temperature by 0.5 ◦C uniformly throughout the winter. Hence, the maximum temperature during winter months without anthropogenic aerosols is estimated by modifying the measured maximum temperature by adding 0.5 ◦C to each day. To study the impact of anthropogenic aerosols, simulation runs of the calibrated APSIM model at the SRFSI nodes were performed for three conditions: (1) with anthropogenic aerosol condition (no change in solar radiation and temperature); (2) without anthropogenic aerosol condition with only radiation effect; and (3) without anthropogenic aerosol condition with radiation and temperature effect. To minimize the effect of irrigation, automated irrigation is switched to 'on' mode with irrigation when available soil water fraction is below 0.5 in all simulations across all the nodes. The APSIM simulation outputs at the SRFSI nodes are compared in terms of grain yield, biomass yield, and crop evapotranspiration.

2.2.4 Economic loss and gain due to anthropogenic aerosols on wheat production

The past five years data on the wheat crop cultivated area and production in the Nepal, India and Bangladesh components of the eastern IGP were obtained from the corresponding national statistics. Based on the simulation results on the average gain or loss in wheat yield due to anthropogenic aerosols in the corresponding nodes in the eastern IGP, the gain or loss of wheat in each country component of the eastern IGP was obtained. By using the average wholesale price of wheat at Patna, a market at eastern IGP over the last 5 years (from April 2014 to April 2019), the total economic loss/gain due to anthropogenic aerosols on wheat production was assessed. Here the economic loss and gain caused by the effect on biomass yield of wheat are not included in the analysis.

3. Results and discussions:

3.1 Atmospheric aerosols in the eastern IGP

The atmospheric aerosols in the eastern IGP are studied using historical AERONET data and field measured particulate matter $PM_{2.5}$ data at eastern IGP stations. The average monthly distribution of AOD at 500 nm and the Angstrom Exponent measured at AERONET stations (Lumbini, Gandhi college, Dhaka and Bhola) in the eastern IGP are presented in Figures 4 and 5 respectively. It is evident from Figure 4 that at all stations the AOD is comparatively less during monsoon season (June - September), which may be due to the wet scavenging of aerosols due to monsoon precipitation. However, AOD increases during the post-monsoon season at all stations and reaches its peak during winter months (December - February), which is similar to the findings of Kumar et al. (2018). The increasing AOD during the post-monsoon season and the peak during the winter season are due to a combination of burning of agricultural residue along with other regular aerosols in those seasons and a shallow boundary layer during winter (Singh et al., 2017; Kumar et al., 2017). The Angstrom exponent at all stations except Bhola during post-monsoon and winter season is between 1.1 to 1.4, which indicates the aerosol particle size is of mixed type (neither fine nor coarse) which is also in line with the findings of Kumar et al. (2018). The AOD pattern in the pre-monsoon season at two stations Lumbini and Gandhi college located in the western part of the eastern IGP is distinctly different from the stations located in Bangladesh (Dhaka and Bhola) with increasing AOD from March to June, which may be due to mineral dust transported from southwest Asia (Middleton, 1986) being deposited before reaching the eastern area of the eastern IGP. This is supported by the comparatively low Angstrom exponent during pre-monsoon months at Gandhi college station in Figure 5. Similarly, a comparatively low Angstrom Exponent during monsoon months at Bhola (located adjacent to the Bay of Bengal) may be due to sea salts brought by the monsoon. From the distribution of AOD in the eastern IGP stations, it can be concluded that except during monsoon season, in all months the AOD is high with a peak during winter in the eastern IGP, which may have strong implications for incoming solar radiation and winter crops due to scattering and absorption of radiation in the atmosphere.

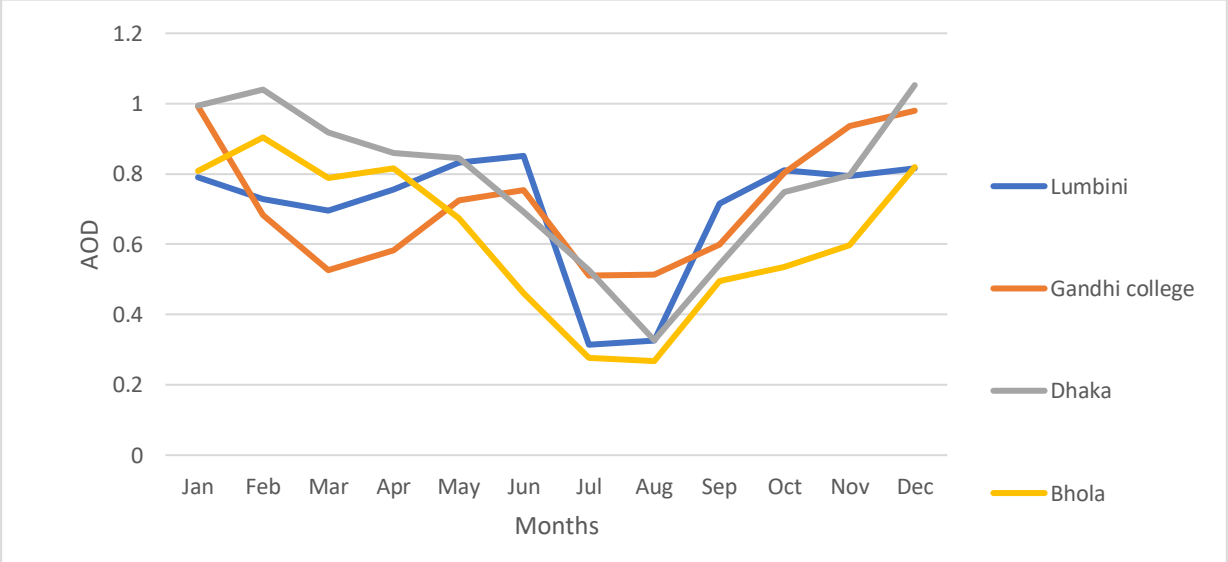

Figure 4: Average monthly distribution of AOD 500 nm based on AERONET data at eastern IGP

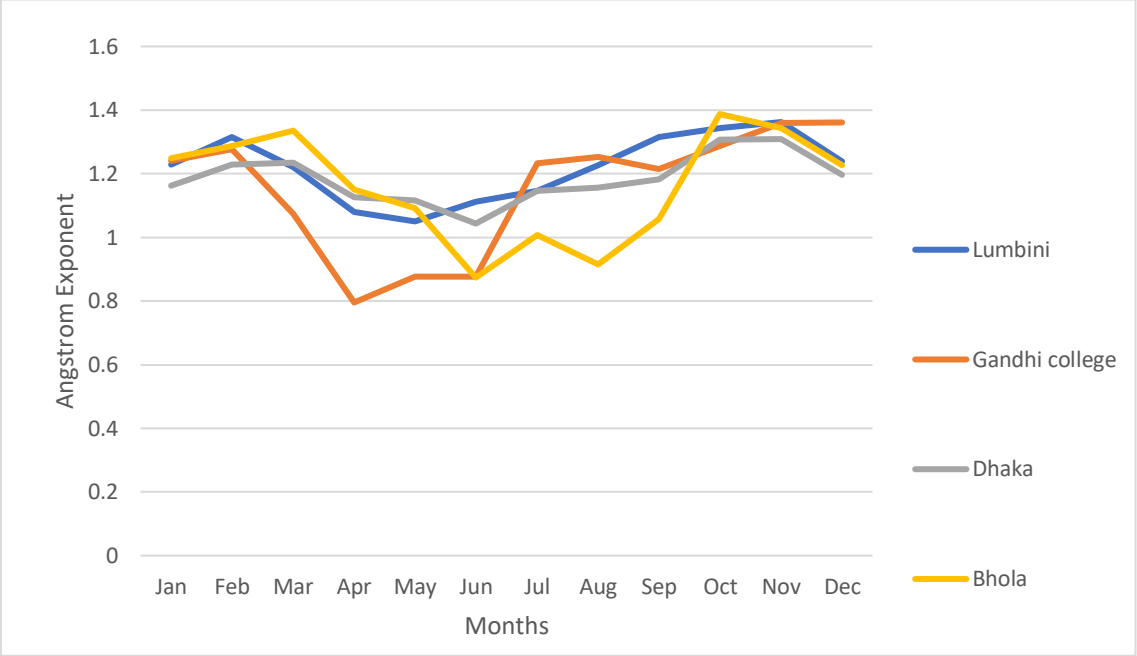

Figure 5: Average monthly distribution of Angstrom exponent (AE) based on AERONET data at eastern IGP

The average monthly particulate matter ($PM_{2.5}$) measured (IQAir AirVisual, 2018) in several eastern IGP stations during 2018 is presented in Figure 6. Annual average $PM_{2.5}$ concentration of those stations is more than 7 to 11 times higher than the World Health Organization (WHO) guideline of 10 µg m^{-3} (WHO, 2006). The monthly distribution of particulate matter also shows a similar pattern to AOD with a minimum during monsoon season and increasing during the post-monsoon season and reaching a peak in the winter season and declining during pre-monsoon season. High particulate matter concentration during winter may be due to increased use of biomass-based fuel for space heating. Moreover, in rural areas of northern India cow dung cake is used as residential fuel for cooking (Banerjee, 2017). From biomass samples from IGP states of India, Singh et al. (2013) found that dung cake produced comparatively more particulate matter than fuelwood and crop residue. Furthermore, Fosu et al. (2017) found a strong relationship between particulate matter and atmospheric stability in the lower troposphere and increased aerosol loading during winter in the IGP, which was caused by enhanced atmospheric stabilization during winter. Stations located in the western area of eastern IGP (viz. Gaya, Varanasi and Patna) show a hump in the month of June, which may be due to mineral dust transported from the western arid/desert regions of the Arabian Peninsula and the Thar Desert in India into the IGP (Gautam et al., 2010). The monthly distribution of particulate matter in the eastern IGP shows critical air quality conditions. The poor air quality is directly linked with negative implications for human health viz. increased risk of premature mortality, respiratory and cardiovascular diseases (Schwartz et al., 2008; Brook et al., 2010).

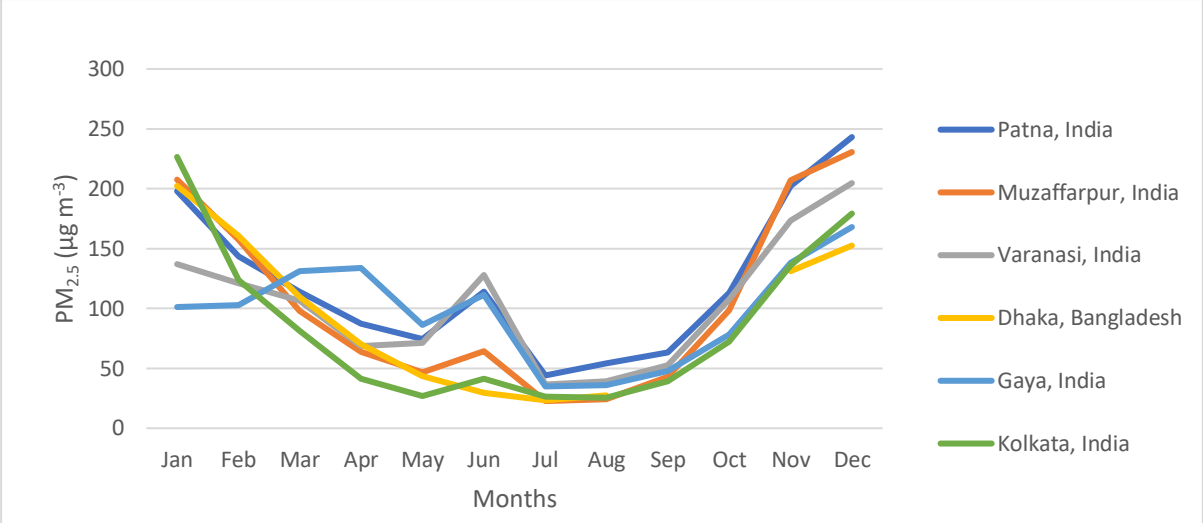

Figure 6: Monthly mean particulate matter distribution in eastern IGP during 2018

3.2 Radiative forcing due to atmospheric aerosols in the eastern IGP

The average seasonal radiative forcing during 2003-2017 due to anthropogenic aerosols estimated by the method outlined in section 2.2.2 at the SRFSI districts is presented in Table 2. The table clearly indicates that compared to other seasons winter season radiative forcing is significantly higher in all the studied districts. High radiative forcing during winter is due to high anthropogenic aerosols in the eastern IGP. During monsoon season, the anthropogenic radiative forcing is minimum which is due to less emission of anthropogenic aerosols during monsoon season and wet scavenging of aerosols due to monsoon precipitation. In all the studied districts, the radiative forcing in post monsoon season is higher than that in pre-monsoon season due to a higher contribution of anthropogenic aerosols. Among the studied districts, the highest average radiative forcing is at Rangapur, followed by Rajshahi and Purnea/Sunsari. The radiative forcing estimated at the SRFSI districts is comparable to the radiative forcing estimated by SBDART model at a station in eastern IGP, Gandhi college as -55.48 Wm^{-2} by using SBDART model (Ramachandran and Kedia, 2012b).

Table 2: Radiative forcing due to anthropogenic aerosols (Wm^{-2}) in the SRFSI districts of eastern IGP

SN	SRFSI nodes in Eastern IGP	Pre-monsoon	Monsoon	Post- Monsoon	Winter	Annual
1	Rangapur	-51.50	-33.26	-60.47	-107.35	-63.15
2	Rajshahi	-51.50	-30.57	-52.17	-88.68	-55.73
3	Purnea/Sunsari	-44.02	-18.23	-52.65	-84.42	-49.83

To obtain the seasonal and annual trend of anthropogenic radiative forcing in the studied districts in eastern IGP during 2003-2017, Mann Kendall (MK) trend analysis is performed and the results are presented in Table 3. From the MK trend analysis results, a significant declining trend on annual radiative forcing is found at all the studied districts at least at the 0.01 level of statistical significance during 2003-2017. The declining trend of radiative forcing in the SRFSI districts in the eastern IGP is due to increasing levels of pollution and hence AOD during the study period. The rate of decline varied from 1.01 Wm^{-2} $year^{-1}$ at Rajshahi to -1.5 Wm^{-2} $year^{-1}$ at Rangapur during 2003-2017. Among the seasonal trends in radiative forcing, it is significantly declining in pre-

monsoon season at all districts and in the winter season at Sunsari and Purnea district at least at the statistically significant level of 0.05.

Table 3: Trend of seasonal and annual average radiative forcing due to atmospheric aerosols estimated during 2003-2017 at eastern IGP study sites

SRFSI districts at Eastern IGP	Seasonal/Annual	Test Z	Significance	Q	B
Rangapur	Pre-monsoon	-2.672	**	-1.279	-97.291
	Monsoon	-1.683	+	-0.908	-58.767
	Post Monsoon	-1.287		-1.379	-66.424
	Winter	-1.782	+	-1.644	-108.673
	Annual	**-2.870**	****	**-1.508**	**-81.855**
Rajshahi	Pre-monsoon	-2.573	*	-1.421	-96.719
	Monsoon	-1.881	+	-0.939	-55.164
	Post Monsoon	-0.891		-1.026	-55.422
	Winter	-1.386		-1.478	-85.368
	Annual	**-2.969**	****	**-1.013**	**-76.012**
Purnea/ Sunsari	Pre-monsoon	-2.672	**	-1.485	-77.761
	Monsoon	-1.584		-0.929	-30.471
	Post Monsoon	-1.881	+	-1.050	-59.648
	Winter	-2.078	*	-2.106	-80.881
	Annual	**-3.563**	****	**-1.209**	**-59.346**

*+ significant at 0.1, * significant at 0.05, ** significant at 0.01, *** significant at 0.001*

3.3 Solar radiation trend at the SRFSI districts in eastern IGP

Historical sunshine hour data of SRFSI district Sunsari in Nepal and Rajshahi in Bangladesh are used for trend analysis of solar radiation. To obtain a monthly and annual trend of sunshine hours at Biratnagar, Sunsari, Nepal during 1990 to 2016, the Mann Kendall (MK) trend analysis is performed and the results are presented in Table 4. The results indicate that the annual daily average sunshine hours are decreasing at the rate of 0.036 hours (0.52%) per annum at a statistically significant level of 0.05 during those 26 years. This result agrees with the findings of Niroula et al. (2015) who indicated surface dimming at a rate of -0.56% per annum in the Terai. Similarly, it is also in line with the findings of Kumari et al. (2007) who found a 5% decline in solar radiation over the Indian region during 1980-2000. The increasing level of atmospheric aerosols has contributed to the reduction of solar radiation in the Indian subcontinent, with pronounced effects in the IGP region (Ramanathan et al., 2001; Ramanathan and Ramana, 2005; Dey and Tripathi, 2007; Srivastava and Ramachandran, 2013). The monthly trend results indicate that there is also a declining trend in sunshine hour at Biratnagar in all the months, but the trend is only statistically significant in January, March, May, and December at the statistically significant level of 0.05. The rate of decline in December and January (winter months) is almost double that in the months of March and May (pre-monsoon months), which may be due to the increased level of aerosols and occurrence of fog events during winter months (December and January) in the Terai area of Nepal

(Shrestha et al., 2018a). The sunshine hour trends at Biratnagar clearly indicate that significant surface dimming is occurring at Biratnagar during winter months, which may affect the production of winter wheat (Yang et al., 2013).

Table 4: Trend of monthly and annual average daily sunshine hour during 1990 to 2016 at Biratnagar, Sunsari, Nepal

Months	Test Z	Slope of a trend line, Q (hr/yr)	Intercept of a trend line, B (hr)	Average daily sunshine hour (hr)	Interannual trend of the average daily sunshine hour (%)
Jan	-3.045	-0.090**	7.221	5.67	-1.59
Feb	-1.842	-0.041+	7.999	7.17	-0.57
Mar	-2.538	-0.043*	8.914	8.29	-0.52
Apr	-1.067	-0.025	8.888	8.33	-0.30
May	-2.030	-0.040*	8.579	8.13	-0.49
Jun	-0.695	-0.031	6.510	6.27	-0.49
Jul	-0.630	-0.008	5.598	5.20	-0.16
Aug	-1.329	-0.054	6.476	5.65	-0.96
Sep	-0.755	-0.023	6.076	5.97	-0.38
Oct	-1.590	-0.036	8.214	7.50	-0.49
Nov	-1.072	-0.028	8.482	7.86	-0.36
Dec	-2.265	-0.082*	7.689	6.49	-1.26
Annual	-2.360	-0.036*	7.266	6.94	-0.52

*+ significant at 0.1, * significant at 0.05, ** significant at 0.01*

Table 5 presents monthly and annual trend analysis results of sunshine hours at Rajshahi, Bangladesh during 1982-2017. The table clearly shows that sunshine hours are declining overall annually as well as in the months of January, March, April, and December at the statistically significant level of at least at 0.05 in Rajshahi, Bangladesh. The annual declining trend of daily sunshine hours at Rajshahi is 0.028 hours per annum. Among the monthly trends, December and January have the largest declining trends with 0.1 and 0.71 hr/annum respectively compared to that of March and April with declining trends of 0.24 and 0.026 hr/annum respectively. The high declining trend during winter months (December and January) compared to other months may be due to the increasing level of atmospheric aerosols (Kar et al., 2010; Kumar et al., 2018) and fog events during winter (Syed et al., 2012) in the region. The trend analysis results indicate that surface dimming is occurring at Rajshahi Bangladesh at a rate of reduction in sunshine hours of 0.42% annually with a very high reduction in winter months January and December of 1.09 and 1.46% respectively. Similar to Biratnagar, Nepal, in Rajshahi, Bangladesh also winter crop production may be affected by declining sunshine hours.

Table 5: Trend of the monthly and annual average daily sunshine hour during 1982 to 2017 at Rajshahi, Bangladesh

Month	Test Z	Slope of a trend line, Q (hr/yr)	Intercept of trend line, B (hr)	Average daily sunshine hour (hr)	Interannual trend of the average daily sunshine hour (%)
Jan	-5.013	-0.071***	7.643	6.52	-1.09
Feb	-1.866	-0.030+	8.665	7.95	-0.38
Mar	-2.465	-0.024*	8.744	8.23	-0.29
Apr	-2.683	-0.026**	8.503	8.05	-0.33
May	-1.131	-0.023	7.646	7.18	-0.31
Jun	-0.994	-0.015	5.312	5.26	-0.29
Jul	0.284	0.003	4.142	4.30	0.07
Aug	-0.852	-0.017	5.397	4.98	-0.35
Sep	0.852	0.019	5.267	5.52	0.34
Oct	-0.966	-0.016	7.687	7.20	-0.22
Nov	-1.562	-0.023	8.165	7.86	-0.29
Dec	-4.573	-0.100***	8.478	6.80	-1.46
Annual	-3.636	-0.028***	7.115	6.66	-0.42

*+ significant at 0.1, * significant at 0.05, ** significant at 0.01, *** significant at 0.001*

3.4 Effect of anthropogenic atmospheric aerosols on wheat production

The simulation results of APSIM on wheat production with and without anthropogenic aerosols at the SRFSI nodes in Nepal, India and Bangladesh are presented in this section. The simulation of wheat production with anthropogenic aerosols at the study nodes is conducted using observed meteorological data. The simulation of wheat production without aerosols is performed in two steps. In the first step, the simulation is performed by considering that anthropogenic aerosols have only affected solar radiation and in the second step, the simulation is run by considering that anthropogenic aerosols have affected solar radiation and daily maximum temperature during winter. The effect of anthropogenic aerosols on wheat production is discussed in terms of the radiation effect only and the combined radiation and temperature effect in the following subsections. The effect of anthropogenic aerosols on wheat production is discussed in terms of wheat grain yield, wheat biomass yield, and total crop evapotranspiration.

3.4.1 Effect of anthropogenic atmospheric aerosols on wheat production by considering only solar radiation effect

The simulation results on wheat production with and without anthropogenic aerosols at the eastern IGP study nodes (listed in Table 1) when considering only the solar radiation effect is covered in this subsection.

3.4.1.1 Effect on wheat grain yield

The APSIM simulation results for wheat grain yield with and without anthropogenic atmospheric aerosols during 2015-2017 at all the eastern IGP nodes are presented in Supplement Table 1. The simulation results indicate that anthropogenic aerosols reduce wheat grain yield in all the study nodes. The loss of wheat grain yield due to anthropogenic aerosols at the nodes ranges from 5.5%

at Tikapatti to 22.2% at Bhaluwa. The reduction of wheat yield due to anthropogenic aerosols is in line with the findings of (Liu et al., 2016) based upon the APSIM model. In addition, the decline of wheat yield under increased anthropogenic aerosols also agrees with the findings of Gupta et al. (2017) and Burney and Ramanathan (2014) based upon the statistical models in India. Country wise, different wheat varieties were cultivated at the nodes in the eastern IGP. The variation in loss of wheat grain yield across the nodes of the eastern IGP could be due to the sensitivity of the cultivated wheat variety to the radiation changes along with the variations in soil type and meteorological parameters. The summarized country wise effect on the wheat grain yield due to anthropogenic aerosols at the nodes of the eastern IGP is presented in Table 6. The table clearly shows that in all the country components of the eastern IGP, the average wheat grain yield is reduced significantly ranging from 6.7% in India to 16.1% in Nepal. The average grain yield across the nodes in the eastern IGP with and without anthropogenic aerosols is 3945.8 and 4560.8 kg/ha showing the loss of 615 kg/ha (13.5 %) on wheat yield during 2015-2017.

Table 6: Effect of anthropogenic aerosols (radiation only) on wheat grain yield in the eastern IGP

Country component of eastern IGP	District	Nodes	Year	Grain Yield (kg/ha)		Gain/loss of grain yield due to aerosols (+/-)	
				With aerosols	Without aerosols	(kg/ha)	%
Nepal	Sunsari	Bhaluwa and Simariya	2015-2016	3987.6	4751.4	-763.8	-16.1
India	Purnea	Tikapatti and Dogachhi	2015-2017	3832.2	4106.6	-274.4	-6.7
Bangladesh	Rajshahi and Rangapur	Baduria, Premtoli, Mohanpur and Kolkondo	2015-2017	3981.7	4692.6	-710.9	-15.1
Average of nodes in eastern IGP				**3945.8**	**4560.8**	**-615.0**	**-13.5**

3.4.1.2 Effect on wheat biomass yield

The APSIM simulation results for wheat biomass yield with and without anthropogenic atmospheric aerosols during 2015-2017 at all the eastern IGP nodes are presented in Supplement Table 2. The results clearly indicate that anthropogenic aerosols reduce wheat biomass yield at all the study nodes, which is due to the reduction in solar radiation. Since APSIM calculates daily biomass production based on light interception and radiation use efficiency (Yang et al., 2013), the biomass yield in the IGP nodes declined with the anthropogenic aerosols due to a reduction in solar radiation. The loss of wheat biomass yield due to anthropogenic aerosols at the eastern IGP nodes ranges from 10.5 % at Simariya and Dogachhi to 39.6 % at Mohonpur. The variation in wheat biomass yield loss across the nodes of the eastern IGP could be due to the sensitiveness of cultivated wheat variety to the change in radiation along with variations in soil type and meteorological parameters. It is observed that comparatively higher biomass loss due to anthropogenic aerosols is observed at nodes in Bangladesh. The summarized country wise effect on wheat biomass yield due to anthropogenic aerosols at the eastern IGP nodes is presented in Table 7. The table clearly shows that in all the country components of the eastern IGP, the wheat

biomass yield is reduced significantly ranging from 11.5 % at the nodes in Nepal and India to 31.4% in Bangladesh. The average biomass yield across the nodes in the eastern IGP with and without anthropogenic aerosols is 8280.5 and 10610.3 kg/ha, which is a loss of 22% of wheat biomass yield during 2015-2017 due to the reduction in solar radiation. Since wheat straw is used as basal feed for dairy livestock in the IGP (Erenstein, 2011), the reduction of wheat biomass by anthropogenic aerosols might have affected its availability in the eastern IGP.

Table 7: Effect of anthropogenic aerosols (radiation only) on wheat biomass yield in the eastern IGP

Country component of eastern IGP	District	Nodes	Year	Biomass Yield (kg/ha)		Gain/loss of biomass yield due to aerosols (+/-)	
				With aerosols	Without aerosols	(kg/ha)	(%)
Nepal	Sunsari	Bhaluwa and Simariya	2015-2016	9367.2	10578.5	-1211.3	-11.5
India	Purnea	Tikapatti and Dogachhi	2015-2017	8486.1	9589.1	-1103.0	-11.5
Bangladesh	Rajshahi and Rangapur	Baduria, Premtoli, Mohanpur and Kolkondo	2015-2017	7634.4	11136.8	-3502.4	-31.4
Average of nodes in eastern IGP				**8280.5**	**10610.3**	**-2329.8**	**-22.0**

3.4.1.3 Effect on wheat crop evapotranspiration

The simulation results on the effect of anthropogenic aerosols (by considering only the radiation effect) on wheat crop evapotranspiration at all the eastern IGP nodes during 2015-2017 are shown in Supplement Table 3. All nodes in the eastern IGP showed less crop evapotranspiration under anthropogenic aerosols due to the reduction in solar radiation. The decline in wheat crop evapotranspiration due to anthropogenic aerosols agrees with the findings of Yang et al. (2013) and Yao (2017). The reduction in crop evapotranspiration varied from 5 percent at Bhaluwa, Nepal to 27.3 percent at Baduria, Bangladesh. The fluctuation in crop evapotranspiration reduction could be due to variations in wheat variety, soil, and meteorological parameters. Comparatively higher loss in crop evapotranspiration due to anthropogenic aerosols is observed in Bangladesh nodes in a similar manner as that of biomass yield loss in those nodes. The summarized country wise effect at the eastern IGP nodes on wheat crop evapotranspiration due to anthropogenic aerosols is presented in Table 8. The table clearly shows that wheat crop evapotranspiration is reduced significantly in all the country component nodes of the eastern IGP, with reductions ranging from 5% at the nodes in Nepal to 20.3% at the nodes in Bangladesh. The average crop evapotranspiration across the nodes in the eastern IGP with and without anthropogenic aerosols are 269.6 and 311.6 mm showing a loss of 13.5% in crop evapotranspiration during 2015-2017. The results shows that the increased anthropogenic aerosols have reduced the irrigation water demand of wheat in the eastern IGP.

Table 8: Effect of anthropogenic aerosols (radiation only) on wheat evapotranspiration in the eastern IGP

Country component of eastern IGP	District	Nodes	Year	Crop Evapotranspiration (mm)		Increase/ decrease on crop evapotranspiration (+/-) due to aerosols	
				With aerosols	Without aerosols	(mm)	%
Nepal	Sunsari	Bhaluwa and Simariya	2015-2016	295.3	310.9	-15.6	-5.0
India	Purnea	Tikapatti and Dogachhi	2015-2017	313.8	346.9	-33.1	-9.5
Bangladesh	Rajshahi and Rangapur	Baduria, Premtoli, Mohanpur and Kolkondo	2015-2017	234.6	294.3	-59.7	-20.3
Average of nodes in eastern IGP				**269.6**	**311.6**	**-42.0**	**-13.5**

3.4.2 Effect of anthropogenic atmospheric aerosols on wheat production by considering the change in solar radiation and maximum winter temperature

The simulation results of wheat crop performance with and without anthropogenic aerosols at the eastern IGP study nodes in the when considering the aerosol effects on daily solar radiation and maximum temperature is covered in this sub section. The effect on anthropogenic aerosols on wheat crop performance is discussed in terms of wheat grain yield, wheat biomass yield and crop evapotranspiration in the following sub sections.

3.4.2.1 Effect on wheat grain yield

The APSIM simulation results for wheat grain yield with and without anthropogenic atmospheric aerosols when considering the aerosol effects on daily solar radiation and maximum temperature during 2015-2017 at all eastern IGP nodes are presented in Supplement Table 4. The simulation results indicate that anthropogenic aerosols reduce wheat grain yield in all study nodes except Simariya. The model indicated comparatively higher nitrogen stress of the wheat crop at Simariya, which could be due to comparatively poor soil fertility. The loss of wheat grain yield due to anthropogenic aerosols at the eastern IGP nodes ranges from -8.5 % at Simariya to 22.3% at Bhaluwa. The variations in wheat grain yield response across the nodes could be due to the sensitivity of the cultivated wheat varieties to radiation and maximum temperature along with variation in soil type, soil fertility, and meteorological parameters. The simulation results indicated that compared to the radiation only effect, the radiation and temperature (maximum) effect of anthropogenic aerosols have less loss in average grain yield in the eastern IGP nodes and this result is supported by the findings of Rao et al. (2015), who clearly indicated a negative correlation of maximum temperature and wheat yield in wheat growing areas in India, including the IGP region. The summarized country wise effect on wheat grain yield due to anthropogenic aerosols at the nodes is presented in Table 9. The table clearly shows that in all the country components of the eastern IGP, wheat grain yield is reduced significantly ranging from 7% in India to 14% in Bangladesh. The average grain yield across the nodes in the eastern IGP with and without

anthropogenic aerosols are 3945.8 and 4444.5 kg/ha showing a loss of 498.7 kg/ha (11.2%) in wheat yield during 2015-2017.

Table 9: Effect of anthropogenic aerosols (radiation and maximum temperature) on wheat grain yield in the eastern IGP

Country component of eastern IGP	District	Nodes	Year	Grain Yield (kg/ha)		Gain/ loss of grain yield due to aerosols (+/-)	
				With aerosols	Without aerosols	(kg/ha)	%
Nepal	Sunsari	Bhaluwa and Simariya	2015-2016	3987.6	4400.1	-412.4	-9.4
India	Purnea	Tikapatti and Dogachhi	2015-2017	3832.2	4122.4	-290.2	-7.0
Bangladesh	Rajshahi and Rangapur	Baduria, Premtoli, Mohanpur and Kolkondo	2015-2017	3981.7	4627.8	-646.1	-14.0
Average of nodes in eastern IGP				**3945.8**	**4444.5**	**-498.7**	**-11.2**

3.4.2.2 Effect on wheat biomass yield

The simulation results for wheat biomass yield with and without anthropogenic atmospheric aerosols during 2015-2017 at all eastern IGP nodes when considering aerosol effects on daily solar radiation and maximum temperature are presented in Supplement Table 5. The results clearly indicate that anthropogenic aerosols reduce wheat biomass yield in all the study nodes. The loss of wheat biomass yield due to anthropogenic aerosols at the nodes ranges from 3.5 % at Simariya to 38.9 % at Mohonpur. The variation in wheat biomass yield loss across the nodes could be due to the sensitivity of the cultivated wheat varieties to radiation and maximum temperature along with variations in soil type, fertility, and meteorological parameters. It is observed that comparatively higher biomass is lost due to anthropogenic aerosols at nodes in Bangladesh. Overall, the reduction in biomass yield when considering the aerosol effects on radiation and temperature is slightly less than when considering the radiation only effect in the eastern IGP (Supplement Table 2 and 5). These results are in line with the findings of Asseng et al. (2004) and Rao et al. (2015), who clearly indicated a negative association of maximum temperature with wheat grain and biomass yield. The summarized country wise effect on wheat biomass yield due to anthropogenic aerosols at the eastern IGP nodes is presented in Table 10. The table clearly shows that in all the country components of the eastern IGP the wheat biomass yield is reduced significantly ranging from 9.7 at the nodes in Nepal to 30.9 in Bangladesh. The average biomass yield across the nodes in the eastern IGP with and without anthropogenic aerosols are 8280.5 and 10511.1 kg/ha, which shows a loss of 21.2% in wheat biomass yield during 2015-2017 due to the reduction in solar radiation and maximum temperature.

Table 10: Effect of anthropogenic aerosols (radiation and maximum temperature) on wheat biomass yield in the eastern IGP

Country component of eastern IGP	District	Nodes	Year	Biomass Yield (kg/ha)		Gain/ loss of biomass yield due to aerosols (+/-)	
				With aerosols	Without aerosols	(kg/ha)	(%)
Nepal	Sunsari	Bhaluwa and Simariya	2015-2016	9367.2	10375.0	-1007.8	-9.7
India	Purnea	Tikapatti and Dogachhi	2015-2017	8486.1	9563.7	-1077.6	-11.3
Bangladesh	Rajshahi and Rangapur	Baduria, Premtoli, Mohanpur and Kolkondo	2015-2017	7634.4	11052.8	-3418.4	-30.9
Average of nodes in eastern IGP				**8280.5**	**10511.1**	**-2230.6**	**-21.2**

3.4.2.3 Effect on wheat crop evapotranspiration

The APSIM simulation results of the effect of anthropogenic aerosols, when considering their effects on solar radiation and maximum temperature, on wheat crop evapotranspiration at the eastern IGP nodes during 2015-2017 are shown in Supplement Table 6. All the nodes in the eastern IGP showed less crop evapotranspiration under anthropogenic aerosols due to the reduction in solar radiation and maximum temperature. The reduction in crop evapotranspiration varied from 8.4 percent at Simariya, Nepal to 27.7 percent at Baduria, Bangladesh. The variations in crop evapotranspiration reduction could be due to variations in the wheat variety, soil, and meteorological parameters. Comparatively higher loss in crop evapotranspiration due to anthropogenic aerosols is observed at Bangladesh nodes in a similar manner as that of biomass yield loss in those nodes. These findings are supported by those of Zhang et al. (2011), who showed a linear relationship between wheat biomass yield and evapotranspiration. The summarized country wise effect at the eastern IGP nodes of the reduction in wheat crop evapotranspiration due to anthropogenic aerosols is presented in Table 11. The table clearly indicates that in all the country components of the eastern IGP, wheat crop evapotranspiration is reduced significantly ranging from 8.5% at the nodes in Nepal to 21.5% at the nodes in Bangladesh. The average crop evapotranspiration across the nodes in the eastern IGP with and without anthropogenic aerosols are 269.6 and 317.4 mm, which is a loss of 15.1% in crop evapotranspiration during 2015-2017.

Table 11: Effect of anthropogenic aerosols (radiation and maximum temperature) on wheat evapotranspiration in the eastern IGP

Country component of eastern IGP	District	Nodes	Year	Crop Evapotranspiration (mm)		Increase/ decrease on crop evapotranspiration (+/-) due to aerosols	
				With aerosols	Without aerosols	(mm)	%
Nepal	Sunsari	Bhaluwa and Simariya	2015-2016	295.3	322.6	-27.3	-8.5
India	Purnea	Tikapatti and Dogachhi	2015-2017	313.8	349.4	-35.5	-10.2
Bangladesh	Rajshahi and Rangapur	Baduria, Premtoli, Mohanpur and Kolkondo	2015-2017	234.6	298.9	-64.3	-21.5
Average of nodes in eastern IGP				**269.6**	**317.4**	**-47.9**	**-15.1**

3.5 Loss due to the reduction in wheat yield

In this subsection, we estimate the loss of wheat production due to anthropogenic aerosols by considering the radiation only effect and the radiation and temperature effects in the eastern IGP region. The estimated loss in wheat production due to anthropogenic aerosols is presented in Table 12. The average area of wheat cultivated in the Nepal component, India component and Bangladesh component of the eastern IGP from 2011 to 2015 were 440,140, 2,447,580 and 402,940 Ha respectively (BBS, 2018; Datanet India, n.d.; MOAD, 2018). Average wheat cultivated area in the eastern IGP region is 3,290,660 ha. While considering only the radiation effect, the average model estimated yield reductions due to anthropogenic aerosols at the nodes in Nepal, India and Bangladesh are 0.764, 0.274, 0.711 t/ha respectively (see Table 6). Similarly, when considering the solar radiation and temperature effect of anthropogenic aerosols, the average yield reduction estimated by the APSIM model at the nodes in Nepal, India and Bangladesh are 0.412, 0.290, 0.646 t/ha respectively (see Table 9). The estimated wheat production reduction in the eastern IGP while considering only the radiation effect is 1293.39 thousand metric tons. While considering both the temperature and radiation effect, the reduction of wheat production by anthropogenic aerosols is estimated to be 1151.44 thousand metric tons. While considering the population of eastern IGP (361 million), the wheat production loss due to anthropogenic aerosols is estimated to be more than 3.2 kg of wheat per capita per annum during the study period. Given that the average wholesale price of wheat at Patna, a market in the eastern IGP from April 2014 to April 2019 is 262.50 USD/ton (FAO, n.d.), then the total estimated loss in wheat production due to anthropogenic aerosols by considering only radiation effect is USD$339.52 million dollars whereas by considering both radiation and temperature effect is USD$302.25 million dollars. In summary, it is estimated that anthropogenic aerosols reduce wheat production in the eastern IGP by more than 1.1 million tons equivalent, which is worth more than USD$300 million dollars. These values indicate the significant contribution an improvement in air quality could achieve in the eastern IGP, even when only considering wheat production.

Generally, the cost of air pollution is estimated based on its negative effect on people's health. For example, the world bank estimated the cost of air pollution (welfare loss from air pollution) in several regions of the world including South Asia by considering the negative health effect on increased premature death and foregone labour output (World Bank Group and IHME, 2016). The report estimated welfare losses from ambient $PM_{2.5}$ in South Asia in the year 2013 as USD$256 billion. While comparing the cost of wheat production loss in the eastern IGP with the loss estimated by the World Bank group over the entire South Asia, it can be concluded that the economic loss of air pollution on agricultural production is significant and needs to be included when assessing the economic losses due to air pollution.

Table 12: Estimated loss in wheat production due to anthropogenic aerosols in the eastern IGP

Country component of eastern IGP	Average area* ('000 Ha)	Reduction in wheat yield due to atmospheric aerosols while considering		Estimated wheat production reduced due to anthropogenic aerosols while considering		Estimated loss# in wheat production due to anthropogenic aerosols while considering	
		Only radiation effect (T/ha)	Radiation & temperature effect (T/ha)	Only radiation effect ('000 T)	Radiation & temperature effect ('000 T)	Only radiation effect (Million USD)	Radiation & temperature effect (Million USD)
Nepal [1]	440.14	-0.764	-0.412	-336.27	-181.34	-88.27	-47.60
India[2]	2447.58	-0.274	-0.290	-670.64	-709.80	-176.04	-186.32
Bangladesh [3]	402.94	-0.711	-0.646	-286.49	-260.30	-75.20	-68.33
Eastern IGP	**3290.66**	**-0.615**	**-0.499**	**-1293.39**	**-1151.44**	**-339.52**	**-302.25**

** based on 5 years (2011- 2015) respective country statistics* (MOAD, 2018)*[1],* (Datanet India, n.d.)*[2] and* (BBS, 2018)*[3]*
 # based on the average wholesale price of wheat (262.50 USD/ton) at Patna (eastern IGP) from April 2014 to April 2019

4.0 Summary and Conclusions

In the context of persistently high levels of anthropogenic aerosols during winter in the eastern IGP, the present study examines the effect of anthropogenic aerosols on one of the important winter crops, wheat, using the process-based APSIM model. The APSIM model was calibrated and validated using data from the SRFSI project on-farm trials of rice-wheat cropping system at 8 nodes in the eastern IGP (4 in Bangladesh and 2 each in Nepal and India). The calibrated APSIM model was run with the observed meteorological data, which provides an estimate of wheat crop performance under anthropogenic aerosols at the eastern IGP nodes. Wheat crop performance without anthropogenic aerosols was obtained in two ways, first by running the model with adjusted observed solar radiation by estimating changed radiative forcing (considering only the radiative effect of anthropogenic aerosols) and second by running the model with adjusted solar radiation and maximum temperature data (considering the radiation as well as temperature effect of anthropogenic aerosols). The radiative effect of anthropogenic aerosols is estimated via the empirical model of clear sky radiative forcing developed by Shrestha et al. (2018) and MERRA cloud fraction and cloud albedo over the SRFSI nodes and seasonal anthropogenic emission coefficients. In addition to the radiative effect, the temperature effect of anthropogenic aerosols in the eastern IGP was adapted in terms of a reduction of 0.5 ◦C on maximum temperature as suggested by Freychet et al. (2019). The impact of anthropogenic aerosols when considering only the radiative effect and the radiative and temperature effects was analysed at all 8 SRFSI nodes during 2015 -2017. In addition, the aerosol loading, its trend, radiative forcing and the solar

radiation trend at the study nodes were also analysed. The major findings of this study are listed below.

The analysis of AERONET AOD in the eastern IGP stations during 2003-2017 indicate that in all months except during monsoon season, the average AOD of eastern IGP stations are high (greater than 0.5) with a peak during winter months. Annual mean particulate matter $PM_{2.5}$ at eastern IGP stations is found to be more than 7 to 11 times higher than WHO guidelines. At all the stations in the eastern IGP, the monthly average particulate matter is increasing in post-monsoon months and reaches a peak during winter, which could be due to increased emissions from biomass burning, fossil fuel emissions, as well as enhanced atmospheric stabilization during winter months.

The estimated average annual radiative forcing due to anthropogenic aerosols at the SRFSI districts in the eastern IGP ranges from -49.83 to -63.15 Wm^{-2}. Regarding the seasonal distribution of radiative forcing, highest radiative forcing is observed during the winter season and lowest radiative forcing is observed during monsoon season. Regarding the annual trend, all the SRFSI districts showed a statistically significant declining trend of radiative forcing during 2003 - 2017 at least at the statistical significance level of 0.01. The rate of decline varied from 1.01 Wm^{-2} $year^{-1}$ at Rajshahi to 1.5 Wm^{-2} $year^{-1}$ at Rangapur during 2003 - 2017. Regarding seasonal radiative forcing, pre-monsoon season radiative forcing shows a declining trend in all SRFSI districts at least at the statistical significance level of 0.05.

The historical trend of annual average sunshine hours at Sunsari and Rajshahi showed a declining trend at the rate of 0.42 and 0.52% per annum at least at the statistical significance level of 0.05. Regarding the monthly average trend in sunshine hours, both districts showed a statistically significant declining trend in the winter months of December and January at the rate of more than 1% per annum. The higher declining trend of sunshine hours during winter months could be due to an increased level of anthropogenic aerosols. Due to the high declining trend of sunshine hours during winter months, it is expected this will affect winter crops significantly.

The APSIM simulation results when only considering the radiative effect of anthropogenic aerosols, indicate that the average grain yield loss in the eastern IGP is 615 kg/ha (13.5%). When considering both the radiative and temperature effects the simulation results showed the average loss of wheat grain yield at 498.7 kg/ha (11.2%) in the eastern IGP nodes. From these results, it can be concluded that anthropogenic aerosols result in significant grain yield loss at the range of 0.5 t/ha in the eastern IGP nodes. It is also revealed that the reduction of per capita wheat production due to anthropogenic aerosols in the eastern IGP is about 3.2 kg per annum. Hence the substantial decline of wheat grain yield indicates a threat to the food security of the eastern IGP by anthropogenic aerosols (air pollution).

The APSIM model results also showed that anthropogenic aerosols reduced biomass yield significantly at all eastern IGP nodes. When considering the radiative only and the radiative and temperature effects of anthropogenic aerosols the average biomass yield in the eastern IGP nodes reduced by 22% and 21.2 % respectively. The reduction in biomass yield by the anthropogenic aerosols may also affect soil organic matter and animal fodder in the eastern IGP.

The APSIM model simulations when considering only the anthropogenic aerosols radiative effect reduced average wheat crop evapotranspiration by 42 mm (13.5%) at the eastern IGP nodes.

When considering both radiative and temperature effects of anthropogenic aerosols, wheat crop evapotranspiration reduced by 47.9 mm (15.1%). Significant reduction in crop evapotranspiration due to anthropogenic aerosols, if considered during irrigation scheduling may significantly save irrigation water.

By combining the average wheat yield loss from nodes in each country due to anthropogenic aerosols, average wheat cultivated area in each country component of the eastern IGP and the average wheat price for the study period, the estimated loss in wheat production due to anthropogenic aerosols was estimated in the eastern IGP. When considering only the radiative effect, wheat production loss caused by anthropogenic aerosols was estimated at USD$339.52 million in the eastern IGP per annum during 2015-2017. When considering both the radiative and temperature effects, wheat production loss caused by anthropogenic aerosols was estimated at USD$302.25 million in the eastern IGP per annum during 2015-2017. As the lost wheat production due to anthropogenic aerosols is found to be a significant amount, similar studies also need to be conducted for the other major crops in the eastern IGP to estimate the total economic loss from all crop production, which would make a significant contribution to assessing the economic loss due to air pollution in the eastern IGP.

References

Agrawal, M., Singh, B., Rajput, M., Marshall, F., Bell, J.N.B., 2003. Effect of air pollution on peri-urban agriculture : a case study. Environ. Pollut. 126, 323–329. https://doi.org/10.1016/S0269-7491(03)00245-8

Archontoulis, S. V, Miguez, F.E., Moore, K.J., 2014. Evaluating APSIM maize , soil water , soil nitrogen , manure , and soil temperature modules in the midwestern United States. Agron. J. 106, 1025–1040. https://doi.org/10.2134/agronj2013.0421

Asseng, S., Fillery, I.R.P., Anderson, G.C., Dolling, P.J., Dunin, F.X., Keating, B.A., 1998. Use of the APSIM wheat model to predict yield, drainage, and NO3 leaching for a deep sand. Aust. J. Agric. Res. 49, 363–77.

Asseng, S., Jamieson, P.D., Kimball, B., Pinter, P., Sayre, K., 2004. Simulated wheat growth affected by rising temperature , increased water deficit and elevated atmospheric CO 2. F. Crop. Res. 85, 85–102. https://doi.org/10.1016/S0378-4290(03)00154-0

Auffhammer, M., Ramanathan, V., Vincent, J.R., 2006. Integrated model shows that atmospheric brown clouds and greenhouse gases have reduced rice harvests in India. PNAS 103.

Babu, S.S., Manoj, M.R., Moorthy, K.K., Gogoi, M.M., Nair, V.S., Kompalli, S.K., Satheesh, S.K., Niranjan, K., Ramagopal, K., Bhuyan, P.K., Singh, D., 2013. Trends in aerosol optical depth over Indian region: Potential causes and impact indicators. J. Geophys. Res. Atmos. 118, 11794–11806. https://doi.org/10.1002/2013JD020507

Balakrishnan, K., Dey, S., Gupta, T., Dhaliwal, R.S., Brauer, M., Cohen, A.J., Stanaway, J.D., Beig, G., Joshi, T.K., Aggarwal, A.N., Sabde, Y., Sadhu, H., Frostad, J., Causey, K., Godwin, W., Shukla, D.K., Kumar, G.A., Varghese, C.M., Muraleedharan, P., Agrawal, A., Anjana, R.M., Bhansali, A., Bhardwaj, D., Burkart, K., Cercy, K., Chakma, J.K., Chowdhury, S., Christopher, D.J., Dutta, E., Furtado, M., Ghosh, S., Ghoshal, A.G., Glenn, S.D., Guleria, R., Gupta, R., Jeemon, P., Kant, R., Kant, S., Kaur, T., Koul, P.A., Krish, V., Krishna, B., Larson, S.L., Madhipatla, K., Mahesh, P.A., Mohan, V., Mukhopadhyay, S., Mutreja, P., Naik, N., Nair, S., Nguyen, G., Odell, C.M., Pandian, J.D., Prabhakaran, D., Prabhakaran, P., Roy, A., Salvi, S., Sambandam, S., Saraf, D., Sharma, M., Shrivastava, A., Singh, V., Tandon, N., Thomas, N.J., Torre, A., Xavier, D., Yadav, G., Singh, S., Shekhar, C., Vos, T., Dandona, R., Reddy, K.S., Lim, S.S., Murray, C.J.L., Venkatesh, S., Dandona, L., 2019. Articles The impact of air pollution on deaths , disease burden , and life expectancy across the states of India : the Global Burden of Disease Study 2017. planetary-health 3. https://doi.org/10.1016/S2542-5196(18)30261-4

Balasubramanian, V., Adhya, T.K., Ladha, J.K., 2013. Enhancing eco-efficiency in the intensive cereal-based systems of the Indo-Gangetic plains, in: Hershey, C.H., Neate, P. (Eds.), Eco-Efficiency: From Vision to Reality (Issues in Tropical Agriculture Series). International Center for Tropical Agriculture, Cali, Colombia, pp. 99–115. https://doi.org/doi:10.1201/b17133-197

Banerjee, T., 2017. Airing ‘ clean air ’ in Clean India Mission. Environ. Sci. Pollut. Res. 24, 6399–6413. https://doi.org/10.1007/s11356-016-8264-y

BBS, 2018. 45 years Agriculture Statistics of Major Crops (Aus , Amon , Boro , Jute , Potato & Wheat) Bangladesh Bureau of Statistics (BBS) Statistics and Informatics Division (SID).

Bergin, M.H., Ghoroi, C., Dixit, D., Schauer, J.J., Shindell, D., 2017. Large reductions in solar energy

production due to dust and particulate air pollution. Environ. Sci. Technol. Lett. acs.estlett.7b00197. https://doi.org/10.1021/acs.estlett.7b00197

Boote, K.J., Jones, J.W., Pickering, N.B., 1996. Potential Uses and Limitations of Crop Models. Agron. J. 88, 704–716. https://doi.org/10.2134/agronj1996.00021962008800050005x

Brook, R.D., Rajagopalan, S., Iii, C.A.P., Brook, J.R., Bhatnagar, A., Diez-roux, A. V, Holguin, F., Hong, Y., Luepker, R. V, Mittleman, M.A., Peters, A., Siscovick, D., Smith, S.C., Whitsel, L., Kaufman, J.D., 2010. Particulate Matter Air Pollution and Cardiovascular Disease An Update to the Scientific Statement From the American. Circulation 21, 2331–2378. https://doi.org/10.1161/CIR.0b013e3181dbece1

Burney, J., Ramanathan, V., 2014. Recent climate and air pollution impacts on India agriculture. Proc. Natl. Acad. Sci. 111, 16319–16324. https://doi.org/10.1073/pnas.1317275111

CBS, 2014. Statistical pocket book of Nepal 2014. Central Bureau of Statistics, National Planning Commission Secretariat, Government of Nepal, Kathmandu, Nepal. https://doi.org/10.2833/77358

Chameides, W.L., Yu, H., Liu, S.C., Bergin, M., Zhou, X., Mearns, L., Wang, G., Kiang, C.S., Saylor, R.D., Luo, C., Huang, Y., Steiner, A., Giorgi, F., 1999. Case study of the effects of atmospheric aerosols and regional haze on agriculture: an opportunity to enhance crop yields in China through emission controls?, in: Proceedings of the National Academy of Sciences of the United States of America. pp. 13626–13633. https://doi.org/10.1073/pnas.96.24.13626

Chen, X., Zhang, Xiaobo, Zhang, Xin, 2018. The impact of exposure to air pollution on cognitive performance. PNAS 115, 9193–9197. https://doi.org/10.1073/pnas.1809474115

Coakley, J.A., Baldwin, D.G., 1984. Towards the Objective Analysis of Clouds from Satellite Imagery Data. J. Clim. Appl. Meteorol. https://doi.org/10.1175/1520-0450(1984)023<1065:ttoaoc>2.0.co;2

Conibear, L., Butt, E.W., Knote, C., Arnold, S.R., Spracklen, D. V., 2018a. Residential energy use emissions dominate health impacts from exposure to ambient particulate matter in India. Nat. Commun. 9, 1–9. https://doi.org/10.1038/s41467-018-02986-7

Conibear, L., Butt, E.W., Knote, C., Arnold, S.R., Spracklen, D. V., 2018b. Stringent emission control policies can provide large improvements in air quality and public health in India. GeoHealth 1–16. https://doi.org/10.1029/2018GH000139

Das, S.K., Chatterjee, A., Ghosh, S.K., Raha, S., 2015. An integrated campaign for investigation of winter-time continental haze over Indo-Gangetic Basin and its radiative effects. Sci. Total Environ. 533, 370–82. https://doi.org/10.1016/j.scitotenv.2015.06.085

Datanet India, n.d. Socio economic statistical information about India [WWW Document]. Indiastat. URL https://www.indiastat.com (accessed 7.7.18).

David, L.M., Ravishankara, A.R., Kodros, J.K., Venkataraman, C., Sadavarte, P., Pierce, J.R., Chaliyakunnel, S., Millet, D.B., 2018. Aerosol optical depth over India. J. Geophys. Res. Atmos. 123, 1–16. https://doi.org/10.1002/2017JD027719

Dey, S., Tripathi, S.N., 2008. Aerosol direct radiative effects over Kanpur in the Indo-Gangetic basin, northern India: Long-term (2001-2005) observations and implications to regional

climate. J. Geophys. Res. Atmos. 113, 1–20. https://doi.org/10.1029/2007JD009029

Dey, S., Tripathi, S.N., 2007. Estimation of aerosol optical properties and radiative effects in the Ganga basin, northern India, during the wintertime. J. Geophys. Res 112, 1–16. https://doi.org/10.1029/2006JD007267

Dey, S., Tripathi, S.N., Singh, R.P., Holben, B.N., 2004. Influence of dust storms on the aerosol optical properties over the Indo-Gangetic basin. J. Geophys. Res. 109, 1–13. https://doi.org/10.1029/2004JD004924

Erenstein, O., 2011. Cropping systems and crop residue management in the Trans-Gangetic Plains: Issues and challenges for conservation agriculture from village surveys. Agric. Syst. 104, 54–62. https://doi.org/10.1016/j.agsy.2010.09.005

Erenstein, O., Thorpe, W., Singh, J., Varma, A., 2007. Crop–livestock interactions and livelihoods in the Trans-Gangetic Plains, India.

FAO, n.d. Food Price monitoring and Analysis [WWW Document]. FPMA. URL http://www.fao.org/giews/food-prices/tool/public/ (accessed 5.9.19).

Fosu, B.O., Wang, S.Y.S., Wang, S.H., Gillies, R.R., Zhao, L., 2017. Greenhouse gases stabilizing winter atmosphere in the Indo-Gangetic plains may increase aerosol loading. Atmos. Sci. Lett. 18, 168–174. https://doi.org/10.1002/asl.739

Freychet, N., Tett, S.F.B., Bollasina, M., Wang, K.C., Hegerl, G.C., 2019. The Local Aerosol Emission Effect on Surface Shortwave Radiation and Temperatures. J. Adv. Model. Earth Syst. https://doi.org/10.1029/2018MS001530

Gathala, M.K., Tiwari, T., Islam, S., Maharjan, S., Gerard, B., 2018. Research synthesis report Sustainable and Resilient Farming Systems Intensification in the Eastern Gangetic Plains. Canberra.

Gautam, R., Hsu, N.C., Kafatos, M., Tsay, S.C., 2007. Influences of winter haze on fog/low cloud over the Indo-Gangetic plains. J. Geophys. Res. Atmos. 112, 1–11. https://doi.org/10.1029/2005JD007036

Gautam, R., Hsu, N.C., Lau, K.M., 2010. Premonsoon aerosol characterization and radiative effects over the Indo-Gangetic plains: Implications for regional climate warming. J. Geophys. Res. Atmos. 115, 1–15. https://doi.org/10.1029/2010JD013819

Gaydon, D., Chaki, A., Dutta, S.K., Laing, A., Poulton, P., 2018. APSIM Modelling for on- farm SRFSI trials in the EGP.

Gaydon, D.S., Wang, E., Poulton, P.L., Ahmad, B., Ahmed, F., Akhter, S., Ali, I., Amarasingha, R., Chaki, A.K., Chen, C., Choudhury, B.U., Darai, R., Das, A., Hochman, Z., Horan, H., Hosang, E.Y., Kumar, P.V., Khan, A.S.M.M.R., Laing, A.M., Liu, L., Malaviachichi, M.A.P.W.K., Mohapatra, K.P., Muttaleb, M.A., Power, B., Radanielson, A.M., Rai, G.S., Rashid, M.H., Rathanayake, W.M.U.K., Sarker, M.M.R., Sena, D.R., Shamim, M., Subash, N., Suriadi, A., Suriyagoda, L.D.B., Wang, G., Wang, J., Yadav, R.K., Roth, C.H., 2017. Field Crops Research Evaluation of the APSIM model in cropping systems of Asia. F. Crop. Res. 204, 52–75. https://doi.org/10.1016/j.fcr.2016.12.015

Gilbert, R.O., 1987. Statistical Methods for Environmental Pollution Monitoring. Van Nostrand

Reinhold Company, New York. https://doi.org/10.2307/1270090

Gilgen, H., Wild, M., Ohmura, A., 1998. Means and trends of shortwave irradiance at the surface estimated from global energy balance archive data. J. Clim. 11, 2042–2061. https://doi.org/10.1175/1520-0442-11.8.2042

Greenwald, R., Bergin, M.H., Xu, J., Cohan, D., Hoogenboom, G., Chameides, W.L., 2006. The influence of aerosols on crop production: A study using the CERES crop model. Agric. Syst. 89, 390–413. https://doi.org/10.1016/j.agsy.2005.10.004

Gupta, R., Seth, A., 2007. A review of resource conserving technologies for sustainable management of the rice-wheat cropping systems of the Indo-Gangetic plains (IGP). Crop Prot. 26, 436–447. https://doi.org/10.1016/j.cropro.2006.04.030

Gupta, R., Somanathan, E., Dey, S., 2017. Global warming and local air pollution have reduced wheat yields in India. Clim. Change 140, 593–604. https://doi.org/10.1007/s10584-016-1878-8

Heagle, A.S., Kress, L.W., Temple, P.J., Kohut, R.J., Miller, J.E., Heggestad, H.E., 1987. Factors influencing ozone dose-yield response relationships in open-top field chamber studies, in: Heck, W.W., Taylor, O.C., Tingey, D.T. (Eds.), Assessment of Crop Loss from Air Pollution. Elsevier Appplied Science, London and New York, pp. 141–180.

Health Effects Institute, 2018. State of global air/ 2018 a special report on global exposure to air pollution and its disease burden. Boston, MA.

Hirano, T., Kiyota, M., Aiga, I., 1995. Physical effects of dust on leaf physiology of cucumber and kidney bean plants. Environ. Pollut. 89, 255–261.

Hunt, J., Norton, R., 2011. Finding an agro-ecological niche for juncea canola, in: 17th Australian Research Assembly on Brassicas (ARAB). pp. 134–138.

Huth, N.I., Possingham, H., 2007. Tradeoffs in Dryland Agroforesty : Birds vs Dollars, in: Oxley, L., Kulasiri, D. (Eds.), MODSIM 2007 International Congress on Modelling and Simulation. Modelling and Simulation Society of Australia and New Zealand, pp. 2250–2256.

IQAir AirVisual, 2018. 2018 WORLD AIR QUALITY REPORT.

Ittersum, M.K. Van, Kropff, M.J., Bastiaans, L., Goudriaan, J., 2003. On approaches and applications of the Wageningen crop models On approaches and applications of the Wageningen crop models. Eur. J. Agron. 18, 201–234. https://doi.org/10.1016/S1161-0301(02)00106-5

Jethva, H., Satheesh, S.K., Srinivasan, J., 2005. Seasonal variability of aerosols over the Indo-Gangetic basin. J. Geophys. Res. Atmos. 110, 1–15. https://doi.org/10.1029/2005JD005938

Jones, J.W., Antle, J.M., Basso, B., Boote, K.J., Conant, R.T., Foster, I., Godfray, H.C.J., Herrero, M., Howitt, R.E., Janssen, S., Keating, B.A., Munoz-carpena, R., Porter, C.H., Rosenzweig, C., Wheeler, T.R., 2016. Brief history of agricultural systems modeling. Agric. Syst. 155, 240–254. https://doi.org/10.1016/j.agsy.2016.05.014

Kar, J., Deeter, M.N., Fishman, J., Liu, Z., Omar, A., Creilson, J.K., Trepte, C.R., Vaughan, M.A., Winker, D.M., 2010. Wintertime pollution over the Eastern Indo-Gangetic Plains as observed from MOPITT, CALIPSO and tropospheric ozone residual data. Atmos. Chem. Phys. 10,

12273–12283. https://doi.org/10.5194/acp-10-12273-2010

Kaskaoutis, D.G., Singh, R.P., Gautam, R., Sharma, M., Kosmopoulos, P.G., Tripathi, S.N., 2012. Variability and trends of aerosol properties over Kanpur, northern India using AERONET data (2001–10). Environ. Res. Lett. 7, 024003. https://doi.org/10.1088/1748-9326/7/2/024003

Keating, B.A., Carberry, P.S., Hammer, G.L., Probert, M.E., Robertson, M.J., Holzworth, D., Huth, N.I., Hargrea, J.N.G., 2003. An o v er v iew of APSIM , a model designed for farming systems simulation. Eur. J. Agron. 18, 267–288.

Krishna Moorthy, K., Suresh Babu, S., Manoj, M.R., Satheesh, S.K., 2013. Buildup of aerosols over the Indian Region. Geophys. Res. Lett. 40, 1011–1014. https://doi.org/10.1002/grl.50165

Kumar, M., Parmar, K.S., Kumar, D.B., Mhawish, A., Broday, D.M., Mall, R.K., Banerjee, T., 2018. Long-term aerosol climatology over Indo-Gangetic Plain: Trend, prediction and potential source fields. Atmos. Environ. 180, 37–50. https://doi.org/10.1016/j.atmosenv.2018.02.027

Kumar, M., Raju, M.P., Singh, R.K., Singh, A.K., Singh, R.S., Banerjee, T., 2017. Wintertime characteristics of aerosols over middle Indo-Gangetic Plain: Vertical profile, transport and radiative forcing. Atmos. Res. 183, 268–282.

Kumari, B.P., Londhe, A.L., Daniel, S., Jadhav, D.B., 2007. Observational evidence of solar dimming : Offsetting surface warming over India 34, 1–5. https://doi.org/10.1029/2007GL031133

Lau, K.M., Kim, K.M., 2006. Observational relationships between aerosol and Asian monsoon rainfall, and circulation. Geophys. Res. Lett. 33, 1–5. https://doi.org/10.1029/2006GL027546

Li-li, M., Li-zhen, Z., Si-ping, Z., Evers, J.B., Wert, W. van der, Jing-jing, W., Hong-quan, S., Zhi-cheng, S., Spiertz, H., 2015. Resource use efficiency, ecological intensification and sustainability of intercropping system. J. Integr. Agric. 14, 1542–1550. https://doi.org/10.1016/S2095-3119(15)61039-5

Liu, X., Sun, H., Feike, T., Zhang, X., Shao, L., Chen, S., 2016. Assessing the impact of air pollution on grain yield of winter wheat - a case study in the North China plain. PLoS One 11, 1–16. https://doi.org/10.1371/journal.pone.0162655

Liu, Y., Wu, W., Jensen, M.P., Toto, T., 2011. Relationship between cloud radiative forcing, cloud fraction and cloud albedo, and new surface-based approach for determining cloud albedo. Atmos. Chem. Phys. 11, 7155–7170. https://doi.org/10.5194/acp-11-7155-2011

Lohmann, U., Feichter, J., 2004. Global indirect aerosol effects: a review. Atmos. Chem. Phys. Discuss. 4, 7561–7614. https://doi.org/10.5194/acpd-4-7561-2004

Maggs, R., Wahid, A., Shamsi, S.R.A., Ashmore, M.R., 1995. Effects of ambient air pollution on wheat and rice yield in Pakistan. Water. Air. Soil Pollut. 85, 1311–1316.

Mamun, M.I., Islam, M., Mondol, P.K., 2014. The seasonal variability of aerosol optical depth over Bangladesh based on satellite data and HYSPLIT model. Am. J. Remote Sens. 2, 20–29. https://doi.org/10.11648/j.ajrs.20140204.11

Mao, K.B., Ma, Y., Xia, L., Chen, W.Y., Shen, X.Y., He, T.J., Xu, T.R., 2014. Global aerosol change in the last decade: An analysis based on MODIS data. Atmos. Environ. 94, 680–686.

https://doi.org/10.1016/j.atmosenv.2014.04.053

McCown, R.L., Hammer, G.L., Hargreaves, J.N.G., Holzworth, D.P., Freebairn, D.M., 1996. APSIM : a novel software system for model development , model testing and simulation in agricultural systems research 50, 255–271.

Meehl, G.A., Arblaster, J.M., Collins, W.D., 2008. Effects of Black Carbon Aerosols on the Indian Monsoon. J. Clim. 21, 2869–2882. https://doi.org/10.1175/2007JCLI1777.1

Mehta, M., Singh, R., Singh, A., Singh, N., Anshumali, 2016. Recent global aerosol optical depth variations and trends - A comparative study using MODIS and MISR level 3 datasets. Remote Sens. Environ. 181, 137–150. https://doi.org/10.1016/j.rse.2016.04.004

Middleton, N.J., 1986. A geography of dust storms in South - West Asia. J. Climatol. 6, 183–196. https://doi.org/10.1002/joc.3370060207

Mina, U., Chandrashekara, T.K., Kumar, S.N., Meena, M.C., Yadav, S., Tiwari, S., Singh, D., Kumar, P., Kumar, R., 2018. Impact of particulate matter on basmati rice varieties grown in Indo-Gangetic Plains of India: Growth, biochemical, physiological and yield attributes. Atmos. Environ. 188, 174–184. https://doi.org/10.1016/j.atmosenv.2018.06.015

MOAD, 2018. Statistical information of Nepalese agriculture. Kanthmandu.

MOAD, 2015. Statistical Information on Nepalese Agriculture. Government of Nepal Ministry of Agricultural Development Agribusiness Promotion and Statistics Division Agri Statistics section, Kathmandu, Nepal.

Monlruzzaman, Rahman, M.S., Karim, M.K., Alam, Q.M., 2009. Agro economic analysis of maize production in bangladesh: a farm level study. Bangladesh J. Agril. Res. 34, 15–24.

Niroula, N., Kobayashi, K., Xu, J., 2015. Sunshine duration is declining in Nepal across the period from 1987 to 2010. J. Agric. Meteorol. 71, 15–23. https://doi.org/10.2480/agrmet.D-14-00025

Pal, D.K., Bhattacharyya, T., Srivastava, P., Chandran, P., Ray, S.K., 2009. Soils of the Indo-Gangetic Plains : their historical perspective and management. Curr. Sci. 96, 1193–1202.

Paliwal, U., Sharma, M., Burkhart, J.F., 2016. Monthly and spatially resolved black carbon emission inventory of India: Uncertainty analysis. Atmos. Chem. Phys. 16, 12457–12476. https://doi.org/10.5194/acp-16-12457-2016

Pandey, S.K., Vinoj, V., Landu, K., Babu, S.S., 2017. Declining pre-monsoon dust loading over South Asia: Signature of a changing regional climate. Sci. Rep. 7, 1–10. https://doi.org/10.1038/s41598-017-16338-w

Paydar, Z., Gallant, J., 2008. A catchment framework for one-dimensional models : introducing FLUSH and its application. Hydrol. Process. 22, 2094–2104. https://doi.org/10.1002/hyp

Przybysz, A., Sæbø, A., Hanslin, H.M., Gawro, S.W., 2014. Accumulation of particulate matter and trace elements on vegetation as affected by pollution level , rainfall and the passage of time. Sci. Total Environ. 481, 360–369. https://doi.org/10.1016/j.scitotenv.2014.02.072

Ramachandran, S., Kedia, S., 2012a. Radiative effects of aerosols over Indo-Gangetic plain:

environmental (urban vs. rural) and seasonal variations. Environ. Sci. Pollut. Res. Int. 19, 2159–2171. https://doi.org/10.1007/s11356-011-0715-x

Ramachandran, S., Kedia, S., 2012b. Radiative effects of aerosols over Indo-Gangetic plain: environmental (urban vs. rural) and seasonal variations. Environ. Sci. Pollut. Res. 19, 2159–2171.

Ramanathan, V., Chung, C., Kim, D., Bettge, T., Buja, L., Kiehl, J.T., Washington, W.M., Fu, Q., Sikka, D.R., Wild, M., 2005. Atmospheric brown clouds: impacts on South Asian climate and hydrological cycle. Proc. Natl. Acad. Sci. U. S. A. 102, 5326–33. https://doi.org/10.1073/pnas.0500656102

Ramanathan, V., Crutzen, P.J., Lelieveld, J., Mitra, a. P., Althausen, D., Anderson, J., Andreae, M.O., Cantrell, W., Cass, G.R., Chung, C.E., Clarke, a. D., Coakley, J. a., Collins, W.D., Conant, W.C., Dulac, F., Heintzenberg, J., Heymsfield, a. J., Holben, B., Howell, S., Hudson, J., Jayaraman, a., Kiehl, J.T., Krishnamurti, T.N., Lubin, D., McFarquhar, G., Novakov, T., Ogren, J. a., Podgorny, I. a., Prather, K., Priestley, K., Prospero, J.M., Quinn, P.K., Rajeev, K., Rasch, P., Rupert, S., Sadourny, R., Satheesh, S.K., Shaw, G.E., Sheridan, P., Valero, F.P.J., 2001. Indian Ocean Experiment: An integrated analysis of the climate forcing and effects of the great Indo-Asian haze. J. Geophys. Res. 106, 28371. https://doi.org/10.1029/2001JD900133

Ramanathan, V., Ramana, M.V., 2005. Persistent , widespread , and strongly absorbing haze over the Himalayan foothills and the Indo-Gangetic Plains. Pure Appl. Geophys. 162, 1609–1626. https://doi.org/10.1007/s00024-005-2685-8

Rao, B.B., Chowdary, P.S., Sandeep, V.M., Pramod, V.P., Rao, V.U.M., 2015. Spatial analysis of the sensitivity of wheat yields to temperature in India. Agric. For. Meteorol. 200, 192–202. https://doi.org/10.1016/j.agrformet.2014.09.023

Russell, P.B., Hobbs, P. V, Stowe, L.L., 1999. Aerosol properties and radiative effects in the United States East Coast haze plume ' An overview of the Tropospheric Aerosol Radiative Forcing Observational Experiment 104, 2213–2222.

Sarkar, S., Singh, R.P., Chauhan, A., 2018. Crop Residue Burning in Northern India : Increasing Threat to Greater India Journal of Geophysical Research : Atmospheres Crop Residue Burning in Northern India : Increasing Threat to Greater India. J. Geophys. Res. Atmos. https://doi.org/10.1029/2018JD028428

Schwartz, J., Coull, B., Laden, F., Ryan, L., 2008. The Effect of Dose and Timing of Dose on the Association between Airborne Particles and Survival. Environ. Health Perspect. 116, 64–69. https://doi.org/10.1289/ehp.9955

Sen, A., Abdelmaksoud, A.S., Nazeer Ahammed, Y., Alghamdi, M.ِ., Banerjee, T., Bhat, M.A., Chatterjee, A., Choudhuri, A.K., Das, T., Dhir, A., Dhyani, P.P., Gadi, R., Ghosh, S., Kumar, K., Khan, A.H., Khoder, M., Maharaj Kumari, K., Kuniyal, J.C., Kumar, M., Lakhani, A., Mahapatra, P.S., Naja, M., Pal, D., Pal, S., Rafiq, M., Romshoo, S.A., Rashid, I., Saikia, P., Shenoy, D.M., Sridhar, V., Verma, N., Vyas, B.M., Saxena, M., Sharma, A., Sharma, S.K., Mandal, T.K., 2017. Variations in particulate matter over Indo-Gangetic Plains and Indo-Himalayan Range during four field campaigns in winter monsoon and summer monsoon: Role of pollution pathways. Atmos. Environ. 154, 200–224. https://doi.org/10.1016/j.atmosenv.2016.12.054

Sharma, B., Amarasinghe, U., Xueliang, C., de Condappa, D., Shah, T., Mukherji, A., Bharati, L., Ambili, G., Qureshi, A., Pant, D., Xenarios, S., Singh, R., Smakhtin, V., 2010. The indus and the

ganges: River basins under extreme pressure. Water Int. 35, 493–521. https://doi.org/10.1080/02508060.2010.512996

Shindell, D.T., Lamarque, J.F., Schulz, M., Flanner, M., Jiao, C., Chin, M., Young, P.J., Lee, Y.H., Rotstayn, L., Mahowald, N., Milly, G., Faluvegi, G., Balkanski, Y., Collins, W.J., Conley, A.J., Dalsoren, S., Easter, R., Ghan, S., Horowitz, L., Liu, X., Myhre, G., Nagashima, T., Naik, V., Rumbold, S.T., Skeie, R., Sudo, K., Szopa, S., Takemura, T., Voulgarakis, A., Yoon, J.H., Lo, F., 2013. Radiative forcing in the ACCMIP historical and future climate simulations. Atmos. Chem. Phys. 13, 2939–2974. https://doi.org/10.5194/acp-13-2939-2013

Shrestha, S., Moore, G.A., Peel, M.C., 2018a. Trends in winter fog events in the Terai region of Nepal. Agric. For. Meteorol. 259, 118–130. https://doi.org/10.1016/j.agrformet.2018.04.018

Shrestha, S., Peel, M.C., Moore, G.A., 2018b. Development of a Regression Model for Estimating Daily Radiative Forcing Due to Atmospheric Aerosols from Moderate Resolution Imaging Spectrometers (MODIS) Data in the Indo Gangetic Plain (IGP). Atmosphere (Basel). 9, 1–26. https://doi.org/10.3390/atmos9100405

Shuai, J., Zhang, Z., Liu, X., Shi, Y.C., Wang, P., Shi, P., 2013. Increasing concentrations of aerosols offset the benefits of climate warming on rice yields during 1980–2008 in Jiangsu Province, China. Reg. Environ. Chang. 13, 287–297. https://doi.org/10.1007/s10113-012-0332-3

Singh, D.P., Gadi, R., Mandal, T.K., Saud, T., Saxena, M., Sharma, S.K., 2013. Emissions estimates of PAH from biomass fuels used in rural sector of Indo-Gangetic Plains of India. Atmos. Enivronment 68, 120–126. https://doi.org/10.1016/j.atmosenv.2012.11.042

Singh, J., Bhattacharya, B.K., Kumar, M., 2012. Solar radiation and evaporation trend over India. J. Earth Sci. Eng. 2, 160–165.

Singh, N., Mhawish, A., Deboudt, K., Singh, R.S., Banerjee, T., 2017. Organic aerosols over Indo-Gangetic Plain: Sources, distributions and climatic implications. Atmos. Environ. 157, 69–74. https://doi.org/10.1016/j.atmosenv.2017.03.008

Singh, S., Singh, D., 2010. Recent Fog trends and its impact on wheat productivity in NW plains in India, in: 5th International Conference on Fog, Fog Collection and Dew Münster, Germany, 25–30 July 2010. Münster, Germany.

Srivastava, A.K., Dey, S., Tripathi, S.N., 2012a. Aerosol Characteristics over the Indo-Gangetic Basin: Implications to Regional Climate, in: Hayder Abdul-Razzak (Ed.), Atmospheric Aerosols - Regional Characteristics - Chemistry and Physics. InTech, pp. 47–79. https://doi.org/DOI: 10.5772/47782

Srivastava, A.K., Singh, S., Tiwari, S., Bisht, D.S., 2012b. Contribution of anthropogenic aerosols in direct radiative forcing and atmospheric heating rate over Delhi in the Indo-Gangetic Basin. Environ. Sci. Pollut. Res. 19, 1144–1158. https://doi.org/10.1007/s11356-011-0633-y

Srivastava, R., Ramachandran, S., 2013. The mixing state of aerosols over the Indo-Gangetic Plain and its impact on radiative forcing. Q. J. R. Meteorol. Soc. 139, 137–151.

Srivastava, S.K., Sharma, A.R., Sachdeva, K., 2016. Spatial and Temporal Variability of Fog Over the Indo-Gangetic Plains, India. Int. J. Environ. Ecol. Eng. 10, 1042–1057.

Sto, C.O., Donatelli, M., Nelson, R., 2003. CropSyst , a cropping systems simulation model. Eur. J.

Agron. 18, 289–307.

Sun, H., Zhang, X., Wang, E., Chen, S., Shao, L., Qin, W., 2016. Field Crops Research Assessing the contribution of weather and management to the annual yield variation of summer maize using APSIM in the North China Plain. F. Crop. Res. 194, 94–102. https://doi.org/10.1016/j.fcr.2016.05.007

Sus, O., Williams, M., Bernhofer, C., Béziat, P., Buchmann, N., Ceschia, E., Doherty, R., Eugster, W., Grünwald, T., Kutsch, W., Smith, P., Wattenbach, M., 2010. Agriculture , Ecosystems and Environment A linked carbon cycle and crop developmental model : Description and evaluation against measurements of carbon fluxes and carbon stocks at several European agricultural sites. "Agriculture, Ecosyst. Environ. 139, 402–418. https://doi.org/10.1016/j.agee.2010.06.012

Syed, F.S., Körnich, H., Tjernström, M., 2012. On the fog variability over south Asia. Clim. Dyn. 39, 2993–3005. https://doi.org/10.1007/s00382-012-1414-0

Taneja, G., Pal, B.D., Joshi, P.K., Aggarwal, P.K., N. K., T., 2014. Farmerss Preferences for Climate-Smart Agriculture: An Assessment in the Indo-Gangetic Plain (No. 01337), Discussion Paper. New Delhi. https://doi.org/10.2139/ssrn.2420547

TERI, 2016. Air pollutant emissions scenario for India, The Energy and Resource Institute. TERI, New Delhi.

Tiwari, S., Hopke, P.K., Thimmaiah, D., Dumka, U.C., Srivastava, A.K., Bisht, D.S., Rao, P.S.P., Chate, D.M., Srivastava, M.K., Tripathi, S.N., 2016. Nature and sources of ionic species in precipitation across the indo-gangetic plains, India. Aerosol Air Qual. Res. 16, 943–957. https://doi.org/10.4209/aaqr.2015.06.0423

Wahid, A., Campus, Q., 1995. Effects of air pollution on rice yield in the Pakistan Punjab. Environ. Pollut. 90, 323–329.

Weerakkody, U., Dover, J.W., Mitchell, P., Reiling, K., 2018. Evaluating the impact of individual leaf traits on atmospheric particulate matter accumulation using natural and synthetic leaves. Urban For. Urban Green. 30, 98–107. https://doi.org/10.1016/j.ufug.2018.01.001

Wester, P., Mishra, A., Mukherji, A., Shrestha, A.B., Change, C., 2019. The Hindu Kush Himalaya assessment : mountains, climate change, sustainability and people. International Center for Integrated Mountain Development (ICIMOD), Hindu Kush Himalayan Monitoring and Assessment Programme (HIMAP) and Springer Open, Kathmandu Nepal.

Whitbread, A.M., Robertson, M.J., Carberry, P.S., Dimes, J.P., 2010. How farming systems simulation can aid the development of more sustainable smallholder farming systems in southern Africa. Eur. J. Agron. 32, 51–58. https://doi.org/10.1016/j.eja.2009.05.004

WHO, 2018. Ambient Air Quality Database, WHO, April 2018 [WWW Document]. URL http://www.who.int/airpollution/en/ (accessed 3.20.19).

WHO, 2006. WHO Air quality guidelines for particulate matter, ozone, nitrogen dioxide and sulfur dioxide: global update 2005: summary of risk assessment, Geneva: World Health Organization. https://doi.org/10.1016/0004-6981(88)90109-6

Wild, M., 2009. Global dimming and brightening: A review. J. Geophys. Res. 114, 1–31.

https://doi.org/10.1029/2008JD011470

World Bank Group, IHME, 2016. The cost of air pollution: Strengthening the Economic Case for Action, The World Bank and Institute for Health Metrics and Evaluation University of Washington, Seattle. https://doi.org/10.1080/000368497326688

Xiao, D., Tao, F., 2016. Contributions of cultivar shift , management practice and climate change to maize yield in North China Plain in 1981 – 2009. Int. J. Biometeorol. 60, 1111–1122. https://doi.org/10.1007/s00484-015-1104-9

Xiao, D., Tao, F., 2014. Contributions of cultivars , management and climate change to winter wheat yield in the North China Plain in the past three decades. Eur. J. Agron. 52, 112–122. https://doi.org/10.1016/j.eja.2013.09.020

Yang, X., Asseng, S., Wong, M.T.F., Yu, Q., Li, J., Liu, E., 2013. Quantifying the interactive impacts of global dimming and warming on wheat yield and water use in China. Agric. For. Meteorol. 182–183, 342–351. https://doi.org/10.1016/j.agrformet.2013.07.006

Yao, L., 2017. Causative impact of air pollution on evapotranspiration in the North China Plain. Environ. Res. 158, 436–442. https://doi.org/10.1016/j.envres.2017.07.007

Zhang, T., Yue, X., Li, T., Unger, N., Yang, X., 2018. Climate effects of stringent air pollution controls mitigate future maize losses in China Climate effects of stringent air pollution controls mitigate future maize losses in China. Environ. Res. Lett. 13, 1–12.

Zhang, X., Chen, S., Sun, H., Shao, L., Wang, Y., 2011. Changes in evapotranspiration over irrigated winter wheat and maize in North China Plain over three decades. Agric. Water Manag. 98, 1097–1104. https://doi.org/10.1016/j.agwat.2011.02.003

Zhang, X., Wang, S., Sun, H., Chen, S., Shao, L., Liu, X., 2013. Contribution of cultivar , fertilizer and weather to yield variation of winter wheat over three decades : A case study in the North China Plain. Eur. J. Agron. 50, 52–59. https://doi.org/10.1016/j.eja.2013.05.005

Zhou, L., Chen, X., Tian, X., 2018. The impact of fi ne particulate matter (PM 2 . 5) on China ' s agricultural production from 2001 to 2010. J. Clean. Prod. 178, 133–141. https://doi.org/10.1016/j.jclepro.2017.12.204

Chapter 7

Summary and Conclusion

1.0 Introduction

The Indo Gangetic plain (IGP) region is regarded as a hot spot with respect to air pollution due to a persistently high level of atmospheric aerosols. The IGP is one of the most densely populated regions of the world. High atmospheric aerosols in this region are not only from the emissions of fossil fuel from industries and vehicles, but also from domestic cooking and space heating due to biomass (fuelwood, animal waste and crop residue) providing a major share of domestic energy use in rural areas (Venkataraman et al., 2006). Moreover, the practice of crop residue (rice and wheat) burning in the field, has a significant contribution of atmospheric aerosols during the harvesting season in the IGP (Kaskaoutis et al., 2014; Rajput et al., 2014). In addition to the increasing and high level of anthropogenic aerosol emissions, the unique topographic features and synoptic meteorological conditions of the region have contributed to the alarming level of atmospheric aerosols in the IGP (Dey and Di Girolamo, 2010; Di Girolamo et al., 2004; Srivastava et al., 2012). The serious effects of atmospheric aerosols on the health of people in the IGP are reportedly result in the second, third and fifth highest mortality burden per annum in the world for IGP countries India (1.2 million), Pakistan (128,000) and Bangladesh (123,000) respectively due to atmospheric aerosols (Health Effects Institute, 2019). In addition to the health effects of atmospheric aerosols, several studies have reported their effect on solar radiation (dimming), monsoon precipitation, glacial retreat, evapotranspiration, etc. in the IGP (Kumari et al., 2007; Liu et al., 2019; Ramanathan and Ramana, 2005; Wild, 2012). Even though the change in solar radiation, monsoon precipitation, evapotranspiration, change in stream discharge due to glacial retreat, etc. could directly impact crop production, there are only a few limited studies on the effect of atmospheric aerosols on crop production in the IGP region. Since the IGP region is a food basket of South Asia, studying the effect of atmospheric aerosols on crop production is very important with respect to the food security and livelihood of farmers in the region.

Several studies have conducted spatial and temporal analysis of atmospheric aerosols in the IGP region and found high aerosol loading in eastern IGP with an increasing trend during the winter season (Dey and Di Girolamo, 2011; Kumar et al., 2018). In addition to high aerosol loading, persistent fog during winter could also adversely affect the main winter crop, wheat, in the eastern IGP as reported by Singh and Singh (2010) in the western IGP. Due to comparatively low crop productivity and high dominance of smallholder farmers in the eastern IGP (Balasubramanian et al., 2013; Taneja et al., 2014), it is very important to

investigate the effect of atmospheric aerosols on crop production due to the possible adverse effects on the food security of millions of people and the livelihoods of farmers in the eastern IGP. In this context, the present study on the physical effect of atmospheric aerosols on winter wheat crop production in the eastern IGP was conducted. This chapter summarizes and concludes the findings by covering the purpose, summary of findings, contributions, and limitations of the study in the following sections. In addition, this chapter also covers the implications and possible applications of the findings, and the recommendations for stakeholders.

2.0 Research Purpose

The main objective of the present research was to study the physical effects of atmospheric aerosols on the winter crop (wheat) production in the eastern IGP region. To address the main objective, the study was conducted in the following four steps. Firstly, the recent increasing trend in persistent winter fog and anthropogenic aerosol levels across the IGP region over the past two decades may affect crop production (Ghude et al., 2017; Syed et al., 2012; Wester et al., 2019). This step addresses a knowledge gap around the status of fog in the Nepal portion of IGP, by investigating the trend in winter fog events in the Terai region of Nepal and their potential effect on crop production. Secondly, an increasing number of cold days, due to increased levels of fog and haze, have been experienced in the Indian component of the IGP (Dash and Mamgain, 2011). This step seeks to address the information gap around extreme cold events and their effect on crop production in the Nepal component of the IGP. A study on cold wave in the Terai region of Nepal and farmer's perceptions of the effect of cold wave and fog events on agriculture was conducted. Thirdly, in order to assess the impact of reduced solar radiation, due to atmospheric aerosols, on crop production a regression modelling study was conducted to estimate daily radiative forcing due to atmospheric aerosols from Moderate Resolution Imaging Spectrometers (MODIS) data in the IGP region. Finally, by using the daily radiative forcing from the developed model and the calibrated Agricultural Production Systems sIMulator (APSIM) model at the Sustainable Resilient Farming Systems Intensifications (SRFSI) project sites of eastern IGP region, the effect on the principal winter crop production due to anthropogenic atmospheric aerosols was studied. Hence, these steps combined seek to contribute to filling the knowledge gaps on the physical effects of high anthropogenic aerosols on crop production in the IGP, the food basket of South Asia.

3.0 Summary of findings

In order to address the main research question, "what are the physical effects of anthropogenic aerosols on winter crop production in the eastern IGP", this study is conducted in four steps to address 5 sub-research questions in chapters 3 (1st sub-research question), 4 (2nd sub-research question), 5 (3rd and 4th sub-research question) and 6 (5th sub-research question). The summary of the findings of those chapters is presented in the following subsections.

3.1 Fog scenario in the Terai region of Nepal

This study component was conducted to address the first sub-research question related to the knowledge gap around fog conditions in the Nepal component of the IGP and its possible impact on crop production. Historical visibility data at four airport stations in Terai region of Nepal (Nepalgunj, Bhairahawa, Simara, and Biratnagar) were investigated to study the fog over time. An attempt was made to develop a simple empirical model to estimate fog events based on meteorological parameters. In addition, the possible effect of fog events on crop production in the Terai region of Nepal was also analyzed. A summary of the findings of this study are listed below.

- In the Terai region of Nepal, fog events begin in November, attain their peak in December/ January and end by the end of February. Based upon visibility data during 1980-2015, the annual average number of foggy days varied from 24 to 56 days across the stations in the Terai region of Nepal. Similarly, the average total day time foggy hours during winter ranged from 71 hours to 169 hours.
- The opacity (reciprocal of visibility) was increasing at all stations in the Terai during winter months in the study period 1980-2015 at least at the statistical significance level of 0.05. The fog-related parameters such as number of foggy days, dense foggy days, foggy hours and dense foggy hours have an increasing trend at least at the 0.1 level of statistical significance.
- To address the unavailability of past visibility data in the Terai region of Nepal, an attempt was made to develop a simple empirical model for estimating foggy day occurrence based on daily meteorological parameters (maximum temperature, minimum temperature, humidity, and precipitation). The developed model was not impressive with a low adjusted R^2, which suggests an improved model may require inclusion of aerosol parameters along with meteorological parameters.
- After analyzing the occurrence of foggy and dense foggy days in combination with the crop calendar of the Terai region of Nepal, the study indicated the potential negative effect of fog on the production of major winter crops like wheat, lintel, potato, winter maize in the Terai region.

3.2 Cold extreme in Terai area of Nepal

In order to address the second sub-research question on the knowledge gap around cold extremes in the Nepal component of the IGP, this study was conducted. After analyzing historical daily maximum and minimum temperature data of 6 Terai stations (Dhangadhi, Nepalgunj, Bhairahawa, Simara, Janakpur and Biratnagar) during 1971-2015, extreme cold events were analyzed in terms of cold days, cold nights, extreme cold days, extreme cold nights, cold wave days and extreme cold wave nights and the major findings are listed below.

- Extreme cold events viz. cold days/nights, extreme cold days/nights and cold wave days occurred during January, February and December in the Terai region of Nepal. The average annual cold days varied from 15.6 to 17.9 days and the average cold nights ranged from 13 to 17.6 days in the Terai region of Nepal. Similarly, the average annual extreme cold days fluctuated from 3.2 to 3.6 days and extreme cold nights varied from 2.6 to 3.4 days in the Terai region.
- All the stations of Terai, except Nepalgunj, showed an increasing trend of cold days and extreme cold days at the statistical significance level of 0.05. Trend analysis of cold nights and extreme cold nights indicated that the majority of Terai stations did not show a statistically significant trend. However, only in Dhangadhi, the cold night and extreme cold nights were showed a declining trend with at a statistical significance level of 0.05.
- The annual average cold wave and extreme cold wave days fluctuated from 9.2 to 13.8 days and 1.4 to 3.8 days in the Terai region of Nepal. By comparing the co-occurrence of foggy days and cold and extreme cold wave days at Biratnagar, Simara, Bhairahawa, and Nepalgunj airport, it was shown that most of the cold and extreme cold wave days were also foggy days.

3.3 Perception of farmers on fog and cold events and its effect on crop production

There is limited ground-level information about the impact of cold wave and fog events on agriculture and the life of people in the Terai region of Nepal, so a study on the farmer's perceptions of the effect of cold wave, fog and their effect on agriculture was conducted in two districts, Sunsari and Dhanusha, through focus group discussions to address the 3rd research sub-question. The summary of findings are listed below.

- Farmer's perceived a significant impact of fog events and cold wave on agriculture, particularly on winter crop cultivation and livestock farming. Potato, tomato, brinjal, wheat, chilly, onion, beans, etc. were identified as the major crops affected by fog and cold wave in the Terai. Conducive environment for fungal infections/late blight and poor vegetative growth were the major effect of cold wave and

fog events on winter crops. Due to late blight during fog/cold wave events in the Terai, up to 100% loss of some crops were reported, especially, tomato, potato and brinjal.

- To prevent late blight on potato during the foggy season, chemical (fungicide) application has significantly increased (on average 6.3 times), which has reportedly increased the cost of cultivation by 18%.
- Livestock production are also reported to be significantly affected by cold wave and fog events. Milk production from cattle was reported to be reduced by 25 to 50% due to cold wave. In addition, goats were also affected by respiratory disease during the cold wave.
- Farm labor productivity was also reported to be significantly reduced during cold wave days because the labourers prefer not to work outdoors during cold wave and foggy events.
- To minimize the effect of cold wave and fog events on crop production, the farmers of Sunsari and Dhanusha districts have adopted several adaptation measures such as fungicide spraying, early planting, irrigation using groundwater (which is warm), and using blight resistant crop varieties. Similarly, adaptation measures adopted by farmers to minimize losses due to cold wave on livestock production are the use of coats for livestock, providing cooked feed and warm water to livestock, and improvement of animal sheds, etc.

3.4 Aerosols and Radiative forcing due to aerosols in the IGP

To assess the physical effects of atmospheric aerosols on crop production requires an estimation of changes in solar radiation at the ground level due to atmospheric aerosols. Hence, to address the 4th research sub-question, a simple regression model to estimate the daily radiative forcing in the IGP region was developed and the major findings are summarized in the following paragraphs.

- A simple year-round multiple regression model was developed to estimate daily direct radiative forcing due to atmospheric aerosols (ADRF) in the IGP by utilizing daily AERONET AOD, atmospheric water vapor and radiative forcing at the surface during 2002 to 2015 at 10 AERONET stations in the IGP. Goodness of fit of the model was shown with an adjusted R^2 value of 0.834. The Jackknife method of delete one group (station data) was used to check the stability of the model and the model was found to be robust because the adjusted R^2 ranged between 0.813 and 0.842 and the model performed well in all stations and seasons.
- To use the developed ADRF model beyond AERONET stations, AOD and atmospheric water vapor products from MODIS Aqua and Terra were compared against AERONET AOD and atmospheric water vapor. After analyzing the root mean square error and correlation coefficient both MODIS Aqua and Terra products of AOD and water vapor were similar to that of AERONET products.

- Estimates of ADRF derived by using MODIS Aqua and Terra products were also evaluated against ADRF from the IGP AERONET stations and the model performed well with Pearson correlation coefficient of 0.66 and 0.65 respectively. The model ADRF estimated results were also compared against SBDART results at Karachi and Lahore and found to be within an acceptable range in spite of fewer input parameters (two compared to more than 60 in SBDART) to estimate radiative forcing at the surface within the IGP. The development of a simple model to estimate radiative forcing due to atmospheric aerosols in the IGP via MODIS products is one of the important contributions of this study.

3.5 Effect of anthropogenic aerosols on winter crop (wheat) production in the eastern IGP

In order to address the 5th research sub-question, a study on the effect of anthropogenic aerosols on winter crop (wheat) production was conducted using the calibrated and validated APSIM model at the SRFSI nodes in the eastern IGP. The effect of anthropogenic aerosols on crop production was obtained by comparing simulation results with, and without, anthropogenic aerosols at the 8 SRFSI nodes in the eastern IGP during 2015-2017. Simulation of the wheat crop with aerosols was performed by using the observed meteorological data. Simulation of the wheat crop without aerosols was performed in two ways, first by only considering the radiative effect (adjusting observed solar radiation data by estimated radiative forcing values), and second by considering the radiative and temperature effects (adding maximum temperature by 0.5 ◦C along with solar radiation data adjustment). In addition, the historical AOD, radiative forcing, and solar radiation were also analyzed at the study nodes. The key findings of this study are listed below.

- Analysis of AERONET AOD in the eastern IGP stations from 2003 to 2017 showed a high level of aerosols (AOD greater than 0.5) in all seasons except monsoon season and a peak during the winter season. The radiative forcing due to anthropogenic aerosols at the SRFSI nodes in the eastern IGP was also comparatively high during the winter season. In addition, there was a declining trend of radiative forcing due to anthropogenic aerosols during 2003-2017 at the SRSFI nodes in the range of -1.5 to -1 Wm^{-2} $year^{-1}$. The decline in radiative forcing due to anthropogenic aerosols were also aligned with the declining trend of average annual sunshine hours and average monthly sunshine hours during winter months of December and January at the SRFSI nodes.
- The results from the calibrated and validated APSIM model at the SRSFI nodes in the eastern IGP showed that the radiative effect of anthropogenic aerosols alone reduced wheat grain yield by 615 kg/ha (13.5%), whereas the combined radiative and temperature effects reduce wheat grain yield by 498.7 kg/ha (11.2%) at the SRSFI nodes in the eastern IGP. The reduction of a significant quantity of

wheat yield due to anthropogenic aerosols at the eastern IGP nodes indicates air pollution is a serious new threat for food security in this region.

- The APSIM results also indicated that average reduction of wheat biomass yield due to anthropogenic aerosols, when considering only the radiative effect and the combined radiative and temperature effects of anthropogenic aerosols at the SRFSI nodes of the eastern IGP during 2015-2017, were 22% and 21.2% respectively. This reduction in wheat biomass yield may also affect the contribution of biomass to soil organic matter and animal fodder in the eastern IGP.
- The APSIM simulation results also showed that average crop evapotranspiration reduced due to anthropogenic aerosols, when consideration only the radiative effect and the combined radiative and temperature effects of anthropogenic aerosols at the SRFSI nodes of the eastern IGP during 2015-2017, was 42 mm (13.5%) and 47.9 mm (15.1%) respectively. This indicates that air pollution has a reduced the irrigation water demand due to the significant reduction in crop evapotranspiration.
- Considering the average wheat cultivated area in each country component of the eastern IGP, the average reduction of yield at the country wise SRSFI nodes, and the average wholesale price of wheat in the region, it was estimated that the economic cost of reduced wheat grain yield due to anthropogenic aerosols in the eastern IGP was more than $US300 million per annum.

4.0 Contributions made by this research

This research sought to address several knowledge gaps in the scientific literature regarding the effect of atmospheric aerosols on crop production in the highly polluted IGP region and has made the following contributions.

- In the context of increasing atmospheric aerosols in the IGP region, for the first time in the Terai region of Nepal (Nepal component of IGP), an increasing trend in winter fog occurrence was established by analyzing historical visibility data.
- This study identified an increasing trend in annual cold days and extreme cold days in the Terai region of Nepal based upon historical daily maximum and minimum temperature data. This supported the previous finding on the increasing trend in winter fog in this region.
- This research reported farmer's perceptions on winter fog and cold events, their perceived effects on agriculture, and the resultant adaptations made by farmers in the eastern Terai region of Nepal (Nepal component of eastern IGP).
- Development of a simple regression model for estimating radiative forcing due to atmospheric aerosols at the surface of the IGP using MODIS data is a major contribution of this study.

- In the scenario of prevalent and persistence of high loading of the anthropogenic atmospheric aerosols during winter, this study quantified the effect of anthropogenic aerosols on winter crop (wheat) yield, biomass, evapotranspiration and value by using process-based model APSIM in the eastern IGP region for the first time. The annual economic cost of anthropogenic aerosols is estimated to be more than $US300 million per annum.

5.0 Limitations of the study

Each of the research chapters provides its own discussion of limitations. The following points cover the overall major limitations of this thesis.

The analysis of fog in the Terai region of Nepal was performed using 3-hour interval day time visibility data from the Meteorological Terminal Air Report (METAR) at 4 airports, which does not include nighttime fog events. The poor performance of the proposed empirical model for estimating foggy days based on daily meteorological parameters (maximum temperature, minimum temperature, humidity, and precipitation) in the Terai region of Nepal could also be due to not considering night time fog.

The perception of the farmers on the effect of cold wave and fog was assessed in only two districts, Dhanusha and Sunsari, of the Terai region of Nepal. Despite this, the study provides an overview of the perceptions of the farmers on the effect of fog and cold events on their agriculture in the Terai region of Nepal. Due to the limited sample size, the findings from the perception of the farmers were not presented with any statistical analysis or statistical level of significance. In addition, the perceptions given were of smallholder farmers of the eastern IGP and it does not represent that of more highly mechanized farmers of the western IGP.

While investigating the physical effect of atmospheric aerosols on winter crop (wheat production) in the eastern IGP, this study only considered the effect of anthropogenic aerosols in the atmosphere and it did not include the effect of deposited atmospheric aerosols on the leaves of the crops. Similarly, this study also did not cover the impact of aerosols on disease infestation, weed cover and fertilization of crop. Due to the majority of annual precipitation (about 85%) occurring during monsoon season and only limited precipitation with a few showers during winter season in the eastern IGP (Gupta and Seth, 2007), the effect of deposited aerosols on the leaves could be significant due to less chance of natural cleaning of the plant leaves by the winter rain.

The APSIM model was used to investigate the effect of anthropogenic aerosols on winter crop production in the eastern IGP. The input meteorological data of the APSIM model are maximum temperature,

minimum temperature, precipitation, and solar radiation at daily time scale. Therefore, any sub-daily variation in the meteorological parameters which may affect crop performance are not covered in this study.

The findings of Freychet et al. (2019) on reduction of maximum temperature by 0.5° C during winter months is used here to study the effect of atmospheric aerosols on temperature along with solar radiation in the performance of wheat crop in the eastern IGP using the APSIM model. In this study, it is assumed that the maximum temperature is uniformly reduced throughout the winter days which may not be true.

In this study, only the effect of anthropogenic atmospheric aerosols on daily global solar radiation availability was considered. The effect of anthropogenic aerosols on direct and diffuse radiation was not considered. According to Roderick et al. (2001), productivity of vegetation is strongly influenced by the diffusion fraction of solar radiation due to clouds and aerosols. Whereas Greenwald et al. (2006) explained that an increase in diffuse fraction has less effect on photosynthesis on overcast days. In the context of the IGP where a significant number of winter days are foggy days, the increased diffuse fraction may have little benefit for the wheat crop (with open and shallow canopy) as suggested by Wild et al. (2012).

6.0 Implications and possible applications of the findings

The implications and possible applications of the findings of this study are listed as follows.

- The findings of this research regarding status and trend of fog events, extreme cold events and farmer's perceptions of the effect on their agriculture can help policy makers to lay appropriate policy to minimize the effect of fog and cold events on the agriculture of the Terai region of Nepal.
- A simple regression model developed to estimate daily average radiative forcing due to atmospheric aerosols in the IGP region could be used by researchers to assess the effect of atmospheric aerosols on the terrestrial ecosystem of the IGP.
- The findings from the assessment of the effect of anthropogenic aerosols on winter wheat crop production in the eastern IGP, could help policy makers and stakeholders in the region to justify more investment in air quality improvement programs in the region.
- In the majority of districts of central and eastern IGP, more than 40 percent of ambient particulate matter is contributed by domestic emissions (Chowdhury et al., 2019). The findings of this study could be used to increase awareness to minimize air pollution (through adoption of improved cook stoves, use of renewable energy sources, avoid crop residue/waste burning, etc.) for health benefits and for better crop yields. Since one of the reasons for the high levels of anthropogenic aerosols in post

monsoon and winter seasons in the IGP is due to increased stubble burning during October-November in the western IGP (Sarkar et al., 2018), there is also need for research and development of crop cultivation methods without stubble burning in the IGP.

- As air pollution in the IGP is a trans boundary issue affecting millions of people in the region, there is need of coordinated effort in the south Asian region to understand the reason behind this and to mitigate at local and national level (Wester et al., 2019). The negative effect of air pollution on the wheat crop production in the eastern IGP, derived from this study may help the policy makers of this region to make policy interventions to control air pollution not only for the sake of health benefits but also for the food security of the region. Favorable policy promoting the use of efficient cook stoves, cleaner brick kilns, improved seeders (to avoid burning of crop residue), clean energy sources and efficient devices with minimal emissions from all sectors (viz. residential, industrial, transport, agricultural etc.) is required.

7.0 Future research directions

Following this research, potential future research directions are listed below.

- As this research has shown significant physical effects of anthropogenic aerosols on wheat production in the eastern IGP, further research to assess the physical effect of anthropogenic aerosols on other important winter crops viz. maize, lentil, potato etc. of the eastern IGP would provide a more complete picture of the effect of anthropogenic aerosols on food security of the eastern IGP.
- The reduction of daily solar radiation by anthropogenic aerosols in the eastern IGP was considered in this study while studying the effect of anthropogenic aerosols on crop production. The increase of atmospheric aerosols reduces the direct radiation and increases the diffuse radiation available to the plants (Kanniah et al., 2010). Hence, in order to study the effect of anthropogenic aerosols on winter crop production in the eastern IGP by considering the availability of direct and diffuse radiation, further research is needed.
- The present study only considers the effect of anthropogenic aerosols in the atmosphere on crop production and does not consider the effect of deposited aerosols on the leaves of the plant. Hence future research should also incorporate the effect of deposited aerosols on the leaves of the plant while assessing the physical effects of anthropogenic aerosols on crop production.
- The IGP area is not only a hotspot of anthropogenic aerosols, but also of climate change (Ericksen et al., 2012). Future research may cover the effect on crop production of considering future scenarios of both climate change and anthropogenic aerosols.

- Experimental field study of the effect of anthropogenic aerosols on crop production could also be future area of research.

8.0 Conclusion

Increasing atmospheric aerosols in the IGP has led to fog becoming an important weather phenomenon in the Nepal component of the IGP (Terai region of Nepal), with an increasing trend in the average number of foggy days (24 to 56 days) over the past 35 years. The annual number of cold days in the Terai region of Nepal also show an increasing trend over the past four decades, which supports the foggy days trend. The farmers of Dhanusha and Sunsari (Terai region of Nepal) perceived that the increased fog events and cold events during winter have significantly affected their winter crops and livestock and they are coping with the extreme cold and fog events by following different adaptation measures. In order to assess the effect of anthropogenic aerosols on crop production in the IGP, a simple model to estimate radiative forcing due to aerosols in the IGP region was developed and evaluated. By using the model estimated radiative forcing due to aerosols with the calibrated and validated process-based crop model APSIM for eastern IGP sites, the effect of anthropogenic aerosols on the important winter crop wheat was assessed. In the eastern IGP, anthropogenic aerosols are estimated to have reduced wheat grain yield by 11.2-13.5%, wheat biomass yield by 21.2-22% and wheat evapotranspiration by 13.5-15.1% during 2015-2017. The economic loss per annum due to reduced wheat grain yield by anthropogenic aerosols in the eastern IGP was estimated to be 302-339 million USD. The major findings of this study regarding the significant effects on winter wheat crop production in the eastern IGP could be utilized by policy makers to make more investment in air pollution control and motivate people and farmers to adopt pollution control measures. Using the methods developed in this study, further future research on the effects of anthropogenic aerosols on other winter crops viz. maize, potato, boro rice could be conducted. In addition, future research on the effect of deposited aerosols on the leaves of winter crops will also help to create a more complete picture of physical effects of atmospheric aerosols on agriculture in the eastern IGP.

References

Balasubramanian, V., Adhya, T.K., Ladha, J.K., 2013. Enhancing eco-efficiency in the intensive cereal-based systems of the Indo-Gangetic plains, in: Hershey, C.H., Neate, P. (Eds.), Eco-Efficiency: From Vision to Reality (Issues in Tropical Agriculture Series). International Center for Tropical Agriculture, Cali, Colombia, pp. 99–115. https://doi.org/doi:10.1201/b17133-197

Chowdhury, S., Dey, S., Guttikunda, S., Pillarisetti, A., Smith, K.R., 2019. Indian annual ambient air quality standard is achievable by completely mitigating emissions from household sources. PNAS 1–6. https://doi.org/10.1073/pnas.1900888116

Dash, S.K., Mamgain, A., 2011. Changes in the frequency of different categories of temperature extremes in India. J. Appl. Meteorol. Climatol. 50, 1842–1858. https://doi.org/10.1175/2011JAMC2687.1

Dey, S., Di Girolamo, L., 2011. A decade of change in aerosol properties over the Indian subcontinent. Geophys. Res. Lett. 38, 1–5. https://doi.org/10.1029/2011GL048153

Dey, S., Di Girolamo, L., 2010. A climatology of aerosol optical and microphysical properties over the Indian subcontinent from 9 years (2000–2008) of Multiangle Imaging Spectroradiometer (MISR) data. J. Geophys. Res. 115, D15204. https://doi.org/10.1029/2009JD013395

Di Girolamo, L., Bond, T.C., Bramer, D., Diner, D.J., Fettinger, F., Kahn, R.A., Martonchik, J. V., Ramana, M. V., Ramanathan, V., Rasch, P.J., 2004. Analysis of multi-angle Imaging SpectroRadiometer (MISR) aerosol optical depths over greater India during winter 2001-2004. Geophys. Res. Lett. 31, 1–5. https://doi.org/10.1029/2004GL021273

Ericksen, P., Thornton, P., Notenbaert, A., Cramer, L., Jones, P., Herrero, M., Ericksen, P., Thornton, P., Cramer, L., Jones, P., 2012. Mapping hotspots of climate change and food insecurity in the global tropics. Copenhagen, Denmark.

Freychet, N., Tett, S.F.B., Bollasina, M., Wang, K.C., Hegerl, G.C., 2019. The Local Aerosol Emission Effect on Surface Shortwave Radiation and Temperatures. J. Adv. Model. Earth Syst. https://doi.org/10.1029/2018MS001530

Ghude, S.D., Bhat, G.S., Prabhakaran, T., Jenamani, R.K., Chate, D.M., Safai, P.D., Karipot, A.K., Konwar, M., Pithani, P., Sinha, V., Rao, P.S.P., Dixit, S.A., Tiwari, S., Todekar, K., Varpe, S., Srivastava, A.K., Bisht, D.S., Murugavel, P., Ali, K., Mina, U., Dharua, M., Rao, J., Padmakumari, B., Hazra, A., Nigam, N., Shende, U., Chandra, B.P., Mishra, A.K., Kumar, A., Hakkim, H., Pawar, H., Acharga, P., Kulkarni, R., Subharthi, C., Balaji, B., Varghese, M., Bera, S., Rajeevan, M., 2017. Winter fog experiment over the Indo-Gangetic plains of India. Curr. Sci. 112, 767–784. https://doi.org/10.18520/cs/v112/i04/767-784

Greenwald, R., Bergin, M.H., Xu, J., Cohan, D., Hoogenboom, G., Chameides, W.L., 2006. The influence of aerosols on crop production: A study using the CERES crop model. Agric. Syst. 89, 390–413. https://doi.org/10.1016/j.agsy.2005.10.004

Gupta, R., Seth, A., 2007. A review of resource conserving technologies for sustainable management of the rice-wheat cropping systems of the Indo-Gangetic plains (IGP). Crop Prot. 26, 436–447. https://doi.org/10.1016/j.cropro.2006.04.030

Health Effects Institute, 2019. State of Global Air 2019. Special Report. Boston, MA.

Kanniah, K.D., Beringer, J., Tapper, N.J., Long, C.N., 2010. Aerosols and their influence on radiation partitioning and savanna productivity in northern Australia. Theor Appl Clim. 100, 423–438. https://doi.org/10.1007/s00704-009-0192-z

Kaskaoutis, D.G., Kumar, S., Sharma, D., Singh, R.P., Kharol, S.K., Sharma, M., Singh, A.K., Singh, S., Singh, A., Singh, D., 2014. Effects of crop residue burning on aerosol properties, plume characteristics, and long-range transport over northern India. J. Geophys. Res. Atmos. 119, 5424–5444. https://doi.org/10.1002/2013JD021357

Kumar, M., Parmar, K.S., Kumar, D.B., Mhawish, A., Broday, D.M., Mall, R.K., Banerjee, T., 2018. Long-term aerosol

climatology over Indo-Gangetic Plain: Trend, prediction and potential source fields. Atmos. Environ. 180, 37–50. https://doi.org/10.1016/j.atmosenv.2018.02.027

Kumari, B.P., Londhe, A.L., Daniel, S., Jadhav, D.B., 2007. Observational evidence of solar dimming : Offsetting surface warming over India 34, 1–5. https://doi.org/10.1029/2007GL031133

Liu, Y., Cai, W., Sun, C., Song, H., Cobb, K.M., 2019. Anthropogenic aerosols cause recent pronounced weakening of Asian Summer Monsoon relative to last four centuries. Geophys. Res. Lett. 0–3. https://doi.org/10.1029/2019GL082497

Rajput, P., Sarin, M., Sharma, D., Singh, D., 2014. Characteristics and emission budget of carbonaceous species from post-harvest agricultural-waste burning in source region of the Indo-Gangetic Plain Characteristics and emission budget of carbonaceous species from post-harvest agricultural-waste burning i. Tellus B Chem. Phys. Meteorol. 0889, 0–11. https://doi.org/10.3402/tellusb.v66.21026

Ramanathan, V., Ramana, M. V, 2005. Persistent, Widespread, and Strongly Absorbing Haze Over the Himalayan Foothills and the Indo-Gangetic Plains. Pure Appl. Geophys. 162, 1609–1626.

Roderick, M.L., Farquhar, G.D., Berry, S.L., Noble, I.R., Roderick, M.L., Farquhar, G.D., Berry, S.L., Noble, I.R., 2001. On the Direct Effect of Clouds and Atmospheric Particles on the Productivity and Structure of Vegetation Published by : Springer in cooperation with International Association for Ecology Stable URL : https://www.jstor.org/stable/4223052 On the direct effe. Int. Assoc. Ecol. 129, 21–30. https://doi.org/10.1007/S004420100760

Sarkar, S., Singh, R.P., Chauhan, A., 2018. Crop Residue Burning in Northern India : Increasing Threat to Greater India Journal of Geophysical Research : Atmospheres Crop Residue Burning in Northern India : Increasing Threat to Greater India. J. Geophys. Res. Atmos. https://doi.org/10.1029/2018JD028428

Singh, S., Singh, D., 2010. Recent Fog trends and its impact on wheat productivity in NW plains in India, in: 5th International Conference on Fog, Fog Collection and Dew Münster, Germany, 25–30 July 2010. Münster, Germany.

Srivastava, A.K., Tripathi, S.N., Dey, S., Kanawade, V.P., Tiwari, S., 2012. Inferring aerosol types over the Indo-Gangetic Basin from ground based sunphotometer measurements. Atmos. Res. 109–110, 64–75. https://doi.org/10.1016/j.atmosres.2012.02.010

Syed, F.S., Körnich, H., Tjernström, M., 2012. On the fog variability over south Asia. Clim. Dyn. 39, 2993–3005. https://doi.org/10.1007/s00382-012-1414-0

Taneja, G., Pal, B.D., Joshi, P.K., Aggarwal, P.K., N. K., T., 2014. Farmerss Preferences for Climate-Smart Agriculture: An Assessment in the Indo-Gangetic Plain (No. 01337), Discussion Paper. New Delhi. https://doi.org/10.2139/ssrn.2420547

Venkataraman, C., Habib, G., Kadamba, D., Shrivastava, M., Leon, J.F., Crouzille, B., Boucher, O., Streets, D.G., 2006. Emissions from open biomass burning in India: Integrating the inventory approach with high-resolution Moderate Resolution Imaging Spectroradiometer (MODIS) active-fire and land cover data. Global Biogeochem. Cycles 20, 1–12. https://doi.org/10.1029/2005GB002547

Wester, P., Mishra, A., Mukherji, A., Shrestha, A.B., Change, C., 2019. The Hindu Kush Himalaya assessment : mountains, climate change, sustainability and people. International Center for Integrated Mountain Development (ICIMOD), Hindu Kush Himalayan Monitoring and Assessment Programme (HIMAP) and Springer Open, Kathmandu Nepal.

Wild, M., 2012. Enlightening Global Dimming and Brightening. Bull. Am. Meteorol. Soc. 93, 27–37. https://doi.org/10.1175/BAMS-D-11-00074.1

Wild, M., Roesch, A., Ammann, C., 2012. Global dimming and brightening - evidence and agricultural implications. CAB Rev. Perspect. Agric. Vet. Sci. Nutr. Nat. Resour. 7, 1–7. https://doi.org/10.1079/PAVSNNR20127003

atmosphere

MDPI

Supplement: Comparison of MODIS and AERONET data

In order to apply MODIS products in the regression model the MODIS Aqua and Terra products of AOD and Precipitable water vapor was compared with that of AERONET in the 10 AERONET sites of the IGP. The results are presented in following figures.

Figure S1. Comparison of MODIS Aqua Derived AOD with AERONET AOD at the IGP stations.
Figure S2. Station wise comparison of MODIS Aqua AOD with AERONET AOD in terms of expected error (EE) for the IGP stations.
Figure S3. Comparison of MODIS Aqua and AERONET derived Atmospheric Water vapour (in cm) at the IGP Stations.
Figure S4. Comparison of MODIS Aqua derived AOD with AERONET AOD in four seasons in the IGP.
Figure S5. Comparison of MODIS Terra derived AOD with AERONET AOD at the IGP stations.
Figure S6. Station wise comparison of MODIS Terra AOD with AERONET AOD in terms of expected error (EE) in the IGP stations.
Figure S7. Comparison of MODIS Terra derived atmospheric water vapour with AERONET atmospheric water vapour at the IGP stations.
Figure S8. Comparison of MODIS Terra derived AOD with AERONET AOD in four seasons in the IGP.

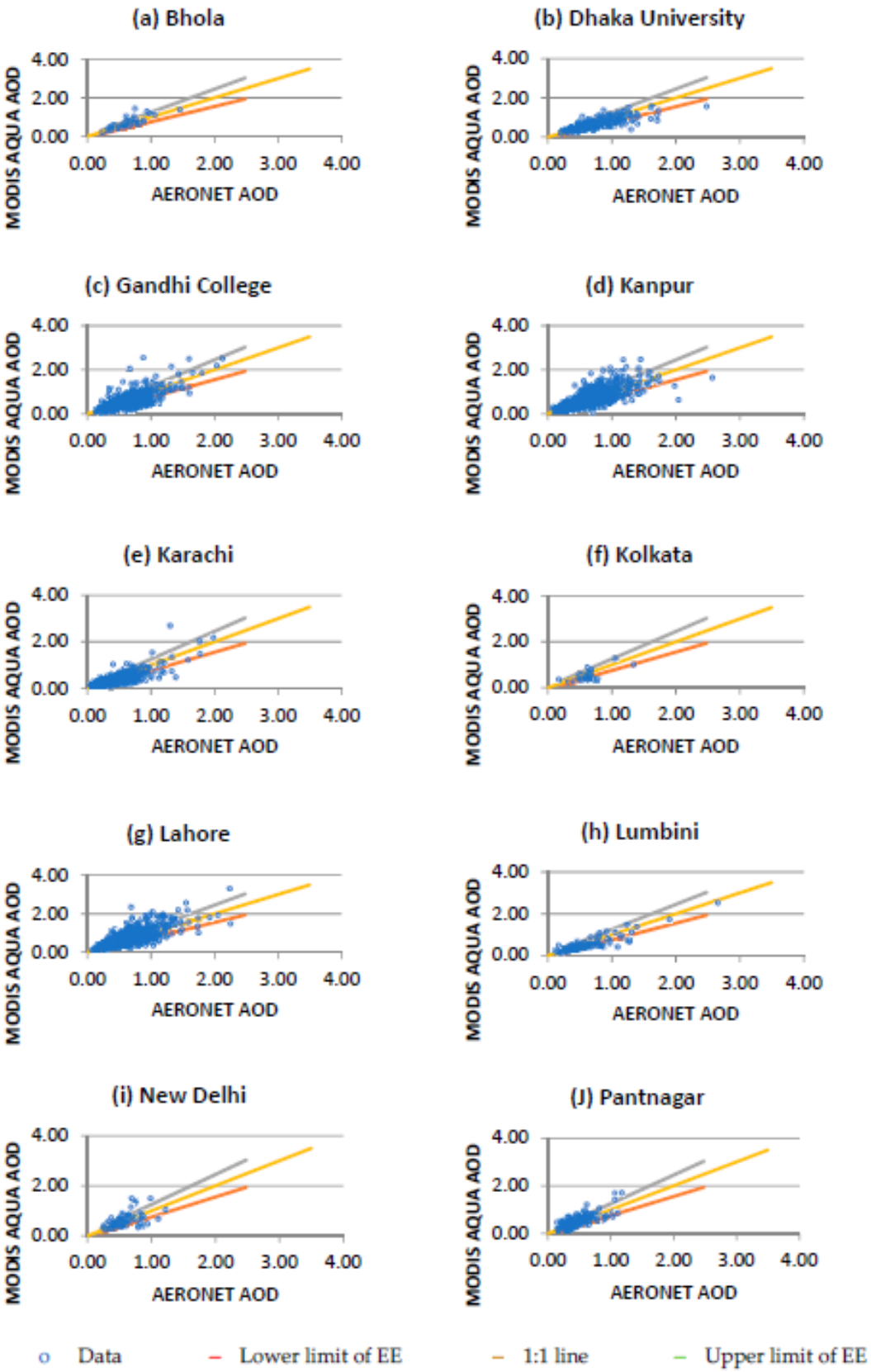

Figure S1. Comparison of MODIS Aqua Derived AOD with AERONET AOD at the IGP stations (**a**) Bhola (**b**) Dhaka University (**c**) Gandhi College (**d**) Kanpur (**e**) Karachi (**f**) Kolkata (**g**) Lahore (**h**) Lumbini (**i**) New Delhi (**j**) Pantnagar. Here EE is expected error range [±(0.05 + 0.2 × AOD)].

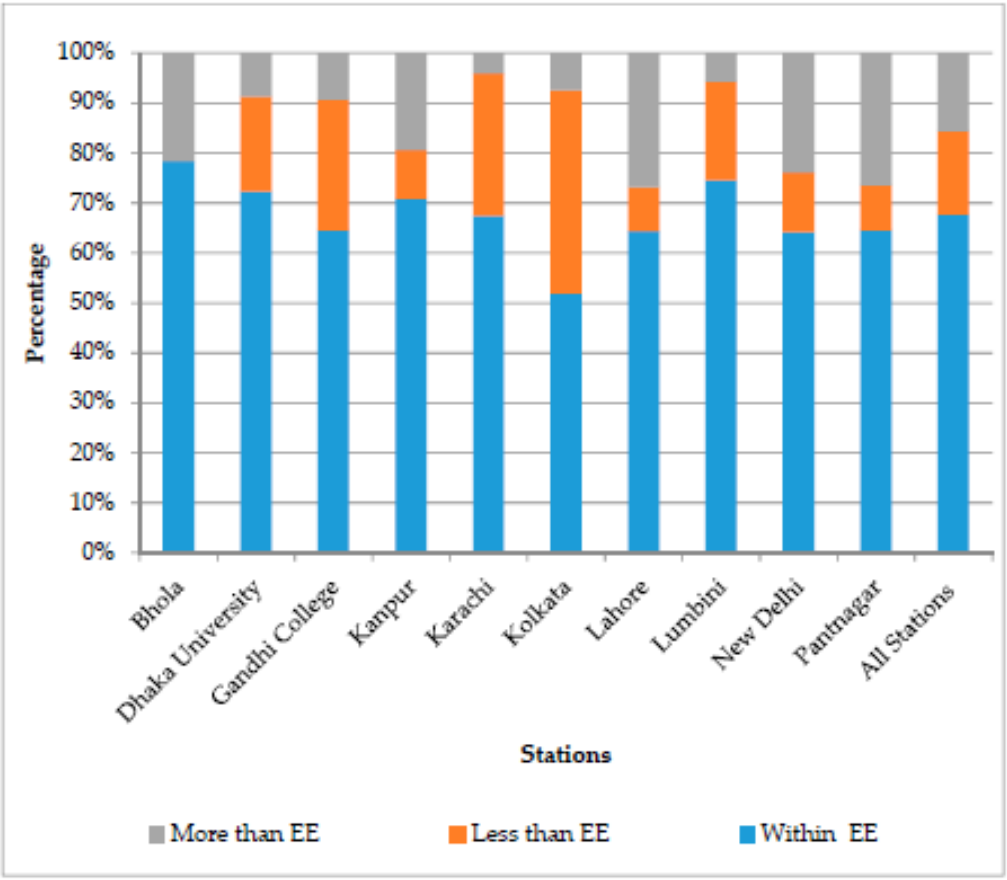

Figure 52. Station wise comparison of MODIS Aqua AOD with AERONET AOD in terms of expected error (EE) for the IGP stations.

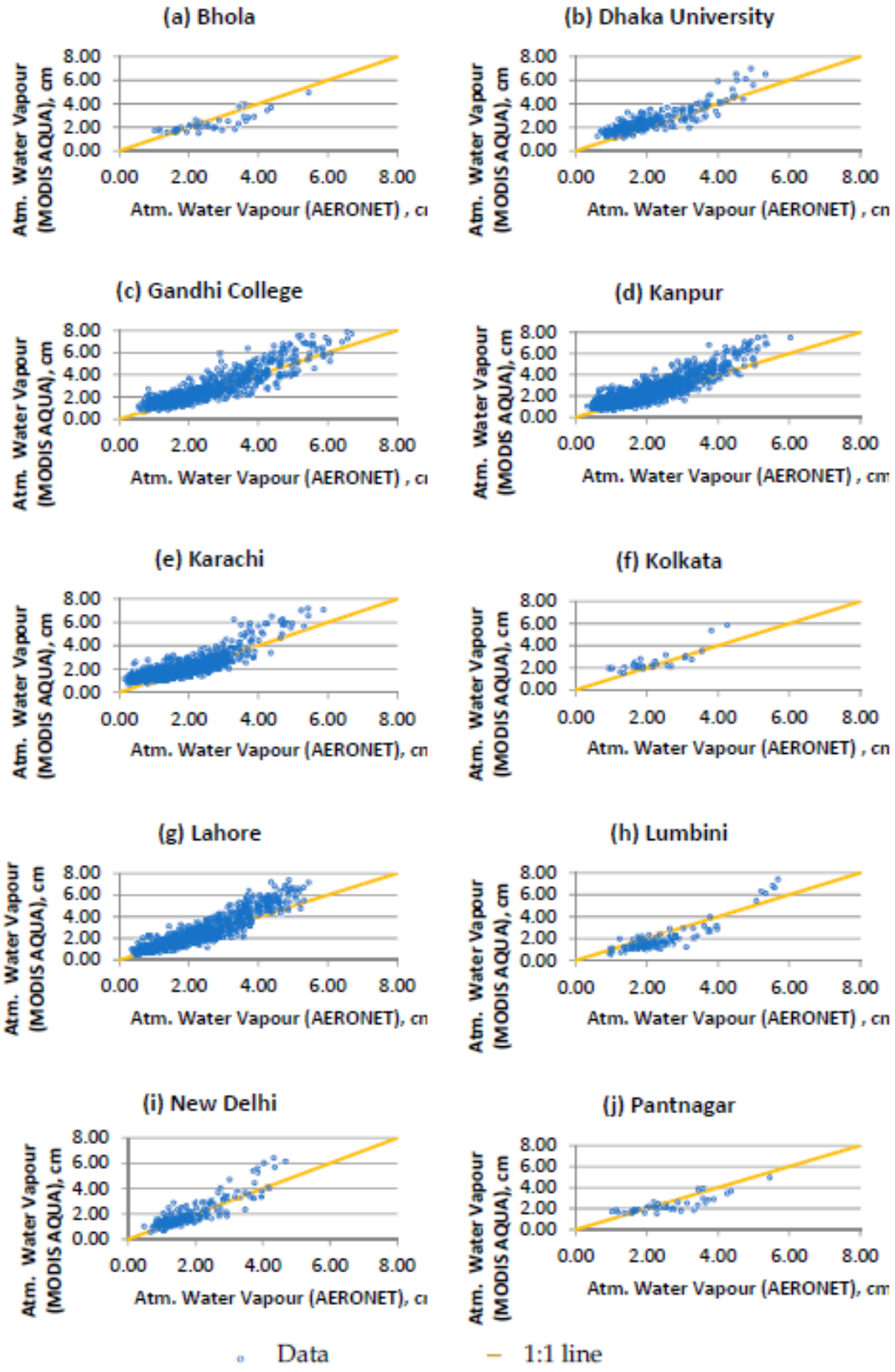

Figure S3. Comparison of MODIS Aqua and AERONET derived Atmospheric Water vapour (in cm) at the IGP Stations (**a**) Bhola (**b**) Dhaka University (**c**) Gandhi College (**d**) Kanpur (**e**) Karachi (**f**)Kolkata (**g**) Lahore (**h**) Lumbini (**i**) New Delhi (**j**) Pantnagar.

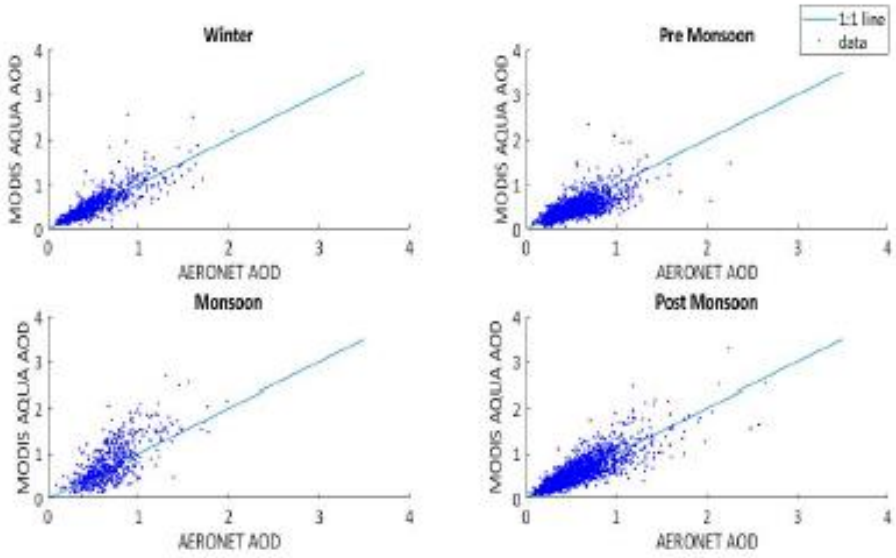

Figure S4. Comparison of MODIS Aqua derived AOD with AERONET AOD in four seasons in the IGP.

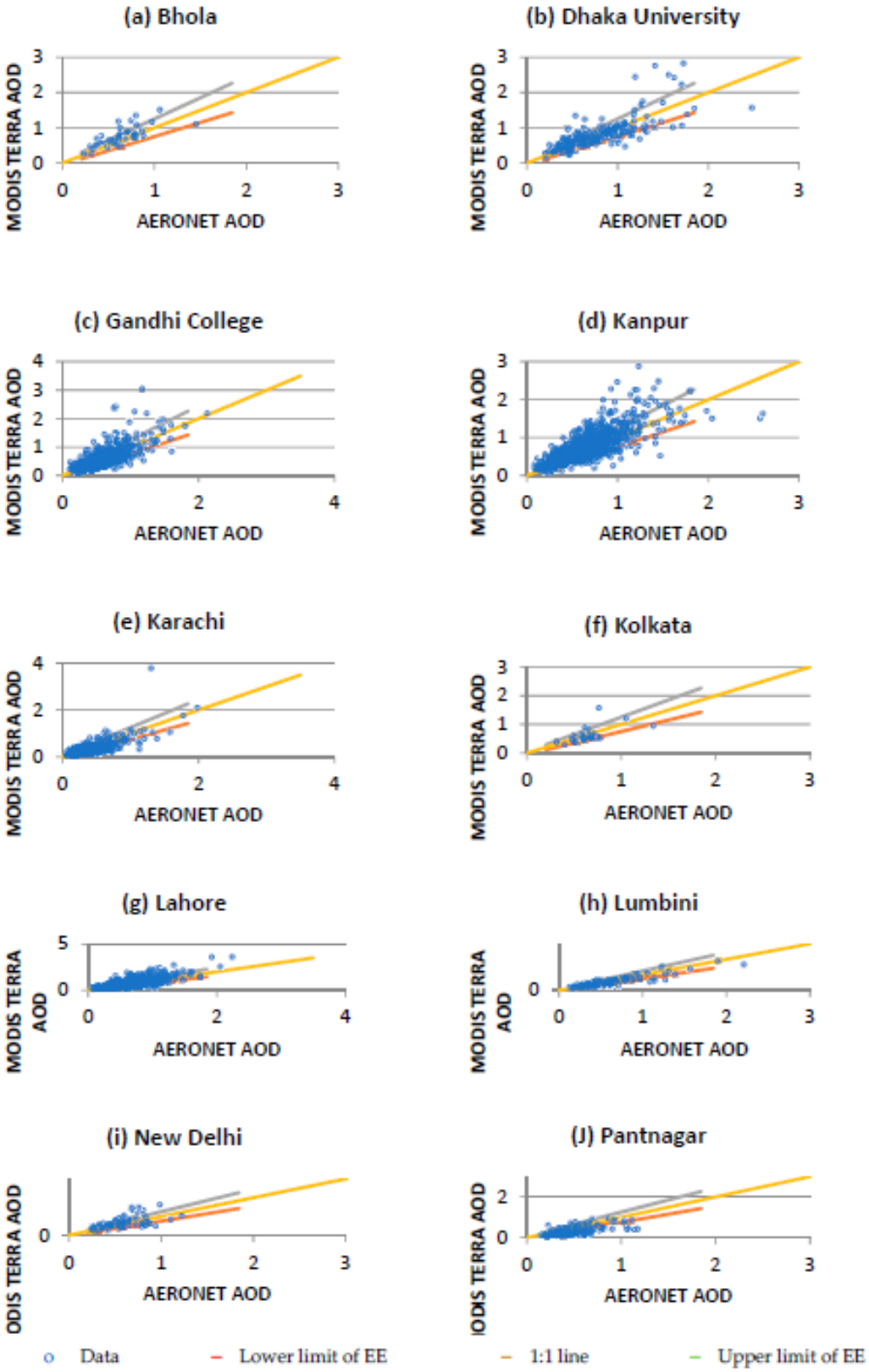

Figure S5. Comparison of MODIS Terra derived AOD with AERONET AOD at the IGP stations (**a**) Bhola (**b**) Dhaka University (**c**) Gandhi College (**d**) Kanpur (**e**) Karachi (**f**) Kolkata (**g**) Lahore (**h**) Lumbini (**i**) New Delhi (**j**) Pantnagar. Here EE is expected error range {±(0.05 + 0.2 × AOD)}.

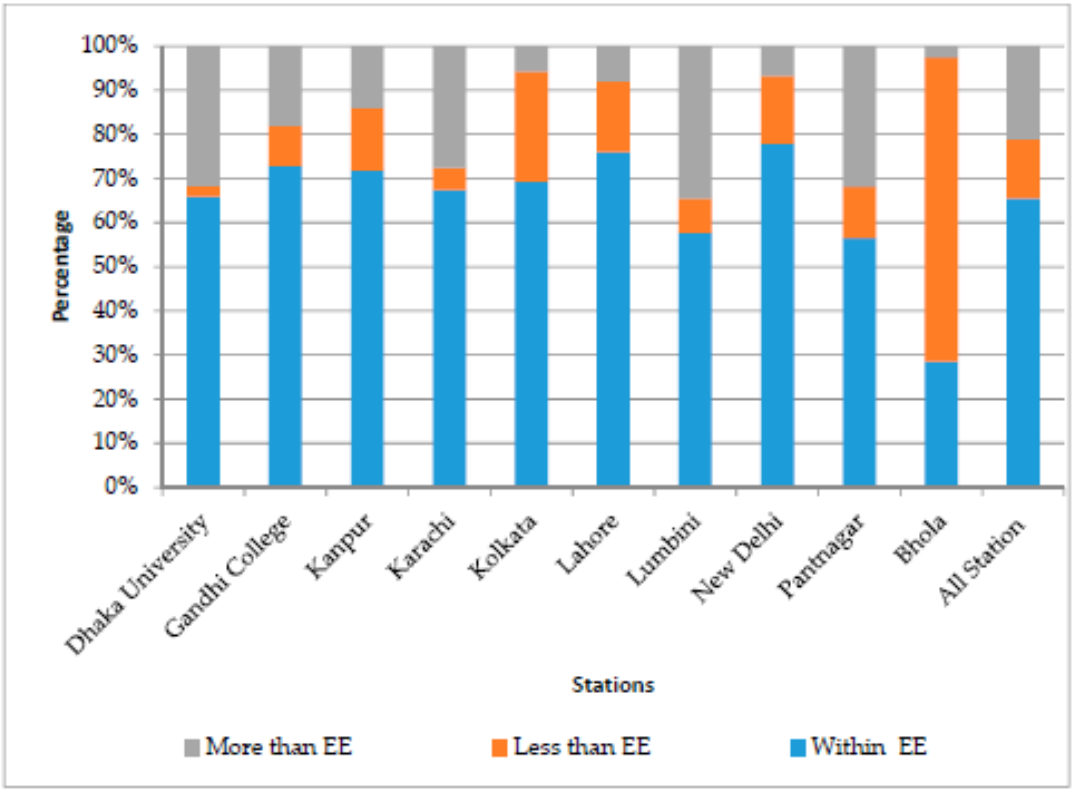

Figure S6. Station wise comparison of MODIS Terra AOD with AERONET AOD in terms of expected error (EE) in the IGP stations.

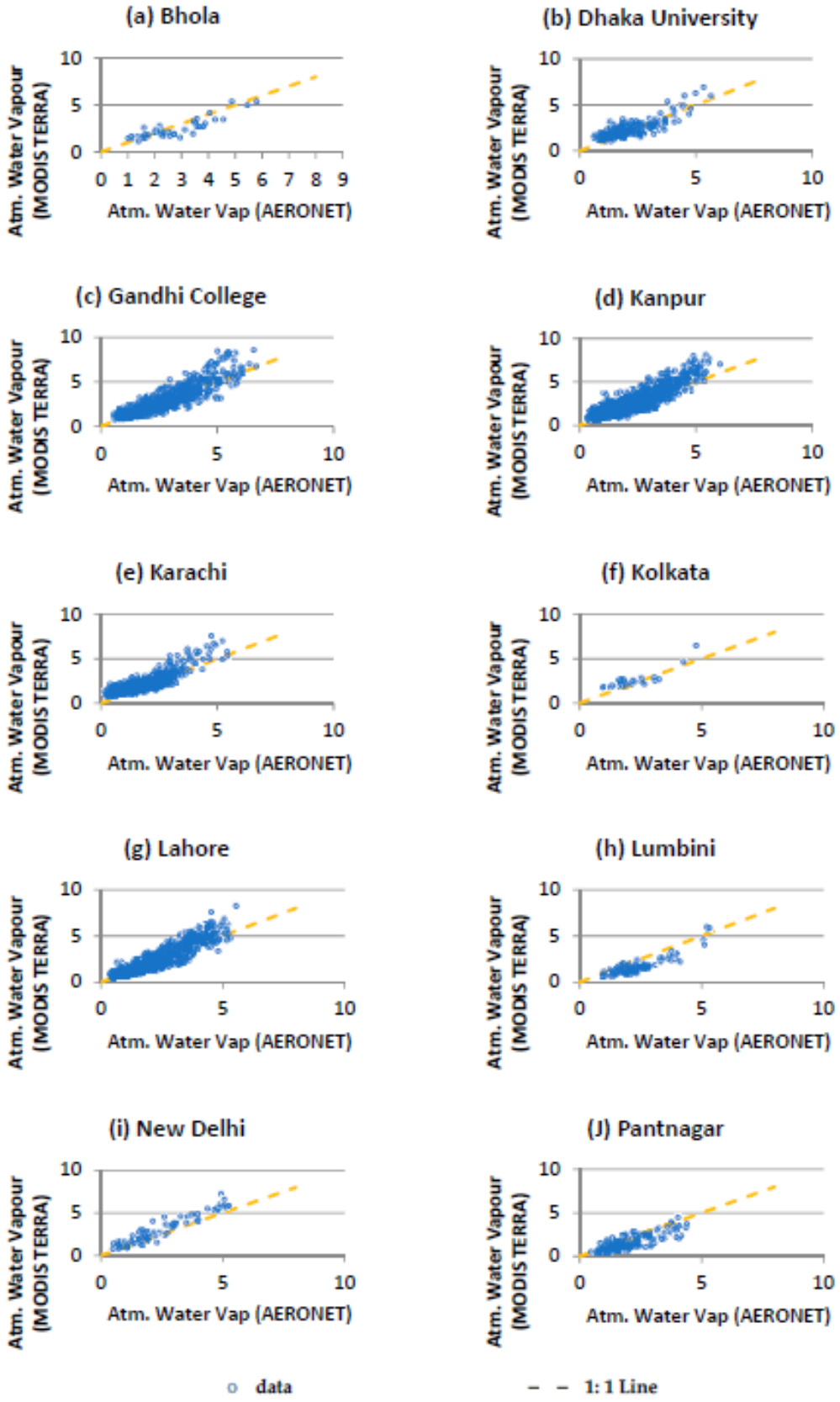

Figure S7. Comparison of MODIS Terra derived atmospheric water vapour with AERONET atmospheric water vapour at the IGP stations (**a**) Bhola (**b**) Dhaka University (**c**) Gandhi College (**d**) Kanpur (**e**) Karachi (**f**)Kolkata (**g**) Lahore (**h**) Lumbini (**i**) New Delhi (**j**) Pantnagar.

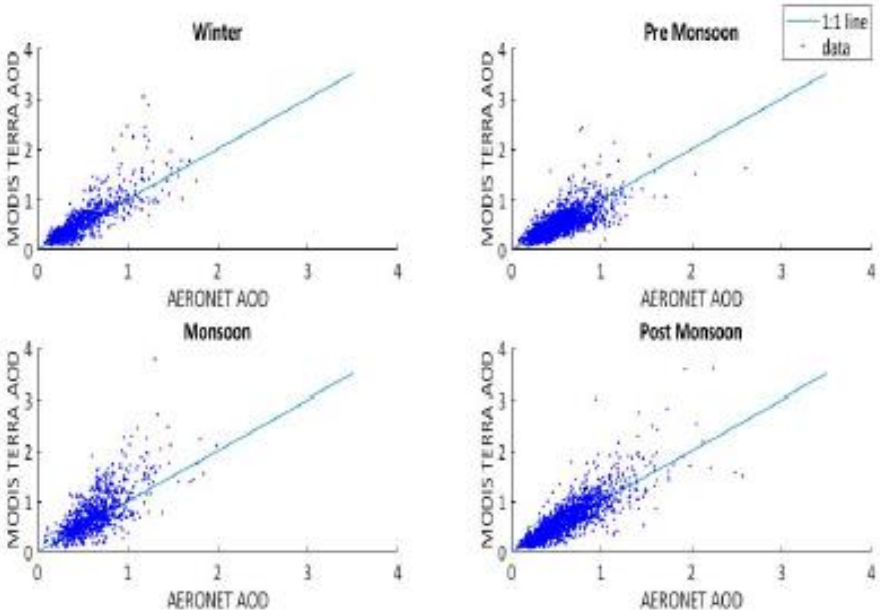

Figure S8. Comparison of MODIS Terra derived AOD with AERONET AOD in four seasons in the IGP.

Supplement Tables:

Supplement Table 1: Effect of anthropogenic aerosols on wheat grain yield in the eastern IGP considering only solar radiation effect

(Details of Table 6)

Country component of eastern IGP	District	Nodes	Year	Grain Yield (kg/ha)		Gain/ loss of grain yield due to aerosols (+/-)	
				With aerosols	Without aerosols	(kg/ha)	(%)
Nepal	**Sunsari**	**Bhaluwa**	2015	3629.0	4782.6	-1153.6	-24.1
			2016	4309.5	5427.5	-1118.0	-20.6
			Average	**3969.3**	**5105.1**	**-1135.8**	**-22.2**
		Simariya	2015	4380.2	4759.4	-379.2	-8.0
			2016	3631.8	4036.0	-404.2	-10.0
			Average	**4006.0**	**4397.7**	**-391.7**	**-8.9**
	Sunsari, Nepal			**3987.6**	**4751.4**	**-763.8**	**-16.1**
India	**Purnea**	**Tikapatti**	2015	4097.6	4198.0	-100.4	-2.4
			2016	2781.1	3063.0	-281.9	-9.2
			2017	3997.3	4242.6	-245.3	-5.8
			Average	**3625.3**	**3834.5**	**-209.2**	**-5.5**
		Dogachhi	2015	3987.8	5257.2	-1269.4	-24.1
			2016	3547.7	3208.6	339.1	10.6
			2017	4581.5	4670.2	-88.7	-1.9
			Average	**4039.0**	**4378.7**	**-339.7**	**-7.8**
	Average of nodes in Purnea, India			**3832.2**	**4106.6**	**-274.4**	**-6.7**
Bangladesh	**Rajshahi**	**Baduria**	2015	4436.6	5760.8	-1324.2	-23.0
			2016	4098.1	5359.2	-1261.1	-23.5
			2017	3280.7	4011.7	-731.0	-18.2
			Average	**3938.5**	**5043.9**	**-1105.4**	**-21.9**
		Premtoli	2015	6145.0	6507.7	-362.7	-5.6
			2016	3687.9	4611.1	-923.2	-20.0
			2017	3341.0	3848.2	-507.2	-13.2
			Average	**4391.3**	**4989.0**	**-597.7**	**-12.0**
	Average of nodes in Rajshahi			**4164.9**	**5016.5**	**-851.6**	**-17.0**
	Rangapur	**Mohonpur**	2015	4449.8	4917.9	-468.1	-9.5
			2016	2908.1	4096.0	-1187.9	-29.0
			Average	**3679.0**	**4507.0**	**-828.0**	**-18.4**
		Kolkondo	2015	4040.5	4662.6	-622.1	-13.3
			2016	3795.7	3798.4	-2.7	-0.1
			Average	**3918.1**	**4230.5**	**-312.4**	**-7.4**
	Average of nodes in Rangapur			**3798.5**	**4368.7**	**-570.2**	**-13.1**
	Average of nodes in Bangladesh			**3981.7**	**4692.6**	**-710.9**	**-15.1**
Average of nodes in eastern IGP				**3945.8**	**4560.8**	**-615.0**	**-13.5**

Supplement Table 2: Effect of anthropogenic aerosols on wheat biomass yield in the eastern IGP considering only solar radiation effect

(Details of Table 7)

Country component of eastern IGP	District	Nodes	Year	Biomass Yield (kg/ha)		Gain/ loss of biomass yield due to aerosols (+/-)	
				With aerosols	Without aerosols	(kg/ha)	(%)
Nepal	Sunsari	Bhaluwa	2015	9727.8	11489.4	-1761.6	-15.3
			2016	10382.3	11430.6	-1048.3	-9.2
			Average	**10055.1**	**11460.0**	**-1405.0**	**-12.3**
		Simariya	2015	9809.8	10767.7	-957.9	-8.9
			2016	7548.8	8626.1	-1077.3	-12.5
			Average	**8679.3**	**9696.9**	**-1017.6**	**-10.5**
	Average of nodes in Sunsari, Nepal			**9367.2**	**10578.5**	**-1211.3**	**-11.5**
India	Purnea	Tikapatti	2015	8857.9	10537.5	-1679.6	-15.9
			2016	6668.5	6801.1	-132.6	-1.9
			2017	8545.5	10214.5	-1669.0	-16.3
			Average	**8024.0**	**9184.4**	**-1160.4**	**-12.6**
		Dogachhi	2015	9159.0	11383.5	-2224.5	-19.5
			2016	7653.0	7539.5	113.5	1.5
			2017	10032.5	11058.2	-1025.7	-9.3
			Average	**8948.2**	**9993.7**	**-1045.6**	**-10.5**
	Average of nodes in Purnea, India			**8486.1**	**9589.1**	**-1103.0**	**-11.5**
Bangladesh	Rajshahi	Baduria	2015	8319.7	13047.4	-4727.7	-36.2
			2016	7954.2	13297.4	-5343.2	-40.2
			2017	7387.3	9605.2	-2217.9	-23.1
			Average	**7887.1**	**11983.3**	**-4096.3**	**-34.2**
		Premtoli	2015	10856.7	14755.1	-3898.4	-26.4
			2016	7511.4	11765.1	-4253.7	-36.2
			2017	7177.2	9423.3	-2246.1	-23.8
			Average	**8515.1**	**11981.2**	**-3466.1**	**-28.9**
	Average of nodes in Rajshahi			**8201.1**	**11982.3**	**-3781.2**	**-31.6**
	Rangapur	Mohonpur	2015	7481.3	10474.1	-2992.8	-28.6
			2016	4806.5	9872	-5065.5	-51.3
			Average	**6143.9**	**10173.1**	**-4029.2**	**-39.6**
		Kolkondo	2015	8903.2	11466.5	-2563.3	-22.4
			2016	7079.9	9352.8	-2272.9	-24.3
			Average	**7991.6**	**10409.7**	**-2418.1**	**-23.2**
	Average of nodes in Rangapur			**7067.7**	**10291.4**	**-3223.6**	**-31.3**
	Average of nodes in Bangladesh			**7634.4**	**11136.8**	**-3502.4**	**-31.4**
Average of nodes in eastern IGP				**8280.5**	**10610.3**	**-2329.8**	**-22.0**

Supplement Table 3: Effect of anthropogenic aerosols on wheat crop evapotranspiration in the eastern IGP considering only solar radiation effect

(Details of Table 8)

Country component of eastern IGP	District	Nodes	Year	Crop evapotranspiration (mm)		Gain/ loss of crop evapotranspiration due to aerosols (+/-)	
				With aerosols	Without aerosols	(mm)	(%)
Nepal	Sunsari	Bhaluwa	2015	326.8	347.4	-20.6	-5.9
			2016	263.8	274.2	-10.4	-3.8
			Average	**295.3**	**310.8**	**-15.5**	**-5.0**
		Simariya	2015	326.8	347.4	-20.6	-5.9
			2016	263.8	274.7	-10.9	-4.0
			Average	**295.3**	**311.0**	**-15.7**	**-5.1**
	Average of nodes in Sunsari, Nepal			**295.3**	**310.9**	**-15.6**	**-5.0**
India	Purnea	Tikapatti	2015	316.0	356.7	-40.7	-11.4
			2016	268.4	278.7	-10.3	-3.7
			2017	314.0	360.7	-46.7	-12.9
			Average	**299.5**	**332.0**	**-32.6**	**-9.8**
		Dogachhi	2015	318.9	368.4	-49.5	-13.4
			2016	314.8	333.4	-18.6	-5.6
			2017	350.9	383.8	-32.9	-8.6
			Average	**328.2**	**361.8**	**-33.7**	**-9.3**
	Average of nodes in Purnea, India			**313.8**	**346.9**	**-33.1**	**-9.5**
Bangladesh	Rajshahi	Baduria	2015	251.2	344.1	-92.9	-27.0
			2016	230.4	348.6	-118.1	-33.9
			2017	231.7	288.6	-56.9	-19.7
			Average	**237.8**	**327.1**	**-89.3**	**-27.3**
		Premtoli	2015	304.5	377.6	-73.1	-19.4
			2016	226.5	317.5	-91.0	-28.7
			2017	206.0	254.4	-48.5	-19.0
			Average	**245.7**	**316.5**	**-70.9**	**-22.4**
	Average of nodes in Rajshahi			**241.72**	**321.80**	**80.1**	**24.9**
	Rangapur	Mohonpur	2015	221.8	252.7	-30.9	-12.2
			2016	215.0	259.1	-44.1	-17.0
			Average	**218.4**	**255.9**	**-37.5**	**-14.7**
		Kolkondo	2015	248.0	290.5	-42.5	-14.6
			2016	225.1	264.9	-39.8	-15.0
			Average	**236.5**	**277.7**	**-41.2**	**-14.8**
	Average of nodes in Rangapur			**227.5**	**266.8**	**-39.3**	**-14.7**
	Average of nodes in Bangladesh			**234.6**	**294.3**	**-59.7**	**-20.3**
Average of nodes in eastern IGP				**269.6**	**311.6**	**-42.0**	**-13.5**

Supplement Table 4: Effect of anthropogenic aerosols on wheat grain yield in the eastern IGP considering the effect on solar radiation and maximum temperature during winter

(Details of Table 9)

Country component of eastern IGP	District	Nodes	Year	Grain Yield (kg/ha)		Gain/ loss of grain yield due to aerosols (+/-)	
				With aerosols	Without aerosols	(kg/ha)	(%)
Nepal	Sunsari	Bhaluwa	2015	3629.0	5225.1	-1596.1	-30.5
			2016	4309.5	4988.9	-679.4	-13.6
			Average	**3969.3**	**5107.0**	**-1137.8**	**-22.3**
		Simariya	2015	4380.2	4322.7	57.5	1.3
			2016	3631.8	3063.5	568.3	18.6
			Average	**4006.0**	**3693.1**	**312.9**	**8.5**
	Average of nodes in Sunsari, Nepal			**3987.6**	**4400.1**	**-412.4**	**-9.4**
India	Purnea	Tikapatti	2015	4097.6	4162.0	-64.4	-1.5
			2016	2781.1	3000.2	-219.1	-7.3
			2017	3997.3	4217.2	-219.9	-5.2
			Average	**3625.3**	**3793.1**	**-167.8**	**-4.4**
		Dogachhi	2015	3987.8	5275.6	-1287.8	-24.4
			2016	3547.7	3354.1	193.6	5.8
			2017	4581.5	4725.3	-143.8	-3.0
			Average	**4039.0**	**4451.7**	**-412.7**	**-9.3**
	Average of nodes in Purnea, India			**3832.2**	**4122.4**	**-290.2**	**-7.0**
Bangladesh	Rajshahi	Baduria	2015	4436.6	5629.2	-1192.6	-21.2
			2016	4098.1	5294.9	-1196.8	-22.6
			2017	3280.7	4074.1	-793.4	-19.5
			Average	**3938.5**	**4999.4**	**-1060.9**	**-21.2**
		Premtoli	2015	6145.0	6538.9	-393.9	-6.0
			2016	3687.9	4612.4	-924.5	-20.0
			2017	3341.0	3869.1	-528.1	-13.6
			Average	**4391.3**	**5006.8**	**-615.5**	**-12.3**
	Average of nodes in Rajshahi			**4164.9**	**5016.5**	**4164.9**	**-16.8**
	Rangapur	Mohonpur	2015	4449.8	4916.6	-466.8	-9.5
			2016	2908.1	3906.1	-998.0	-25.5
			Average	**3679.0**	**4411.4**	**-732.4**	**-16.6**
		Kolkondo	2015	4040.5	4497.3	-456.8	-10.2
			2016	3795.7	3690.2	105.5	2.9
			Average	**3918.1**	**4093.8**	**-175.7**	**-4.3**
	Average of nodes in Rangapur			**3798.5**	**4252.6**	**-454.0**	**-10.7**
	Average of nodes in Bangladesh			**3981.7**	**4627.8**	**-646.1**	**-14.0**
Average of nodes in eastern IGP				**3945.8**	**4444.5**	**-498.7**	**-11.2**

Supplement Table 5: Effect of anthropogenic aerosols on wheat biomass yield in the eastern IGP considering the effect on solar radiation and maximum temperature during winter

(Details of Table 10)

Country component of eastern IGP	District	Nodes	Year	Biomass Yield (kg/ha)		Gain/ loss of biomass yield due to aerosols (+/-)	
				With aerosols	Without aerosols	(kg/ha)	(%)
Nepal	Sunsari	Bhaluwa	2015	9727.8	12354.7	-2626.9	-21.3
			2016	10382.3	11160.1	-777.8	-7.0
			Average	**10055.1**	**11757.4**	**-1702.4**	**-14.5**
		Simariya	2015	9809.8	10481.2	-671.4	-6.4
			2016	7548.8	7504.0	44.8	0.6
			Average	**8679.3**	**8992.6**	**-313.3**	**-3.5**
	Average of nodes in Sunsari, Nepal Average			**9367.2**	**10375.0**	**-1007.8**	**-9.7**
India	Purnea	Tikapatti	2015	8857.9	10451.3	-1593.4	-15.2
			2016	6668.5	6637.4	31.1	0.5
			2017	8545.5	10117	-1571.5	-15.5
			Average	**8024.0**	**9068.6**	**-1044.6**	**-11.5**
		Dogachhi	2015	9159.0	11425.1	-2266.1	-19.8
			2016	7653.0	7655.0	-2.0	0.0
			2017	10032.5	11096.1	-1063.6	-9.6
			Average	**8948.2**	**10058.7**	**-1110.6**	**-11.0**
	Average of nodes in Purnea, India Average			**8486.1**	**9563.7**	**-1077.6**	**-11.3**
Bangladesh	Rajshahi	Baduria	2015	8319.7	12818.8	-4499.1	-35.1
			2016	7954.2	13164.3	-5210.1	-39.6
			2017	7387.3	9601.9	-2214.6	-23.1
			Average	**7887.1**	**11861.7**	**-3974.6**	**-33.5**
		Premtoli	2015	10856.7	14683.5	-3826.8	-26.1
			2016	7511.4	11743.9	-4232.5	-36.0
			2017	7177.2	9399.5	-2222.3	-23.6
			Average	**8515.1**	**11942.3**	**-3427.2**	**-28.7**
	Average of nodes in Rajshahi Average			**8201.1**	**11902.0**	**-3700.9**	**-31.1**
	Rangapur	Mohonpur	2015	7481.3	10573.5	-3092.2	-29.2
			2016	4806.5	9536.2	-4729.7	-49.6
			Average	**6143.9**	**10054.9**	**-3911.0**	**-38.9**
		Kolkondo	2015	8903.2	11375.7	-2472.5	-21.7
			2016	7079.9	9329.1	-2249.2	-24.1
			Average	**7991.6**	**10352.4**	**-2360.9**	**-22.8**
	Average of nodes in Rangapur Average			**7067.7**	**10203.6**	**-3135.9**	**-30.7**
	Average of nodes in Bangladesh Average			**7634.4**	**11052.8**	**-3418.4**	**-30.9**
Average of nodes in eastern IGP				**8280.5**	**10511.1**	**-2230.6**	**-21.2**

Supplement Table 6: Effect of anthropogenic aerosols on wheat crop evapotranspiration in the eastern IGP considering the effect on solar radiation and maximum temperature during winter

(Details of Table 11)

Country component of eastern IGP	District	Nodes	Year	Crop evapotranspiration (mm)		Gain/ loss of crop evapotranspiration due to aerosols (+/-)	
				With aerosols	Without aerosols	(mm)	(%)
Nepal	Sunsari	Bhaluwa	2015	326.8	352.6	-25.8	-7.3
			2016	263.8	293.4	-29.6	-10.1
			Average	**295.3**	**323.0**	**-27.7**	**-8.6**
		Simariya	2015	326.8	357.8	-31.0	-8.7
			2016	263.8	286.7	-22.9	-8.0
			Average	**295.3**	**322.2**	**-26.9**	**-8.4**
	Average of nodes in Sunsari, Nepal			**295.3**	**322.6**	**-27.3**	**-8.5**
India	Purnea	Tikapatti	2015	316.0	360.7	-44.7	-12.4
			2016	268.4	277.2	-8.7	-3.1
			2017	314.0	365.0	-51.0	-14.0
			Average	**299.5**	**334.3**	**-34.8**	**-10.4**
		Dogachhi	2015	318.9	375.4	-56.5	-15.1
			2016	314.8	321.4	-6.6	-2.0
			2017	350.9	396.7	-45.8	-11.5
			Average	**328.2**	**364.5**	**-36.3**	**-10.0**
	Average of nodes in Purnea, India			**313.8**	**349.4**	**-35.5**	**-10.2**
Bangladesh	Rajshahi	Baduria	2015	251.2	346.4	-95.2	-27.5
			2016	230.4	348.9	-118.5	-34.0
			2017	231.7	291.2	-59.5	-20.4
			Average	**237.8**	**328.8**	**-91.1**	**-27.7**
		Premtoli	2015	304.5	384.7	-80.2	-20.9
			2016	226.5	326.6	-100.0	-30.6
			2017	206.0	261.6	-55.6	-21.2
			Average	**245.7**	**324.3**	**-78.6**	**-24.2**
	Average of nodes in Rajshahi			**241.72**	**326.6**	**-84.8**	**-26.0**
	Rangapur	Mohonpur	2015	221.8	265.8	-44.0	-16.5
			2016	215.0	264.2	-49.2	-18.6
			Average	**218.4**	**265.0**	**-46.6**	**-17.6**
		Kolkondo	2015	248.0	291.3	-43.4	-14.9
			2016	225.1	263.6	-38.5	-14.6
			Average	**236.5**	**277.4**	**-40.9**	**-14.7**
	Average of nodes in Rangapur			**227.5**	**271.2**	**-43.7**	**-16.1**
	Average of nodes in Bangladesh			**234.6**	**298.9**	**-64.3**	**-21.5**
Average of nodes in eastern IGP				**269.6**	**317.4**	**-47.9**	**-15.1**